Transition-Metal-Catalyzed C−C and C−Heteroatom Bonds Formation using Strained Rings: Enroute to Spiro and Heterocyclic Congeners

A Thesis Submitted

in Partial Fulfilment of the Requirements

for the Degree of

DOCTOR OF PHILOSOPHY IN CHEMISTRY

By

Bijoy Debnath

Roll No. 196122008

Department of Chemistry
Indian Institute of Technology Guwahati
Guwahati 781039
February 2025

Dedicated To

My Family

INDIAN INSTITUTE OF TECHNOLOGY GUWAHATI

Department of Chemistry

STATEMENT

I hereby declare that the matter embodied in this thesis is the result of investigations carried out by me in the Department of Chemistry, Indian Institute of Technology Guwahati, Guwahati, India under the supervision of Prof. Tharmalingam Punniyamurthy.

In keeping with the general practice of reporting scientific observations, due acknowledgement has been made wherever the work described is based on the findings of other investigators.

Guwahati — Bijoy Debnath

February 2025

INDIAN INSTITUTE OF TECHNOLOGY GUWAHATI

Department of Chemistry

CERTIFICATE

This is to certify that Mr. Bijoy Debnath has been working under my supervision since July 2019. I am forwarding his thesis entitled "*Transition-Metal-Catalyzed C−C and C−Heteroatom Bonds Formation using Strained Rings: Enroute to Spiro and Heterocyclic Congeners*" being submitted for the Ph.D. degree of this institute. I certify that he has fulfilled all the requirements according to the rules of this institute, and regarding the investigations embodied in his thesis and this work has not been submitted elsewhere for a degree.

Guwahati

February 2025

Prof. Tharmalingam Punniyamurthy

Supervisor

ACKNOWLEDGEMENT

I want to take the opportunity to express my gratitude to my mentor and supervisor, **Prof. Tharmalingam Punniyamurthy**, for introducing me to the captivating field of synthetic chemistry and granting me the opportunity and freedom to conduct this research. I am deeply indebted to him for his unwavering interest, invaluable guidance, constant motivation, and continuous support. Thank you, Sir! for consistently motivating and helping me achieve this milestone. I will remain eternally grateful for the opportunities you have provided and the doors you have opened for me. In addition to my supervisor, I would also like to acknowledge my doctoral committee members **Prof. G. Krishnamoorthy**, **Prof. A. S. Achalkumar**, Department of Chemistry, and **Prof. Vishal Trivedi**, Department of Biosciences and Bioengineering for their insightful suggestions and feedback throughout the evaluation process of my doctoral thesis.

I am truly delighted to express my heartfelt gratitude to my labmates Dr. Subhasish Roy, Dr. S. Vivek Kumar, Dr. Tariq A. Shah, Dr. Dinesh Kumar Nayak, Dr. R. Arunachalam, Dr. Vijay Murugan, Dr. Pinaki Bhusan De, Dr. Sourav Pradhan, Dr. Bijay Ketan Das, Dr. Tanumay Sarkar, Dr. Kangkan Talukdar, Dr. Sonbidya Banerjee, Dr. Manmath Mishra, Dr. Pallab Karjee, Dr. Muthuraja Perumal, Dr. V. Tamilthendral, Mr. Shubhajit Basak, Ms. Tripti Paul, Ms. Subhradeep Kar, Mr. Prabhat Kumar Maharana, Mr. Santu Mondal, Mr. Hemanga Bhattacharyya, Mr. Kshitiz Verma, Mr. Sharajit Saha, Ms. Swati Samantaray, Mr. Maniya V. N, Mr. Madhab Barman, Ms. Anita Sahoo, Mr. Sajal Roy, Ms. Priya Patra, Ms. Ravina Yadav, Mr. Vishwanath Kumar, Mr. Nicky jones Lyngdoh Marshillong for their unwavering moral support, invaluable encouragement, and for always being there whenever I reached out. I also deeply appreciate the friendly and collaborative relationship we shared.

I sincerely appreciate the support and assistance provided by all the faculty members of the Department of Chemistry, the staff of the Central Instruments Facility, and the non-teaching staff of the Department of Chemistry during my entire Ph.D. journey.

I am deeply thankful to UGC, India for fellowship and IIT Guwahati for providing me with access to all the necessary facilities. I also extend my thanks to the Central Instrument Facility (CIF) and North East Centre for Biological Sciences and Healthcare Engineering (NECBH), IIT Guwahati for offering the instrumentation resources, and to DST for providing the X-ray facility.

I am delighted to extend my heartfelt gratitude to my wonderful friends at IIT Guwahati. I deeply appreciate the support and the joyful moments shared with my Ph.D. batchmates (July, 2019), fellow research scholars in the Chemistry Department, and my B.Sc. and M.Sc. friends.

I am fortunate enough to have nice friends Mr. Ratnadeep Nath and Ms. Kuheli Deb for their moral support in my tough times.

Finally, I profoundly render my deep regards to my beloved parents (Mr. Laxmi Kanta Debnath & Mrs. Mina Rani Debnath) and elder brothers (Mr. Sajay Debnath and Mr. Ajoy Debnath), my sister Ms. Jayashree Debnath and my uncle (Mr. Gurudas Debnath) for their endless patience, countless sacrifices, sincere encouragement, and inspiration. Thank you for keeping your faith in me and giving me the freedom and opportunities to pursue my dreams. This journey would have been incredibly difficult without your blessings, love and unwavering moral support. I am deeply indebted to your love, care, affection, and blessings.

Last but certainly not least, I am deeply grateful to the almighty God. I humbly surrender myself to you for showering your blessings upon me and granting me the strength and ability to complete this thesis work.

God bless you all!

Bijoy Debnath

List of Abbreviations

Å	Angstrom (10^{-8} cm)
Ar	Aryl
BHT	2,6-di-*tert*-butyl-4-methylphenol
Bn	Benzyl
Boc	*Tert*-butyloxycarbonyl
CCDC	Cambridge crystallographic data center
DAC	Donor-acceptor cyclopropane
DIPEA	*N,N*-diisopropylethylamine
DMSO	Dimethylsulfoxide
DMF	*N,N*-dimethylformamide
dppp	1,3-Bis(diphenylphosphino)propane
dppb	1,4-Bis(diphenylphosphino)butane
dppe	1,2-Bis(diphenylphosphino)ethane
DBN	1,5-Diazabicyclo[4.3.0]non-5-ene
DABCO	1,4-Diazabicyclo[2.2.2]octane
DTPB	2, 6-Di-tert-butylpyridine
DIPEA	*N,N*-diisopropylethylamine
DBU	1,8-Diazabicyclo[5.4.0]undec-7-ene
DMF	Dimethylformamide
DMSO	Dimethyl sulfoxide
EDG	Electron donating group
equiv	Equivalent
ESI	Electrospray ionization

EWG	Electron withdrawing group
FT-IR	Fourier transform infrared spectroscopy
HFIP	Hexafluoroisopropanol
Het	Hetero
HRMS	High-resolution mass spectrometry
Hz	Hertz
m/z	Mass to charge ratio
mp	Melting point
MHz	Megahertz
NMR	Nuclear magnetic resonance
nd	Not detected
ORTEP	Oak ridge thermal ellipsoid plot
R_f	Retardation factor
rt	Room temperature
TEMPO	2,2,6,6-Tetramethyl-1-piperidinyloxy
TFE	2,2,2-Trifluoroethanol
Tf	Trifluoromethanesulfonyl
THF	Tetrahydrofuran
Ts	Toluenesulfonyl
TLC	Thin layer chromatography
TMS	Trimethylsilyl
TM	Transition metal
μL	Microliter

Abstract

The thesis is structured into four chapters. The first chapter emphasizes the significance of spiro and heterocyclic scaffolds and the transition-metal-catalyzed reactivity of strained rings, leading to cyclic congeners. The second chapter explores the diastereoselective synthesis of spirooxindole cycloadducts through the annulative C−C coupling of spirovinylcyclopropyl oxindoles with *p*-quinone methides. The third chapter discusses the synthesis of fused 1,4-oxazines *via* C−N/C−O coupling between aziridines and 2,4-dienals. The fourth chapter addresses the C−H/C−C activation/annulation of quinoline *N*-oxides with cyclopropenones to produce functionalized 2-quinolones.

Chapter I. Spiro/Heterocyclic Scaffolds and Reactivity of Strained Rings

Hetero- and spirocyclic scaffolds play a vital role as fundamental elements in various organic compounds, such as pharmaceuticals, natural products, and functional materials. They display a broad spectrum of biological activities and are present in numerous types of natural compounds. Hence research and development of these compounds are of significant interest and continue to be important in organic synthesis. In recent decade, three-membered rings, owing to their staple architecture and facile reactivity have garnered significant attention for construction of complex cyclic scaffolds. In this chapter, the synthetic methodologies involving transition-metal-catalyzed reactions of three-membered rings with dipolarophiles, leading to fabrication of cyclic frameworks have been discussed (Scheme 1).

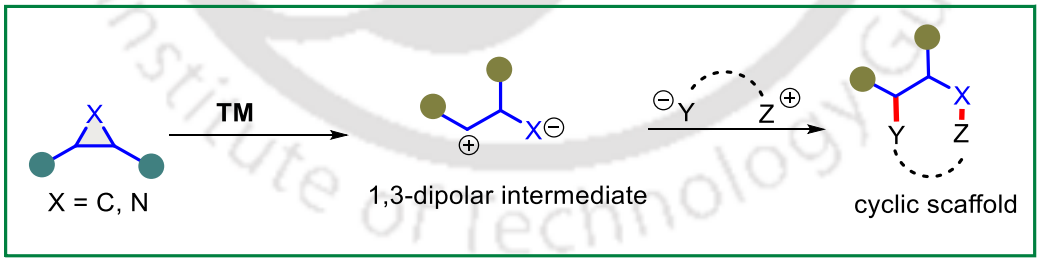

Scheme 1. Synthesis of Cyclic Scaffolds using Three-membered Rings

Chapter II. [3+2]-Annulation of Spirovinylcyclopropyl Oxindoles with *p*-Quinone Methides

The synthesis of spiro-ring fused cyclic scaffolds has garnered increased attention in scientific research. In particular, spirocyclic oxindoles have become a focus in contemporary drug discovery due to their three-dimensional structures, versatile architectures, and common

occurrence in bioactive compounds. Despite their significance, the synthesis of spirooxindole derivatives remains complex, often demanding extensive and multi-step synthetic processes. As a result, the development of efficient methods for synthesizing these scaffolds using readily accessible reagents has become an area of active interest. In this chapter, we described a palladium-catalyzed [3+3]-annulative C−C coupling using spirovinylcycloproyl oxindoles (SVCPs) and *p*-quinone methides (p-QMs) to produce functionalized bis-spirocyclopentane oxindole derivatives (Scheme 2). The reaction proceeds *via* a [3+3]-annulation pathway.

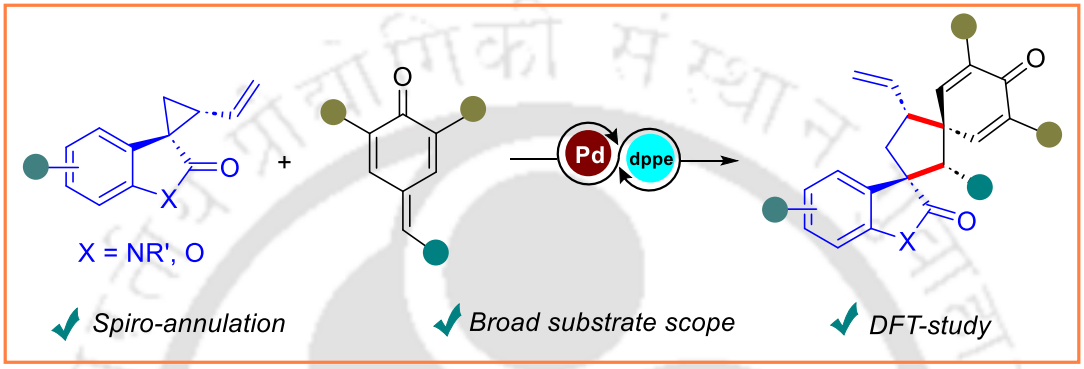

J. Org. Chem. **2023**, *88*, 9704

Scheme 2. Pd-Catalyzed [3+2]-Annulation of SVCPs and *p*-QMs

Chapter III. [3+3]-Annulation of 2,4-Dienals with Aziridines: Access to Fused Morpholines

Fused small cyclic molecules, on account of their rigid conformations and moderate ring sizes exhibit excellent physicochemical properties. Consequently, advancing synthetic methods for such molecular frameworks has emerged as a leading research focus. However, traditional synthetic techniques for these fused systems often depend on costly catalysts and lack efficiency in terms of atom and step economy. Therefore, developing cost-effective strategies to achieve these structural units using easily accessible catalysts and reagents remains a significant challenge and is highly sought after. Herein, we entitled C−O/C−N coupling of aziridines with 2,4-dienals under earth abundant iron-catalysis to furnish fused morpholines derivatives (Scheme 3). Substrate scope, mild reaction conditions and cost-effective catalyst are important practical features.

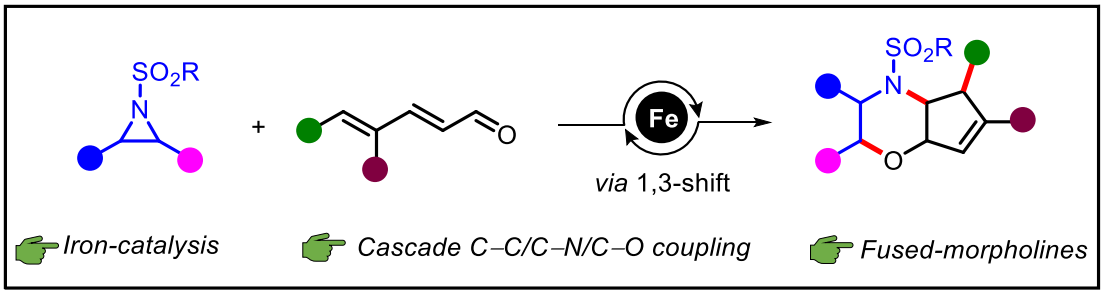

Scheme 3. Fe-Catalyzed [3+3]-Annulation of Aziridines and 2,4-Dienals

Chapter IV. Cascade C−H/C−C-Activation/Annulation of Quinoline *N*-oxides and Cyclopropenones

In recent years, cascade annulation reactions *via* C−H activation have attracted significant attention, as these strategies serve as elegant tool to simplify the lengthy and complex synthesis processes. One promising approach is the use of auxiliary facilitated synthesis or modification of essential molecular frameworks. In this vein, the site-selective C−H functionalization of quinoline cores has garnered considerable interest. However, strategies involving C−H activation/annulation with quinoline cores are still scarce and challenging. Thus, we envisioned merging C−H/C−C activation and annulation strategy utilizing quinoline *N*-oxides with strained rings could offer a more facile strategy for generating a variety of substituted cyclic structures. This chapter deals with a robust strategy of C−H/C−C activation employing quinoline *N*-oxides with cyclopropenones under rhodium-catalysis (Scheme 4). The protocol offers generation of functionalized 2-quinolone derivatives *via* sequential C−C/C−N bond formation, mechanistic aspect and valuable synthetic transformation as key features.

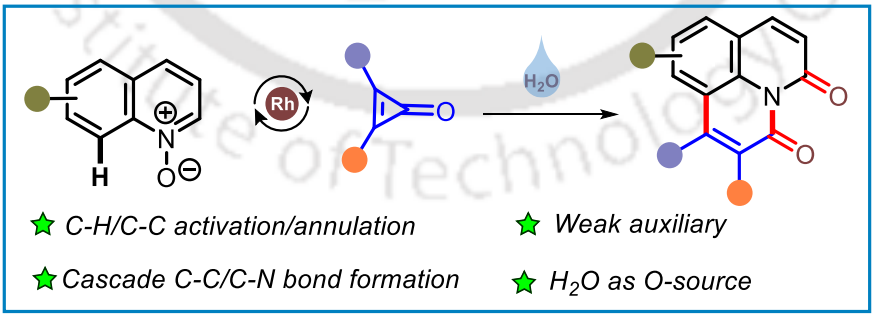

Chem. Commun. **2025**, *61*, 7875

Scheme 4. Rh-Catalyzed Annulation of Quinoline *N*-oxides and Cyclopropenones

Contents

Chapter I

Spiro/Heterocyclic Scaffolds and Reactivity of Strained Rings

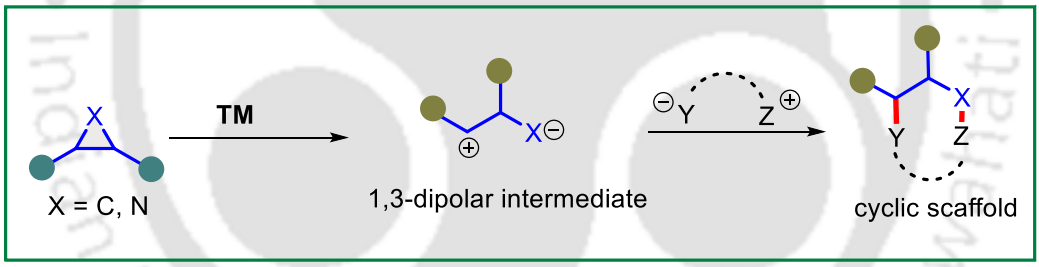

Spiro/Heterocyclic Scaffolds and Reactivity of Strained Rings

1.1 Importance of Spiro- and Heterocycles

Spiro cyclic compounds are a class of bicyclic organic molecules where two rings are connected by a single atom.[1] Baeyer first coined the term spiro-cycle from his groundbreaking research in 1900. The unique three-dimensional structural features of such compounds provide them structural rigidity and conformational restrictions.[2] These properties enable spiro compounds to be versatile in various biological and catalytic activities, making them more selectively targeted than other flat or aromatic structures. Moreover, natural spiro compounds like acorenone B, rosmadial, β-vetivone, pandamarine, spinol etc. (Figure 1.1), exhibit a wide range of medicinal and material properties as well as stereo-control catalytic activities.[2,3] Cyclic

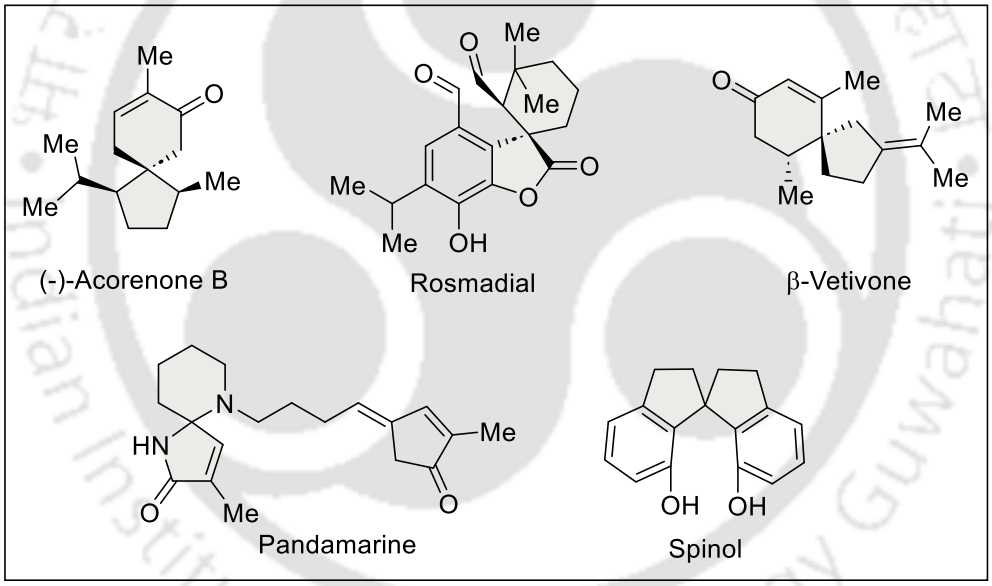

Figure 1.1. Selective Examples of Vital Natural Spirocyclic Compounds

compounds with one or more hetero atoms are termed as heterocyclic compounds.[4] Moreover, heterocyclic compounds are among the most common organic structures and are widely distributed in various applications across medicinal and industrial fields.[5] In this context, nitrogen containing hetero cycles has gained profuse prominence due to their omnipresence in numerous natural sources and medicinal molecules.[6] For instance, five and six membered nitrogen containing heterocycles like pyrroles, pyrimidines, morpholines, oxindoles, indoles, quinolines etc. (Figure 1.2) are found to have vast range of medicinal applications. Further, recent study revealed 60% of U.S. FDA drugs are composed of *N*-heterocycles.[6b] Owing to

such potentiality, these cyclic scaffolds have attracted scientific fronts for laboratory synthesis, property modification, and the design of new hetero- and spirocyclic molecules to increase their usability. However, synthesis of these compounds poses several challenges like functional group compatibility, further derivatisation of the rings and intricacies involved in synthesizing quaternary centres. Thus, development of new methodologies to construct such molecular frameworks are highly demanding.

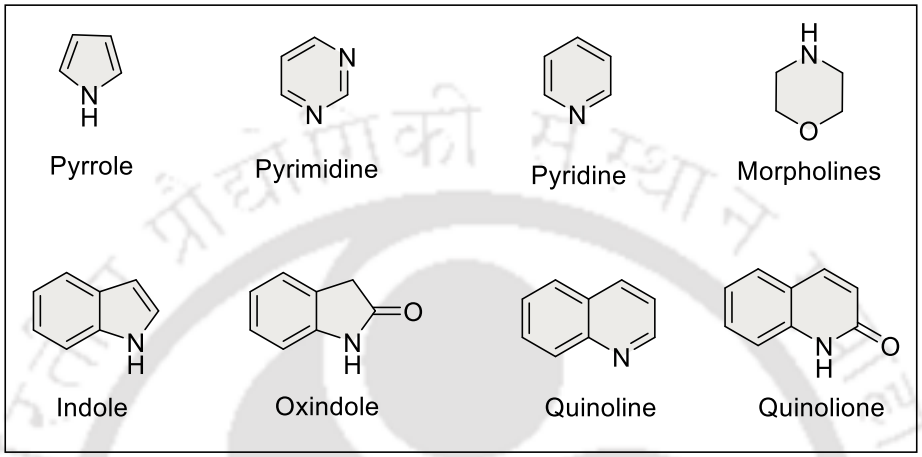

Figure 1.2. Selective Examples of Vital *N*-Heterocycles

1.2 Strained Ring: A Versatile Tool to Synthesize Cyclic Congeners

In recent time, among the quest of regal strategies for the synthesis and modification of essential cyclic frameworks, strained rings surfaced as a one of the best coupling partners.[7] Due to high ring strain, staple molecular geometry, easy accessibility, and high stability, strained rings continue to be captivating research interest (Figure 1.3).[7g] In this realm, three membered rings such as aziridines, vinylcyclopropanes and cyclopropenones, stood out as versatile precursors to architect and fabricate valuable cyclic motifs. Synthetic methodologies using such strained rings display excellent approach to mitigate the challenges like atom and step-economy, functional group tolerance, regioselectivity etc. associated with other synthetic methods that need tedious efforts. This chapter presents the reactivity of vinylcyclopropanes, aziridines, and cyclopropenones under transition metal-catalysis and their utility for the synthesis of value-added spiro- and hetero-cyclic skeletal structures.

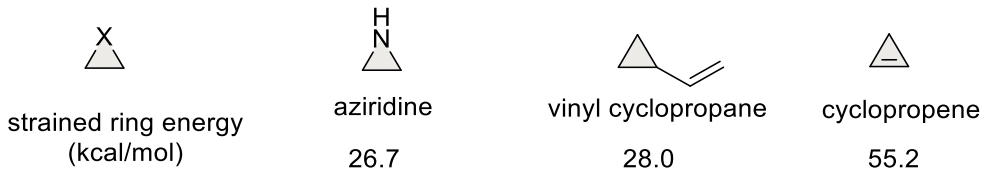

Figure 1.3. Comparative Ring Strain Energy of Three-Membered Rings

1.3 Synthetic Strategy for Construction of Cyclic Scaffolds using Three-Membered Rings

In presence of metal-catalysts, the innate ring strain acts as a driving force that led to release of ring strain *via* thermodynamically favourable ring opening that can lead to generation of 1,3-dipolar intermediate, which can undergo annulation or cyclization with dipolarophile to furnish cyclic scaffolds (Scheme 1.1).

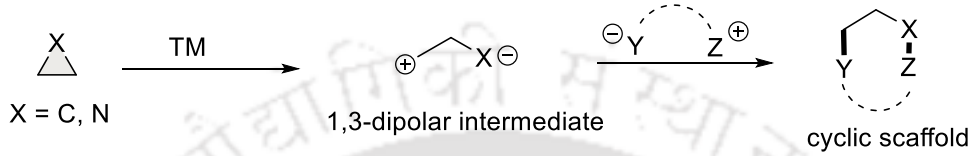

Scheme 1.1. Ring-opening/Annulation Strategy using Three-membered Rings

1.4 Classification and Reactivity of Vinylcyclopropanes

VCPs can be classified into two categories based on their substitutions: (i) activated or donor-acceptor (DA) VCPs which contain a vinyl group that acts as an electron-donating group and

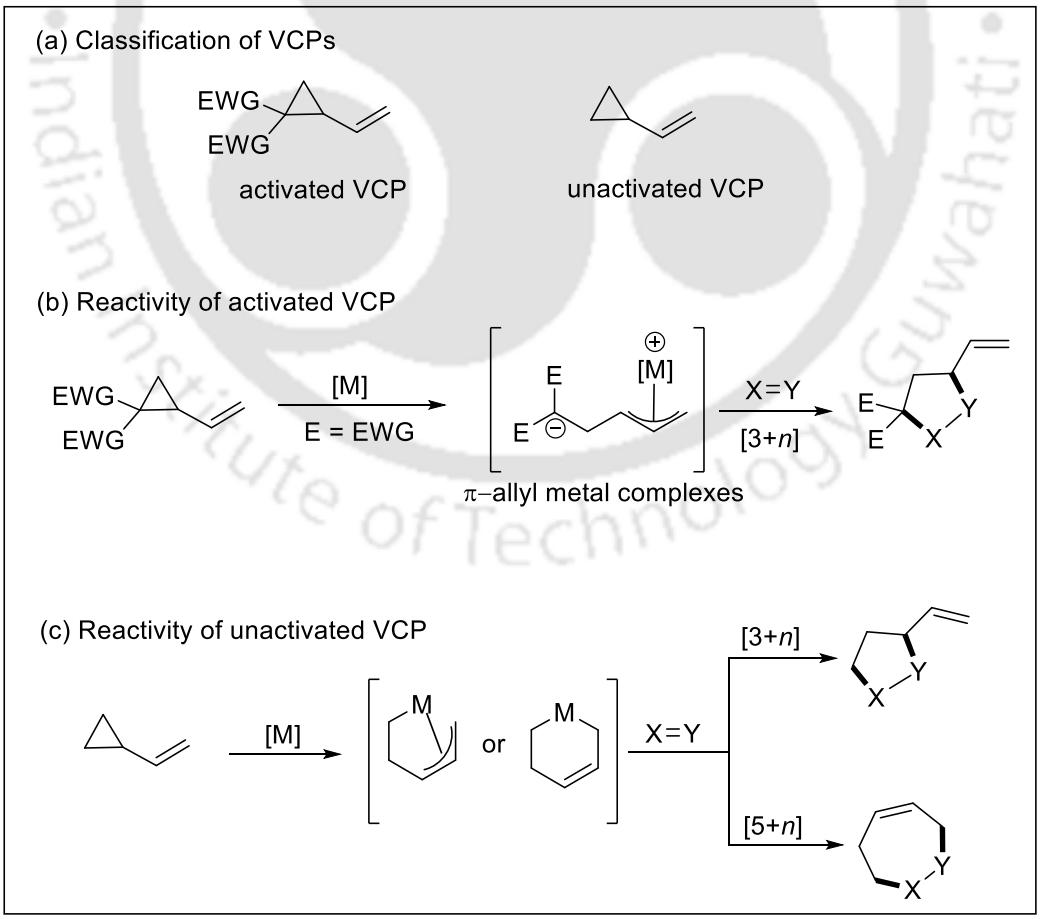

Figure 1.4. Classification and General Reactivity of VCP

a geminal electron-withdrawing group, while, (ii) unactivated VCPs, lacks the EWGs (Figure 1.4a).[8] Considering the general reactivity of activated VCPs, vinylic C=C bonds effectively assist transition-metal for the selective C−C bond cleavage. Additionally, the innate strain energy (28 kcal/mol approx.) and EWGs facilitate energetically favourable ring opening and formation of active π-allyl-metal complexes. Such, π-allyl metal complexes act as 1,3- or 1,5-dipole that serve as three carbon or 5-carbon synthon. Consequently, combination of such synthons with various unsaturated acceptors can lead to the [3+*n*] or [5+*n*] -annulation reactions (Figure 1.4b). However, in the presence of a metal catalyst, unactivated VCPs undergo oxidative addition to form a metallacycle, which can act as three or five-carbon synthon for subsequent annulation with dipolarophiles (Figure 1.4c). Notably, activated VCP generally prefers [3+*n*]-annulation over [5+*n*]-annulation, while non-activated VCP follows the vice-versa reactivity depending on the orientation of dipolarophiles.

1.4.1 Synthesis of Carbo- and Heterocycles using VCP

1.4.1.1 [3+2]-Annulation Reactions

Trost and co-workers developed [3+2]-annulation of Meldrum's acid-substituted VCP and alkylidenes to yield bis-spirocyclopantane derivatives (Scheme 1.2).[9] The methodology showed well compatibility to various functional groups to produce spiro-cyclopentanes. The catalytic pocket of Pd-phosphines exhibited excellent regioselectivity to furnish the spiro-annulated cyclopropane with good yield and diastereoselectivity.

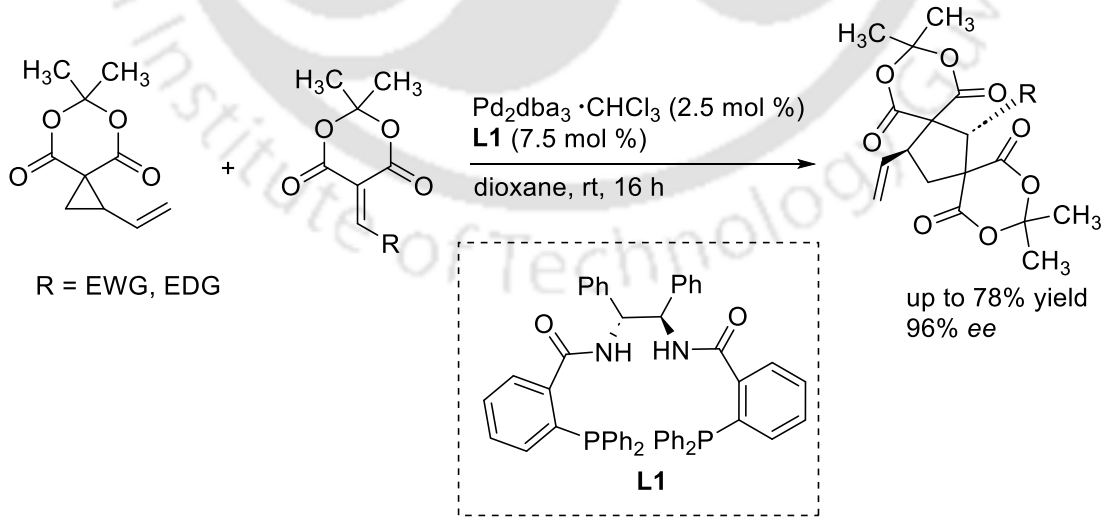

Scheme 1.2. Pd-Catalyzed [3+2]-Annulation of VCP with Azalactone Alkylidenes

They extended the scope of the protocol by reacting of azlactone alkylidenes with VCP to yield mono-spiro cyclopentanes under Pd/phosphine catalysis (Scheme 1.3).[9]

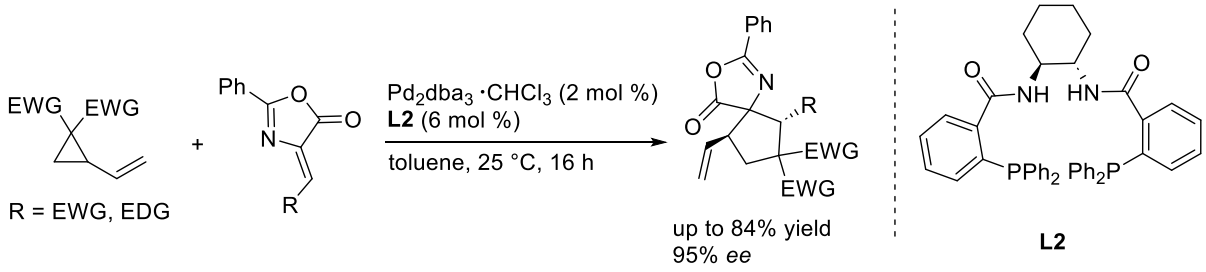

Scheme 1.3. Pd-Catalyzed [3+2]-Annulation of VCP with Alkylidenes

Plietker and co-workers demonstrated Fe/NHC-catalyzed [3+2]-annulation of activated VCPs with imines to synthesize pyrrole (Scheme 1.4).[10] The protocol showed well tolerance to a wide range of functional groups to yield pyrrole derivatives.

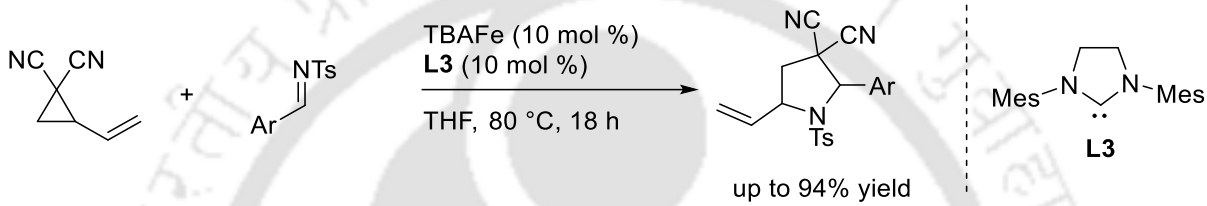

Scheme 1.4. Fe/NHC-Catalyzed [3+2]-Annulation of VCP with Imine

Ni-catalyzed [3+2]-annulation of activated VCPs with imines afforded tetrahydro pyrroles (Scheme 1.5).[11] Use of Ni-catalyst found to be excellent for harnessing chemoselective *cis*-pyrroles as major isomer. In addition, the synthetic method showed well compatibility to various functional groups installed imines to deliver the substituted pyrrole derivatives in high yields.

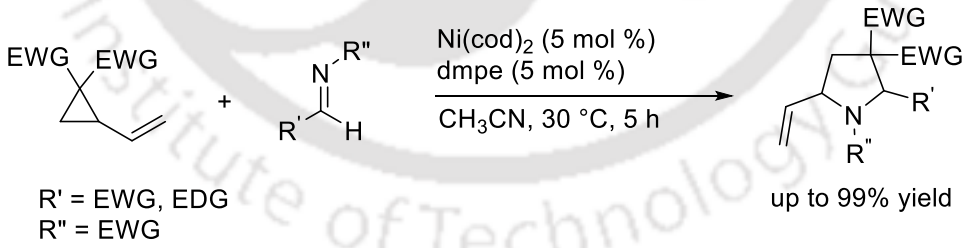

Scheme 1.5. Ni-Catalyzed [3+2]-Annulation of VCP with Imine

Vitale and co-workers synthesize 2,3-fused cyclopentannulated indolines by employing VCP and 3-nitroindoles under Pd-catalysis at room temperature (Scheme 1.6).[12] The protocol furnished the *cis*-fused indolines as major isomer with high yield *via* [3+2]-annulation pathway.

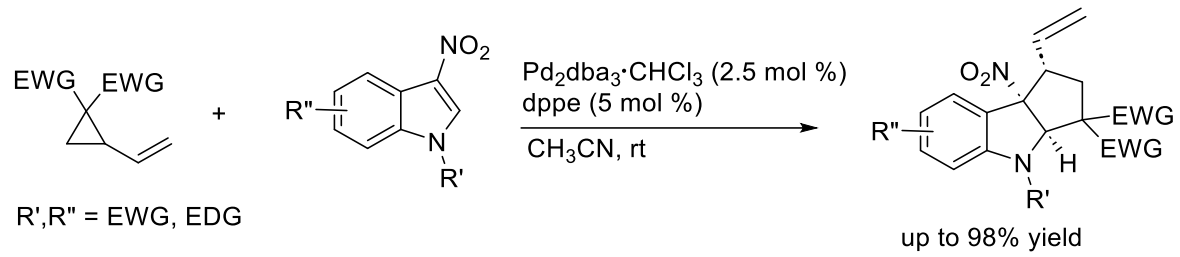

Scheme 1.6. Pd-Catalyzed [3+2]-Annulation of VCP and 3-Nitroindole

Yu and coworkers reported an elusive asymmetric synthesis of bicyclo[3.3.0] compounds using unactivated VCPs under Rh-catalysis (Scheme 1.7).[13] The protocol exhibited good compatibility to diverse functional groups to produce bicyclo compounds in high yield and enantiomeric excess. The reaction proceeds *via* oxidative addition and intramolecular [3+2]-annulation. Moreover, the substituents in alkyl part and the rigid phosphine ligand core played vital role to control the enantioselective outcome.

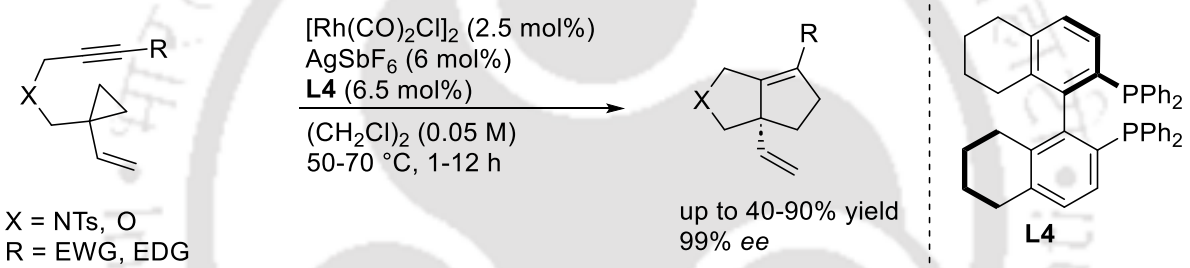

Scheme 1.7. Rh-Catalyzed [3+2]-Annulation of VCP

1.4.1.2 [3+4]-Annulation Reactions

Very recently, a streamline approach for the synthesis of benzoepoxyazepines utilizing VCP and anthranil has been realized (Scheme 1.8).[14] The methodology followed a dearomatized [3+4]-annulation path to produce various benzoepoxyazepine derivatives. Further, borane pays the vital role for activation of anthranil, resulting in formation of borane–anthranil complex.

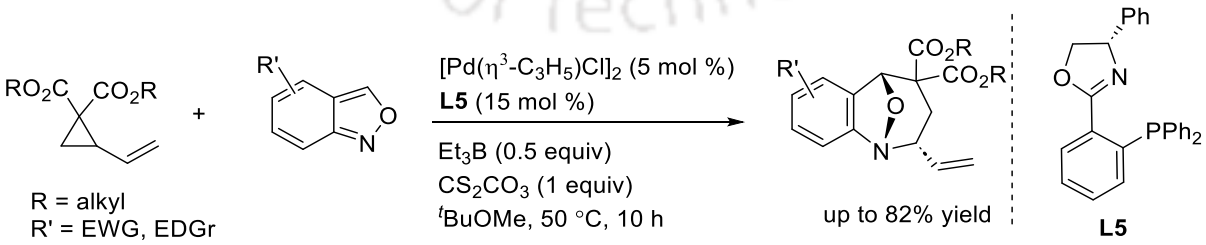

Scheme 1.8. Pd-Catalyzed Dearomatized [3+4]-Annulation of VCP and Anthranil

1.4.1.3 [5+2]-Annulation Reactions

Anderson and co-workers showed Rh-catalyzed synthesis of seven-membered fused tetrahydro pyrrole or [5.3.0]-azabicycles utilizing VCP (Scheme 1.9).[15] Under Rh-catalysis, VCP undergoes a diastereoselective intramolecular [5+2]-cycloisomerization that lead to formation of fused seven-membered cycloadduct. In addition, asymmetric catalysis using Rh/phosphoramidite produced the product in high enantiomeric excess. Further, DFT-study revealed the mechanistic route in a unique fashion.

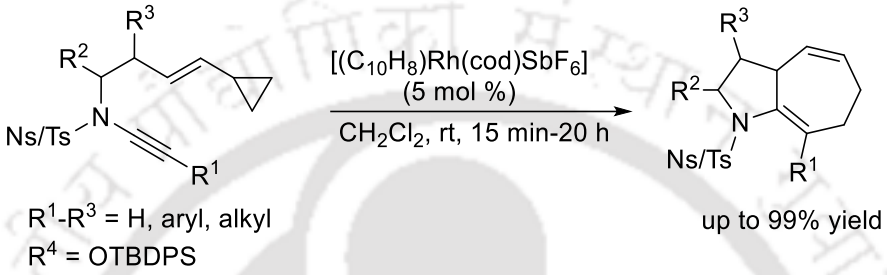

Scheme 1.9. Rh-Catalyzed [5+2]-Cycloisomerization of Ynamide VCP

1.4.1.4 [5+4]-Annulation Reactions

Archambeau and co-workers developed an exquisite Pd-catalyzed [5+4]-annulation by employing VCP with benzofuran-azadienes (Scheme 1.10).[16] The protocol leads to formation of benzofuran-azonanes. The Pd/phenanthroline catalysis enforces the VCP to act as 1,5-synthon *via* formation of 1,5-π-allyl zwitterion that furnished the nine-membered cycloadduct in a [5+4]-annulation pathway. Additionally, extension of the reaction conditions with linear 1-azadienes afforded the tetrahydro-azonines with excess isomeric ratio and good yields.

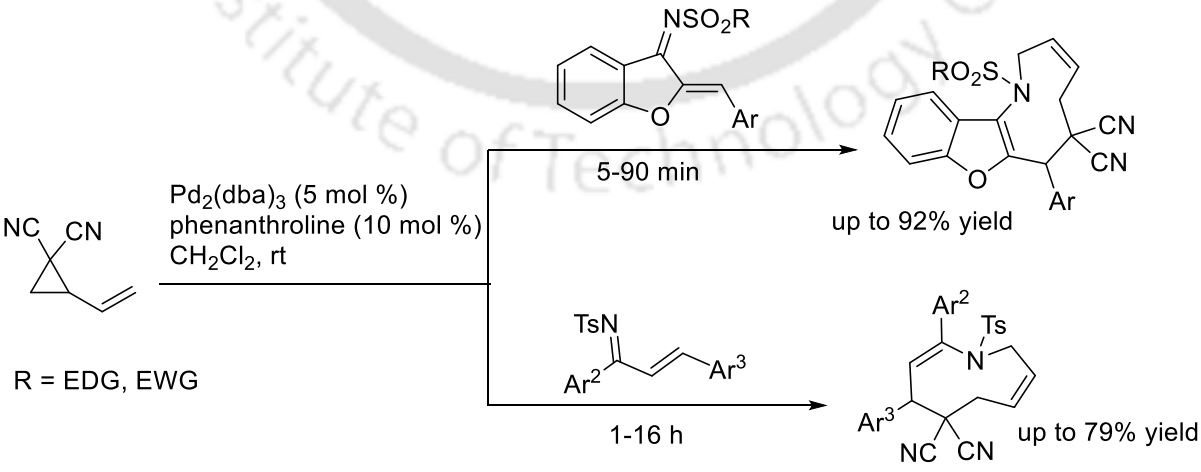

Scheme 1.10. Pd-Catalyzed [5+4]-Annulation of VCP with Benzofuran-azadienes

1.5 Classification and Reactivity of Aziridines

Aziridine, the smallest saturated azaheterocycle has gained surge attention as a nitrogen bearing synthon that can convey to [3+*n*]-annulation or cycloaddition reactions. This enables aziridine to be use in synthesis of plethora of ubiquitous heterocyclic molecular scaffolds. Aziridine can be classified in two types (i) activated aziridine and (ii) unactivated aziridine (Figure 1.5a). Under transition-metal-catalysis, activated aziridines undergo heterolytic C−N cleavage to furnish nitrogen bearing 1,3-zwitterionic intermediate that could afford [3+*n*]-annulation with coupling partners *via* ring opening/cyclization or tandem C-N/C-C bond formation (Figure 1.5b).[18] Whereas, reaction of unactivated aziridines proceeds *via* formation of azomethine ylide intermediate in presence of nucleophile and metal catalysis (Figure 1.5c). [17]

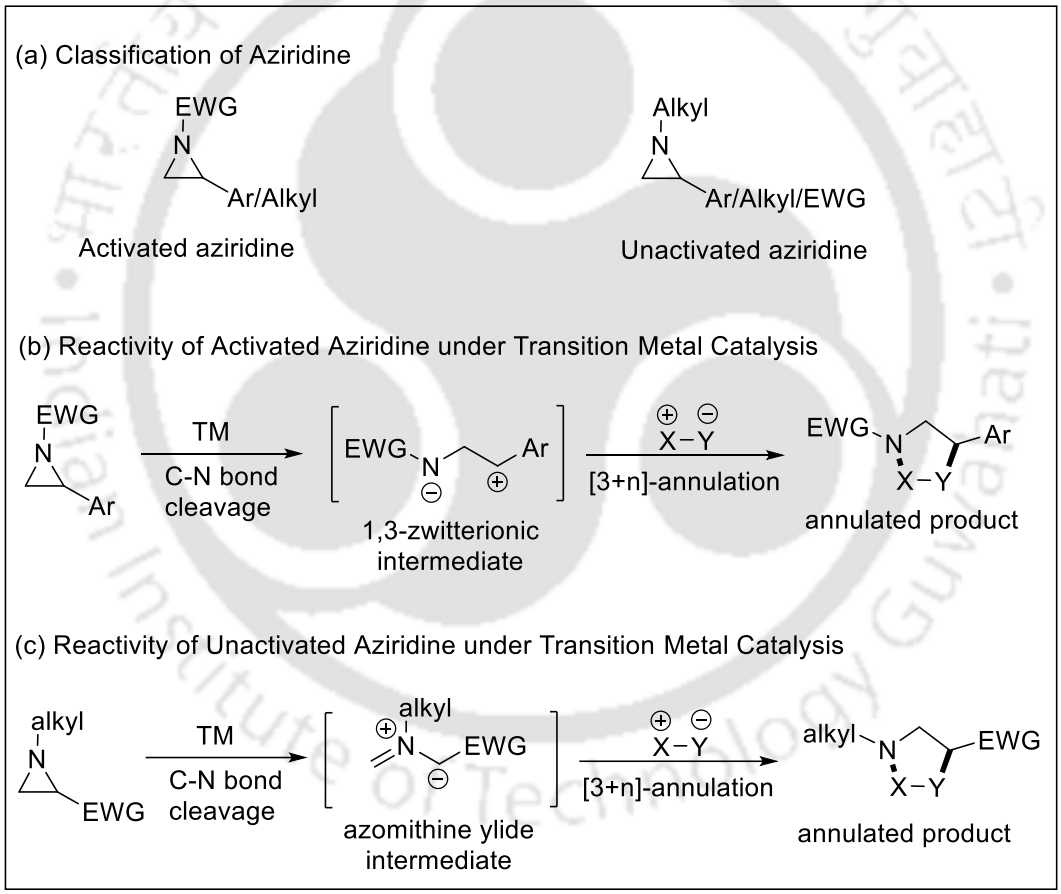

Figure 1.5. General Reactivity of Aziridine under Transition Metal Catalysis

1.5.1 Synthesis of Heterocycles using Aziridines

1.5.1.1 [3+2]-Annulation Reactions

Strand and co-workers developed a regioselective approach for [3+2]-annulation of aziridines with alkynes at room temperature under silver catalysis (Scheme 1.11).[19] The reaction resulted

in formation of 2,3-dihydropyrroles with excellent regioselectivity. A wide range of internal and terminal alkynes showed well tolerance to furnish the coupled products in good yields.

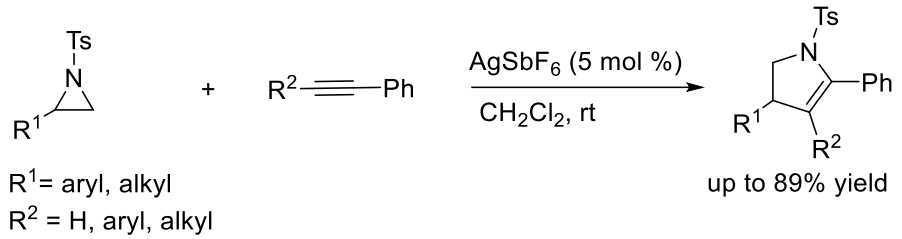

Scheme 1.11. Ag-Catalyzed [3+2]-Annulation of Aziridines with Alkynes

Our group accomplished a Fe-catalyzed [3+2]-annulation of N-alkylaziridines with heterocumulenes (Scheme 1.12).[20] The reaction furnished functionalized iminoazo-selenolidine derivatives in a sustainable approach using water as solvent. Various functional group tolerance, use of inexpensive iron catalyst and green solvent are the main practical features.

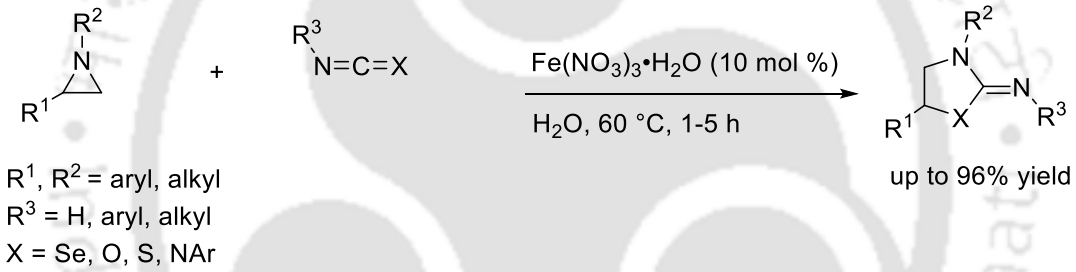

Scheme 1.12. Fe-Catalyzed [3+2]-Annulation of *N*-Alkylaziridines with Heterocumulenes

Murakami and co-workers described a Cu/bipyridine-catalyzed [3+2]-annulation of aziridine and diazetidine to synthesize imidazolidine (Scheme 1.13).[21] The reaction involves annulation of aziridines with *in situ* generated imines involving a stereospecific ring-opening pathway.

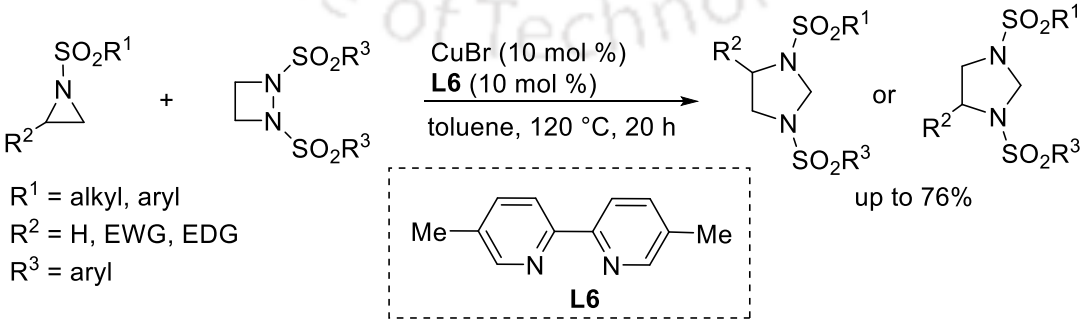

Scheme 1.13. Cu/Bipyridine-Catalyzed [3+2]-Annulation of Aziridines and Diazetidines

1.5.1.2 [3+3]-Annulation Reactions

Wang group demonstrated a [3+3]-annulation of aziridines with hydrazones under Cu-catalysis to synthesize functionalized tetrahydrotriazine derivatives (Scheme 1.14).[22] The presence of air is crucial to forward the reaction. Moreover, the reaction is found to furnish the cycloadduct *via* formation of *β*-hydrazinylamin intermediate.

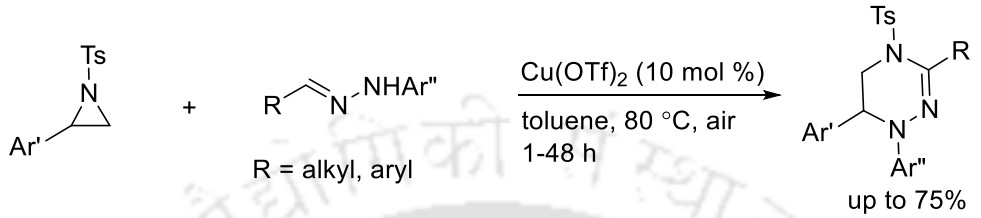

Scheme 1.14. Cu-Catalyzed [3+3]-Annulation of Aziridines and Hydrazones

Our group accomplished a Cu-catalyzed annulation cycloisomerization of aziridines with propargylamines *via* [3+3]-annulation (Scheme 1.15).[23] This strategy offered formation of piperazines *via* a stereospecific ring opening/annulation of aziridine followed by a base assisted hydroamination process. The methodology was extended to accomplish piperazine derivatives in high enantiomeric excess by using enantiopure aziridines.

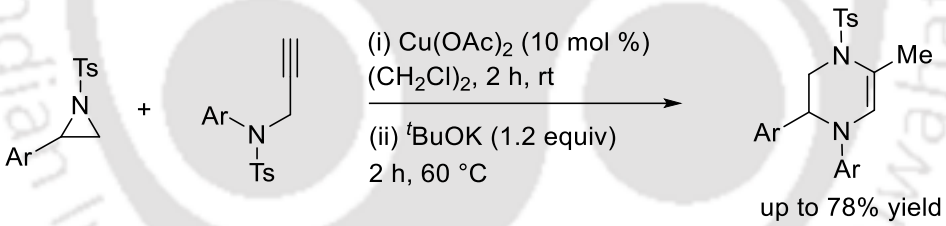

Scheme 1.15. Cu-Catalyzed Ring-opening and Cycloisomerization of Aziridines and Propargylamines

Zhao and co-workers described synthesis of tetrahydropyrimidines *via* [3+3]-annulation of aziridines and iso-cyanoacetates using phosphine-copper complex (Scheme 1.16).[24] The protocol was amenable to pursue stereoselective tetrahydropyrimidines from chiral aziridines with high enantiomeric excess. Moreover, the post-synthetic transformation of the cycloadduct to valuable amino alcohol derivatives describes the synthetic importance.

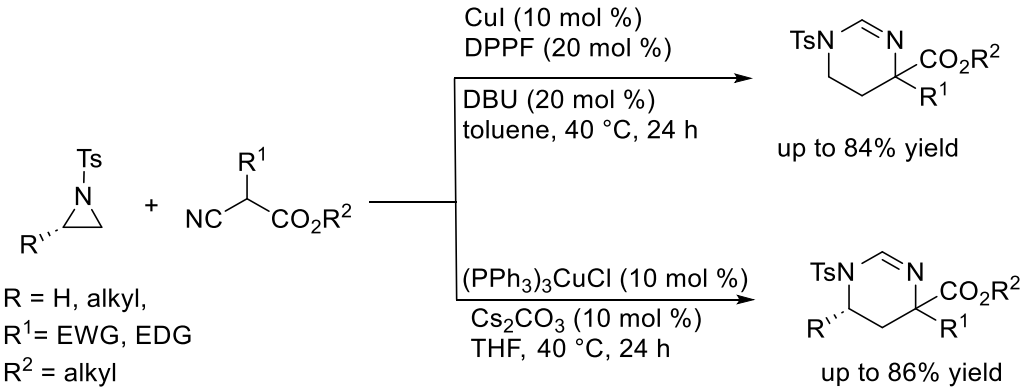

Scheme 1.16. Cu/Phosphine-Catalyzed [3+4]-Annulation of Aziridines and *Iso*-cyanoacetates

1.5.1.3 [3+4]-Annulation Reactions

Shi and co-workers showcased [3+4]-annulation using vinyl aziridines and *p*-quinone methides under Ir-catalysis to accomplish synthetically important benzoxazepines (Scheme 1.17).[25] The synthetic methodology elaborated using chiral-phosphine/palladium catalysis to yield benzoxazepines in high enantiomeric excess.

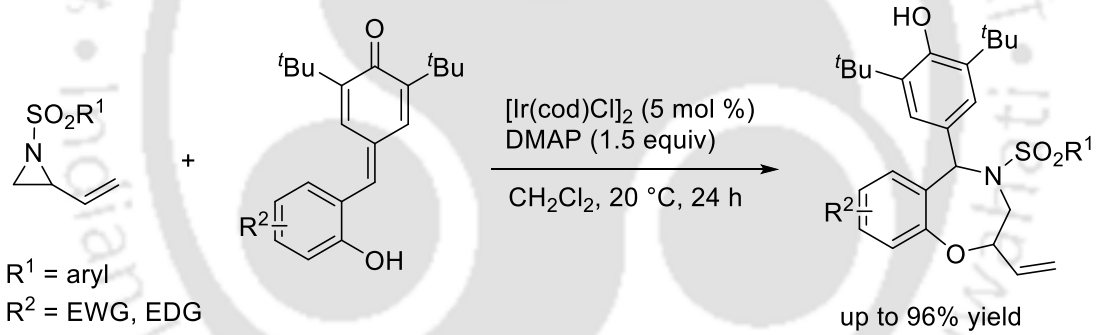

Scheme 1.17. Ir-Catalyzed [3+4]-Annulation of Vinyl Aziridines and *p*-Quinone Methides

Recently, our group discovered facile approach of Cu-catalyzed [3+4]-annulation of aziridines and indoles (Scheme 1.18). The reaction showed well tolerance to various functional groups to deliver azepinoindoles in good yield and diastereoselectivity. An asymmetric approach of the protocol in presence of Cu/(*R*)-BINAP successfully resulted in azepinoindole derivatives with high enantiomeric excess.

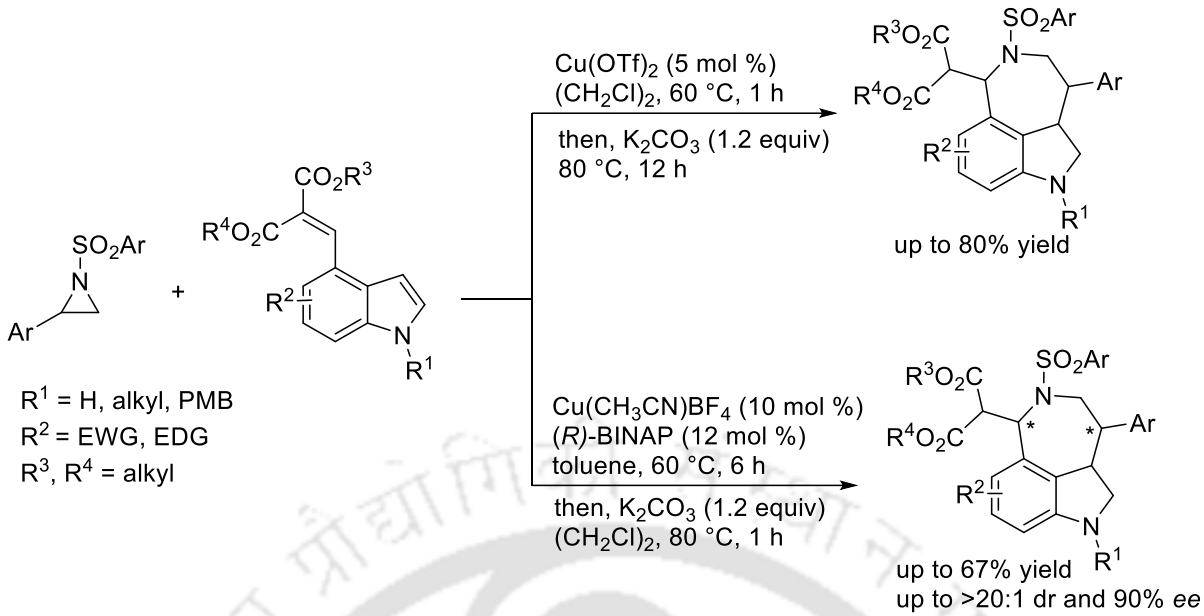

Scheme 1.18. Cu-Catalyzed [3+4]-Annulation of Aziridines and Indoles

1.6 Reactivity of Cyclopropenones

Cyclopropenone are the resonance stabilized smallest ring that follow Hückle's rule of aromaticity.[27] In recent times, cyclopropenone received remarkable attention as a coupling partner for construction of carbo or heterocyclic frameworks. In presence of metal, the three membered ring can undergo C−C bond cleavage through two modes (i) 1,2-nucleophilic addition followed by a β-carbon elimination and (ii) oxidative addition of metal to C−C=O bond (Figure 1.6).[28] This enables cyclopropenone to serve as crucial three-carbon synthon for annulation reactions.

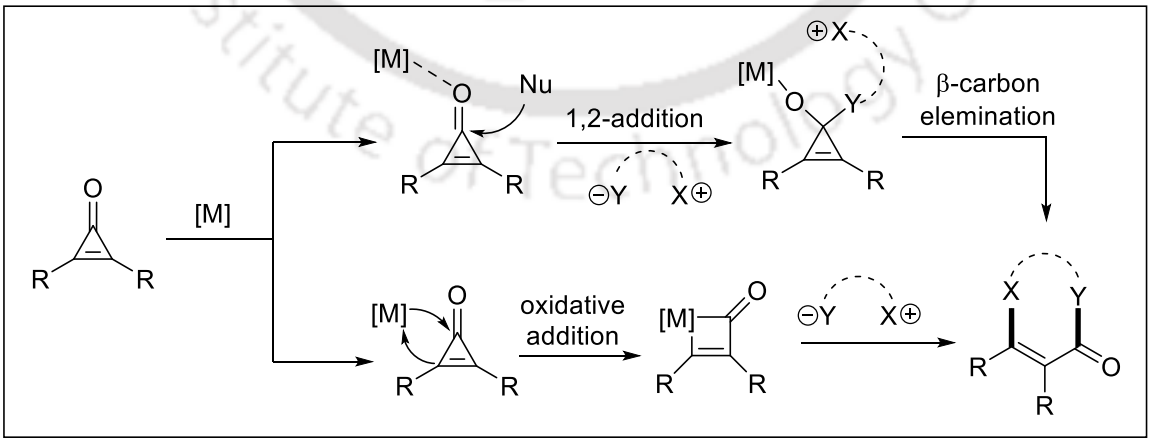

Figure 1.6. Reactivity of Cyclopropenone

1.6.1 Synthesis of Carbo- and Heterocycles using Cyclopropenones

1.6.1.1 1,2-Addition/ β-Carbon Elimination Reactions

Sakurai and co-workers developed Au-catalyzed spiroannulation of cyclopropenones with enyne (Scheme 1.19).[29] The strategy provides a fascinating path for the construction of synthetically important spiro[4.4]octane skeletons. Further, the residual water served as the source of alcohol group.

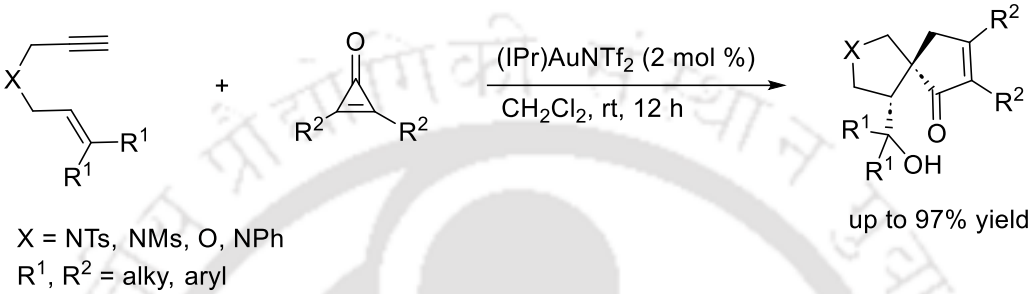

Scheme 1.19. Au-Catalyzed Spiroannulation of Cyclopropenones with Enynes

Sun and co-workers discovered Ag-catalyzed [3+2]-annulation of cyclopropenones and formamides (Scheme 1.20).[30] The reaction serve as an eminent strategy involving a 1,2-addition followed by a *β*-carbon elimination path to deliver *γ*-aminobutenolides. In addition, the method exhibited excellent regio and chemo selectivity to deliver the final product in high yield.

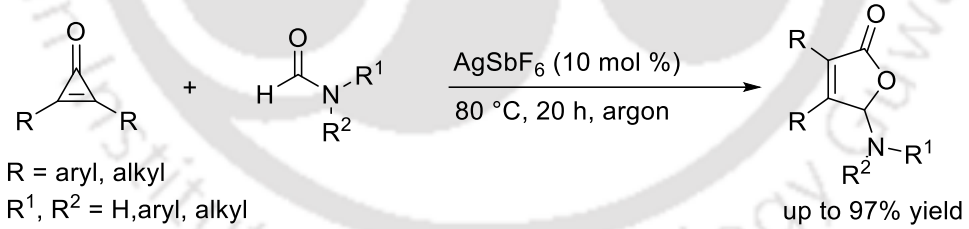

Scheme 1.20. Ag-catalyzed [3+2]-Annulation of Cyclopropenones and Formamides

Wu research group accomplished Ag-promoted ring-opening/annulation of cyclopropenones with oximes (Scheme 1.21).[31] The reaction resulted in formation of ubiquitous 1,3-oxazinone derivatives in moderate to high yields with well functional group tolerance. Considering the reactivity, the strategy involves ring opening *via* β-carbon elimination along with *in situ* generated ketene intermediate to accomplish the annulated product.

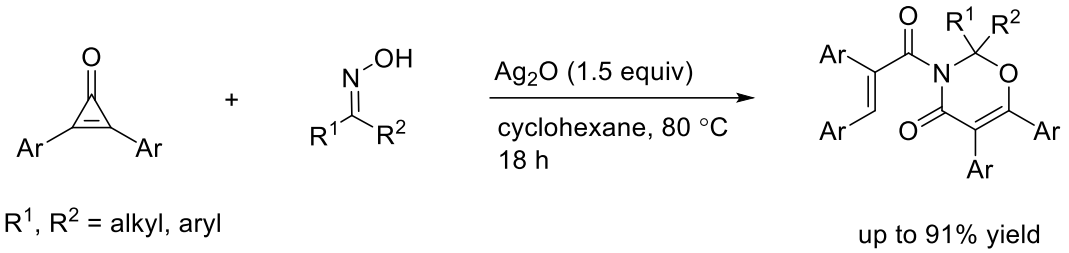

Scheme 1.21. Ag_2O-Promoted Ring-opening/annulation of Cyclopropenones with Oximes

1.6.1.2 Oxidative Addition Reactions

Williams and co-workers developed Rh-catalyzed [3+2]-annulation of cyclopropenones and alkynes to synthesize cyclopentadienone (Scheme 1.22).[32] The reaction tiggered *via* oxidative addition of cyclopropenone, which on regioselective co-ordination with alkyne delivered the target annulated product.

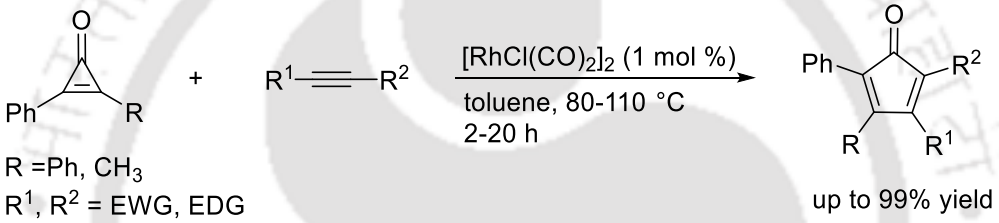

Scheme 1.22. Rh-Catalyzed [3+2]-Annulation of Cyclopropenones and Alkynes

Xu and co-workers demonstrated Pd-catalyzed a (3+2)-asymmetric spiroannulation of cyclopropenones and cyclic 1,3-diketones at room temperature to construct oxaspiro adducts (Scheme 1.23).[33] The protocol proceeds *via* C−C bond activation and desymmetrization to furnish the spiro adducts. Further, the catalytic cavity provided by the ligand **L4** found to be vital to achieve enantiomeric excess and diastereoselectivity.

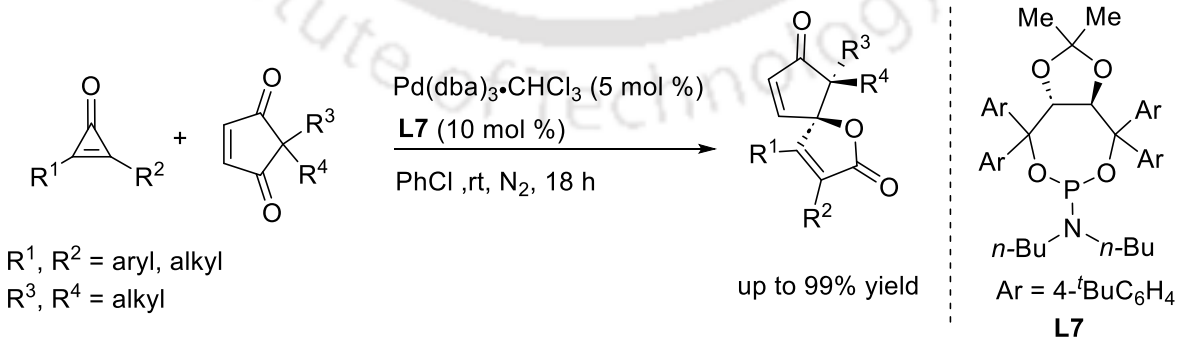

Scheme 1.23. Pd-Catalyzed (3+2)-Asymmetric Spiroannulation of Cyclopropenones and Cyclic 1,3-Diketones

Zhao group reported synthesis of dihydropyridones by employing cyclopropenones and aziridines under Pd-catalysis (Scheme 1.24).[34] The role of CuBr found to be crucial in activating the aziridine ring. In addition, reaction with optically pure aziridine confirms the annulation reaction proceeds *via* S_N2 pathway.

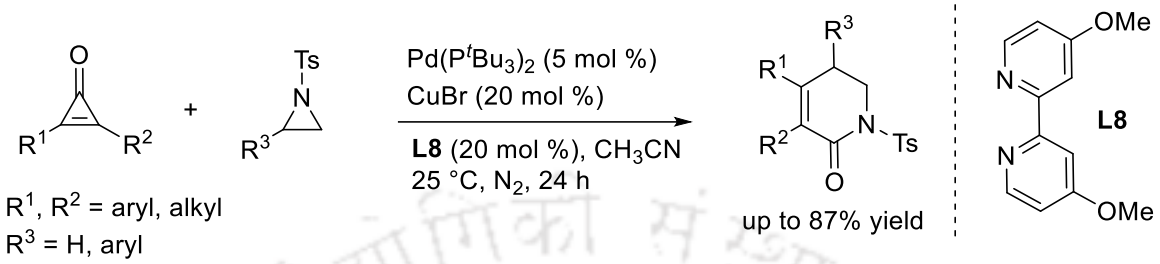

Scheme 1.24. Pd-Catalyzed [3+3]-Annulation of Cyclopropenones and Aziridines

1.7 Objectives of the Thesis

The above literature studies elaborate, the use of strained rings for synthesis of complex molecular architecture *via* more facile and atom economical approach. However, these studies also shed light on the following domains for further research objectives.

- Spirocyclic compounds are very fascinating because of the ring constrains and rigid cyclic core. Considering the reactivity of VCPs, spirovinylcyclopropanes can be used as a pivotal precursor of synthesis of challenging spirocyclic motifs in step- and atom-economic approach.
- Studies towards synthesis of heterocycles using aziridines are focused on using expensive transition metals. However, methods using inexpensive and Earth abundant metal catalyst would be more valuable in synthetic point of view.
- In recent years, C−H activation reactions are surfaced as a robust strategy for fabricating plethora of complex molecular frameworks. Thus, merging C−H activation and annulation strategy employing strained rings can lead to new avenues for synthesis of vital and complex molecules in more facile pathway.

1.8 References

1. Baeyer, A. von. *Ber. Dtsch. Chem. Ges*. **1900**, *33*, 3771.
2. Ding, A.; Meazza, M.; Guo, H.; Yang, J. W.; Rios, R. *Chem. Soc. Rev*. **2018**, *47*, 5946.
3. (a) Smith, L. K.; Baxendale, I. R. *Org. Biomol. Chem*. **2015**, *13*, 9907. (b) Mardjan, M. I. D.; Mayooufi, A.; Parrain, J.-L.; Thibonnet, J.; Commeiras, L. *Org. Process Res. Dev*. **2020**, *24*, 606. (c) Gilles, L.; Antoniotti, S. *Chem Plus Chem*. **2022**, *87*, e202200227.
4. Joule, J. A; Mills, K. Heterocyclic Chemistry. Fifth Edition, **2010**, ISBN: 978-1-405-13300-5.
5. Taylor, R. D.; MacCoss, M.; Lawson, A. D. G. *J. Med. Chem*. **2014**, *57*, 5845.
6. (a) Vitaku, E.; Smith, D. T.; Njardarson, J. T. J. Med. Chem. 2014, 57, 10257. (b) Heravi, M. M.; Zadsirjan, V. *RSC Adv*. **2020**, *10*, 44247.
7. (a) Carson, C. A.; Kerr, M. A. *Chem. Soc. Rev*. **2009**, *38*, 3051. (b) He, Z.; Zajdlik, A.; Yudin, A. K. *Acc. Chem. Res*. **2014**, *47*, 1029. (c) Cavitt, M. A.; Phuna, L. H.; France, S. *Chem. Soc. Rev*. **2014**, *43*, 804. (d) Schneider, T. F.; Kaschel, J.; Werz, D. B. *Angew. Chem., Int. Ed*. **2014**, *53*, 5504. (e) Xia, Y.; Liu, Xi.; Feng, X. *Angew. Chem., Int. Ed*. **2021**, *60*, 9192. (f) Wang, J.; Blaszczyk, S. A.; Li, X.; Tang, W. *Chem. Rev*. **2021**, *121*, 110. (g) Wang, H.-H.; Wang, X.-D.; Yin, G.-F.; Zeng, Y.-F.; Chen, J.; Wang, Z. *ACS Catal*. **2022**, *12*, 2330.
8. Wang, J.-H.; Blaszczyk, S. A.; Li, X.-X.; Tang, W.-P. *Chem. Rev*. **2021**, *121*, 110.
9. Trost, B. M.; Morris, P. J.; Sprague, S. J. *J. Am. Chem. Soc*. **2012**, *134*, 17823.
10. Dieskau, A. P.; Holzwarth, M. S.; Plietker, B. *J. Am. Chem. Soc*. **2012**, *134*, 5048.
11. Tombe, R.; Kurahashi, T.; Matsubara, S. *Org. Lett*. **2013**, *15*, 1791.
12. Laugeois, M.; Ling, J.; Férard, C.; Michelet, V.; Ratovelomanana-Vidal, V.; Vitale, M. R. *Org. Lett*. **2017**, *19*, 2266.
13. Lin, M.; Kang, G. Y.; Guo, Y. A.; Yu, Z. X. *J. Am. Chem. Soc*. **2012**, *134*, 398.
14. Cheng, Q.; Xie, J.-H.; Weng, Y.-C.; You, S.-L. *Angew. Chem., Int. Ed.* **2019**, *58*, 5739.
15. Straker, R. N.; Peng, Q.; Mekareeya, A.; Paton, R. S.; Anderson, E. A. *Nat. Commun*. **2016**, *7*, 10109.
16. Scuiller, A.; Karnat, A.; Casaretto, N.; Archambeau, A. *Org. Lett*. **2021**, *23*, 2332.
17. Dauban, P.; Malik, G. *Angew. Chem., Int. Ed*. **2009**, *48*, 9026.
18. (a) Huang, C.-Y.; Doyle, A. G. *Chem. Rev*. **2014**, *114*, 8153. (b) Feng, J.-J.; Zhang, J. *ACS Catal*. **2016**, *6*, 6651.
19. Wender, P. A.; Strand, D. *J. Am. Chem. Soc*. **2009**, *131*, 7528.

20. Sengoden, M.; Punniyamurthy, T. *Angew. Chem. Int. Ed*. **2013**, *52*, 572.
21. Higuchi, D.; Matsubara, S.; Kadowaki, H.; Tanaka, D; Murakami, K. *Chem.-Eur. J.* **2023**, *29*, e202301071.
22. Hong, D.; Lin, X.; Zhu, Y.; Lei, M.; Wang, Y. *Org. Lett*. **2009**, *11*, 5678.
23. Das, B. K.; Pradhan, S.; Punniyamurthy, T. *Org. Lett*. **2018**, *20*, 4444.
24. Kok, G. P. Y.; Yang, H.; Wong, M. W.; Zhao, Y. *Org. Lett.* **2018**, *20*, 5112.
25. Jiang, F.; Yuan, F.-R.; Jin, L.-W.; Mei, G.-J.; Shi, F. *ACS Catal.* **2018**, *8*, 10234.
26. Kar, S.; Maharana, P. K.; Punniyamurthy, T.; Trivedi, V. *Org. Lett*. **2023**, *25*, 8850.
27. Wang, X.; Seidel, F. W.; Nozaki, K. *Angew. Chem. Int. Ed*. **2019**, *58*, 12955.
28. Luo, Y.; Shan, C.; Liu, S.; Zhang, T.; Zhu, L.; Zhong, K.; Bai, R.; Lan, Y. *ACS Catal.* **2019**, *9*, 10876.
29. Matsuda, T.; Sakurai, Y. *J. Org. Chem*. **2014**, *79*, 2739
30. Ren, J.-T.; Wang, J.-X.; Tian, H.; Xu, J.-L.; Hu, H.; Aslam, M.; Sun, M. *Org. Lett*. **2018**, *20*, 6636.
31. Yang, Y.-F.; Huang, X.-B.; Gao, W.-X.; Zhou, Y.-B.; Liu, M.-C.; Wu, H.-Y. *Org. Biomol. Chem*. **2020**, *18*, 5822.
32. Wender, P. A.; Paxton, T. J.; Williams, T. J. *J. Am. Chem. Soc*. **2006**, *128*, 14814.
33. Zhou, H.-Q.; Gu, X.-W.; Zhou, X.-H.; Li, L.; Ye, F.; Yin, G.-W.; Xu, Z.; Xu, L.-W. *Chem. Sci*. **2021**, *12*, 13737.
34. Li, R.; Li, B.; Zhang, H.; Ju, C.-W.; Qin, Y.; Xue, X.-S.; Zhao, D. *Nat. Chem*. **2021**, *13*, 1006.

Chapter II

[3+2]-Annulation of Spirovinylcyclopropyl Oxindoles with *p*-Quinone Methides

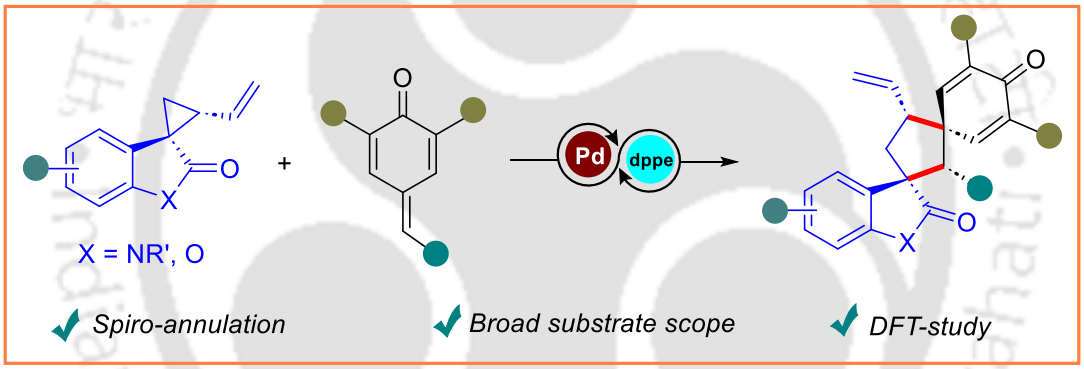

J. Org. Chem. **2023**, *88*, 9704

[3+2]-Annulation of Spirovinylcyclopropyl Oxindoles with *p*-Quinone Methides

The increasing emphasis on expanding structural diversity has sparked considerable scientific attention in recent decades, leading to the creation of synthetic strategies that explore new, uncharted chemical spaces.[1] In this vein, the synthesis of spiro-ring fused cyclic scaffolds have received surge attention in scientific fronts. Specifically, spirocyclic oxindoles have gained significant attention in modern drug discovery because of their three-dimensional structures, diverse architectures, and widespread presence in compounds with medicinal properties (Figure 2.1).[2] However, synthesizing these spirooxindole derivatives remains challenging and requires considerable effort and multistep synthetic approaches. Therefore, developing efficient methods to synthesize such scaffolds using easily available reactants become a topic of ongoing interest.[3] In this context, oxindole derived spirocyclopropanes, owing to their easy accessibility and tandem reactive behaviour received immense attention.[4-7] In addition, use of such spirocyclopropanes has reduced the multistep efforts involved for synthesis of complex spirooxindole derivatives. Under metal catalysis, these spirocyclopropanes can undergo ring cleavage and function as 1,3-dipolar species. Theses dipolar species upon reaction with dipolarophiles, produce diverse spirocyclic scaffolds.[8] Further, *p*-quinone methides (*p*- QM), known for its role as vital coupling partner for fabricating ubiquitous cyclic and spirocyclic scaffolds of natural and bio-relevant importance.[9] Considering the reactivity, the carbonyl group conjugated to the olefinic bond of *p*-QMs drives it behave as Michael acceptor *via* 1,6-addition reactions, thus allowing *p*-QM to electron deficient exocyclic olefin coupling partner to synthesize spirocyclic frameworks.[10-12] However, such reactivity of *p*-QM is limited to certain examples because of the more favourable aromatization of quinone core to phenol.[13] Thus, utilizing *p*-QM for fabrication of cyclic scaffolds *via* annulation strategy has become a demanding research topic. In this chapter, we report a [3+2]-annulation strategy by employing spirovinylcyclopropyl oxindoles (SVCP) with *p*-QMs under palladium-phosphine-catalysis to furnish multi spiro-centered functionalized bis-spirocyclopentane oxindole derivatives. Key aspects of this strategy include the use of mild reaction conditions, substrate scope, and the potential biological applications of the synthesized spiro-adduct.

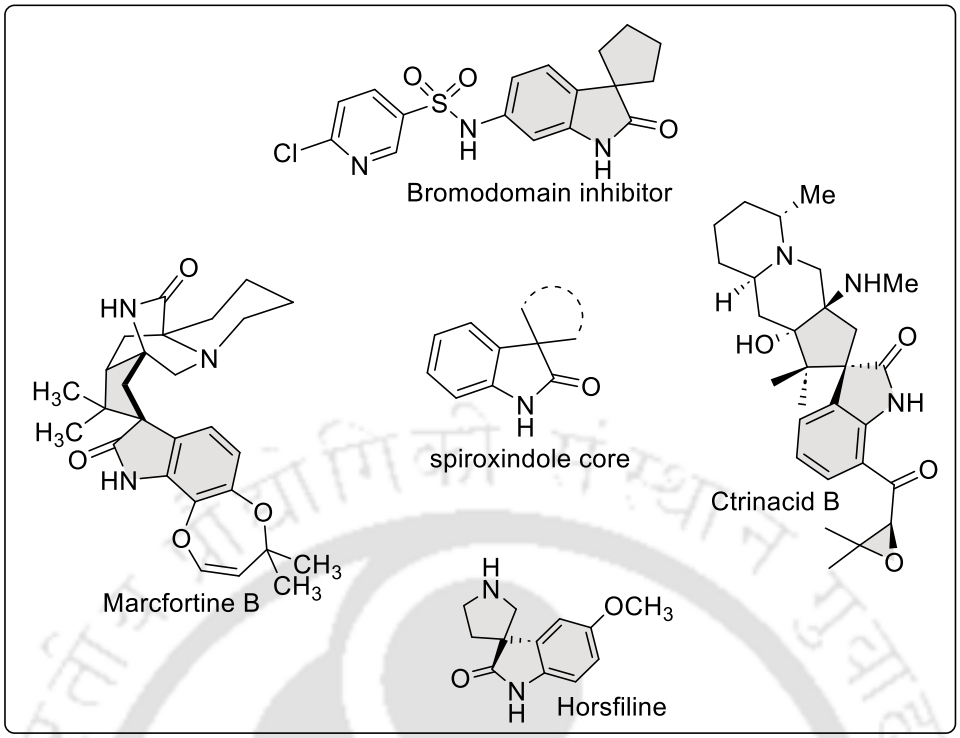

Figure 2.1. Selected Examples of Biorelevant Spirooxindole Scaffolds

2.1 Reactivity of Spirocyclopropyl Oxindoles

Carriera and co-workers rationalized synthesis of spiro[pyrrolidine-3,3′-oxindole] derivatives by reacting spirocyclopropyl-oxindole and aldimine under Mg-catalysis (Scheme 2.1).[4] The protocol was tolerated with diversely aldimines, to access functionalized spirotryptoisatins in high yields.

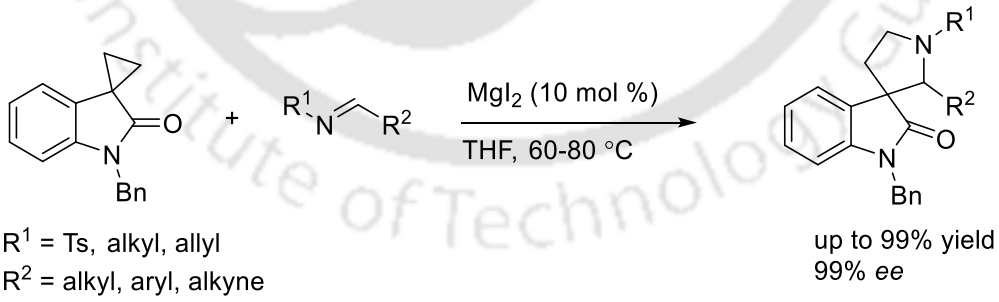

Scheme 2.1. Mg-Catalyzed [3+2]-Annulation of Spirocyclopropyl-oxindoles and Aldimines

Zhou and co-workers showcased enantioselective synthesis of spiro[tetrahydro oxazine-4,3'-oxindole] derivatives using spirocyclopropyl-oxindole and nitrones under Ni-bisoxazoline-catalysis (Scheme 2.2).[5] The methodology executed excellent stereoselectivity. Further, *N*-diethoxyphosphoryl exhibited a dual role for the activation of spirocyclopropyl oxindole.

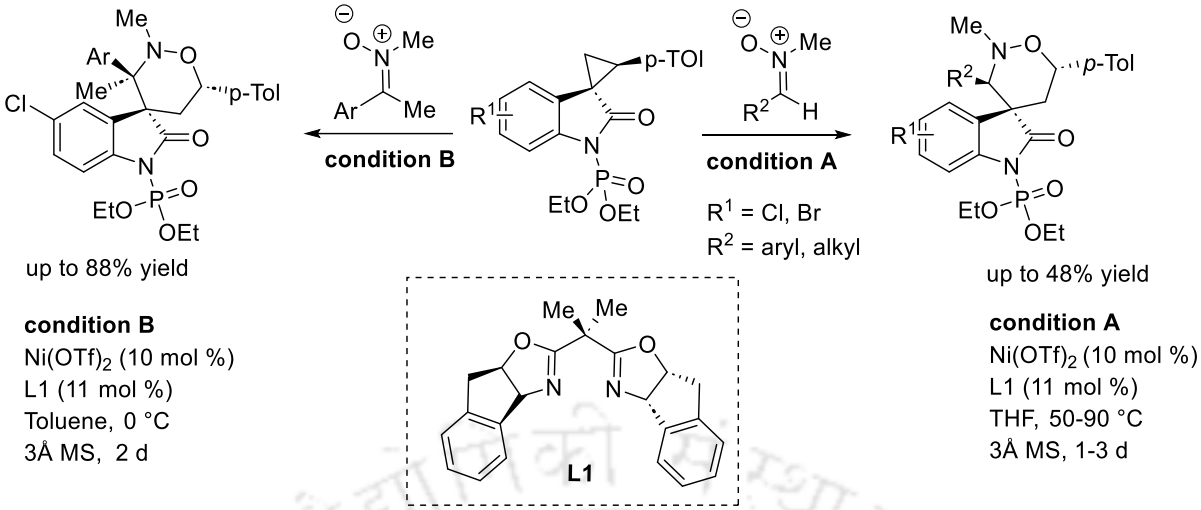

Scheme 2.2. Ni-Catalyzed [3+3]-Annulation of Spirocyclopropyl-oxindoles and Nitrones

Budynina research group illustrated synthesis of spiro[2-pyrrolidinone-5,3'-oxindole] frameworks using donor-acceptor spirocylopropyl oxindoles and amine under Ni-catalysis (Scheme 2.3).[6] The protocol involves a ring opening followed by ring closing pathway to afford the spiro adducts in moderate to good yields and diastereoseletivity.

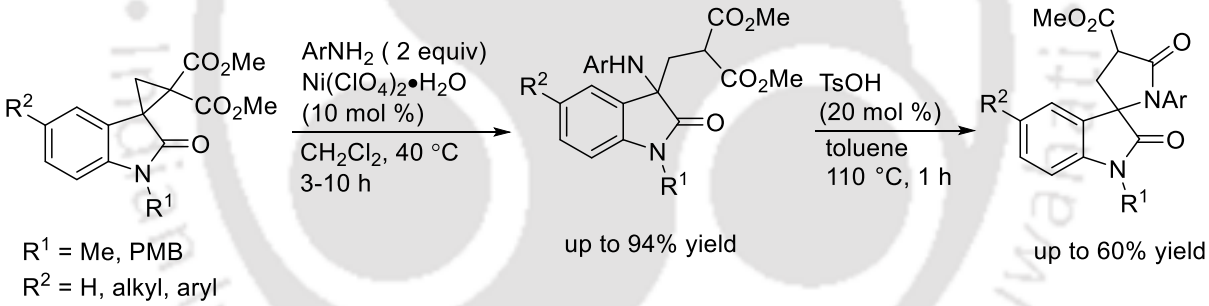

Scheme 2.3. Ni-Catalyzed Ring-opening/cyclization of Spirocyclopropyl-oxindoles and Amines

Du and co-workers depicted an excellent bimetallic asymmetric approach to access bio-relevant 3-spirocyclopentane-2-oxindoles utilizing spirovinylcylopropyl oxindoles and α, β-unsaturated 2-acyl imidazoles (Scheme 2.4).[7] The rhodium-complex exhibited the crucial role to achieve the target spiro-adduct in stereoselectively. Moreover, the synthetic strategy showed well compatibility with widely substituted cyclopropanes and amines.

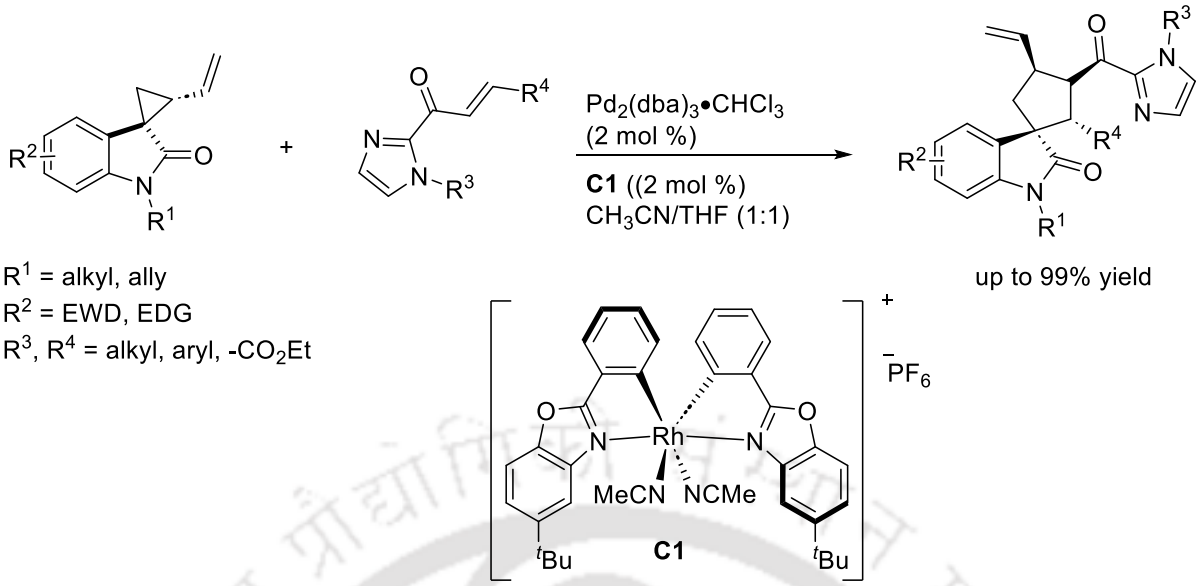

Scheme 2.4. Pd-Catalyzed [3+2]-Annulation of Spirovinylcyclopropyl-oxindoles.

2.2 Reactivity of *para*-Quinone Methides (*p*-QMs)

Synthesis of spiro[2.5]octa-4,7-dien-6-one scaffolds by reaction of *p*-QM and diethyl 2-bromomalonate under basic condition was demonstrated (Scheme 2.5).[10] The methodology procced *via* 1,6-conjugate addition of malonate to *p*-QM followed by an intramolecular dearomatization lead to formation of spiro-adduct. Further, the protocol was tolerated to *p*-QMs bearing various electron-donating and withdrawing functional groups.

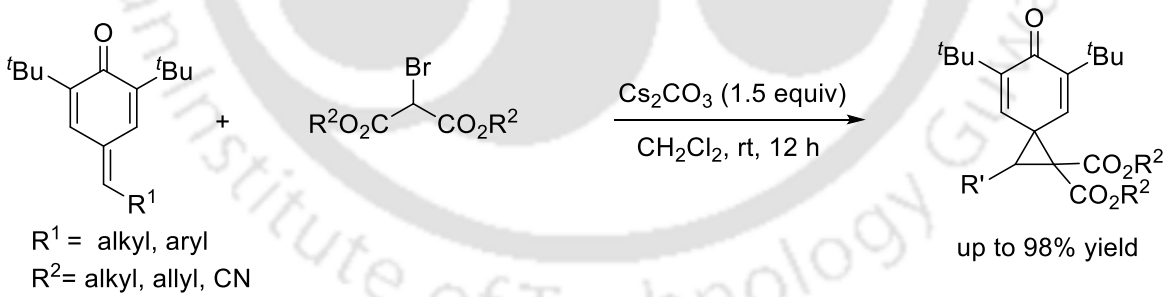

Scheme 2.5. Base-mediated 1,6-addition/cyclization of *p*-QMs 2-Bromomalonate

Lin group demonstrated Ag-catalyzed 1,6-addition/cyclization of *p*-QMs with propargyl malonates (Scheme 2.6).[11] The reaction accomplished a wide range of diverse substituents to synthesize spiro[4.5]deca-6,9-dien-8-one derivatives in high yields.

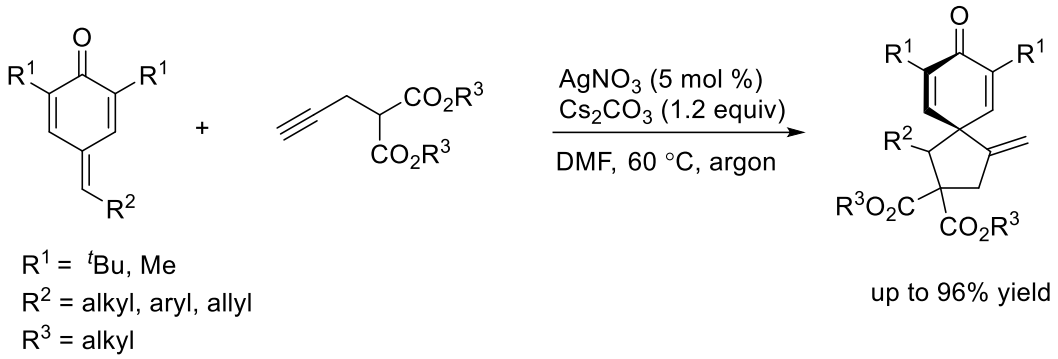

Scheme 2.6. Ag-Catalyzed 1,6-addition/cyclization of *p*-QMs with Propargyl Malonates

An elegant [4+2]-annulation strategy utilizing *p*-QM with sulfonyl allenols under Pd-catalysis was described to afford spiro[5.5]undeca-1,4-dien-3-one scaffolds (Scheme 2.7).[12] The reaction was initiated by 1,6-conjugate addition of in situ generated enolate ion from sulfonyl allenols. In addition, the protocol displays good functional group compatibility and stereoselectivity to produce the spiro adducts.

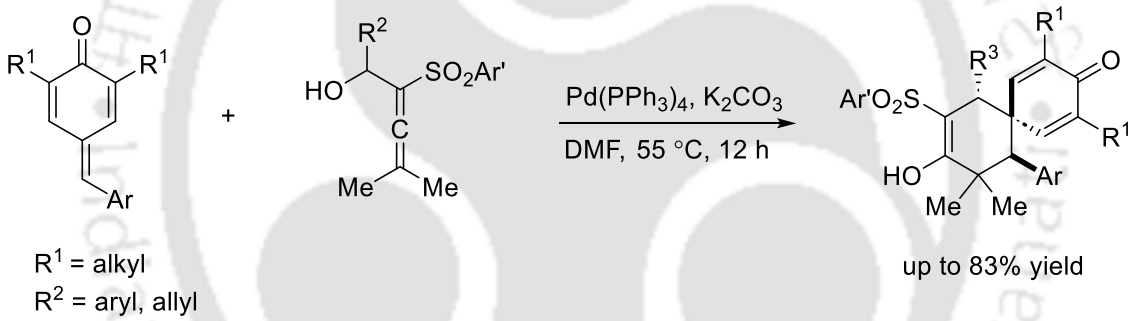

Scheme 2.7. Pd-Catalyzed [4+2]-Annulation of *p*-QMs with Sulfonyl Allenols

2.3 Present Study

We have here described a Pd/phosphine-catalyzed [3+2]-annulation of spirovinylcyclopropane oxindoles with *p*-QMs to produce spiro-centred 3-spirocyclopentane oxindole derivatives, providing opportunities to explore spiro-cyclization approaches. We begin the optimisation studies by reacting SVCP **1a** and *p*-QM **2a** as the model substrates in presence of various Pd-sources, ligands, additives and solvents (Table 2.1-2.4). To our delight, the cycloadduct **3aa** was obtained in 51% yield with a 1.2:1 mixture of diastereomers, when the substrates were stirred with 5 mol % $Pd(OAc)_2$ and 10 mol % 1,2-bis(diphenylphosphino)ethane (dppe) in CH_2Cl_2 at room temperature for 48 h. Screening of other Pd-salts, *viz*. $Pd(OAc)_2$, $PdCl_2$, $Pd(PPh_3)_2Cl_2$, $Pd_2(dba)_3$ and $Pd(PPh_3)_4$ revealed that $Pd(OAc)_2$ yielded the best result (Table 2.1). Further, the addition of 1,8-diazabicyclo[5.4.0]undec-7-ene (DBU) as an additive led to

improve the yield to 75% with high diastereoselectivity (dr = 17:1). Among the other additives screened, DBU was superior to DBN, DABCO, DTPB, quinidine, DIPEA (Table 2.2). In a set of phosphine-based ligands studied, dppe, xanthphos, BINAP, dppp, dppb and PPh_3, dppe produced the superior result(Table 2.3). Further, CH_2Cl_2 was the solvent of choice compared to other solvents, toluene, CH_3CN, THF, methanol, DMF and $(CH_2Cl)_2$ (Table 2.4). In addition, control experiment confirmed that combination of [Pd]-salt and phosphine ligand are essential for the annulation. The stereochemistry of the major isomer **3aa** was determined using a single-crystal X-ray analysis (CCDC 2158075) and NOESY experiment.

Optimization of the Reaction Conditions

Table 2.1. Screening of Palladium-salts[a]

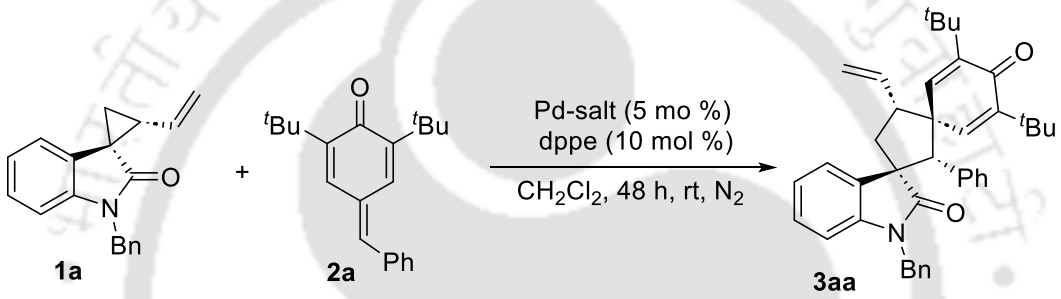

Entry	[Pd]-salt	Yield (%)[b]	dr[c]
1	$Pd(OAc)_2$	51	1.2: 1
2	$PdCl_2$	nr	-
3	$Pd(PPh_3)_2Cl_2$	42	1.1: 1
4	$Pd_2(dba)_3$	40	1.5 :1
5	$Pd(PPh_3)_4$	44	1:1
6[d]	$Pd(OAc)_2$	nr	-

[a]Reaction conditions: **1a** (0.1 mmol), **2a** (0.1 mmol), [Pd]-salt (5 mol %), dppe (10 mol %), CH_2Cl_2 (2 mL), rt, N_2-atmosphere, 48 h. [b]Isolated yield. [c]The dr was determined by ^1H NMR of isolated product. [d]In absence of dppe.

Table 2.2. Screening of Additive[a]

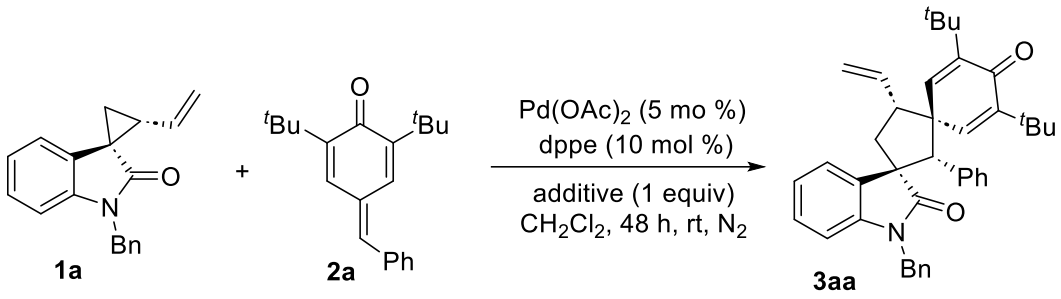

Entry	Additive	Yield (%)[b]	dr[c]
1	**DBU**	**75**	**17:1**
2	DBN	70	4:1
3	DABCO	48	1.6: 1
4	DTBP	30	1.2: 1
5	Quinidine	45	7: 1
6	DIPEA	26	1: 1

[a]Reaction conditions: **1a** (0.1 mmol), **2a** (0.1 mmol), $Pd(OAc)_2$ (5 mol %), dppe (10 mol %), additive (0.1 mmol), CH_2Cl_2 (2 mL), rt, N_2-atmosphere, 48 h. [b]Isolated yield. [c]The dr was determined by ^1H NMR of isolated product.

Table 2.3. Screening of Ligand[a]

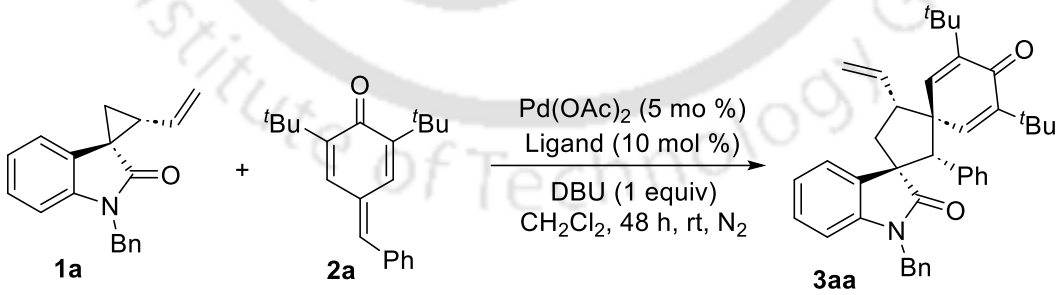

Entry	Ligand	Yield (%)[b]	dr[c]
1	Xanthphos	45	3.8: 1
2	BINAP	45	2: 1
3	dppp	64	14.8: 1

4	dppb	55	12: 1
5	PPh_3	58	2.5: 1

[a]Reaction conditions: **1a** (0.1 mmol), **2a** (0.1 mmol), $Pd(OAc)_2$ (5 mol %), ligand (10 mol %), DBU (0.1 mmol), CH_2Cl_2 (2 mL), rt, N_2-atmosphere, 48 h. [b]Isolated yield. [c]The dr was determined by ^1H NMR of isolated product.

Table 2.4. Screening of Solvent[a]

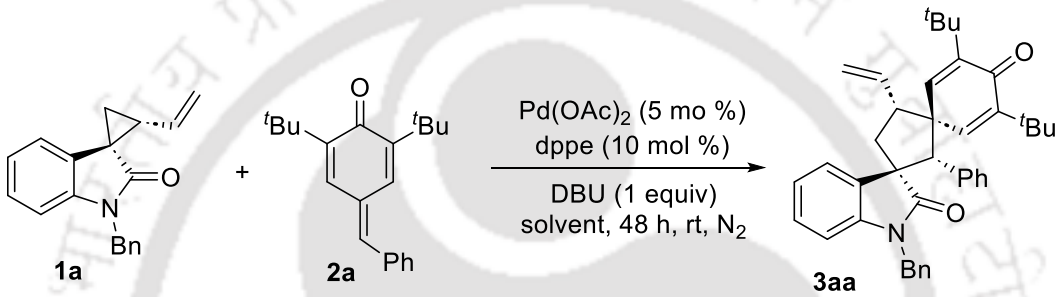

Entry	Solvent	Yield (%)[b]	dr[c]
1	Toluene	50	1.5: 1
2	CH_3CN	55	12: 1
3	THF	60	6: 1
4	CH_3OH	51	2.6: 1
5	DMF	70	14: 1
6	$(CH_2Cl)_2$	55	14: 1

[a]Reaction conditions: **1a** (0.1 mmol), **2a** (0.1 mmol), $Pd(OAc)_2$ (5 mol %), dppe (10 mol %), DBU (0.1 mmol), solvent (2 mL), rt, N_2-atmosphere, 48 h. [b]Isolated yield. [c]The dr was determined by ^1H NMR of isolated product.

Table 2.5. Substrate Scope with Respect to SVCPs[a]

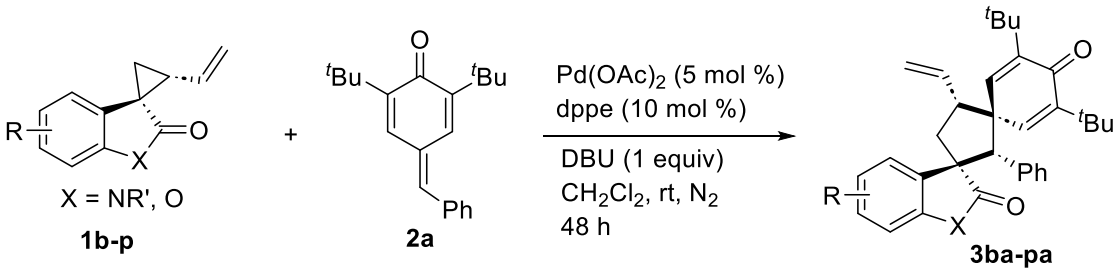

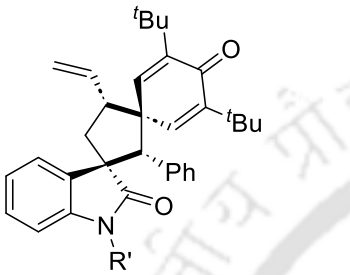

R' = allyl, **3ba**, 71%, >20:1 dr
= Boc, **3ca**, 59%, 12:1 dr
= Me, **3da**, 70%, 14:1 dr
= octyl, **3ea**, 69%, >20:1 dr
= H, **3fa**, n.r.

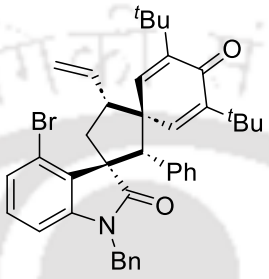

3ga, 70%, >20:1 dr

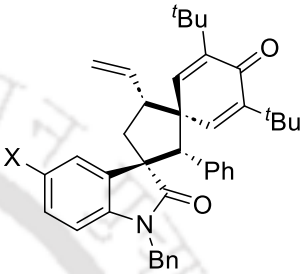

X = Br, **3ha**, 72%, 15:1 dr
= F, **3ia**, 62%, 16:1 dr
= OMe, **3ja,** 77%, 15:1 dr
= Me, **3ka,** 76%, 17:1 dr
= NO_2, **3la,** 65%, >20:1 dr
= Ph, **3ma,** 71%, 15:1 dr

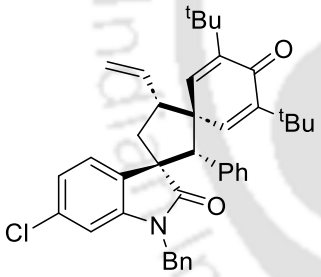

3na, 68%, 19:1 dr

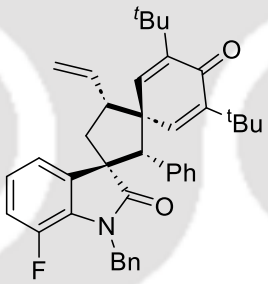

3oa, 64%, >20:1 dr

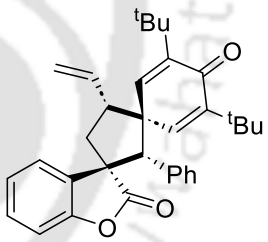

3pa, 49%, >20:1

[a]Reaction conditions: **1b-p** (0.1 mmol), **2a** (0.1 mmol), $Pd(OAc)_2$ (5 mol %), dppe (10 mol %), DBU (0.1 mmol), CH_2Cl_2 (2 mL), rt, N_2-atmosphere, 48 h. [b]Isolated yield. [c]The dr was determined by ^1H NMR of isolated product.

With the optimal reaction conditions, we investigated the scope of the protocol employing diverse SVCPs **1b-p** with **2a** as the representative substrate (Table 2.5). The reaction of SVCPs bearing allyl **1b**, *tert*-butyloxycarbonyl **1c**, methyl **1d** and octyl **1e** substituents at the *N*-centre afforded the cycloadducts **3ba-ea** in 59-75% yields with ≥12:1 dr, whereas unsubstituted SVCPs **1f** was unsuccessful substrate, might be due to complexation of metals with nitrogen. However, 4-bromo substituted **1g** furnished **3ga** with 70% yield and >20:1 dr. Similarly,

substituents at the C5 position comprising electron-rich and -deficient functionalities such as bromo **1h**, fluoro **1i**, methoxy **1j**, methyl **1k**, nitro **1l** and phenyl **1m** participated efficiently to give **3ha-ma** in 62-77% yield and ≥15:1 dr. Further, 6-chloro **1n** and 7-fluoro **1o** substituted SVCPs proved amenable to deliver **3na** and **3oa** in 68% (19:1 dr) and 64% (>20 :1 dr) yields, respectively. Moreover, the reaction using 2-coumaranone derived spirocyclopropane **1p** produced **3pa** with >20:1 dr, in 49% yield.

Table 2.6. Substrate Scope with Respect to *p*-QMs[a]

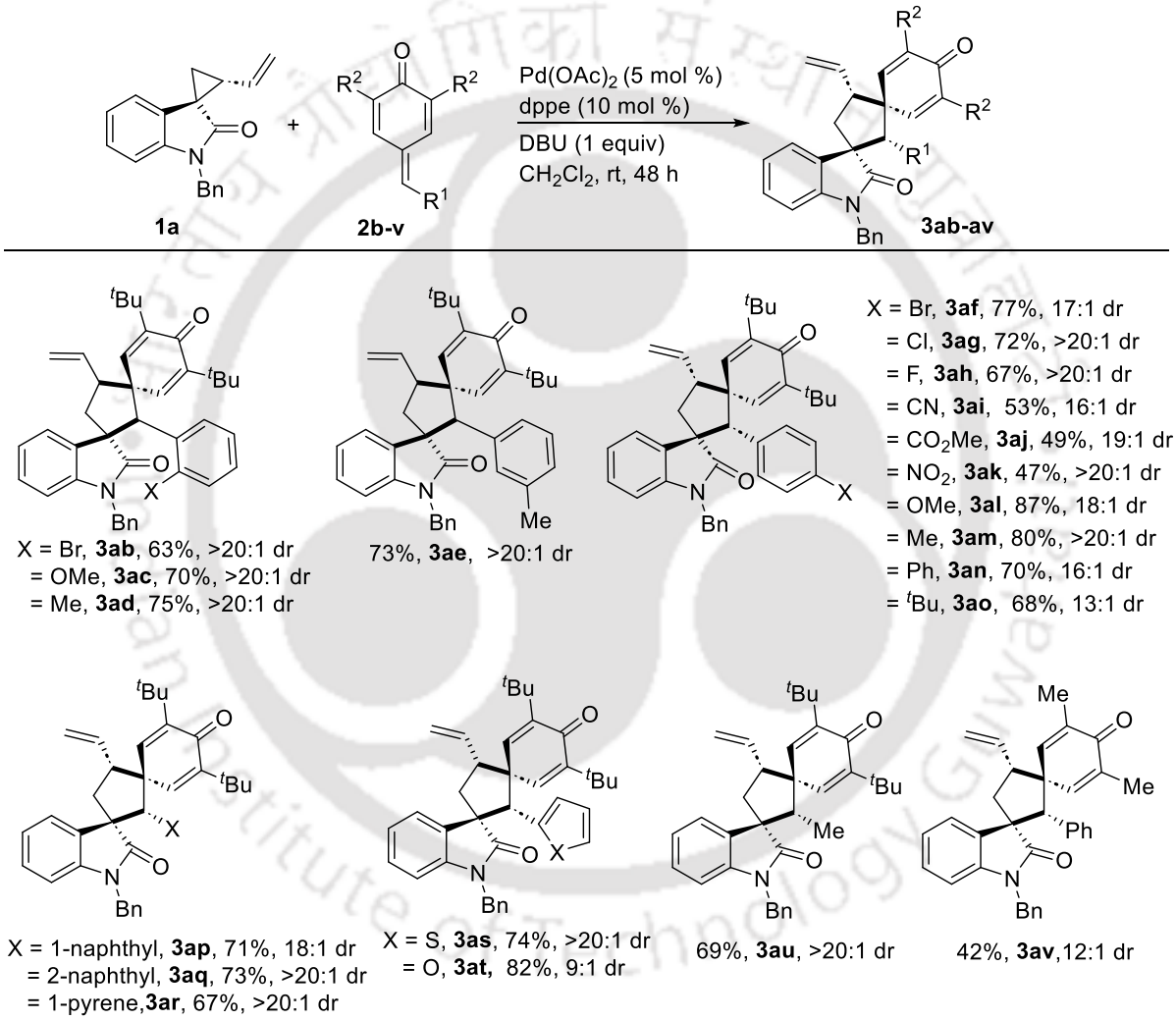

[a]Reaction conditions: **1a** (0.1 mmol), **2b-v** (0.1 mmol), $Pd(OAc)_2$ (5 mol %), dppe (10 mol %), DBU (0.1 mmol), CH_2Cl_2 (2 mL), rt, N_2-atmosphere, 48 h. [b]Isolated yield. [c]The dr was determined by ^1H NMR of isolated product.

The scope of the procedure further extended to the coupling of substituted *p*-QMs **2b-v** with SVCP **1a** as the representative substrate (Table 2.6). *p*-QMs having substitution at the aryl ring with 2-bromo **2b**, 2-methoxy **2c** and 2-methyl **2d** groups furnished **3ab-ad** in 63-75% yields

and >20:1 dr. Similarly, 3-methyl **2e** group substituted substrate delivered **3ae** in 73% yield. Further, the reactions with halogen substituted *p*-QMs, such as 4-bromo **2f**, 4-chloro **2g** and 4-fluoro **2h** groups, occurredto give the cycloadducts **3af-ah** in 67-77% yields and ≥17:1 dr. In addition, *p*-QMs with electron-deficient 4-cyano **2i**, 4-methoxycarbonyl **2j** and 4-nitro **2k** groups produced **3ai-ak** in 47-53% yields and ≥16:1 dr. While, electron-rich groups at the 4-position with methoxy **2l**, methyl **2m**, phenyl **2n** and *tert*-butyl **2o** groups afforded **3al-ao** in 68-87% yields and ≥13:1dr. Moreover, p-QMs bearing poly-aromatic substitutions *viz.,*1-naphthyl **2p**, 2-naphthyl **2q** and 1-pyryl **2r** were successful to produce **3ap-ar** in 67-73% yields and ≥18:1 dr. In addition, p-QMs containing heterocyclic substitutions, 2-thiophenyl **2s** and 2-furfuryl **2t** were exhibited **3as** and **3at** in 74% and 82% yields, respectively. These results suggest the potentiality of the protocol to access a series of functionalized 3-spirocyclopantane oxindole in high yields and dr.

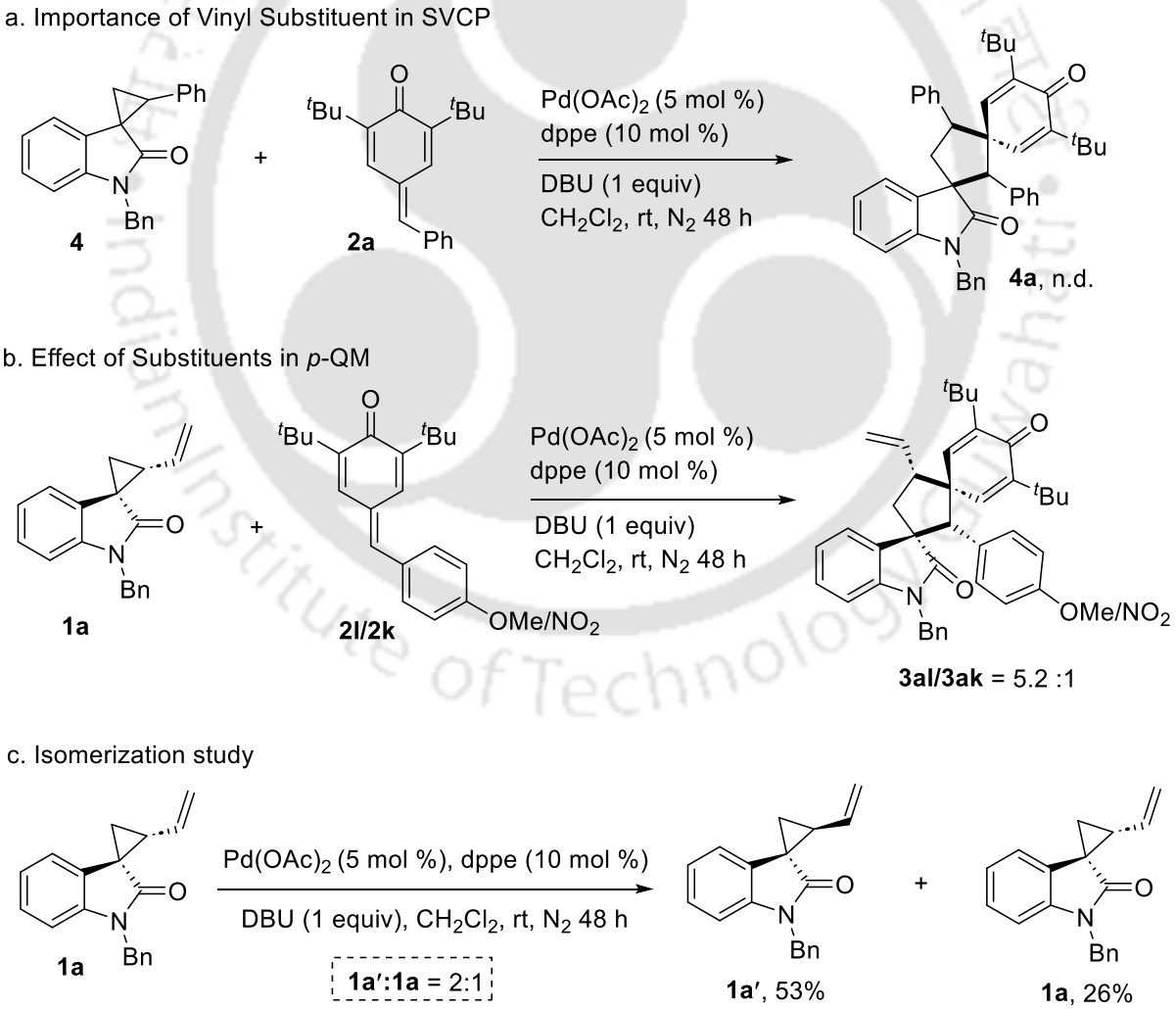

Scheme 2.8. Control Experiments

To unveil reaction pathways control experiments were performed (Scheme 8). The reaction of spirocyclopropyl oxindole **4** with **2a** was performed under standard conditions. However, no annulated product was observed which confides the necessity of vinyl substituent (Scheme 2.8a). Further, the intermolecular competitive experiment showed *p*-QM **2l** with electron donating methoxy group has greater reactivity compared to **2k** bearing electron withdrawing nitro group (Scheme 2.8b) which may be due to presence of electron withdrawing group destabilizes the *p*-QMs. Moreover, **1a** in absence of *p*-QM could be isomerized to a mixture of diastereomers (**1a'**:**1a** = 2:1 dr) *via* an intramolecular rearrangement (Scheme 2.8c).

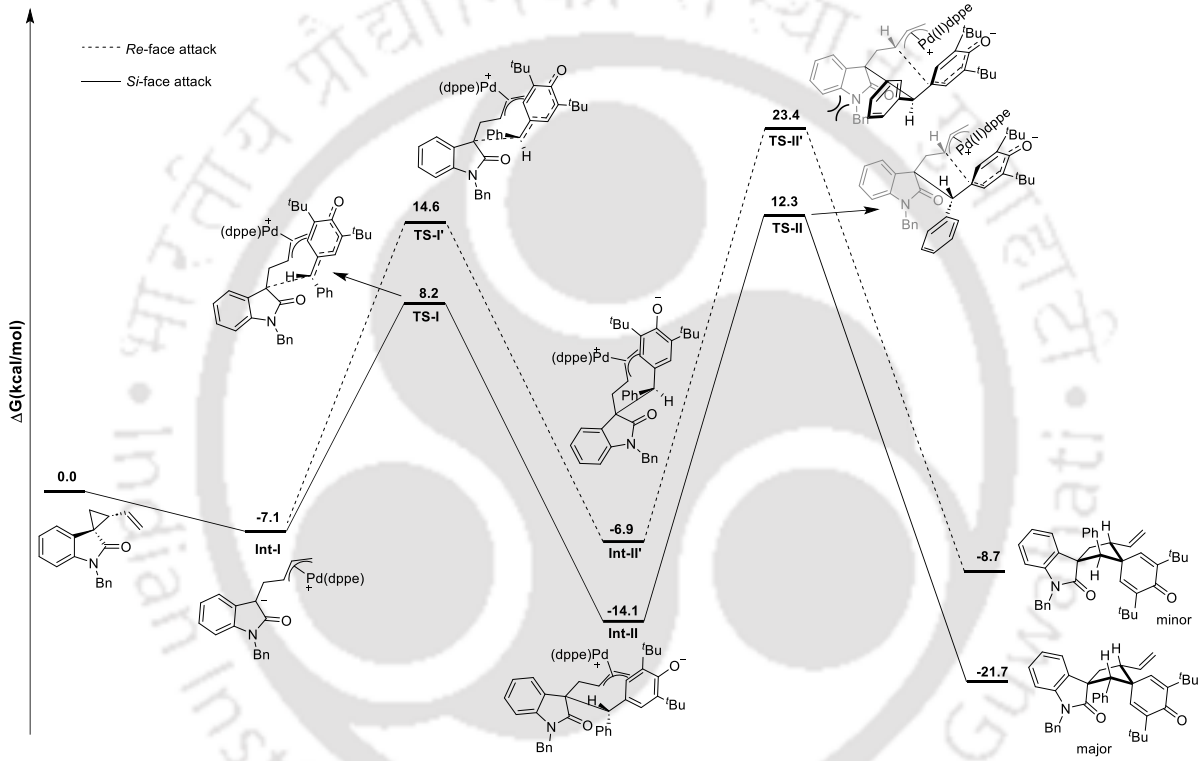

Scheme 2.9. Plausible Reaction Mechanism using DFT-study

To understand the mechanistic pathways,[14,15] DFT-calculations were performed by taking **1a** and **2a** as the model substrates at 298 K in gas phase (Scheme 2.9). At first, Pd-catalyzed ring opening of **1a** may produce the zwitterionic π-allyl palladium-complex **Int-I** *via* exergonic pathway (ΔG298 = -7.1 kcal/mol) which involve nucleophilic attack of stabilized carbanion at more electron deficient benzyl carbon. Si-face approach of *p*-QM to **Int-I** may form **Int-II** involving the transition state **TS-I** with an energy barrier of 15.3 kcal/mol. Then **Int-II** may afford the major isomer *via* **TS-II** with an activation energy barrier of 26.4 kcal/mol. However, the Re-face attack may lead to generation of comparatively higher energy transition states **TS-**

I′ and **TS-II′**, which may produce the other isomer as minor isomer. This result suggests that the Si-face attack is more favourable.

To demonstrate the utility of the developed protocol, we performed scale-up synthesis (Scheme 10). Scale-up synthesis using **1a** and **2a** successfully afforded **3aa** in 68% yield with >13:1 dr (Scheme 2.10a). Further, to showcase the potentiality of the spiro-product, we carried out post-synthetic transformation using **3aa** (Scheme 2.10b). Reaction of **3aa** with *m*CPBA successfully accomplished epoxide **5** (52% yield, >20:1 dr) whose relative configuration was determined by analysis of 2D NOESY experiment. Wacker oxidation of **3aa** yielded the aldehyde **6** in 55% yield (>20:1 dr). Moreover, hydrogenation of **3aa** produce **7** (81% yield, >20:1 dr) and Heck coupling of **3aa** with phenyl iodide resulted in **8** (76% yield, >20:1 dr).

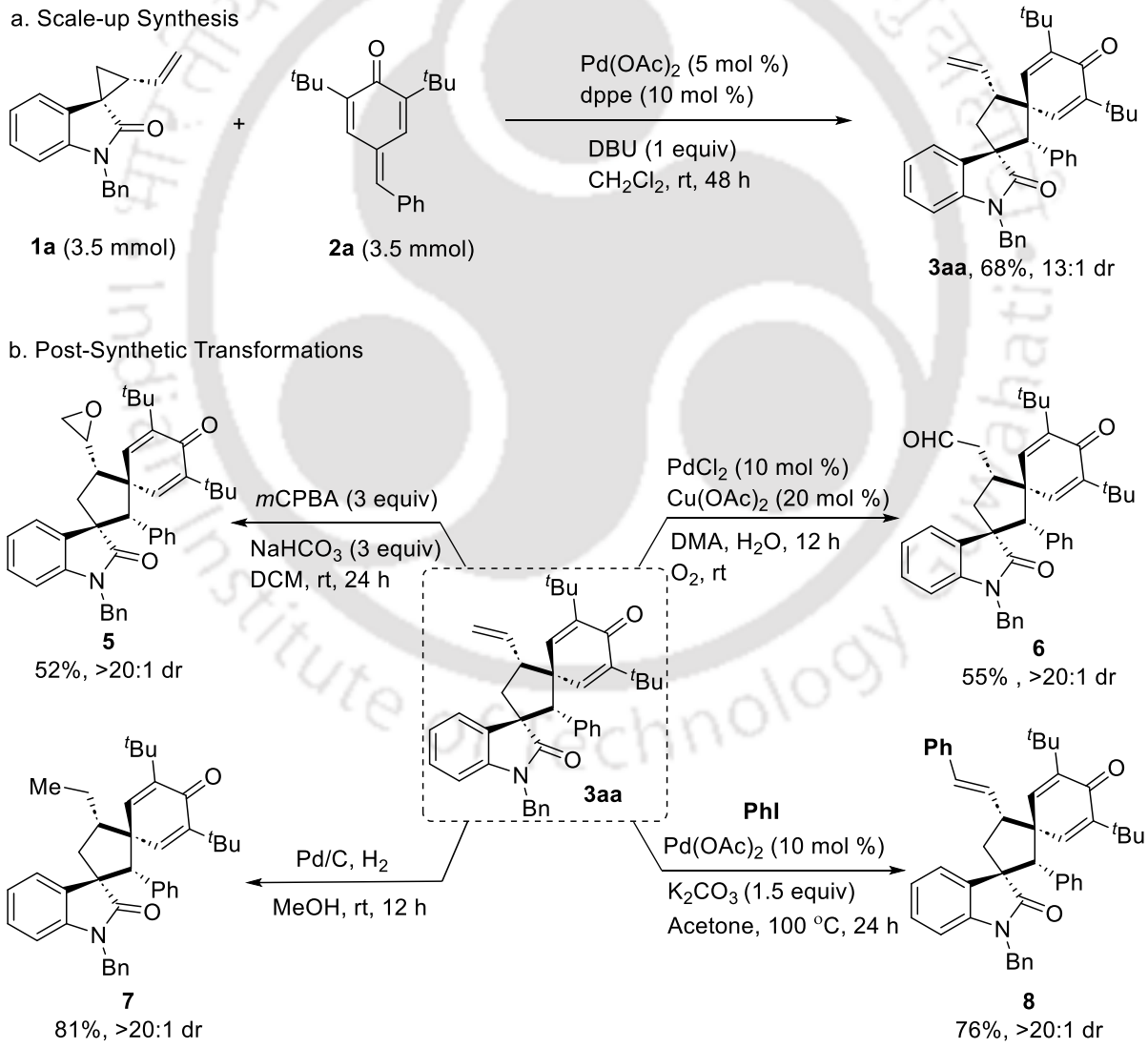

Scheme 2.10. Synthetic Utilities

Moreover, MTT cell viability assay was performed against MDAMB-231 by employing our designed spiro-adduct **3**. Gratifyingly, the pyryl ring containing spiro-adduct **3ar** exhibited cytotoxicity against the cancer cells with $IC_{50} = 61.6 \pm 4.6$ µM (Figure 2). This biological study displayed the useability of the spiro-adduct in medicinal field.

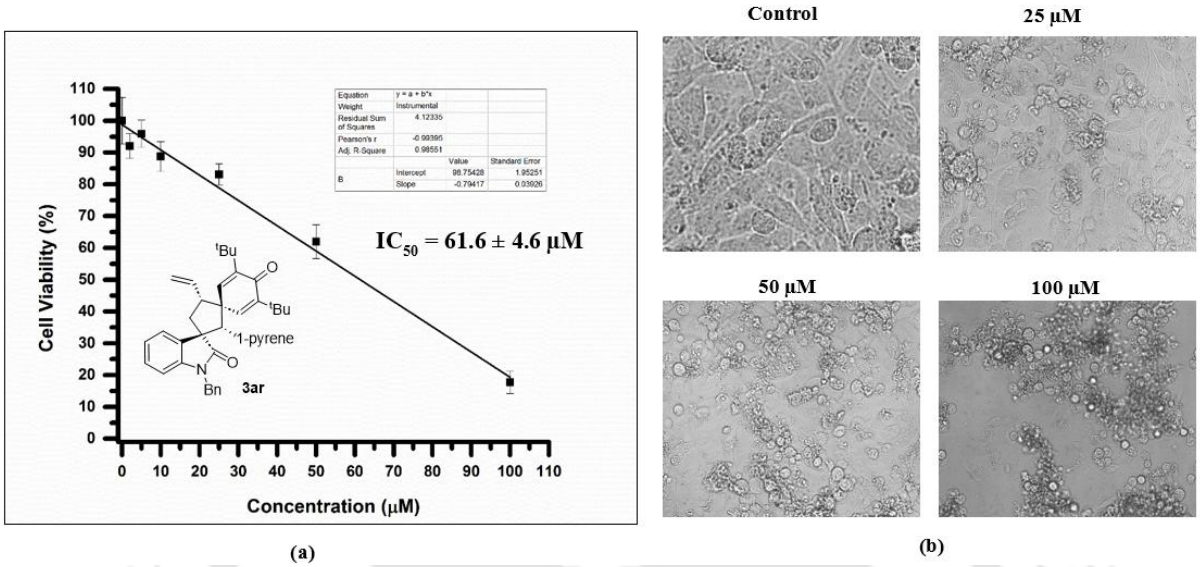

Figure 2.2. MTT assay against cancer cell MDAMB-231. (a) Graphical plot of concentration dependent killing activity by compound **3ar**, (b) Cytell images of cancer cells at different concentrations of **3ar**.

In summary, we have developed a synthetic strategy for construction of diversely substituted 3-spirocyclopantane oxindoles under mild reaction conditions. The substrate scope, functional group diversity, DFT studies, scale-up synthesis and post-synthetic transformations are the important features.

2.4 Experimental Section

General Information. $Pd(OAc)_2$ (98%), $PdCl_2$ (99%), $Pd(PPh_3)_2Cl_2$ (>99%), $Pd_2(dba)_3$ (97%), $Pd(PPh_3)_4$ (99%), dppe (99%), xanthphos (97%), BINAP (97%), dppp (97%), dppb (98%) and PPh_3 (99%) of Aldrich used as received. Spirovinylcyclopropanes[7] and *p*-quinone methides[10-12] were prepared according to literature. SRL silica gel G/GF 254 plates were used for analytical TLC and SRL silica gel (100-200 mesh) was used for column chromatography. NMR (^1H, ^{13}C, ^{19}F and NOESY) spectra were recorded with Bruker Ascend 400, 500 and 600 MHz spectrometers using $CDCl_3$ as solvent and TMS as an internal standard. Chemical shifts (δ) and spin-spin coupling constant (*J*) are reported in ppm and in Hz, respectively, and other data are reported as mentioned: s = singlet, d = doublet, t = triplet, m = multiplet, q = quartet. HRMS

was recorded with Q-Tof ESI-MS instrument (model HAB 273 and Xevo G2-XS). Perkin Elmer FT-IR spectrometer was used to record IR spectra. Melting points were determined using a Büchi B-540 apparatus and are uncorrected. Single crystal X-ray data was collected on a Bruker SMART APEX equipped with a CCD area detector using Mo/Kα radiation and the structure was solved by direct method using SHELXL-14 (Göttingen, Germany).

General Procedure for the Synthesis of Spirovinylcyclopropanyl Oxindoles.[7]

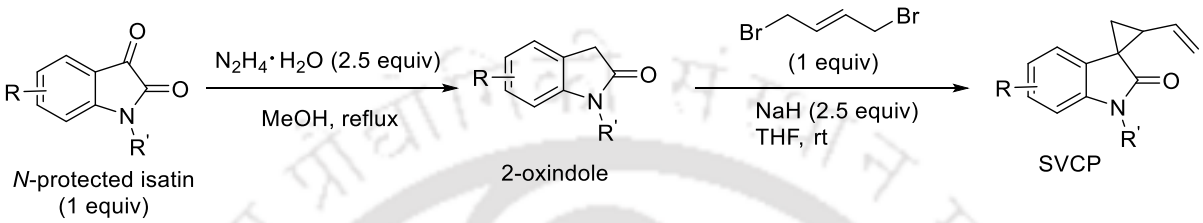

N-protected isatin derivative (2.1 mmol) was dissolved in MeOH (10 mL) and allowed to stir at room temperature. To it hydrazine hydrate (5.25 mmol, 2.5 equiv) was added and the resultant mixture was refluxed for 2 h. Then the reaction mixture was cooled and concentrated using rotary evaporator. The residue was dissolved in ethyl acetate, washed with brine (5 mL x 2), and dried over Na_2SO_4. Evaporation of the solvent gave 2-oxindole derivative that was used for next step without further purification.

To a stirred solution of the above 2-oxindole derivative in dry THF (10 mL), NaH (5.25 mmol, 2.5 equiv) was added and the reaction was allowed to stir at room temperature for 5 minutes. Then a solution of trans-1,4-dibromo-2-butene (2.1 mmol, 1 equiv) in dry THF (5 mL) was added to it in dropwise manner and the stirring was allowed to continue for another 15 minutes. Then ice cold water (10 mL) was added in the reaction mixture to quench the excess of NaH. The organic part was extracted with ethyl acetate (20 mL x 3), washed with brine (5 mL x 2) and dried over Na_2SO_4. Evaporation of the solvent produced a crude residue that was purified on silica gel column chromatography using hexane/ethyl acetate mixture as an eluent to afford SVCP.

General Procedure for the Synthesis of *para*-Quinone Methides (*p*-QMs).[16]

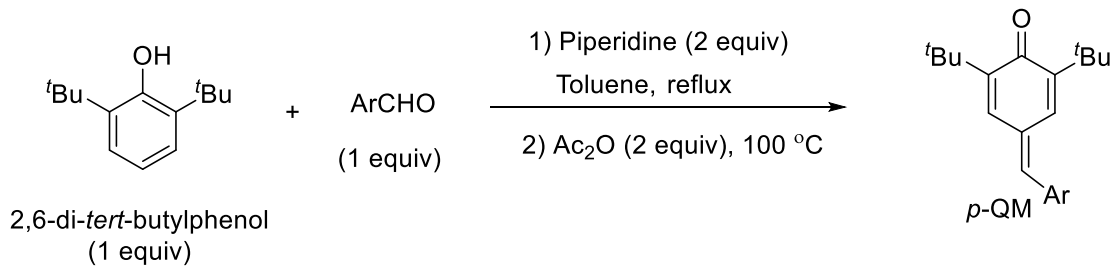

A solution of 2,6-di-*tert*-butylphenol (2.4 mmol) and aldehyde (2.4 mmol) in toluene (20 mL) was refluxed using Dean-stark apparatus for 30 minutes. Then, piperidine (4.8 mmol, 2 equiv) was added and the reflux was continued till the completion of the reaction (monitored using TLC). The reaction mixture was then cooled, acetic anhydride (4.8 mmol, 2 equiv) was added and the reaction was continued for another 15 minutes at 100 °C. The reaction mixture was then cooled to room temperature and water (10 mL) was added. The organic part was extracted with ethyl acetate (20 mL x 3), washed with brine (10 mL x 2) and dried over Na_2SO_4. Evaporation of the solvent produced residue that was purified on silica gel column chromatography using hexane/ethyl acetate mixture as an eluent to afford *p*-QM.

General Procedure for Pd-Catalyzed (3+2)-Annulative Coupling of SVCPs with *p*-QMs. To a stirred solution of $Pd(OAc)_2$ (5 mol %, 1.2 mg) and dppe (10 mol %, 4 mg) in CH_2Cl_2 (2 mL) at room temperature under nitrogen atmosphere for 30 minutes, substrate **1** (0.1 mmol), substrate **2** (0.1 mmol) and DBU (0.1 mmol, 15 µL) were added. The resultant solution was stirred for an additional 48 h. The reaction was diluted with CH_2Cl_2 (10 mL) and passed through a short celite pad. Evaporation of the solvent produced a residue, which was purified on silica gel column chromatography using hexane/ethyl acetate mixture as an eluent to afford **3**. The dr was determined using ^1H NMR analysis.

Scale-up Synthesis of 3aa. To a stirred solution of $Pd(OAc)_2$ (5 mol %, 39 mg), dppe (10 mol %, 139.3 mg) in CH_2Cl_2 (10 mL) at room temperature for 30 mins under nitrogen atmosphere, **1a** (3.5 mmol, 0.96 g), **2a** (3.5 mmol, 1 g) and DBU (3.5 mmol, 532 µL) were added and the stirring was continued for an additional 48 h. The reaction mixture was diluted with CH_2Cl_2 (20 mL) and passed through a short celite pad. Evaporation of the solvent gave a residue which was purified on silica gel column chromatography using hexane/ethyl acetate as an eluent to yield **3aa** in 68% (1.34 g) with 13:1 dr.

Synthesis of 5. To an ice cooled solution of **3aa** (0.1 mmol, 56.9 mg) in CH_2Cl_2 (3 mL), $NaHCO_3$ (0.3 mmol, 25.2 mg) was added and the mixture was allowed to stir for 5 minutes. Then, *m*CPBA (0.3 mmol, 52 mg) was added portion wise and the reaction mixture was stirred for additional 24 h at room temperature. The reaction mixture was treated with saturated aqueous solution of $Na_2S_2O_3$ and extracted using CH_2Cl_2 (3 x 5 mL). The combined organic layer was washed with water (5 mL) and dried over Na_2SO_4. Evaporation of the solvent gave a residue that was purified on silica gel chromatography to afford **5** in 52% (30.5 mg) yield.

Synthesis of 6. To a stirred solution a **3aa** (0.1 mmol, 56.9 mg) in DMF (0.7 mL), $PdCl_2$ (10 mol %, 2.2 mg), $Cu(OAc)_2$ (20 mol %, 3.6 mg) and water (0.1 mL) were added. The stirring was allowed to continue for 12 h at room temperature under oxygen balloon. The reaction was then treated with water (1 mL) and extracted using ethyl acetate (2 x 10 mL). The organic layer was washed with brine (5 mL), water (5 mL) and dried over Na_2SO_4. Evaporation of the solvent gave a residue that was purified on silica gel column chromatography to produce **6** in 55% (32.1 mg) yield.

Synthesis of 7. To a stirred solution of **3aa** (0.1 mmol, 56.9 mg) in MeOH (2 mL), Pd/C (10 mol %, 1 mg) were added and the resultant mixture was allowed to stir at room temperature for 12 h under hydrogen balloon. Then the reaction mixture was diluted with ethyl acetate (10 mL) and passed through a short celite pad. Evaporation of the solvent gave a residue which was purified on silica gel column chromatography to yield **7** in 81% (46.2 mg) yield.

Synthesis of 8. In sealed tube, **3aa** (0.1 mmol, 56.9 mg), iodobenzene (0.15 mmol, 17 µL), $Pd(OAc)_2$ (10 mol %, 2.2 mg), K_2CO_3 (0.15 mmol, 21 mg) and acetone (1 mL) were stirred at 100 °C under nitrogen atmosphere for 24 h. Then the reaction mixture was diluted with ethyl acetate (10 mL) and passed through a short pad of celite. Evaporation of the solvent gave a residue that was purified on silica gel column chromatography to get **8** in 76% (49 mg) yield.

Control Experiments

Reaction of Spirocyclopropyl Oxindole (4) with 2a (Scheme 8a). A solution of $Pd(OAc)_2$ (5 mol %, 1.2 mg) and dppe (10 mol %, 4 mg) in CH_2Cl_2 (2 mL) was allowed to stir at room temperature under nitrogen atmosphere for 30 minutes. Then, **4** (0.1 mmol, 32.5 mg), **2a** (0.1 mmol, 29.5 mg) and DBU (0.1 mmol, 15 µL) were added. The resultant solution was stirred for an additional 48 h. Analysis of the reaction mixture was performed using TLC and HRMS.

Intermolecular Competitive Experiments using 1a with 2k and 2l (Scheme 8b). To a stirred solution of $Pd(OAc)_2$ (5 mol %, 1.2 mg) and dppe (10 mol %, 4mg) in CH_2Cl_2 (4 mL) for 30 mins at room temperature, **1a** (0.1 mmol, 27.5 mg), **2k** (0.5 mmol, 169.5 mg), **2l** (0.5 mmol, 162 mg) and DBU (0.1 mmol, 15 µL) were added. The stirring was continued for 48 h and passed through a short of pad of celite using CH_2Cl_2 (10 mL). Evaporation of the solvent produced a residue, whose ^1H NMR was used to determine the conversion ratio (**3al** : **3ak** = 5.2:1).

Isomerization Study (Scheme 8c). A solution of $Pd(OAc)_2$ (5 mol %, 1.2 mg) and dppe (10 mol %, 4 mg) in CH_2Cl_2 (2 mL) was allowed to stir at room temperature under nitrogen atmosphere for 30 minutes. Then, **1a** (0.1 mmol, 27.5 mg) and DBU (0.1 mmol, 15 μL) were added and the resultant solution was stirred for an additional 48 h. Purification of the reaction mixture was performed according to general procedure as described to isolate mixture of **1a'/1a** in 79% (21.7 mg) whose ratio (2:1) was calculated using ^{1}H NMR analysis.

2.5 Characterization Data

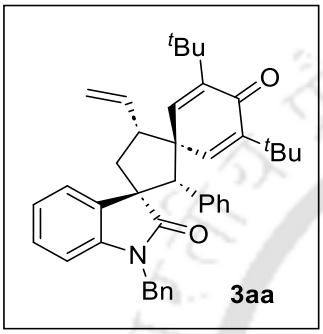

1''-Benzyl-3,5-di-*tert*-butyl-2'-phenyl-4'-vinyldispiro-[cyclohexane-1,3'-cyclopentane-1',3''-indoline]-2,5-diene-2'',4-dione 3aa. Analytical TLC on silica gel, 1:49 ethyl acetate/hexane R_f = 0.25; colorless solid; mp 167-168 °C; yield 75% (43 mg); major diastereomer (17:1 dr); ^{1}H NMR (500 MHz, $CDCl_3$) δ 8.05 (m, 1H), 7.47 (d, *J* = 7.0 Hz, 1H), 7.06-6.99 (m, 4H), 6.97-6.91 (m, 4H), 6.83-6.82 (m, 1H), 6.40 (d, *J* = 7.5 Hz, 2H), 6.32-6.29 (m, 2H), 5.47-5.40 (m, 1H), 5.06 (d, *J* =16.5 Hz, 1H), 4.96-4.92 (m, 2H), 4.23 (d, *J* = 15.6 Hz, 1H), 3.73 (s, 1H), 3.18-3.12 (m, 1H), 2.84-2.79 (m, 1H), 2.39-2.35 (m, 1H), 1.31 (s, 9H), 1.02 (s, 9H); ^{13}C{^{1}H} NMR (150 MHz, $CDCl_3$) δ 186.6, 179.1, 150.2, 148.5, 143.5, 142.1, 140.1, 136.1, 135.3, 135.0, 134.8, 129.4, 128.6, 128.1, 127.8, 127.6, 127.1, 126.4, 123.2, 122.0, 117.1, 109.1, 69.3, 58.5, 56.4, 55.5, 43.8, 41.9, 35.7, 34.8, 29.64, 29.62; FT-IR (KBr) 2955, 1708, 1636, 1489, 1363, 1171 cm^{-1}; HRMS (ESI) m/z: $[M+H]^+$ Calcd for $C_{40}H_{44}NO_2$ 570.3367; Found 570.3371.

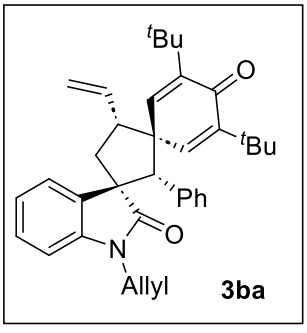

1''-Allyl-3,5-di-*tert*-butyl-2'-phenyl-4'-vinyldispiro[cyclohexane-1,3'-cyclopentane-1',3''-indoline]-2,5-diene-2'',4-dione 3ba. Analytical TLC on silica gel,

1:49 ethyl acetate/hexane R_f = 0.24; colorless solid; mp 143-144 °C; yield 71% (36.9 mg); major diastereomer (>20:1 dr): ^{1}H NMR (500 MHz, $CDCl_3$) δ 7.998-7.993 (m, 1H), 7.45-7.44 (m, 1H), 7.14-7.11 (m, 1H), 7.09-7.06 (m, 1H), 6.97-6.94 (m, 1H), 6.89-6.86 (m, 2H), 6.75-6.74 (m, 2H), 6.54 (d, *J* = 7.5 Hz, 1H), 6.28-6.28 (m, 1H), 5.46-5.39 (m, 1H), 5.28-5.21 (m, 1H), 4.95-4.91 (m, 2H), 4.77 (d, *J* = 10.5 Hz, 1H), 4.40 (d, *J* =17.5 Hz, 1H), 4.29-4.25 (m, 1H), 3.78-3.74 (m, 1H), 3.66 (s, 1H), 3.15-3.10 (m, 1H), 2.79-2.74 (m, 1H), 2.36-2.32 (m, 1H), 1.29 (s, 9H), 1.02 (s, 9H); ^{13}C NMR (125 MHz, $CDCl_3$) δ 186.7, 178.9, 150.4, 148.8, 143.6, 142.4, 140.0, 136.3, 135.6, 134.9, 130.9, 129.4, 128.2, 127.7, 127.6, 123.2, 122.1, 117.1, 116.9, 108.9, 69.7, 58.6, 56.5, 55.7, 42.4, 41.5, 35.8, 34.9, 29.8, 29.7; FT-IR (KBr) 2953, 1705, 1657, 1634, 1611, 1488, 1466, 1362, 919, 742, 696 cm^{-1}; HRMS (ESI) m/z: $[M+H]^+$ Calcd for $C_{36}H_{42}NO_2$ 520.3210; Found 520.3209.

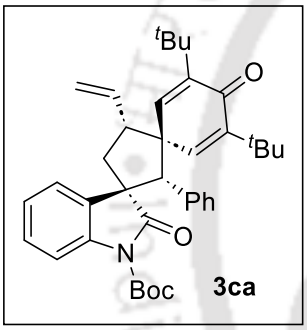

***tert*-Butyl-3,5-di-*tert*-butyl-2'',4-dioxo-2'-phenyl-4'-vinyldispiro [cyclohexane-1,3'-cyclopentane-1',3''-indoline]-2,5-diene-1''-carboxylate 3ca.** Analytical TLC on silica gel, 1:24 ethyl acetate/hexane R_f = 0.25; colorless solid; mp 139-140 °C; yield 59% (34.2 mg); major diastereomer (12:1 dr): ^{1}H NMR (500 MHz, $CDCl_3$) δ 7.83-7.82 (m, 1H), 7.52-7.51 (m, 1H), 7.44-7.42 (m, 1H), 7.20-7.18 (m, 2H), 7.00-6.97 (m, 1H), 6.92-6.89 (m, 2H), 6.71-6.70 (d, *J* = 7.5 Hz, 2H), 6.24-6,23 (m, 1H), 5.48-5.41 (m, 1H), 4.97-4.93 (m, 2H), 3.52 (s, 1H), 3.14-3.09 (m, 1H), 2.88-2.83 (m, 1H), 2.39-2.35 (m, 1H), 1.43 (s, 9H), 1.27 (s, 9H), 1.00 (s, 9H); ^{13}C NMR (125 MHz, $CDCl_3$) δ 186.4, 178.4, 150.4, 148.9, 148.7, 143.2, 139.1, 138.8, 135.3, 134.7, 133.8, 129.2, 128.4, 127.8, 127.6, 125.1, 121.9, 117.1, 114.7, 84.0, 71.5, 58.8, 56.6, 55.4, 41.3, 35.7, 34.8, 29.6, 28.0; FT-IR (KBr) 2955, 1758, 1732, 1635, 1480, 1355, 1292, 1149, 747, 696 cm^{-1}; HRMS (ESI) m/z: $[M+H]^+$ Calcd for $C_{38}H_{46}NO_4$ 580.3421; Found 580.3429.

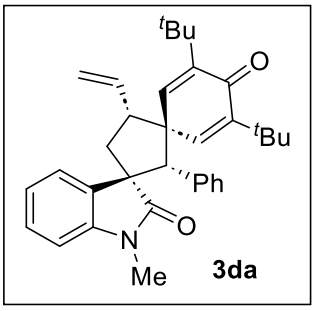

3,5-Di-*tert*-butyl-1''-methyl-2'-phenyl-4'-vinyldispiro [cyclohexane-1,3'-cyclopentane-1',3''-indoline]-2,5-diene-2'',4-dione 3da. Analytical TLC on silica gel, 1:49 ethyl acetate/hexane R_f = 0.24; colorless solid; mp 177-178 °C; yield 70% (34.7 mg); major diastereomer (14:1 dr): ^{1}H NMR (500 MHz, $CDCl_3$) δ 7.99-7.98 (m, 1H), 7.44-7.43 (m, 1H), 7.18-7.15 (m, 1H), 7.10-7.07 (m, 1H), 6.97-6.94 (m, 1H), 6.90-6.87 (m, 2H), 6.74-6.73 (m, 2H), 6.58 (d, *J* = 7.5 Hz, 1H), 6.29-6.28 (m, 1H), 5.45-5.38 (m, 1H), 4.95-4.90 (m, 2H), 3.66 (s, 1H), 3.13-3.08 (m 1H), 2.86 (s, 3H), 2.76-2.71 (m, 1H), 2.34-2.29 (m, 1H), 1.29 (s, 9H), 1.02 (s, 9H); ^{13}C NMR (125 MHz, $CDCl_3$) δ 186.8, 179.4, 150.5, 148.9, 143.8, 143.2, 140.2, 136.5, 135.7, 135.2, 129.3, 128.4, 127.71, 127.70, 123.3, 122.2, 117.3, 108.1, 69.4, 58.6, 56.6, 55.7, 41.8, 36.0, 35.0, 29.9, 26.5; FT-IR (KBr) 2955, 1710, 1636, 1489, 1363, 742 cm^{-1}; HRMS (ESI) m/z: $[M+H]^+$ Calcd for $C_{34}H_{40}NO_2$ 494.3054; Found 494.3054.

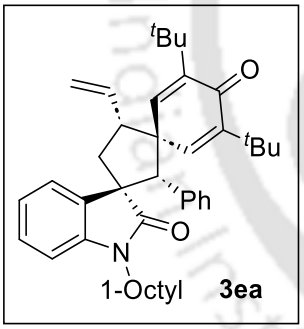

3,5-Di-*tert*-butyl-1''-octyl-2'-phenyl-4'-vinyldispiro[cyclohexane-1,3'-cyclopentane-1',3''-indoline]-2,5-diene-2'',4-dione 3ea. Analytical TLC on silica gel, 1:49 ethyl acetate/hexane R_f = 0.24; colorless solid; mp 189-190 °C; yield 69% (40.8 mg); major diastereomer (>20:1 dr): ^{1}H NMR (500 MHz, $CDCl_3$) δ 8.00-7.99 (m, 1H), 7.44-7.42 (m, 1H), 7.18-7.14 (m, 1H), 7.08-7.05 (m, 1H), 6.95-6.93 (m, 1H), 6.88-6.85 (m, 2H), 6.74-6.72 (m, 2H), 6.58 (d, *J* = 8.0 Hz, 1H), 6.28-6.27 (m, 1H), 5.45-5.38 (m, 1H), 4.95-4.90 (m, 2H), 3.64 (s, 1H), 3.57-3.51 (m, 1H), 3.16-3.08 (m, 2H), 2.75-2.70 (m, 1H), 2.32-2.28 (m, 1H), 1.30 (s, 9H), 1.22-1.17 (m, 3H), 1.15- 1.07 (m, 7H), 1.02 (s, 9H), 0.96-0.88 (m, 2H), 0.81-0.78 (m, 3H); ^{13}C NMR (125 MHz, $CDCl_3$) δ 186.6, 178.7, 150.2, 148.6, 143.6, 142.7, 140.1, 136.4, 135.5, 134.9, 129.1, 128.1, 127.4, 122.8, 122.1, 117.0, 108.1, 69.3, 58.3, 56.3, 55.6, 41.4, 40.2, 35.7, 34.8, 31.9, 29.7, 29.6, 29.3, 29.1, 27.2, 26.8, 22.7, 14.1; FT-IR (KBr) 2958, 2928, 1708,

1638, 1611, 1466, 1364, 745, 697 cm^{-1}; HRMS (ESI) m/z: $[M+H]^+$ Calcd for $C_{41}H_{54}NO_2$ 592.4149; Found 592.4150.

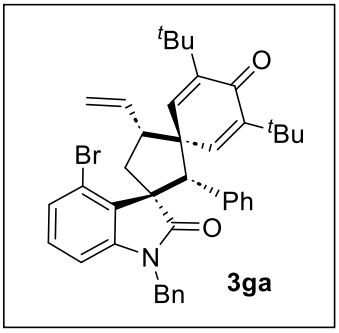

1''-Benzyl-4''-bromo-3,5-di-*tert*-butyl-2'-phenyl-4'-vinyldispiro [cyclohexane-1,3'-cyclopentane-1',3''-indoline]-2,5-diene-2'',4-dione 3ga. Analytical TLC on silica gel, 1:49 ethyl acetate/hexane R_f = 0.24; colorless solid; mp 192-193 °C; yield 70% (45.6 mg); major diastereomer (>20:1 dr): ^{1}H NMR (500 MHz, $CDCl_3$) δ 8.15-8.14 (m, 1H), 7.17-7.15 (m, 1H), 7.07-7.03 (m, 2H), 6.99-6.96 (m, 2H), 6.93-6.90 (m, 2H), 6.86-6.81 (m, 3H), 6.38-6.37 (m, 2H), 6.35-6.34 (m, 3H), 6.23 (d, *J* = 7.5 Hz, 1H), 5.51-5.44 (m, 1H), 4.98-4.92 (m, 3H), 4.32 (s, 1H), 4.24 (d, *J* = 16.0 Hz, 1H), 3.76-3.70 (m, 1H), 2.79-2.74 (m, 1H), 2.70-2.65 (m, 1H), 1.30 (s, 9H), 1.01 (s, 9H); ^{13}C NMR (125 MHz, $CDCl_3$) δ 186.6, 178.8, 150.2, 147.9, 144.6, 143.7, 141.0, 136.0, 134.7, 131.2, 129.74, 129.71, 128.7, 127.879, 127.870, 127.7, 127.4, 127.3, 126.4, 118.0, 116.5, 108.5, 63.0, 60.8, 56.8, 54.3, 44.0, 38.2, 35.7, 34.7, 29.67, 29.66; FT-IR (KBr) 2953, 1711, 1635, 1601, 1453, 1357, 736, 696 cm^{-1}; HRMS (ESI) m/z: $[M+H]^+$ Calcd for $C_{40}H_{43}BrNO_2$ 648.2472; Found 648.2473.

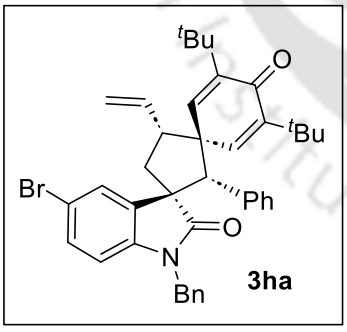

1''-Benzyl-5''-bromo-3,5-di-*tert*-butyl-2'-phenyl-4'-vinyl-dispiro[cyclohexane-1,3'-cyclopentane-1',3''-indoline]-2,5-diene-2'',4-dione 3ha. Analytical TLC on silica gel, 1:49 ethyl acetate/hexane R_f = 0.24; colorless solid; mp >200 °C; yield 72% (46.7 mg); major diastereomer (15:1 dr): ^{1}H NMR (600 MHz, $CDCl_3$) δ 8.074-8.070 (m, 1H), 7.646-7.644 (m, 1H), 7.26-7.19 (m, 1H), 7.18-7.16 (m, 1H), 7.13-7.10 (m, 1H), 7.05-7.02 (m, 4H), 6.92-6.91 (m, 2H), 6.42 (d, *J* = 7.2 Hz, 2H), 6.385-6.380 (m, 1H), 6.27 (d, *J* = 8.3 Hz, 1H), 5.52-5.47 (m, 1H), 5.14 (d, *J* = 16.2 Hz, 1H), 5.06-5.01 (m, 2H), 4.27 (d, *J* = 16.2 Hz, 1H), 3.74 (s, 1H), 3.22-3.18 (m, 1H), 2.91-2.86 (m, 1H), 2.46-2.42 (m, 1H), 1.38 (s, 9H),

1.10 (s, 9H); ^{13}C NMR (150 MHz, $CDCl_3$) δ 186.5, 178.5, 150.5, 148.7, 143.3, 141.2, 139.7, 138.2, 135.1, 134.5, 134.4, 131.1, 129.5, 128.8, 128.0, 127.9, 127.4, 126.4, 125.3, 117.5, 115.7, 110.8, 77.3, 76.9, 69.4, 58.7, 56.4, 55.4, 43.9, 41.8, 35.8, 34.9, 29.7, 29.6; FT-IR (KBr) 2955, 1709, 1636, 1481, 1342, 1259, 805, 737, 696 cm^{-1}; HRMS (ESI) m/z: $[M+H]^+$ Calcd for $C_{40}H_{43}BrNO_2$ 648.2472; Found 648.2472.

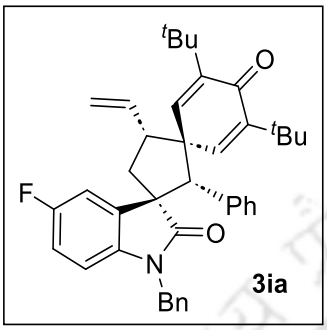

1''-Benzyl-3,5-di-*tert*-butyl-5''-fluoro-2'-phenyl-4'-vinyldispiro [cyclohexane-1,3'-cyclopentane-1',3''-indoline]-2,5-diene-2'',4-dione 3ia. Analytical TLC on silica gel, 1:49 ethyl acetate/hexane R_f = 0.22; colorless solid; mp 179-180 °C; yield 62% (36.4 mg); major diastereomer (16:1 dr): ^{1}H NMR (500 MHz, $CDCl_3$) δ 8.02-8.01 (m, 1H), 7.21-7.19 (m, 1H), 7.09-7.02 (m, 2H), 6.98-6.93 (m, 4H), 6.85-6.84 (m, 2H), 6.72-6.68 (m, 1H), 6.40-6.38 (m, 2H), 6.286-6.280 (m, 1H), 6.23-6.21 (m, 1H), 5.47-5.40 (m, 1H), 5.04 (d, J = 16.0 Hz, 1H), 4.97-4.93 (m, 2H), 4.22 (d, J = 16.0 Hz, 1H), 3.65 (s, 1H), 3.15-3.09 (m, 1H), 2.85-2.80 (m, 1H), 2.38-2.34 (m, 1H), 1.30 (s, 9H), 1.02 (s, 9H); ^{13}C NMR (125 MHz, $CDCl_3$) δ 186.5, 178.8, 160.6 ($J_{C\text{-}F}$ = 239.8 Hz), 150.5, 148.8, 143.2, 139.6, 138.1 ($J_{C\text{-}F}$ = 1.8 Hz), 137.8 ($J_{C\text{-}F}$ = 7.3 Hz), 135.2, 134.8, 134.5, 129.5, 128.7, 127.9, 127.8, 127.3, 126.5, 117.2, 114.5 ($J_{C\text{-}F}$ = 23.1 Hz), 110.2 ($J_{C\text{-}F}$ = 24.3 Hz), 109.8 ($J_{C\text{-}F}$ = 7.8 Hz), 69.5, 58.9, 58.9, 56.4, 55.4, 44.0, 41.8, 35.8, 34.8, 29.6; ^{19}F NMR (471 MHz, $CDCl_3$) δ -119.5; FT-IR (KBr) 2955, 2921, 1710, 1493, 1454, 1363, 1344, 1257, 696 cm^{-1}; HRMS (ESI) m/z: $[M+H]^+$ Calcd for $C_{40}H_{43}FNO_2$ 588.3272; Found 588.3272.

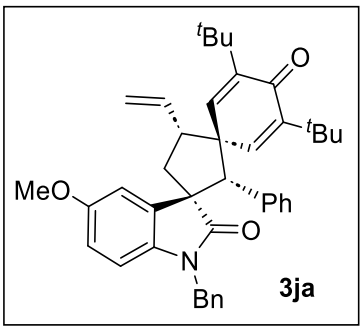

1''-Benzyl-3,5-di-*tert*-butyl-5''-methoxy-2'-phenyl-4'-vinyl-dispiro[cyclohexane-1,3'-cyclopentane-1',3''-indoline]-2,5-diene-2'',4-dione 3ja. Analytical TLC on silica gel, 1:24 ethyl acetate/hexane R_f = 0.22; colorless solid; mp 157-158

°C; yield 77% (46.2 mg); major diastereomer (15:1 dr): ^{1}H NMR (400 MHz, $CDCl_3$) δ 8.04-8.03 (m, 1H), 7.09-7.02 (m, 3H), 6.99-6.92 (m, 4H), 6.86-6.84 (m, 2H), 6.54-6.52 (m, 1H), 6.42-6.40 (m, 2H), 6.29-6.28 (m 1H), 6.23 (d, *J* = 8.4 Hz, 1H), 5.48-5.39 (m, 1H), 5.05 (d, *J* = 15.6 Hz, 1H), 4.97-4.92 (m, 2H), 4.22 (d, *J* = 16.0 Hz, 1H), 3.75 (s, 3H), 3.68 (s, 1H), 3.15-3.08 (m, 1H), 2.85-2.79 (m, 1H), 2.38-2.33 (m, 1H), 1.30 (s, 9H), 1.02 (s, 9H); ^{13}C NMR (125 MHz, $CDCl_3$) δ 186.6, 178.8, 156.5, 150.4, 148.7, 143.5, 140.0, 137.7, 135.8, 135.4, 135.3, 134.9, 129.6, 128.6, 127.8, 127.7, 127.2, 126.6, 117.1, 111.6, 110.3, 109.4, 69.6, 58.9, 56.5, 56.0, 55.5, 44.0, 42.0, 35.8, 34.8, 29.6; FT-IR (KBr) 2954, 1703, 1636, 1469, 1455, 1365, 1177, 748, 696 cm^{-1}; HRMS (ESI) m/z: $[M+H]^+$ Calcd for $C_{41}H_{46}NO_3$ 600.3472; Found 600.3472.

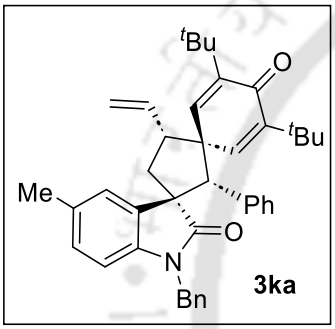

1''-Benzyl-3,5-di-*tert*-butyl-5''-methyl-2'-phenyl-4'-vinyl-dispiro[cyclohexane-1,3'-cyclopentane-1',3''-indoline]-2,5-diene-2'',4-dione 3ka. Analytical TLC on silica gel, 1:48 ethyl acetate/hexane R_f = 0.26; colorless solid; mp 189-190 °C; yield 76% (44.4 mg); major diastereomer (17:1 dr): ^{1}H NMR (500 MHz, $CDCl_3$) δ 8.058-5.052 (m, 1H), 7.25 (s, 1H), 7.07-7.01 (m, 2H), 6.98-6.91 (m, 4H), 6.84-6.80 (m, 3H), 6.42 (d, *J* = 7.0 Hz, 2H), 6.32-6.31 (m, 1H), 6.22 (d, *J* = 8.0 Hz, 1H), 5.47-5.41 (m, 1H), 5.04 (d, *J* = 16.0 Hz, 1H), 4.97-4.93 (m, 2H), 4.23 (d, *J* = 16.0 Hz, 1H), 3.70 (s, 1H), 3.17-3.11 (m, 1H), 2.83-2.78 (m, 1H), 2.37-2.34 (m, 1H), 2.33 (s, 3H), 1.30 (s, 9H), 1.03 (s, 9H); ^{13}C NMR (125 MHz, $CDCl_3$) δ 186.6, 179.1, 150.3, 148.6, 143.5, 140.1, 139.8, 136.3, 135.5, 135.3, 135.0, 132.7, 129.5, 128.6, 128.4, 127.8, 127.6, 127.1, 126.6, 122.7, 117.0, 108.9, 69.3, 58.6, 56.5, 55.5, 43.9, 42.1, 35.8, 34.8, 29.7, 29.6, 21.4; FT-IR (KBr) 2953, 1703, 1635, 1496, 1454, 1363, 1189, 806, 695 cm^{-1}; HRMS (ESI) m/z: $[M+H]^+$ Calcd for $C_{41}H_{46}NO_2$ 584.3523; Found 584.3528.

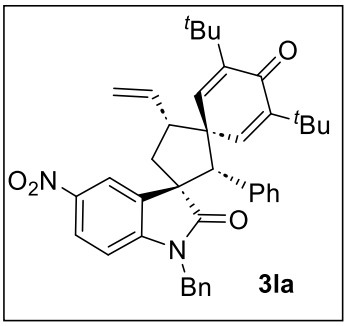

1''-Benzyl-3,5-di-*tert*-butyl-5''-nitro-2'-phenyl-4'-vinyldispiro [cyclohexane-1,3'-cyclopentane-1',3''-indoline]-2,5-diene-2'',4-dione 3la. Analytical TLC on silica gel, 1:24 ethyl acetate/hexane R_f = 0.21; colorless solid; mp >200 °C; yield 65% (40 mg); major diastereomer (>20:1 dr): ^{1}H NMR (500 MHz, $CDCl_3$) δ 8.358-8.353 (m, 1H), 8.01-7.99 (m, 1H), 7.947-7.941 (m, 1H), 7.12-7.06 (m, 2H), 7.01-6.94 (m, 4H), 6.83-6.81 (m, 2H), 6.41-6.33 (m, 4H), 5.48-5.41 (m, 1H), 5.11 (d, *J* = 16.0 Hz, 1H), 5.01- 4.98 (m, 2H), 4.30 (d, *J* = 16.0 Hz, 1H), 3.72 (s, 1H), 3.25-3.20 (m, 1H), 2.87-2.82 (m, 1H), 2.44-2.40 (m, 1H), 1.31 (s, 9H), 1.03 (s, 9H); ^{13}C NMR (150 MHz, $CDCl_3$) δ 186.3, 179.2, 150.8, 149.0, 147.9, 143.8, 142.8, 138.9, 137.0, 134.8, 133.9, 129.5, 128.9, 128.2, 128.1, 127.7, 126.4, 125.5, 118.0, 117.7, 108.8, 69.5, 58.4, 56.4, 55.3, 44.2, 41.7, 35.8, 34.9, 29.65, 29.61; FT-IR (KBr) 2954, 1723, 1614, 1519, 1490, 1335 cm^{-1}; HRMS (ESI) m/z: $[M+H]^+$ Calcd for $C_{40}H_{43}N_2O_4$ 615.3217; Found 615.3215.

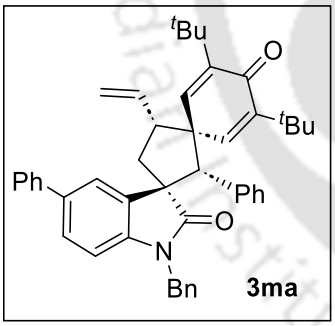

1''-Benzyl-3,5-di-*tert*-butyl-2',5''-diphenyl-4'-vinyldispiro [cyclohexane-1,3'-cyclopenta-ne-1',3''-indoline]-2,5-diene-2'',4-dione 3ma. Analytical TLC on silica gel, 1:49 ethyl acetate/hexane R_f = 0.25; colorless solid; mp 197-198 °C; yield 71% (45.8 mg); major diastereomer (15:1 dr): ^{1}H NMR (600 MHz, $CDCl_3$) δ 8.0 (s, 1H), 7.635-7.633 (m, 1H), 7.53-7.52 (m, 2H), 7.3 (t, *J* =7.8 Hz, 2H), 7.29-7.26 (m, 1H), 7.23-7.22 (m, 1H), 7.08-7.02 (m, 2H), 6.99-6.96 (m, 2H), 6.95-6.92 (m, 2H), 6.85-6.84 (m, 2H), 6.43 (d, *J* = 7.2 Hz, 2H), 6.39 (d, *J* = 7.8 Hz, 1H), 6.30 (s, 1H), 5.48-5.42 (m, 1H), 5.09 (d, *J* = 16.2 Hz, 1H), 4.97-4.94 (m, 2H), 4.26 (d, *J* = 16.2 Hz, 1H), 3.76 (s, 1H), 3.20-3.16 (m, 1H), 2.88-2.83 (m, 1H), 2.45-2.2 (m, 1H), 1.31 (s, 9H), 1.01 (s, 9H); ^{13}C NMR (150 MHz, $CDCl_3$) δ 186.5, 179.1, 150.4, 148.6, 143.4, 141.6, 141.1, 139.9, 136.8, 136.7, 135.3, 135.0, 134.7, 129.5, 129.0,

128.6, 127.9, 127.7, 127.3, 127.2, 127.19, 127.10, 126.5, 120.9, 117.2, 109.3, 69.5, 58.7, 56.5, 55.5, 43.9, 42.0, 35.7, 34.8, 29.67, 29.66; FT-IR (KBr) 2954,1706, 1631, 1484, 1357, 698 cm^{-1}; HRMS (ESI) m/z: $[M+H]^+$ Calcd for $C_{46}H_{48}NO_2$ 646.3680; Found 646.3679.

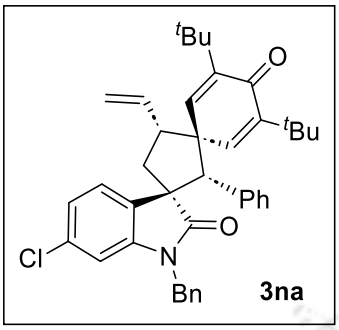

1''-Benzyl-3,5-di-*tert*-butyl-6''-chloro-2'-phenyl-4'-vinyldispiro [cyclohexane-1,3'-cyclopentane-1',3''-indoline]-2,5-diene-2'',4-dione 3na. Analytical TLC on silica gel, 1:24 ethyl acetate/hexane R_f = 0.23; colorless solid; mp 187-188 °C; yield 68% (41 mg); major diastereomer (19:1 dr): ^{1}H NMR (500 MHz, $CDCl_3$) δ 7.995-7.990 (m, 1H), 7.38 (d, *J* = 8.0 Hz, 1H), 7.09-7.01 (m, 3H), 6.99-6.93 (m, 4H), 6.83-6.81(m, 2H), 6.40 (d, *J* = 7.5 Hz, 2H), 6.32-6.31(m, 1H), 6.27-6.26 (m, 1H), 5.46-5.39 (m, 1H), 5.03 (d, *J* = 16.0 Hz, 1H), 4.97-4.92 (m, 2H), 4.21 (d, *J* = 16.0 Hz, 1H), 3.66 (s, 1H), 3.14-3.09 (m, 1H), 2.83-2.78 (m, 1H), 2.35-2.31 (m, 1H), 1.30 (s, 9H), 1.01 (s, 9H); ^{13}C NMR (150 MHz, $CDCl_3$) δ 186.4, 179.0, 150.3, 148.6, 143.3, 143.2, 139.7, 135.1, 134.47, 134.42, 133.7, 129.4, 128.7, 127.9, 127.8, 127.3, 126.3, 123.05, 123.02, 117.3, 109.7, 69.2, 58.2, 56.3, 55.4, 43.8, 41.8, 35.7, 34.8, 29.6, 29.5; FT-IR (KBr) 2954, 1712, 1634, 1607, 1366, 1254, 739, 696 cm^{-1}; HRMS (ESI) m/z: $[M+H]^+$ Calcd for $C_{40}H_{43}ClNO_2$ 604.2977; Found 604.2975.

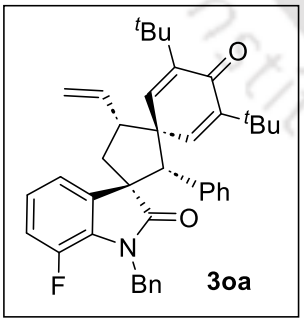

1''-Benzyl-3,5-di-*tert*-butyl-7''-fluoro-2'-phenyl-4'-vinyldispiro [cyclohexane-1,3'-cyclopentane-1',3''-indoline]-2,5-diene-2'',4-dione 3oa. Analytical TLC on silica gel, 1:24 ethyl acetate/hexane R_f = 0.23; colorless solid; mp 179-180 °C; yield 64% (37.8 mg); major diastereomer (>20:1 dr): ^{1}H NMR (500 MHz, $CDCl_3$) δ 8.079-8.073 (m, 1H), 7.34 (d, *J* = 7.5 Hz, 1H), 7.14-7.04 (m, 5H), 7.01-6.98 (m, 2H), 6.90-6.85 (m, 3H), 6.60-6.59 (m, 2H), 6.35-6.34 (m, 1H), 5.54-5.47 (m, 1H), 5.07-4.99 (m, 3H), 4.64 (d, *J* = 15.5 Hz, 1H), 3.77 (s, 1H), 3.23-3.17 (m, 1H), 2.91-2.86 (m, 1H), 2.45-2.40 (m, 1H), 1.37 (s, 9H), 1.09 (s,

9H); ^{13}C NMR (125 MHz, $CDCl_3$) δ 186.5, 178.8, 150.5, 148.8, 148.0 (J_{C-F} = 244.0 Hz), 143.2, 139.7, 139.2 (J_{C-F} = 3.1 Hz), 136.5, 135.2, 134.5, 129.5, 129.0 (J_{C-F} = 9.0 Hz), 128.4, 127.9, 127.8, 127.0, 126.5, 123.8 (J_{C-F} = 6.3 Hz), 118.0 (J_{C-F} = 2.8 Hz), 117.2, 116.4 (J_{C-F} = 19.5 Hz), 69.5, 58.8, 56.5, 55.4, 45.3, 42.5, 35.8, 34.8, 29.6; ^{19}F NMR (471 MHz, $CDCl_3$) δ -134.2; FT-IR (KBr) 2955, 1711, 1633, 1481, 1356, 1188, 702 cm^{-1}; HRMS (ESI) m/z: $[M+H]^+$ Calcd for $C_{40}H_{43}FNO_2$ 588.3272; Found 588.3274.

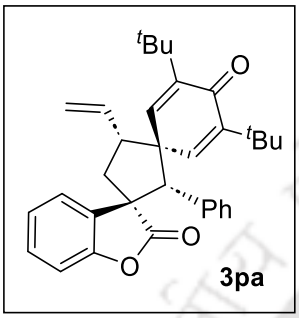

3'',5''-Di-*tert*-butyl-2'-phenyl-4'-vinyl-2H-dispiro[benzofuran-3,1'-cyclopentane-3',1''-cyclohexane]-2'',5''-diene-2,4''-dione 3pa. Analytical TLC on silica gel, 1:24 ethyl acetate/hexane R_f = 0.20; colorless solid; mp 167-168 °C; yield 49% (23.6 mg); major diastereomer (>20:1 dr): ^{1}H NMR (500 MHz, $CDCl_3$) δ 7.74-7.73 (m, 1H), 7.45-7.43 (m, 1H), 7.21-7.18 (m, 2H), 7.04-7.01 (m, 1H), 6.96-6.92 (m, 2H), 6.87-6.85 (m, 1H), 6.75-6.73 (m, 2H), 6.257-6.251 (m, 1H), 5.45-5.38 (m, 1H), 4.99-4.97 (m, 2H), 3.62 (s, 1H), 3.15-3.10 (m, 1H), 2.85-2.79 (m, 1H), 2.47-2.43 (m, 1H), 1.28 (s, 9H), 1.02 (s, 9H); ^{13}C NMR (150 MHz, $CDCl_3$) δ 186.4, 179.4, 152.5, 150.7, 149.4, 142.8, 138.6, 134.8, 133.9, 133.9, 129.2, 129.0, 128.2, 128.1, 125.1, 122.4, 117.7, 110.8, 69.9, 57.5, 56.4, 55.3, 42.7, 35.8, 35.0, 29.69, 29.63; FT-IR (KBr) 2955, 1795, 1635, 1463, 1042, 751 cm^{-1}; HRMS (ESI) m/z: $[M+H]^+$ Calcd for $C_{33}H_{37}O_3$ 481.2737; Found 481.2734.

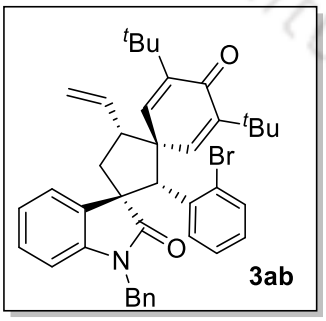

1''-Benzyl-2'-(2-bromophenyl)-3,5-di-*tert*-butyl-4'-vinyldispiro[cyclohexane-1,3'-cyclopentane-1',3''-indoline]-2,5-diene-2'',4-dione 3ab. Analytical TLC on silica gel, 1:49 ethyl acetate/hexane R_f = 0.25; colorless solid; mp > 200 °C; yield 63% (40.8 mg); major diastereomer (>20:1 dr): ^{1}H NMR (400 MHz, $CDCl_3$) δ 7.84-7.83 (m, 1H), 7.56-7.54 (m, 1H), 7.46-7.43 (m, 1H), 7.22-7.20 (m, 1H), 7.06-6.95 (m, 5H), 6.91-6.83 (m, 2H),

6.57-6.55 (m, 2H), 6.52-6.51 (m, 1H), 6.35-6.33 (m, 1H), 5.56-5.47 (m, 1H), 5.08-4.95 (m, 3H), 4.74 (s, 1H), 4.36 (d, J = 16.0 Hz, 1H), 3.31-3.24 (m, 1H), 2.94-2.87 (m, 1H), 2.45-2.39 (m, 1H), 1.26 (s, 9H), 1.01 (s, 9H); ^{13}C NMR (150 MHz, $CDCl_3$) δ 186.4, 179.2, 150.0, 149.2, 142.6, 141.8, 138.9, 135.7, 135.2, 134.7, 133.3, 132.3, 132.0, 129.0, 128.6, 128.2, 127.2, 126.78, 126.74, 126.5, 123.4, 123.0, 116.8, 109.0, 64.2, 58.1, 57.7, 55.0, 43.8, 42.0, 35.7, 34.8, 29.6, 29.4; FT-IR (KBr) 2954, 2867, 1702, 1636, 1467, 1364, 744 cm^{-1}; HRMS (ESI) m/z: $[M+H]^+$ Calcd for $C_{40}H_{43}BrNO_2$ 648.2472; Found 648.2470.

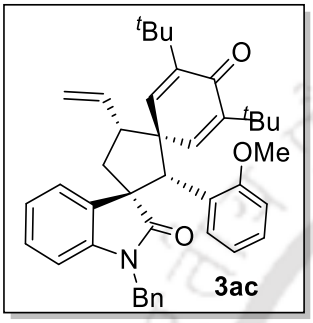

1''-Benzyl-3,5-di-*tert*-butyl-2'-(2-methoxyphenyl)-4'-vinyldispiro [cyclohexane-1,3'-cyclopentane-1',3''-indoline]-2,5-diene-2'',4-dione 3ac. Analytical TLC on silica gel, 1:24 ethyl acetate/hexane R_f = 0.20; colorless solid; mp 194-195 °C; yield 70% (42.1 mg); major diastereomer (>20:1 dr): ^{1}H NMR (400 MHz, $CDCl_3$) δ 8.00-7.99 (m, 1H), 7.50 (d, J = 7.2 Hz, 1H), 7.35-7.33 (m, 1H), 7.06-6.93 (m, 6H), 6.61-6.57 (m, 1H), 6.51-6.47 (m, 3H), 6.38-6.37 (m, 1H), 6.30 (d, J = 7.8 Hz, 1H), 5.51-5.43 (m, 1H), 5.12 (d, J = 16.0 Hz, 1H), 4.97-4.93 (m, 2H), 4.69 (s, 1H), 4.27 (d, J = 16.0 Hz, 1H), 3.25-3.19 (m, 1H), 3.16 (s, 3H), 2.88-2.81 (m, 1H), 2.40-2.34 (m, 1H), 1.29 (s, 9H), 1.00 (s, 9H); ^{13}C NMR (150 MHz, $CDCl_3$) δ 186.7, 179.7, 157.6, 149.7, 148.4, 143.7, 141.9, 140.5, 136.3, 135.9, 135.3, 130.8, 128.6, 128.3, 127.6, 127.1, 126.6, 123.4, 122.7, 122.6, 120.1, 116.7, 110.5, 108.8, 58.1, 57.4, 57.0, 55.6, 55.3, 43.8, 42.2, 35.7, 34.7, 29.6; FT-IR (KBr) 2953, 1704, 1634, 1489, 1466, 1364, 1243, 1104, 747 cm^{-1}; HRMS (ESI) m/z: $[M+H]^+$ Calcd for $C_{41}H_{46}NO_3$ 600.3472; Found: 600.3476.

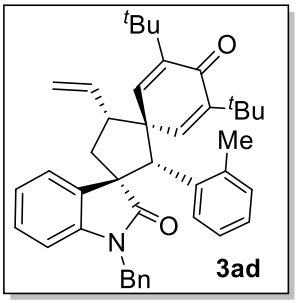

1''-Benzyl-3,5-di-*tert*-butyl-2'-(*o*-tolyl)-4'-vinyldispiro [cyclohexane-1,3'-cyclopentane-1',3''-indoline]-2,5-diene-2'',4-dione 3ad. Analytical TLC

on silica gel, 1:49 ethyl acetate/hexane R_f = 0.24; colorless solid; mp 187-189 °C; yield 75% (43.7 mg); major diastereomer (>20:1 dr): ^{1}H NMR (400 MHz, $CDCl_3$) δ 7.91-.90 (m, 1H), 7.49 (d, *J* = 7.2 Hz, 1H), 7.34 (d, *J* = 8.0 Hz, 1H), 7.03-6.90 (m, 6H), 6.83-6.77 (m, 2H), 6.40-6.38 (m, 2H), 6.33-6.32 (m, 1H), 6.28 (d, *J* = 7.6 Hz, 1H), 5.55-5.46 (m, 1H), 5.12 (d, *J* = 16.0 Hz, 1H), 5.00-4.95 (m, 2H), 4.24 (s, 1H), 3.26-3.19 (m, 1H), 2.95-2.89 (m, 1H), 2.43-2.38 (m, 1H), 1.75 (s, 3H), 1.29 (s, 9H), 0.98 (s, 9H); ^{13}C NMR (100 MHz, $CDCl_3$) δ 186.5, 179.4, 150.2, 148.6, 142.7, 142.1, 139.8, 136.6, 135.9, 135.1, 132.6, 130.5, 129.8, 128.6, 128.2, 127.4, 127.1, 126.4, 125.5, 122.8, 122.3, 116.7, 109.2, 62.9, 58.4, 57.7, 55.5, 43.8, 41.5, 35.7, 34.7, 29.6, 29.5, 20.6; FT-IR (KBr) 2953, 1706, 1636, 1488, 1467, 1363, 747 cm^{-1}; HRMS (ESI) m/z: $[M+H]^+$ Calcd for $C_{41}H_{46}NO_2$ 584.3523; Found 584.3524.

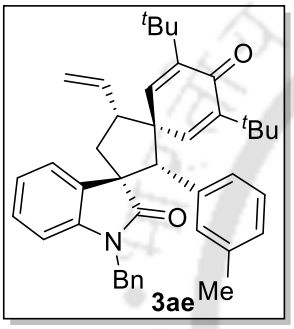

3ae

1''-Benzyl-3,5-di-*tert*-butyl-2'-(*m*-tolyl)-4'-vinyldispiro [cyclohexane-1,3'-cyclopentane-1',3''-indoline]-2,5-diene-2'',4-dione 3ae. Analytical TLC on silica gel, 1:49 ethyl acetate/hexane R_f = 0.25; colorless solid; mp 127-128 °C; yield 73% (42.4 mg); major diastereomer (>20:1 dr): ^{1}H NMR (400 MHz, $CDCl_3$) δ 8.05-8.04 (m, 1H), 7.46-7.44 (m, 1H), 7.05-7.01 (m, 2H), 6.99-6.95 (m, 2H), 6.87-6.85 (m, 1H), 6.81-6.77 (m, 1H), 6.70 (s, 1H), 6.53-6.51 (m, 1H), 6.45-6.43 (m, 2H), 6.35 (d, *J* = 7.2 Hz, 1H), 6.29-6.28 (m, 1H), 5.47-5.38 (m, 1H), 5.09 (d, *J* = 16.0 Hz, 1H), 4.96-4.91 (m, 2H), 4.24 (d, *J* = 16.0 Hz, 1H), 3.69 (s, 1H), 3.16-3.09 (m, 1H), 2.83-2.76 (m, 1H), 2.38-2.33 (m, 1H), 1.98 (s, 3H), 1.30 (s, 9H), 1.03 (s, 9H); ^{13}C NMR (150 MHz, $CDCl_3$) δ 186.7, 179.2, 150.1, 148.4, 143.7, 142.2, 140.2, 137.2, 136.2, 135.4, 135.2, 134.8, 129.9, 128.6, 128.4, 128.1, 127.7, 127.1, 126.6, 126.4, 123.1, 122.0, 117.1, 109.0, 69.1, 58.5, 56.4, 55.5, 43.8, 42.0, 35.7, 34.8, 29.6, 29.6, 21.4; FT-IR (KBr) 2953, 1704, 1633, 1611, 1362, 737, 694 cm^{-1}; HRMS (ESI) m/z: $[M+H]^+$ Calcd for $C_{41}H_{46}NO_2$ 584.3523; Found 584.3526.

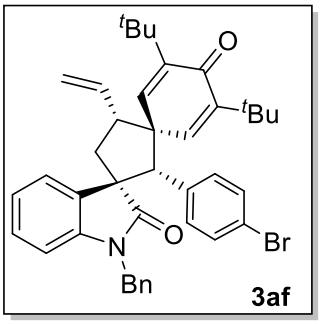

1''-Benzyl-2'-(4-bromophenyl)-3,5-di-*tert*-butyl-4'-vinyldispiro [cyclohexane-1,3'-cyclopentane-1',3''-indoline]-2,5-diene-2'',4-dione 3af. Analytical TLC on silica gel, 1:49 ethyl acetate/hexane R_f = 0.23; colorless solid; mp 189-190 °C; yield 77% (49.9 mg); major diastereomer (17:1 dr): ^{1}H NMR (600 MHz, $CDCl_3$) δ 8.029-8.024 (m, 1H), 7.46 (d, *J* = 6.6 Hz, 1H), 7.11-7.03 (m, 7H), 6.71 (d, *J* = 8.4 Hz, 1H), 6.40-6.37 (m, 3H), 6.276-6.272 (m, 1H), 5.44-5.38 (m, 1H), 5.12 (d, *J* = 15.6 Hz, 1H), 4.97-4.92 (m, 2H), 4.21 (d, *J* = 16.2 Hz, 1H), 3.67 (s, 1H), 3.16-3.11 (m, 1H), 2.81-2.77 (m, 1H), 2.39-2.35 (m, 1H), 1.30 (s, 9H), 1.03 (s, 9H); ^{13}C NMR (150 MHz, $CDCl_3$) δ 186.4, 178.8, 150.6, 149.0, 143.0, 142.1, 139.5, 135.7, 135.1, 135.0, 134.0, 131.1, 131.0, 128.7, 128.3, 127.4, 126.5, 123.3, 122.0, 121.9, 117.3, 109.2, 68.4, 58.4, 56.2, 55.6, 43.9, 41.9, 35.8, 34.9, 29.69, 29.66; FT-IR (KBr) 2954, 2919, 1707, 1635, 1612, 1489, 1363, 747, 696 cm^{-1}; HRMS (ESI) m/z: $[M+H]^+$ Calcd for $C_{40}H_{43}BrNO_2$ 648.2472; Found 648.2472.

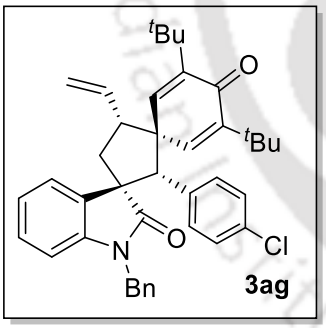

1''-Benzyl-3,5-di-*tert*-butyl-2'-(4-chlorophenyl)-4'-vinyldispiro [cyclohexane-1,3'-cyclopentane-1',3''-indoline]-2,5-diene-2'',4-dione 3ag. Analytical TLC on silica gel, 1:49 ethyl acetate/hexane R_f = 0.24; colorless solid; mp 172-173 °C; yield 72% (43.5 mg); major diastereomer (>20:1 dr): ^{1}H NMR (400 MHz, $CDCl_3$) δ 8.02-8.01 (m, 1H), 7.46-7.43 (m, 1H), 7.10-7.02 (m, 5H), 6.91-6.89 (m, 2H), 6.77-6.75 (m, 2H), 6.44-6.42 (m, 2H), 6.39-6.37 (m, 1H), 6.27-6.26 (m, 1H), 5.46-5.38 (m, 1H), 5.09 (d, *J* = 16.0 Hz, 1H), 4.98-4.92 (m, 2H), 4.23 (d, *J* = 16.0 Hz, 1H), 3.68 (s, 1H), 3.17-3.10 (m, 1H), 2.83-2.76 (m, 1H), 2.39-2.34 (m, 1H), 1.30 (s, 9H), 1.03 (s, 9H); ^{13}C NMR (100 MHz, $CDCl_3$) δ 186.4, 178.8, 150.7, 149.0, 143.1, 142.2, 139.5, 135.8, 135.1, 135.0, 133.7, 133.5, 130.8, 128.6, 128.4, 128.1, 127.4, 126.5, 123.3, 122.0, 117.3, 109.2, 68.5, 58.503, 56.3, 55.6, 43.9, 41.9, 35.8, 34.9, 29.7,

29.6; FT-IR (KBr) 2955, 1705, 1634, 1490, 1363, 1092, 710, 695 cm^{-1}; HRMS (ESI) m/z: $[M+H]^+$ Calcd for $C_{40}H_{43}ClNO_2$ 604.2977; Found 604.2978.

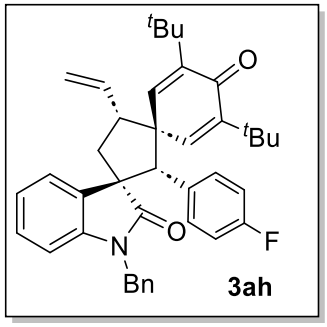

1''-Benzyl-3,5-di-*tert*-butyl-2'-(4-fluorophenyl)-4'-vinyldispiro [cyclohexane-1,3'-cyclopentane-1',3''-indoline]-2,5-diene-2'',4-dione 3ah. Analytical TLC on silica gel, 1:24 ethyl acetate/hexane R_f = 0.12; colorless solid; mp 143-145 °C; yield 67% (39.4 mg); major diastereomer (>20:1 dr): ^{1}H NMR (600 MHz, $CDCl_3$) δ 8.01-8.00 (m, 1H), 7.46-7.44 (m, 1H), 7.08-6.99 (m, 5H), 6.82-6.78 (m, 2H), 6.63-6.59 (m, 2H), 6.45-6.43 (m, 2H), 6.39-6-6.37 (m, 1H), 6.27-6.26 (m, 1H), 5.48-5.39 (m, 1H), 5.07 (d, *J* = 24.0 Hz, 1H),), 4.97-4.92 (m, 2H), 4.26 (d, *J* = 24.0 Hz, 1H), 3.69 (s, 1H), 3.17-3.10 (m, 1H), 2.84-2.77 (m, 1H), 2.40-2.34 (m, 1H), 1.30 (s, 9H), 1.03 (s, 9H); ^{13}C NMR (100 MHz, $CDCl_3$) δ 186.5, 178.9, 163.7 (J_{C-F} = 247.2 Hz), 150.6, 149.0, 143.2, 142.2, 139.6, 135.9, 135.3, 135.1, 131.2 (J_{C-F} = 7.7Hz), 130.7 (J_{C-F} = 3.2), 128.6, 128.3, 127.4, 126.5, 123.3, 122.0, 117.2, 114.8 (J_{C-F} = 21.1 Hz), 109.1, 68.5, 58.5, 56.4, 55.4, 43.8, 41.8, 35.8, 34.9, 29.6, 29.6; ^{19}F NMR (377 MHz, $CDCl_3$) δ -114.7; FT-IR (KBr) 2955, 1707, 1636, 1612, 1363, 1230, 747 cm^{-1}; HRMS (ESI) m/z: $[M+H]^+$ Calcd for $C_{40}H_{43}FNO_2$ 588.3272; Found 588.3285.

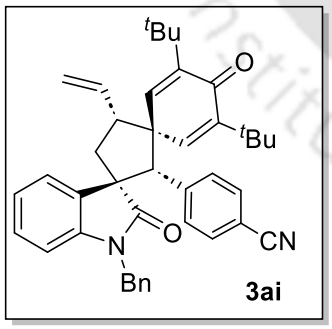

1''-Benzyl-3,5-di-*tert*-butyl-2'',4-dioxo-4'-vinyldispiro [cyclohexane-1,3'-cyclopentane-1',3''-indoline]-2,5-dien-2'-yl)benzonitrile 3ai. Analytical TLC on silica gel, 1:24 ethyl acetate/hexane R_f = 0.22; colorless solid; mp 172-173 °C; yield 53% (31.5 mg); major diastereomer (16:1 dr): ^{1}H NMR (500 MHz, $CDCl_3$) δ 7.997-7.992 (m, 1H), 7.47-7.45 (m, 1H), 7.18 (d, *J* = 8.0 Hz, 1H), 7.13-7.07 (m, 3H), 7.06-7.03 (m, 2H), 6.92 (d, *J* = 8.5 Hz, 2H), 6.51 (d, *J* = 7.5 Hz, 2H) 6.47-6.45 (m, 1H), 6.266-6.260 (m, 1H), 5.45-5.38 (m, 1H), 4.99-4.94 (m, 3H), 4.28 (d, *J* = 16.0 Hz, 1H), 3.72 (s, 1H), 3.18-3.13 (m, 1H),

2.83-2.78 (m, 1H), 2.41-2.36 (m, 1H), 1.30 (s, 1H), 1.02 (s, 1H); ^{13}C NMR (150 MHz, $CDCl_3$) δ 186.2, 178.5, 150.9, 149.3, 142.5, 142.1, 140.5, 139.0, 135.3, 135.0, 134.7, 131.5, 130.1, 128.69, 128.67, 126.6, 123.5, 122.1, 118.6, 117.6, 111.6, 109.2, 68.5, 58.3, 56.2, 55.6, 43.9, 42.0, 35.8, 34.9, 29.6; FT-IR (KBr) 2955, 2923, 2227, 1706, 1636, 1610, 1364, 748 cm^{-1}; HRMS (ESI) m/z: $[M+H]^+$ Calcd for $C_{41}H_{43}N_2O_2$ 595.3319; Found: 595.3321.

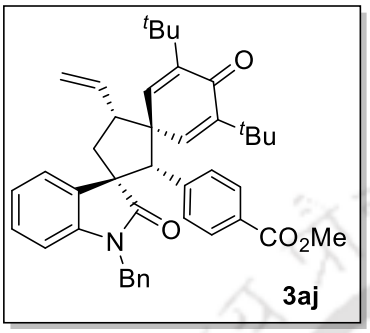

Methyl-4-(1''-benzyl-3,5-di-*tert*-butyl-2'',4-dioxo-4'-vinyldispiro[cyclohexane-1,3'-cyclopentane-1',3''-indoline]-2,5-dien-2'-yl) benzoate 3aj. Analytical TLC on silica gel, 1:49 ethyl acetate/hexane R_f = 0.23; coloress solid; mp 167-168 °C; yield 49% (30.8 mg); major diastereomer (16:1 dr): ^{1}H NMR (500 MHz, $CDCl_3$) δ 8.06-8.05 (m, 1H), 7.60 (d, *J* = 8.5 Hz, 2H), 7.48-7.46 (m, 1H), 7.08-7.00 (m, 3H), 6.95-6.92 (m, 2H), 6.89 (d, *J* = 5.0 Hz, 2H), 6.46 (d, *J* = 7.5 Hz, 2H), 6.39 (d, *J* = 7.5 Hz, 1H), 6.29-6.28 (m, 1H), 5.46-5.39 (m, 1H), 4.98-4.93 (m, 3H), 4.26 (d, *J* = 16.0 Hz, 1H), 3.76 (s, 4H), 3.19-3.13 (m, 1H), 2.84-2.78 (m, 1H), 2.40-2.36 (m, 1H), 1.31 (s, 9H), 1.02 (s, 9H); ^{13}C NMR (150 MHz, $CDCl_3$) δ 186.3, 178.7, 166.8, 150.6, 148.9, 142.9, 142.1, 140.3, 139.6, 135.6, 135.09, 135.03, 129.4, 129.3, 129.1, 128.5, 128.4, 127.3, 126.6, 123.3, 122.0, 117.4, 109.2, 68.7, 58.4, 56.2, 55.6, 52.1, 43.9, 41.9, 35.8, 34.8, 29.6; FT-IR (KBr) 2953, 1710, 1632, 1614, 1360, 1279, 1110, 744 cm^{-1}; HRMS (ESI) m/z: $[M+H]^+$ Calcd for $C_{42}H_{46}NO_4$ 628.3421; Found 628.3416.

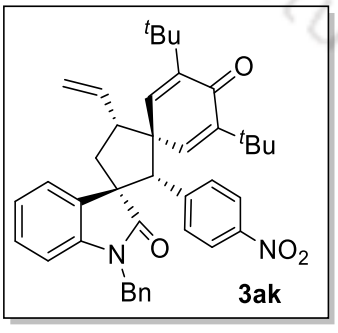

1''-Benzyl-3,5-di-*tert*-butyl-2'-(4-nitrophenyl)-4'-vinyldispiro [cyclohexane-1,3'-cyclopentane-1',3''-indoline]-2,5-diene-2'',4-dione 3ak. Analytical TLC on silica gel, 1:49 ethyl acetate/hexane R_f = 0.20; colorless solid; mp 169-170 °C; yield 47% (28.9 mg); major diastereomer (>20:1 dr): ^{1}H NMR (500 MHz, $CDCl_3$) δ 8.025-8.020 (m, 1H), 7.72 (d, *J* = 8.5 Hz, 1H), 7.49-7.47 (m, 1H), 7.11-7.09 (m, 2H), 7.05-7.02 (m, 1H), 6.96-6.93

(m, 4H), 6.56 (d, J = 7.5 Hz, 2H), 6.51-6.49 (m, 1H), 6.279-6.274 (m, 1H), 5.45-5.38 (m, 1H), 5.00-4.92 (m, 3H), 4.29 (d, J = 16.0 Hz, 1H), 3.79 (s, 1H), 3.19-3.14 (m, 1H), 2.34-2.78 (m, 1H), 2.42-2.37 (m, 1H), 1.31 (s, 9H), 1.02 (s, 9H); ^{13}C NMR (150 MHz, $CDCl_3$) δ 186.2, 178.4, 151.0, 149.4, 147.3, 142.7, 142.4, 142.1, 139.0, 135.3, 135.1, 134.7, 130.1, 128.7, 128.5, 127.7, 126.8, 123.5, 122.9, 122.1, 117.7, 109.2, 68.0, 58.4, 56.2, 55.7, 43.9, 42.0, 35.9, 34.9, 29.6; FT-IR (KBr) 2956, 1704, 1519, 1344 cm^{-1}; HRMS (ESI) m/z: $[M+H]^+$ Calcd for $C_{40}H_{43}N_2O_4$ 615.3217; Found 615.3217.

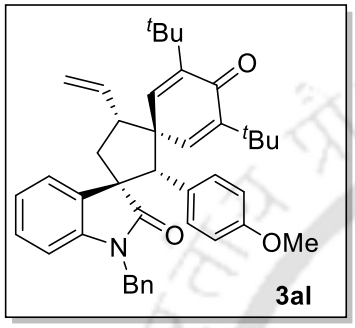

1''-Benzyl-3,5-di-*tert*-butyl-2'-(4-methoxyphenyl)-4'-vinyl-dispiro[cyclohexane-1,3'-cyclopentane-1',3''-indoline]-2,5-diene-2'',4-dione 3al. Analytical TLC on silica gel, 1:24 ethyl acetate/hexane R_f = 0.19; colorless solid; mp 187-188 °C; yield 87% (52.2 mg); major diastereomer (18:1 dr): ^{1}H NMR (600 MHz, $CDCl_3$) δ 8.039-8.034 (m, 1H), 7.46 (d, J = 7.2 Hz, 1H), 7.07-6.96 (m, 5H), 6.75-6.73 (m, 2H), 6.46 (d, J = 8.4 Hz, 2H), 6.39 (d, J = 7.2 Hz, 2H), 6.34 (d, J =7.8 Hz, 1H), 6.29-6.28 (m, 1H), 5.46-5.40 (m, 1H), 5.11 (d, J = 16.2 Hz, 1H), 4.96-4.92 (m, 2H), 4.22 (d, J = 16.2 Hz, 1H), 3.68 (s, 1H), 3.60 (s, 3H), 3.15-3.11 (m, 1H), 2.82-2.78 (m, 1H), 2.37-2.34 (m, 1H), 1.31(s, 9H), 1.03 (s, 9H); ^{13}C NMR (150 MHz, $CDCl_3$) δ 186.6, 179.2, 159.0, 150.3, 148.6, 143.7, 142.2, 140.1, 136.2, 135.5, 135.1, 130.6, 128.5, 128.1, 127.2, 126.8, 126.5, 123.1, 122.0, 117.0, 113.1, 109.1, 68.8, 58.6, 56.5, 55.5, 55.0, 43.7, 41.7, 35.7, 34.8, 29.7, 29.6; FT-IR (KBr) 2955, 1704, 1611, 1513, 1466, 1362, 1250, 735, 696 cm^{-1}; HRMS (ESI) m/z: $[M+H]^+$ Calcd for $C_{41}H_{46}NO_3$ 600.3472; Found 600.3471.

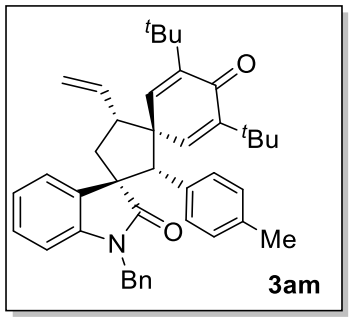

1''-Benzyl-3,5-di-*tert*-butyl-2'-(*p*-tolyl)-4'-vinyldispiro [cyclohexane-1,3'-cyclopentane-1',3''-indoline]-2,5-diene-2'',4-dione 3am. Analytical

TLC on silica gel, 1:24 ethyl acetate/hexane R_f = 0.25; colorless solid; mp 177-178 °C; yield 80% (47 mg); major diastereomer (>20:1 dr): ^{1}H NMR (400 MHz, $CDCl_3$) δ 8.05-8.04 (m, 1H), 7.46 (d, *J* = 7.2 Hz, 1H), 7.06-6.93 (m, 5H), 6.74-6.68 (m, 4H), 6.42-6.40 (m, 2H), 6.32-6.28 (m, 2H), 5.47- 5.38 (m, 1H), 5.10 (d, *J* = 16.0 Hz, 1H), 4.96-4.91 (m, 2H), 4.22 (d, *J* = 16.0 Hz, 1H), 3.69 (s, 1H), 3.17-3.10 (m, 1H), 2.83-2.77 (m, 1H), 2.38-2.32 (m, 1H), 2.14 (s, 1H), 1.31 (s, 9H), 1.03 (s, 9H); ^{13}C NMR (100 MHz, $CDCl_3$) δ 186.6, 179.1, 150.2, 148.5, 143.6, 142.2, 140.2, 137.0, 136.2, 135.4, 135.2, 131.8, 129.3, 128.5, 128.4, 128.1, 127.1, 126.6, 123.1, 122.0, 117.0, 109.1, 69.1, 58.6, 56.5, 55.5, 43.8, 41.9, 35.7, 34.8, 29.7, 29.6, 21.1; FT-IR (KBr) 2954, 1705, 1656, 1634, 1611, 1362, 806, 736, 696 cm^{-1}; HRMS (ESI) m/z: $[M+H]^+$ Calcd for $C_{41}H_{46}NO_2$ 584.3523; Found 584.3522.

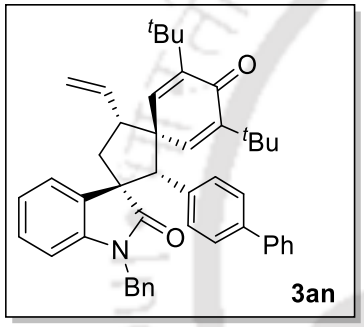

([1,1'-Biphenyl]-4-yl)-1''-benzyl-3,5-di-*tert*-butyl-4'-vinyl-dispiro[cyclohexane-1,3'-cyclopentane-1',3''-indoline]-2,5-diene-2'',4-dione 3an. Analytical TLC on silica gel, 1:49 ethyl acetate/hexane R_f = 0.23; colorless solid; mp >200 °C; yield 70% (45 mg); major diastereomer (16:1 dr): ^{1}H NMR (600 MHz, $CDCl_3$) δ 8.17-8.16 (m, 1H), 7.58-8.56 (m, 1H), 7.49-7.47 (m, 2H), 7.39-7.36 (m, 2H), 7.31-7.27 (m, 3H), 7.17-7.14 (m, 1H), 7.11-7.09 (m, 1H), 6.99-6.95 (m, 3H), 6.91-6.88 (m, 2H), 6.49-6.48 (m, 2H), 6.42-6.40 (m, 2H), 5.55-5.49 (m, 1H), 5.22 (d, *J* = 16.2 Hz, 1H), 5.05-5.01 (m, 2H), 4.30 (d, *J* = 16.2 Hz, 1H), 3.86 (s, 1H), 3.28-3.23 (m, 1H), 2.94-2.89 (m, 1H), 2.49-2.45 (m, 1H), 1.40 (s, 9H), 1.11 (s, 9H); ^{13}C NMR (150 MHz, $CDCl_3$) δ 186.5, 179.1, 150.3, 148.6, 143.5, 142.1, 140.4, 140.1, 140.0, 136.1, 135.3, 135.0, 134.0, 129.9, 128.8, 128.6, 128.2, 127.3, 127.1, 126.9, 126.4, 126.3, 123.2, 122.0, 117.2, 109.2, 68.9, 58.5, 56.5, 55.5, 43.8, 41.9, 35.8, 34.8, 29.6; FT-IR (KBr) 2954, 2915, 1707, 1635, 1488, 1363, 747, 696 cm^{-1}; HRMS (ESI) m/z: $[M+H]^+$ Calcd for $C_{46}H_{48}NO_2$ 646.3680; Found 646.3680.

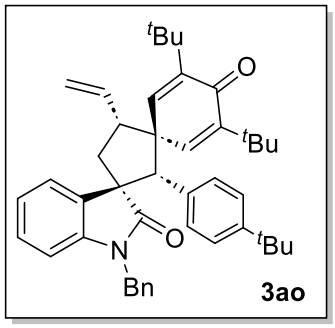

1''-Benzyl-3,5-di-*tert*-butyl-2'-(4-(*tert*-butyl)phenyl)-4'-vinyl-dispiro[cyclohexane-1,3'-cyclopentane-1',3''-indoline]-2,5-diene-2'',4-dione 3ao. Analytical TLC on silica gel, 1:49 ethyl acetate/hexane R_f = 0.37; colorless solid; mp 197-198 °C; yield 68% (42.4 mg); major diastereomer (13:1 dr): ^{1}H NMR (400 MHz, $CDCl_3$) δ 7.99-7.98 (m, 1H), 7.46-7.44 (m, 1H), 7.06-6.98 (m, 5H), 6.94-6.92 (m, 2H), 6.76-6.74 (m, 2H), 6.66-6.64 (m, 2H), 6.35 (d, *J* = 7.2 Hz, 1H), 6.299-6.292 (m, 1H), 5.49-5.40 (m, 1H), 5.05 (d, *J* = 16.0 Hz, 1H), 4.96-4.92 (m, 2H), 4.34 (d, *J* = 16.0 Hz, 1H), 3.72 (s, 1H), 3.17-3.10 (m, 1H), 2.85-2.78 (m, 1H), 2.37-2.32 (m, 1H), 1.29 (s, 1H), 1.11 (s, 1H), 1.01 (s, 1H); ^{13}C NMR (100 MHz, $CDCl_3$) δ 186.5, 179.4, 150.3, 150.1, 148.6, 143.7, 142.2, 140.1, 136.6, 135.6, 135.3, 131.8, 129.2, 128.6, 128.1, 127.2, 126.8, 124.4, 123.1, 122.0, 117.0, 109.3, 68.7, 58.1, 56.7, 55.2, 44.0, 42.5, 35.7, 34.8, 34.4, 31.3, 29.6, 29.5; FT-IR (KBr) 2955, 1707, 1636, 1466, 1363, 747 cm^{-1}. HRMS (ESI) m/z: $[M+H]^+$ Calcd for $C_{44}H_{52}NO_2$ 626.3993; Found 626.3995.

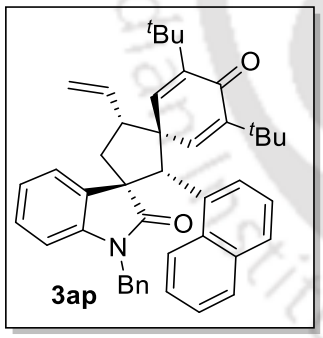

1''-Benzyl-3,5-di-*tert*-butyl-2'-(naphthalen-1-yl)-4'-vinyldispiro [cyclohexane-1,3'-cyclopentane-1',3''-indoline]-2,5-diene-2'',4-dione 3ap. Analytical TLC on silica gel, 1:49 ethyl acetate/hexane R_f = 0.30; colorless solid; mp 197-198 °C; yield 71% (44 mg); major diastereomer (18:1 dr): ^{1}H NMR (400 MHz, $CDCl_3$) δ 8.029-8.022 (m, 1H), 7.66-7.65 (m, 1H), 7.62-7.60 (m, 2H), 7.55 (d, *J* = 8.4 Hz, 2H), 7.20-7.18 (m, 1H), 7.12-7.04 (m, 3H), 6.97-6.94 (m, 1H), 6.92-6.88 (m, 1H), 6.85-6.81 (m, 2H), 6.31-6.27 (m, 3H), 6.15 (d, *J* = 8.0 Hz, 1H), 5.59-5.50 (m, 1H), 5.03-5.02 (m, 1H), 5.00-4.98 (m, 2H), 4.86 (s, 1H), 4.23 (d, *J* = 16.0 Hz, 1H), 3.38-3.31 (m, 1H), 3.04-2.97 (m, 1H), 2.53-2.47 (m, 1H), 1.31 (s, 9H), 0.74 (s, 9H); ^{13}C NMR (100 MHz, $CDCl_3$) δ 186.3, 179.5, 150.0, 148.9, 143.1, 142.1, 139.8, 135.8, 135.7, 135.0, 133.6, 132.6, 130.1, 128.9, 128.5, 128.4, 128.26, 128.23, 127.1, 126.3,

125.7, 124.9, 124.7, 123.0, 122.17, 122.12, 116.9, 109.2, 61.0, 58.5, 57.7, 55.5, 43.8, 41.9, 35.7, 34.6, 29.6, 29.2; FT-IR (KBr) 2954, 1706, 1612, 1488, 1363, 744, 696 cm^{-1}; HRMS (ESI) m/z: $[M+H]^+$ Calcd for $C_{44}H_{46}NO_2$ 620.3523; Found 620.3523.

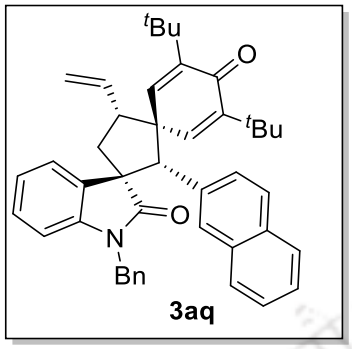

1''-Benzyl-3,5-di-*tert*-butyl-2'-(naphthalen-2-yl)-4'-vinyl-dispiro[cyclohexane-1,3'-cyclopentane-1',3''-indoline]-2,5-diene-2'',4-dione 3aq. Analytical TLC on silica gel, 1:49 ethyl acetate/hexane R_f = 0.30; colorless solid; 157-158 °C; yield 73% (45.2 mg); major diastereomer (>20:1 dr): ^{1}H NMR (500 MHz, $CDCl_3$) δ 8.217-8.214 (m, 1H), 7.62 (d, *J* = 8.0 Hz, 1H), 7.53 (d, *J* = 7.5 Hz, 1H), 7.47-7.46 (m, 1H), 7.38-7.35 (m, 2H), 7.34-7.31(m, 1H), 7.29-7.26 (m, 1H), 7.10-7.07 (m, 1H), 7.04-7.01 (m, 1H), 6.87-6.86 (m, 1H), 6.82-6.79 (m, 1H), 6.46-6.43 (m, 2H), 6.359-6.354 (m, 1H), 6.31 (d, *J* = 8.0 Hz, 1H), 6.19-6.17 (m, 2H), 5.49-5.42 (m, 1H), 5.02-4.94 (m, 3H), 4.14 (d, *J* = 16.0 Hz, 1H), 3.92 (s, 1H), 3.23-3.17 (m, 1H), 2.88-2.83 (m, 1H), 2.43-2.39 (m, 1H), 1.36 (s, 9H), 1.00 (s, 9H); ^{13}C NMR (125 MHz, $CDCl_3$) δ 186.7, 179.2, 150.6, 148.9, 143.6, 142.4, 140.3, 136.3, 135.4, 135.0, 133.1, 133.0, 132.9, 128.4, 128.4, 127.66, 127.63, 127.5, 127.2, 126.5, 126.07, 126.05, 123.3, 122.2, 117.4, 109.3, 69.3, 58.8, 56.6, 55.9, 44.0, 42.3, 36.0, 35.0, 29.9, 29.8; FT-IR (KBr) 2955, 2918, 1707, 1635, 1467, 1363, 745 cm^{-1}; HRMS (ESI) m/z: $[M+H]^+$ Calcd for $C_{44}H_{46}NO_2$ 620.3523; Found 620.3524.

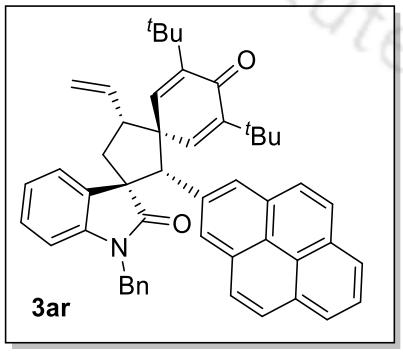

1''-Benzyl-3,5-di-*tert*-butyl-2'-(pyren-1-yl)-4'-vinyldispiro [cyclohexane-1,3'-cyclopentane-1',3''-indoline]-2,5-diene-2'',4-dione 3ar. Analytical TLC on silica gel, 1:49 ethyl acetate/hexane R_f = 0.22; colorless solid; mp >200 °C; yield 67% (46.4 mg); major diastereomer (>20:1 dr): ^{1}H NMR (500 MHz, $CDCl_3$) δ 8.249-8.2444 (m, 1H), 8.16

(d, J = 8.5 Hz, 1H), 8.06-8.04 (m, 1H), 7.95-7.93 (m, 1Hz), 7.86-7.83 (m, 2H), 7.81-7.79 (m, 1H), 7.76-7.75 (m, 2H), 7.69-7.67 (m, 1H), 7.13-7.10 (m, 1H), 6.89-6.86 (m, 1H), 6.66-6.63 (m, 1H), 6.418-6.412 (m, 1H), 6.24-6.21 (m, 2H), 6.02 (d, J = 8.0 Hz, 1H), 5.87 (d, J = 8.0 Hz, 2H), 5.61-5.54 (m, 1H), 5.14 (s, 1H), 5.06-5.02 (m, 2H), 4.95 (d, J = 16.0 Hz, 1H), 4.09 (d, J = 16.0 Hz, 1H), 3.47-3.41 (m, 1H), 3.11-3.05 (m, 1H), 2.60-2.56 (m, 1H), 1.38 (s, 9H), 0.74 (s, 9H); ^{13}C NMR (125 MHz, $CDCl_3$) δ 186.4, 179.3, 150.4, 148.9, 143.0, 142.2, 140.1, 135.7, 135.4, 134.6, 131.3, 130.6, 130.4, 129.9, 128.5, 128.3, 128.1, 128.0, 127.7, 127.4, 127.3, 126.8, 125.9, 125.8, 125.3, 124.9, 124.7, 124.6, 124.3, 123.1, 122.2, 121.9, 117.1, 109.2, 62.0, 59.1, 57.8, 56.0, 43.7, 41.7, 35.9, 34.6, 29.7, 29.4; FT-IR (KBr) 2954, 2914, 1704, 1636, 1466, 1363, 843, 746 cm^{-1}; HRMS (ESI) m/z: $[M+H]^+$ Calcd for $C_{50}H_{48}NO_2$ 694.3680; Found 694.3678.

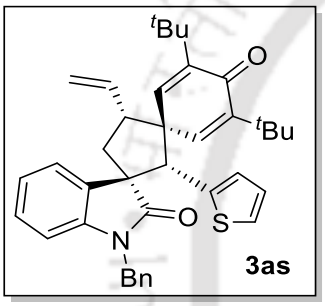

1''-Benzyl-3,5-di-*tert*-butyl-2'-(thiophen-2-yl)-4'-vinyldispiro [cyclohexane-1,3'-cyclopenta-ne-1',3''-indoline]-2,5-diene-2'',4-dione 3as. Analytical TLC on silica gel, 1:49 ethyl acetate/hexane R_f = 0.30; colorless solid; mp 147-148 °C; yield 74% (42.6 mg); major diastereomer (>20:1 dr): ^{1}H NMR (500 MHz, $CDCl_3$) δ 8.00-7.99 (m, 1H), 7.43-7.42 (m, 1H), 7.06-7.05 (m, 5H), 6.90-6.89 (m, 1H), 6.64-6.62 (m, 1H), 6.58-6.57 (m, 2H), 6.43-6.41 (m, 2H), 6.29-6.28 (m, 1H), 5.44-5.38 (m, 1H), 5.05 (d, J = 16.0 Hz, 1H), 4.96-4.91 (m, 2H), 4.32 (d, J = 16.0 Hz, 1H), 4.05 (s, 1H), 3.15-3.09 (m, 1H), 2.79-2.74 (m, 1H), 2.38-2.33 (m, 1H), 1.31(s, 9H), 1.07 (s, 9H); ^{13}C NMR (125 MHz, $CDCl_3$) δ 186.6, 178.8, 150.8, 149.8, 143.0, 142.5, 139.0, 136.3, 135.9, 135.3, 135.2, 128.7, 128.3, 127.2, 126.79, 126.77, 126.2, 124.4, 123.2, 122.0, 117.3, 109.2, 63.7, 58.6, 56.6, 55.4, 44.0, 41.9, 35.8, 34.9, 29.7, 29.5; FT-IR (KBr) 2954, 2913, 1706, 1635, 1612, 1488, 1466, 1362, 740, 696 cm^{-1}; HRMS (ESI) m/z: $[M+H]^+$ Calcd for $C_{38}H_{42}NO_2S$ 576.2931; Found 576.2935.

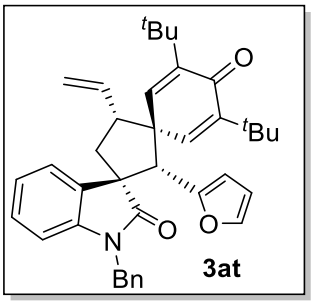

1''-Benzyl-3,5-di-*tert*-butyl-2'-(furan-2-yl)-4'-vinyldispiro [cyclohexane-1,3'-cyclopentane-1',3''-indoline]-2,5-diene-2'',4-dione 3at. Analytical TLC on silica gel, 1:49 ethyl acetate/hexane R_f = 0.29; colorless solid; mp 179-180 °C; yield 82% (45.9 mg); major diastereomer (9:1 dr): ^{1}H NMR (500 MHz, $CDCl_3$) δ 7.83-7.82 (m, 1H), 7.41-7.40 (m, 1H), 7.14-7.13 (m, 3H), 7.08-7.03 (m, 2H), 6.91-6.89 (m, 3H), 6.52-6.51 (m, 1H), 6.35-6.36 (m, 1H), 6.02-6.01 (m, 1H), 5.876-5.870 (m, 1H), 5.43-5.36 (m, 1H), 5.06 (d, *J* = 16.0 Hz, 1H), 4.96-4.91 (m, 2H), 4.48 (d, *J* = 15.5 Hz, 1H), 3.92 (s, 1H), 3.14-3.08 (m, 1H), 2.75-2.69 (m, 1H), 2.32-2.28 (m, 1H), 1.26 (s, 9H), 1.12 (s, 9H); ^{13}C NMR (125 MHz, $CDCl_3$) δ 186.7, 178.8, 150.5, 149.8, 149.1, 142.9, 142.3, 141.0, 139.4, 136.40, 135.60, 135.0, 128.7, 128.2, 127.4, 127.1, 123.2, 122.0, 117.4, 110.3, 109.2, 108.4, 60.8, 57.0, 55.6, 55.3, 44.0, 42.8, 35.7, 34.9, 29.73, 29.71; FT-IR (KBr) 2953, 1705, 1634, 1612, 1493, 1469, 1376, 1347, 742, 702 cm^{-1}; HRMS (ESI) m/z: $[M+H]^+$ Calcd for $C_{38}H_{42}NO_3$ 560.3159; Found 560.3158.

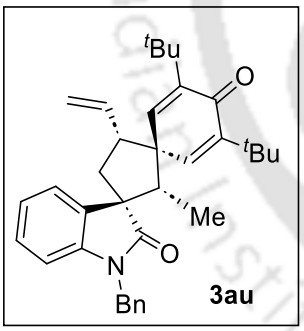

1''-Benzyl-3,5-di-*tert*-butyl-2'-methyl-4'-vinyldispiro [cyclohexane-1,3'-cyclopentane-1',3''-indoline]-2,5-diene-2'',4-dione 3au. Analytical TLC on silica gel; 1:49 ethyl acetate/hexane R_f = 0.29; colorless solid; mp 169-170 °C; yield 69% (70 mg); major diastereomer (>20:1 dr): ^{1}H NMR (500 MHz, $CDCl_3$) δ 7.58 (s, 1H), 7.38 (d, *J* = 7.0 Hz, 1H), 7.23-7.25 (m, 5H), 7.17-7.14 (m, 1H), 7.10-7.07 (m, 1H), 6.69 (d, *J* = 7.5 Hz, 1H), 6.34 (s, 1H), 5.51-5.44 (m, 1H), 5.12 (d, *J* = 15.5 Hz, 1H), 4.99-4.96 (m, 2H), 4.77 (d, *J* = 16.0 Hz, 1H), 3.12-3.07 (m, 1H), 2.71-2.66 (m, 1H), 2.62 (q, *J* = 7.2 Hz, 1H), 2.35-2.28 (m, 1H), 1.33 (s, 9H), 1.25 (s, 9H), 0.62 (d, *J* = 7.0 Hz, 3H); ^{13}C NMR (125 MHz, $CDCl_3$) δ 187.1, 179.2, 150.5, 149.4, 143.8, 142.3, 139.6, 136.7, 136.0, 135.7, 128.8, 127.9, 127.7, 127.3, 123.1, 122.3, 116.6, 109.0, 57.0, 56.8, 55.8, 55.3, 44.1, 42.3, 35.7, 35.0, 29.9, 29.8, 10.3; FT-IR (KBr)

2954, 2867, 1705, 1635, 1612, 1487, 1456, 1358, 1171, 921, 741 cm^{-1}; HRMS (ESI) m/z: $[M+H]^+$ Calcd for $C_{35}H_{42}NO_2$ 508.3210; Found 508.3238.

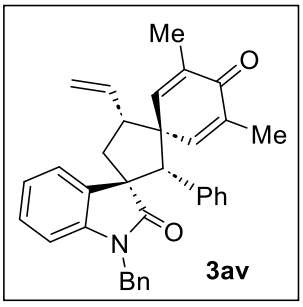

1''-Benzyl-3,5-dimethyl-2'-phenyl-4'-vinyldispiro[cyclohexane-1,3'-cyclopentane-1',3''-indoline]-2,5-diene-2'', 4-dione 3av. Analytical TLC on silica gel; 1:20 ethyl acetate/hexane R_f= 0.21; colorless solid; mp 183-184 °C; yield 42% (45 mg); major diastereomer 12:1 dr): ^{1}H NMR (400 MHz, $CDCl_3$) δ 8.25-8.24 (m, 1H), 7.52-7.50 (m, 1H), 7.18-7.09 (m, 4H), 7.07-7.00 (m, 4H), 6.89-6.87 (m, 2H), 6.51-6.50 (m, 1H), 6.45-6.41 (m, 3H), 5.58-5.49 (m, 1H), 5.098-5.02 (m, 3H), 4.29 (d, *J* = 16.0 Hz, 1H), 3.83 (s, 1H), 3.28-3.21 (m, 1H), 2.90-2.83 (m, 1H), 2.45-2.40 (m, 1H), 2.10 (s, 3H), 1.80 (s, 3H); ^{13}C NMR (125 MHz, $CDCl_3$) δ 187.5, 178.8, 147.6, 144.1, 142.1, 137.8, 136.9, 135.7, 135.1, 134.9, 134.7, 129.1, 128.5, 128.1, 128.0, 127.712, 127.1, 126.4, 123.1, 121.9, 117.4, 109.0, 68.8, 58.6, 57.3, 55.4, 43.822, 41.7, 16.6, 16.2; FT-IR (KBr) 2923, 1705, 1630, 1491, 1467, 1358, 1176, 741, 697 cm^{-1}; HRMS (ESI) m/z: $[M+H]^+$ Calcd for $C_{34}H_{32}NO_2$ 486.2428; Found 486.2427.

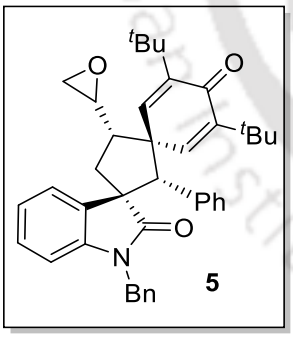

1''-Benzyl-3,5-di-*tert*-butyl-4'-(oxiran-2-yl)-2'-phenyldispiro [cyclohexane-1,3'-cyclopentane-1',3''-indoline]-2,5-diene-2'',4-dione 5. Analytical TLC on silica gel, 1:20 ethyl acetate/hexane R_f = 0.20; colorless solid; mp 147-148 °C; yield 52% (30.5 mg); major diastereomer (>20:1 dr): ^{1}H NMR (600 MHz, $CDCl_3$) δ 8.28 (d, *J* = 3.0 Hz, 1H), 7.48-7.47 (m, 1H), 7.16-7.08 (m, 4H), 7.05-6.99 (m, 4H), 6.90 (d, *J* = 7.2 Hz, 2H), 6.49 (d, *J* = 7.5 Hz, 2H), 6.40 (d, *J* = 7.2 Hz, 1H), 6.367-6.362 (m, 1H), 5.14 (d, *J* = 16.2 Hz, 1H), 4.33 (d, *J* = 16.2 Hz, 1H), 3.77 (s, 1H), 2.98-2.94 (m, 1H), 2.76-2.74 (m, 1H), 2.67-2.65 (m, 1H), 2.54-2.51 (m, 1H), 2.47-2.42 (m, 1H), 2.40-2.39 (m, 1H), 1.40 (s, 9H), 1.09 (s, 9H); ^{13}C NMR (125 MHz, $CDCl_3$) δ 186.2, 179.0, 150.3, 148.4, 143.3, 142.2, 139.8, 135.7, 135.1, 134.1,

129.6, 128.6, 128.3, 127.9, 127.8, 127.2, 126.5, 123.2, 122.0, 109.2, 69.8, 58.4, 55.7, 54.0, 51.7, 45.7, 43.9, 39.6, 35.8, 34.8, 29.5, 29.4; FT-IR (KBr) 2953, 1705, 1629, 1461, 1360, 743, 698 cm^{-1}; HRMS (ESI) m/z: $[M+H]^+$ Calcd for $C_{40}H_{44}NO_3$ 586.3316; Found 586.3326.

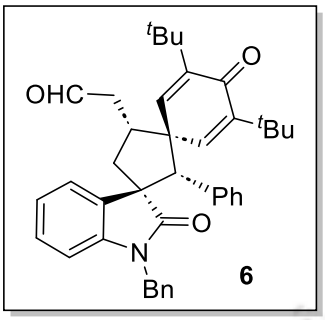

1''-Benzyl-3,5-di-*tert*-butyl-2'',4-dioxo-2'-phenyldispiro [cyclohexane-1,1'-cyclopentane-3',3''-indoline]-2,5-dien-5'-yl)acetaldehyde 6. Analytical TLC on silica gel; 1:20 ethyl acetate/hexane R_f = 0.22; colorless solid; mp 167-168 °C; yield 55% (32.1 mg); major diastereomer (>20:1 dr): ^{1}H NMR (600 MHz, $CDCl_3$) δ 9.69 (s, 1H), 8.044-8.040 (m, 1H), 7.52 (d, *J* = 7.2 Hz, 1H), 7.09-7.06 (m, 2H), 7.04-7.01 (m, 2H), 6.98-6.96 (m, 2H), 6.95-6.92 (m, 2H), 6.83-6.82 (m, 2H), 6.42-6.41 (m, 2H), 6.33 (d, *J* = 7.8 Hz, 1H), 6.29-6.28 (m, 1H), 5.05 (d, *J* = 16.2 Hz, 1H), 4.26 (d, *J* = 16.2 Hz, 1H), 3.73 (s, 1H), 3.13-3.07 (m, 1H), 2.59-2.49 (m, 2H), 2.38-2.28 (m, 2H), 1.33 (s, 9H), 1.00 (s, 9H); ^{13}C NMR (150 MHz, $CDCl_3$) δ 200.5, 186.2, 179.0, 150.6, 149.3, 143.4, 142.1, 139.7, 135.8, 135.0, 134.4, 129.6, 128.6, 128.2, 127.88, 127.83, 127.2, 126.5, 123.3, 122.2, 109.2, 69.5, 58.6, 55.6, 44.8, 43.8, 42.7, 35.9, 34.9, 29.6, 29.4; FT-IR (KBr) 2954, 1703,1634, 1611, 1488, 1467, 737, 697 cm^{-1}; HRMS (ESI) m/z: $[M+H]^+$ Calcd for $C_{40}H_{44}NO_3$ 586.3316; Found 586.3317.

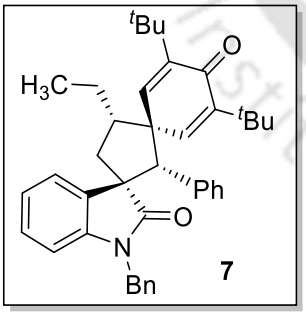

1''-Benzyl-3,5-di-*tert*-butyl-4'-ethyl-2'-phenyldispiro [cyclohexane-1,3'-cyclopentane-1',3''-indoline]-2,5-diene-2'',4-dione 7. Analytical TLC on silica gel, 1:49 ethyl acetate/hexane R_f = 0.30; colorless solid; mp 197-198 °C; yield 81% (46.2 mg); major diastereomer (>20:1 dr): ^{1}H NMR (500 MHz, $CDCl_3$) δ 8.00-7.99 (m, 1H), 7.46 (d, *J* = 7.0 Hz, 1H), 7.06-7.00 (m, 4H), 6.98-6.95 (m, 2H), 6.93-6.89 (m, 2H), 6.83-6.81 (m, 2H), 6.44 (d, *J* = 7.5 Hz, 2H), 6.32-6.29 (m, 2H), 5.05 (d, *J* = 16.0 Hz, 1H), 4.26 (d, *J* = 16.0 Hz, 1H), 3.66 (s, 1H), 2.57-2.51 m, 1H), 2.46-2.40 (m, 2H), 1.31 (s, 9H), 1.19-1.13 (m, 2H), 1.01

(s, 9H), 0.82 (t, J = 7.4 Hz, 3H); ^{13}C NMR (125 MHz, $CDCl_3$) δ 186.7, 179.3, 149.6, 148.4, 144.6, 142.2, 140.7, 136.5, 135.2, 134.8, 129.8, 128.6, 128.0, 127.7, 127.6, 127.1, 126.5, 123.1, 122.0, 109.1, 70.1, 58.4, 56.2, 53.7, 43.8, 43.1, 35.8, 34.7, 29.6, 29.5, 24.0, 13.1; FT-IR (KBr) 2955, 1706, 1634, 1612, 1466, 1363, 744, 697 cm^{-1}; HRMS (ESI) m/z: $[M+H]^+$ Calcd for $C_{40}H_{46}NO_2$ 572.3523; Found 572.3523.

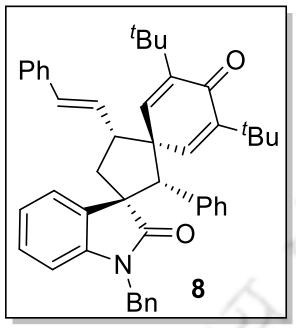

1''-Benzyl-3,5-di-*tert*-butyl-2'-phenyl-4'-((E)-styryl)dispiro-[cyclohexane-1,3'-cyclopentane-1',3''-indoline]-2,5-diene-2'',4-dione 8. Analytical TLC on silica gel, 1:49 ethyl acetate/hexane R_f = 0.30; colorless solid, mp >200 °C; yield 76% (49 mg); major diastereomer (>20:1 dr): ^{1}H NMR (600 MHz, $CDCl_3$) δ 8.178-8.174 m, 1H), 7.51 (d, J = 7.2 Hz, 1H), 7.20-7.10 (m, 6H), 7.09-7.07 (m, 2H), 7.05-7.02 (m, 2H), 6.99-6.94 (m, 4H), 6.85-6.84 (m, 2H), 6.43 (d, J = 7.2 Hz, 2H), 6.36-6.34 (m, 2H), 6.30 (d, J = 15.6 Hz, 1H), 5.81-5.77 (m, 1H), 5.08 (d, J = 16.2 Hz, 1H), 4.25 (d, J = 16.2 Hz, 1H), 3.79 (s, 1H), 3.33-3.29 (m, 1H), 2.92-2.88 (m, 1H), 2.48-2.44 (m, 1H), 1.30 (s, 9H), 1.01 (s, 9H); ^{13}C NMR (150 MHz, $CDCl_3$) δ 186.4, 179.1, 150.5, 148.8, 143.4, 142.2, 140.1, 136.9, 136.1, 135.1, 135.0, 132.4, 129.4, 128.69, 128.67, 128.2, 127.9, 127.7, 127.6, 127.21, 127.20, 126.5, 126.2, 123.2, 122.1, 109.2, 69.1, 58.7, 57.1, 55.1, 43.9, 42.6, 35.7, 34.8, 29.7, 29.6; FT-IR (KBr) 2953, 1704, 1633, 1612, 1488, 1362, 742, 695 cm^{-1}; HRMS (ESI) m/z: $[M+H]^+$ Calcd for $C_{46}H_{48}NO_2$ 646.3680; Found 646.3680.

Crystal Structure and Data of 3aa (major isomer)

Sample Preparation for Crystal Growth. The compound **3aa** was dissolved in acetonitrile and kept for slow evaporation (3 days). Block shaped crystal (dimensions of 0.36 mm X 0.31 mm X 0.28 mm) was formed whose X-ray analysis was performed.

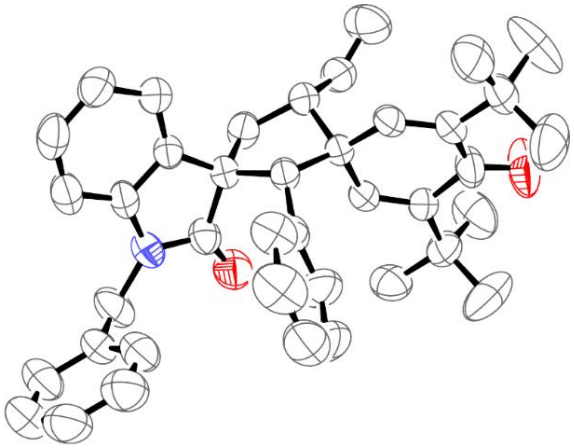

Figure 3. ORTEP diagram of **3aa** (major isomer) with 50% probability (CCDC 2158075). H-Atoms omitted for clarity.

Identification code	**3aa**
Empirical formula	'C40 H43 N O2'
Formula weight	569.75
Crystal habit, colour	Needle/Colorless
Temperature, *T*/K	296 K
Wavelength, *λ*/Å	0.71073
Crystal system	'monoclinic'
Space group	'P 21/c'
Unit cell dimensions	a= 13.7443 (10) Å
	b= 9.2387 (8) Å
	c= 27.6804 (19)Å
	α = 90
	β = 102.625(2)
	γ = 90
Volume, *V*/Å^3	3429.9(5)

Z	4
Calculated density, $Mg \cdot m^{-3}$	1.103
Absorption coefficient, μ/mm^{-1}	0.067
$F(000)$	1224.0
θ range for data collection	1.89 to 25°
Limiting indices	$-16 \leq h \leq 16$, $-11 \leq k \leq 11$, $-32 \leq l \leq 32$
Reflection collected / unique	3450/2277
Completeness to θ	100%
Absorption correction	Multi-scan
Max. and min. transmission	0.976 and 0.981
Refinement method	'SHELXL-2014/7 (Sheldrick, 2014)'
Data / restraints / parameters	6066/0/394
Goodness–of–fit on F^2	1.066
Final R indices [I>2sigma(I)]	R1 = 0.0639, wR2 = 0.1435
R indices (all data)	R1 = 0.1289, wR2 = 0.1743

2.6 Computational Details

All the structures were fully optimized without any symmetry constraint at M06-2X/def2TZVP level.[13] Harmonic vibrational frequency calculations were performed at the same level of theory to understand the nature of the stationary points. All intermediates are characterized by real values of the Hessian matrix while the transition states were characterized by one imaginary value of the Hessian matrix. All these calculations were performed using Gaussian 16 suite performed.[14]

Total Energy, Imaginary Frequency and Bond lengths (Å) of the Optimized Geometries:

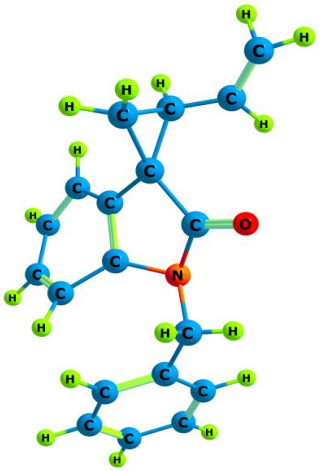

1a

Total Energy: − 863.555012

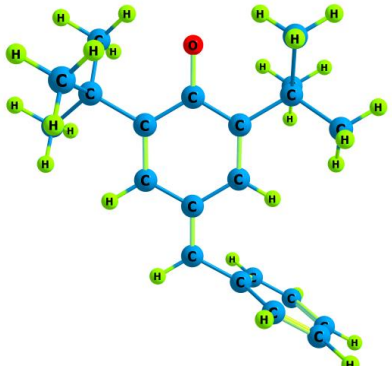

2a

Total Energy: − 443.029781

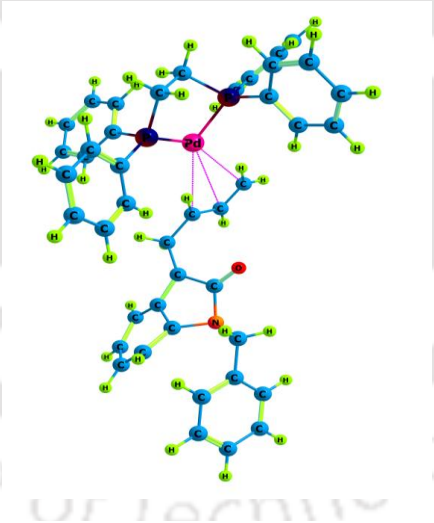

Int-I

Total Energy: − 2718.020012

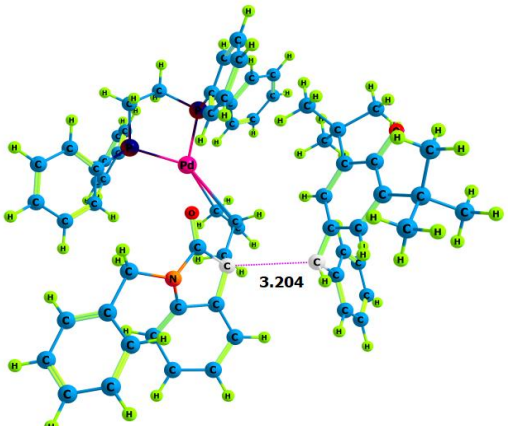

TS-I

Total Energy: − 3161.02503

ν_1 = − 288.4 cm^{-1}

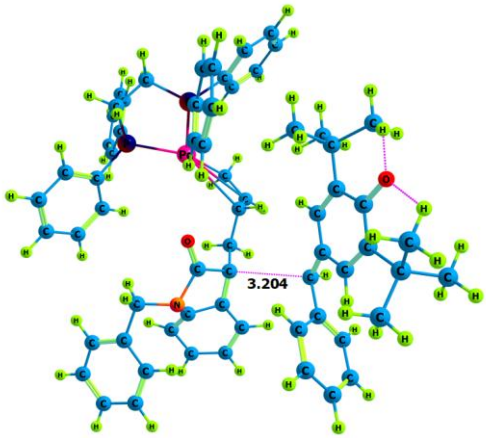

TS-I'

Total Energy: − 3161.0153

ν_1 = − 302.6 cm^{-1}

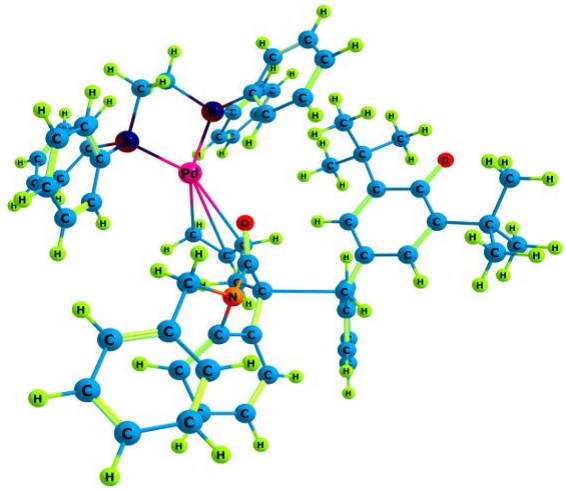

Int-II

Total Energy: − 3161.06103

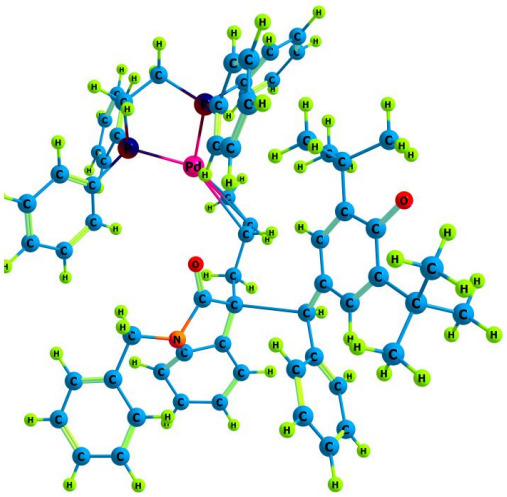

Int-II'

Total Energy: − 3161.04530

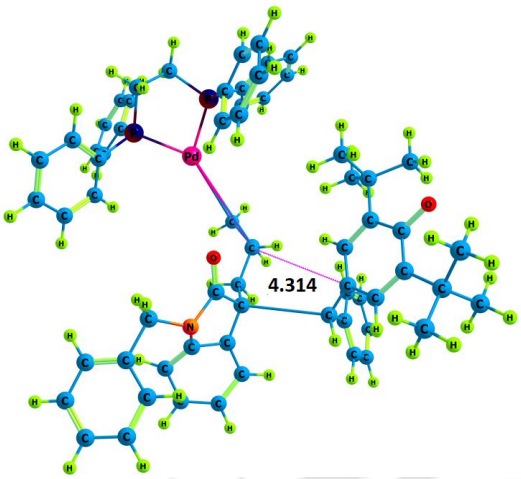

TS-II

Total Energy: − 3161.03503

ν_1 = − 641.4 cm^{-1}

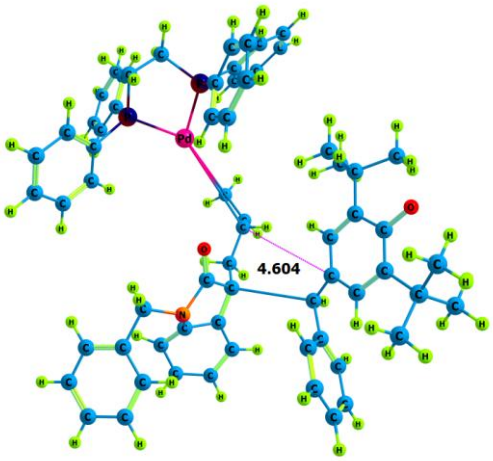

TS-II'

Total Energy: − 3160.99701

ν_1 = − 549.2 cm^{-1}

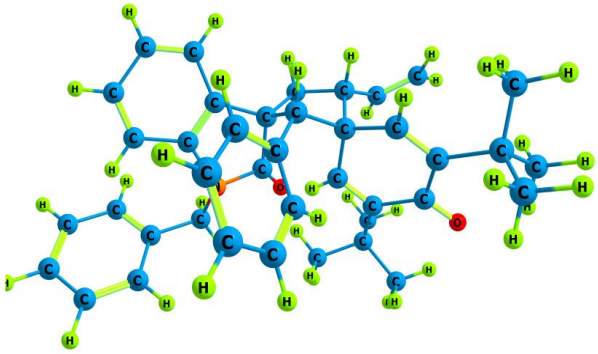

3aa (Major Product)

Total Energy: − 3161.08921

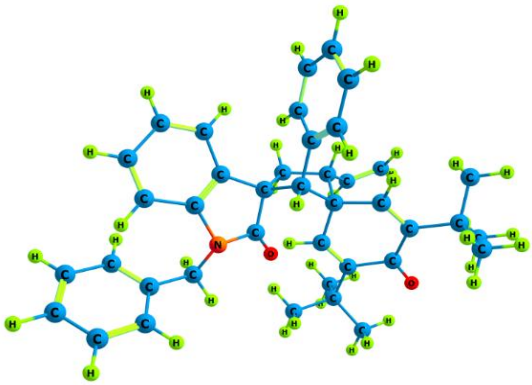

3aa' (Minor Product):

Total Energy: −

2.7 References

1. (a) Trost, B. M. *Acc. Chem. Res*. **2002**, *35*, 695. (b) Lovering, F.; Bikkerand, J.; Humblet, C. *J. Med. Chem*. **2009**, *52*, 6752. (c) Newton, C. G.; Wang, S.-G.; Oliveira, C. C.; Cramer, N. *Chem. Rev*. **2017**, *117*, 8908. (d) Caplin, M. J.; Foley, D. J. *Chem. Sci.* **2021**, *12*, 4646. (e) Boddy, A. J.; Bull, J. A. *Org. Chem. Front*. **2021**, *8*, 1026.
2. Galliford, C. V.; Scheidt, K. A. *Angew. Chem., Int. Ed*. **2007**, *46*,8748. (b) Zheng, Y.; Tice, C. M.; Singh, S. B. *Bioorg. Med. Chem. Lett*. **2014**, *24*, 3673. (c) Cao, Z.-Y.; Zhou, F.; Zhou, *J. Acc. Chem. Res*. **2018**, *51*, 1443.
3. Ding, A.; Meazza, M.; Guo, H.; Yang, J. W.; Rios, R. *Chem. Soc. Rev*. **2018**, *47*, 5946. (b) Gui, H.-Z.; Wei, Y.; Shi, M. *Chem. Asian J*. **2020**, *15*, 1225.
4. Alper, P. B.; Meyers, C.; Lerchner, A.; Siegel, D. R.; Carreira, E. M. *Angew. Chem., Int. Ed.* **1999**, *38*, 3186.
5. Xu, P.-W.; Liu, J.-K.; Shen, L.; Cao, Z.-Y.; Zhao, X.-L.; Yan, J.; Zhou, J. *Nat. Commun*. **2017**, *8*, 1619.
6. Akaev, A. A.; Melnikov, M. Ya.; Budynina, E. M. *Org. Lett*. **2019**, *21*, 9795.
7. Wan, Q.; Chen, L.; Li, S.; Kang, Q.; Yuan, Y.; Du, Y. *Org. Lett*. **2020**, *22*, 9539.
8. Sarkar, T.; Das, B. K.; Talukdar, K.; Shah, T.A.; Punniyamurthy, T. *ACS Omega* **2020**, *5*, 26316.
9. Lima, C. G. S.; Pauli, F. P.; Costa, D. C. S.;de Souza, A. S.; Forezi, L. S. M.; Ferreira, V. F.; de Carvalho da Silva, F. Eur. *J. Org. Chem*. **2020**, 2650.
10. Gai, K.; Fang, X.; Li, X.; Xu, J.; Wu, X.; Lin, A.; Yao, H. *Chem. Commun*. **2015**, *51*, 15831.
11. Yuan, Z.; Liu, L.; Pan, R.; Yao, H.; Lin, A. *J. Org. Chem*. **2017**, *82*, 8743.
12. Ghotekar, G. S.; Shirsath, S. R.; Shaikh, A. C.; Muthukrishnan, M. *Chem. Commun*. **2020**, *56*, 5022.
13. (a) Chu, W.-D.; Zhang, L.-F.; Bao, X.; Zhao, X.-H.; Zeng, C.; Du, J.-Y.; Zhang, G.-B.; Wang, F.-X.; Ma, X.-Y.; Fan, C.-A. *Angew. Chem., Int. Ed*. **2013**, *52*, 9229. (b) Caruana, L.; Kniep, F.; Johansen, T. K.; Poulsen, P. H.; Jørgensen, K. A. *J. Am. Chem. Soc*. **2014**, *136*, 15929. (c) Lou, Y.; Cao, P.; Jia, T.; Zhang, Y.; Wang, M.; Liao, J. *Angew. Chem., Int. Ed*. **2015**, *54*, 12134.
14. (a) Zhao, Y.; Truhlar, D. G. *Theor. Chem. Acc*. **2008**, *120*, 215. (b) D. J. Fox et al. Gaussian, Inc., Wallingford CT, **2016**.

15. (a) Li, S. H.; Liu, Y.Y.; Huang, B.; Zhou, T.; Tao, H. M.; Xiao, Y. J.; Liu, L.; Zhang, J. L. *ACS Catal*. **2017**, *7*, 2805. (b) Dennis, J. M.; White, N. A.; Liu, R. Y.; Buchwald, S. L. *ACS Catal*. **2019**, *9*, 3822. (c) Lau, S. H.; Yu, P.; Chen, L.; Madsen-Duggan, C. B.; Williams, M. J.; Carrow, B. P. *J. Am. Chem. Soc.* **2020**, *142*, 20030. (d) Bitai, J.; Nimmo, A. J.; Slawin, A. M.-Z.; Smith, A. D. *Angew. Chem., Int. Ed*. **2022**, *61*, e202202621.
16. (a) López, A.; Parra, A.; Jarava-Barrera, C.; Tortosa, M. *Chem. Commun*. **2015**, *51*, 17684. (b) Reddy, V.; Anand, R. V. *Org. Lett*. **2015**, *17*, 3390. (c) Jillella, R.; Oh, D. H.; Oh, C. H. *New J. Chem*. **2018**, *42*, 16886. (d) Burra, A. G.; Uredi, D.; Motati, D. R.; Fronczek, F. R.; Watkins, E. B. *Eur. J. Org. Chem*. **2022**, e202200191.

2.8 Selected NMR Spectra

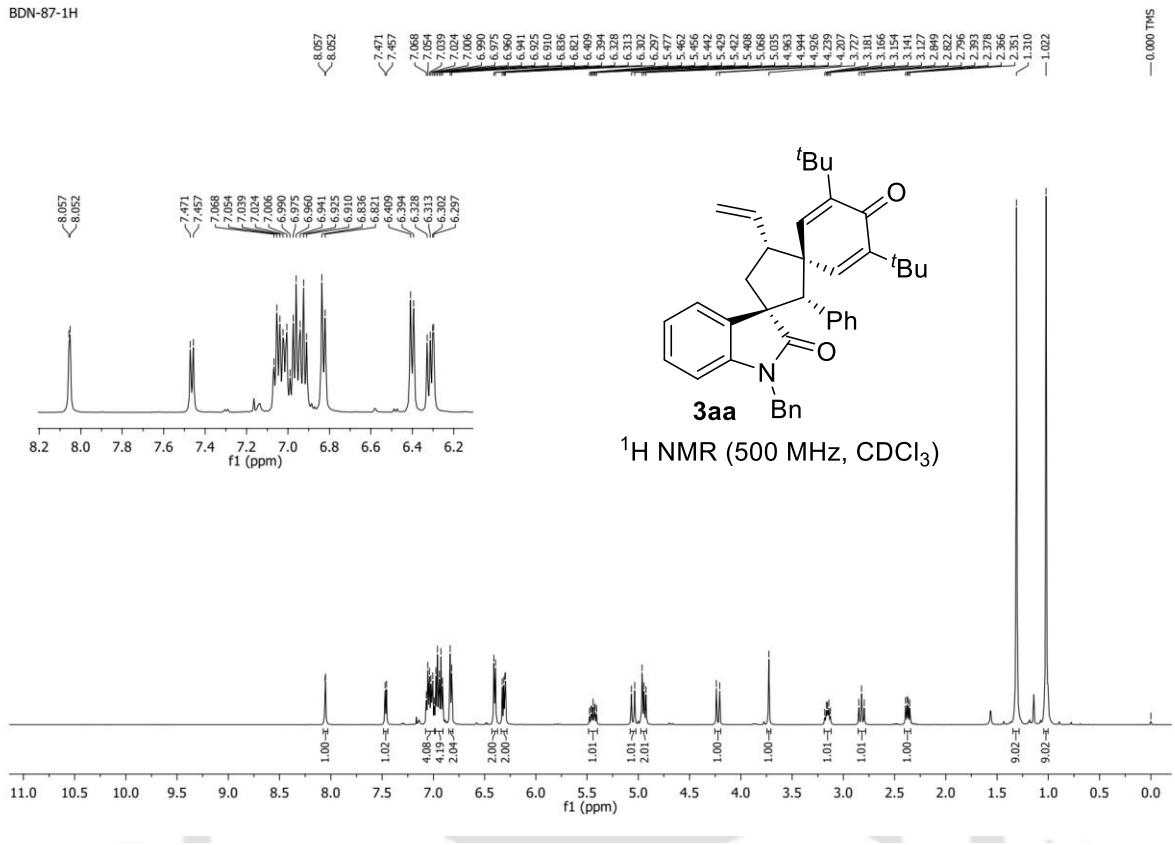

^{1}H NMR (500 MHz, $CDCl_3$)

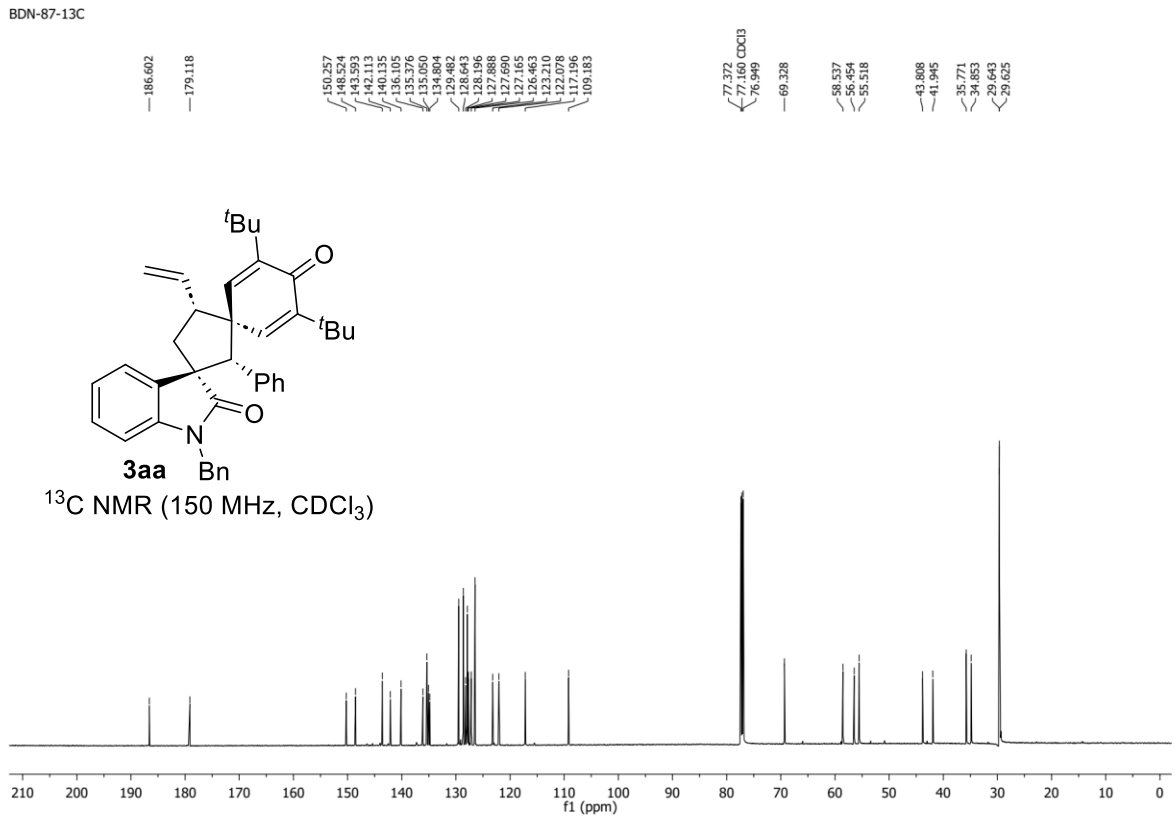

^{13}C NMR (150 MHz, $CDCl_3$)

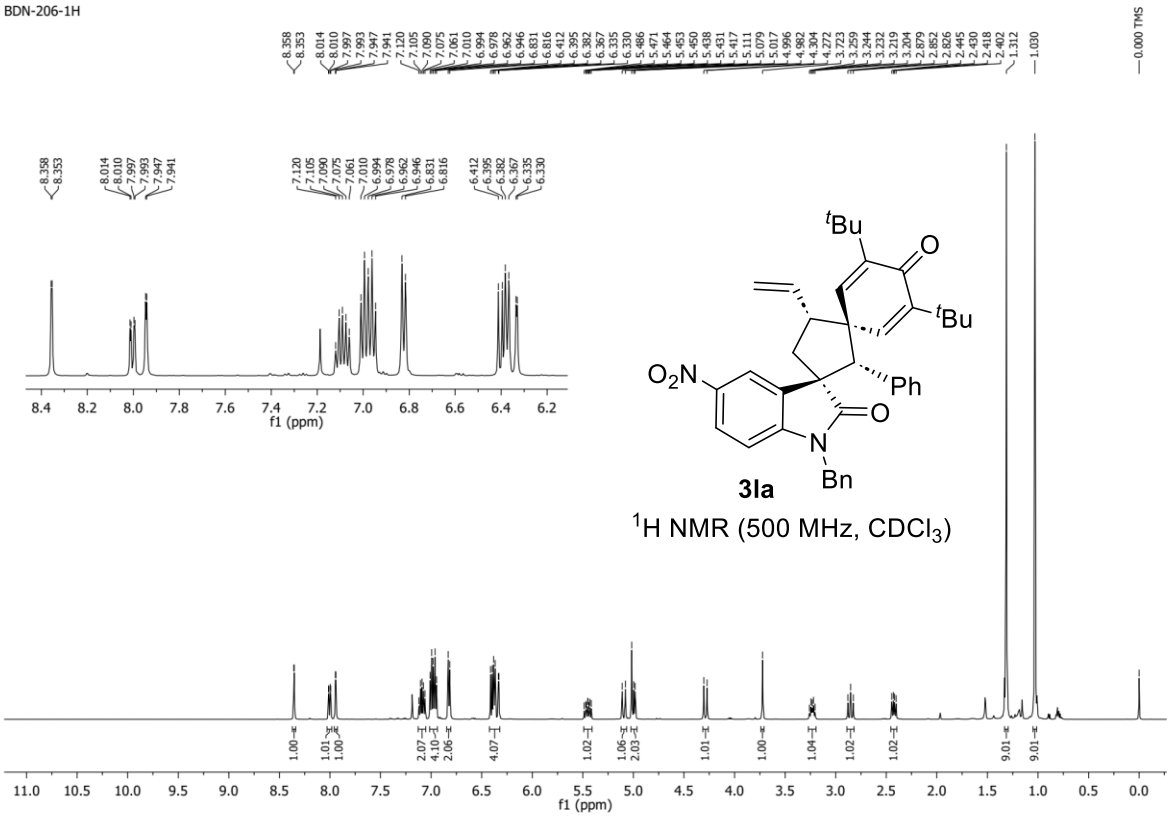

3la

^{1}H NMR (500 MHz, $CDCl_3$)

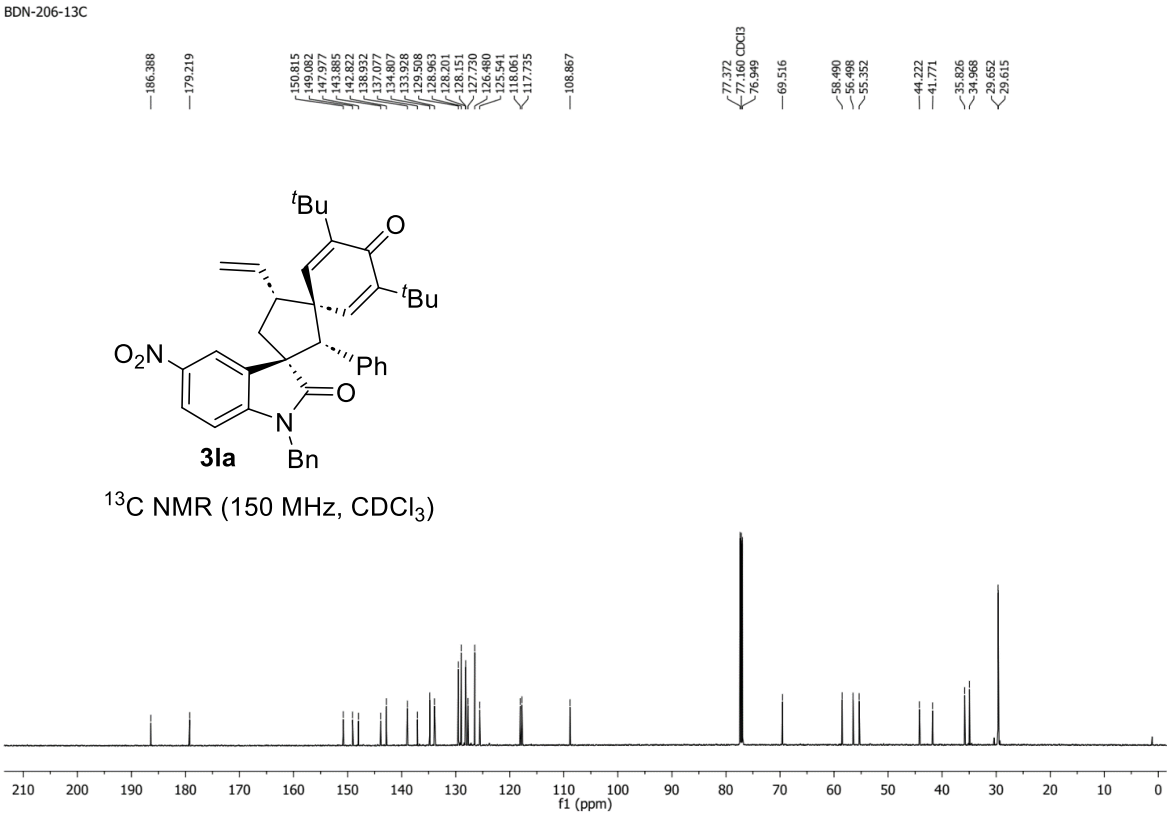

3la

^{13}C NMR (150 MHz, $CDCl_3$)

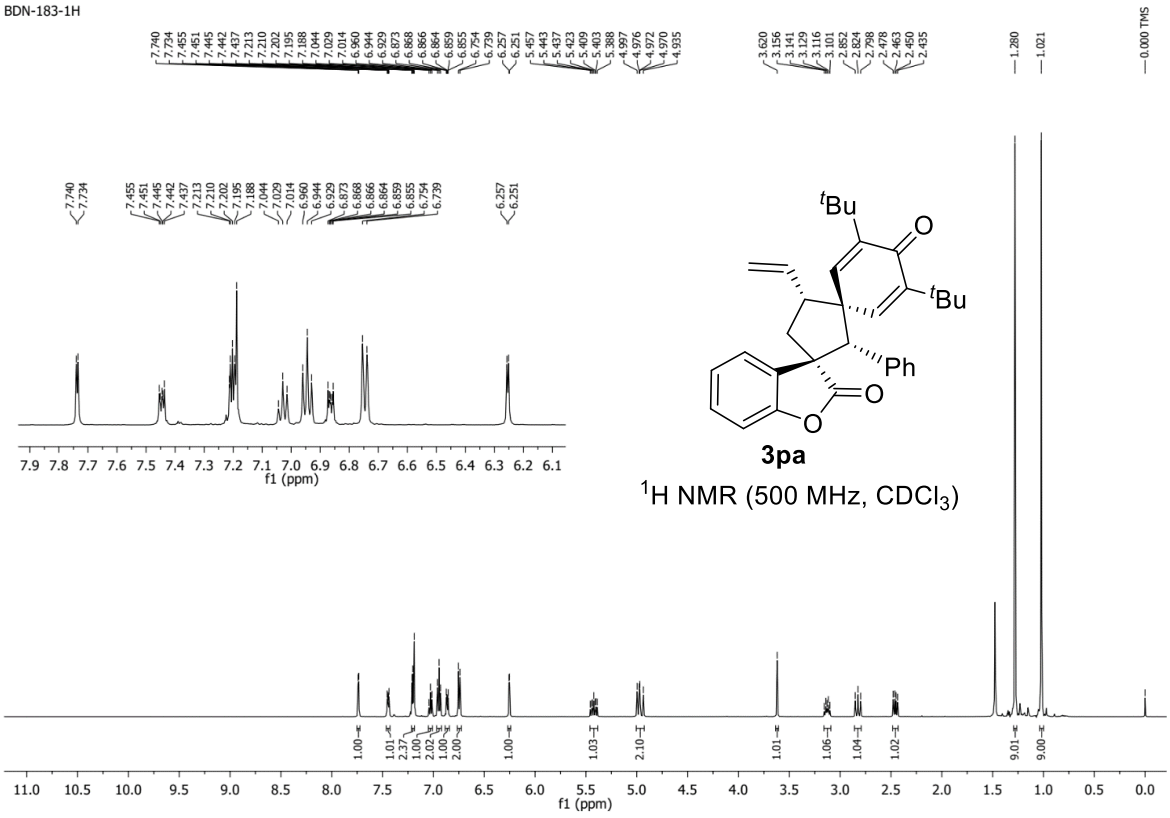

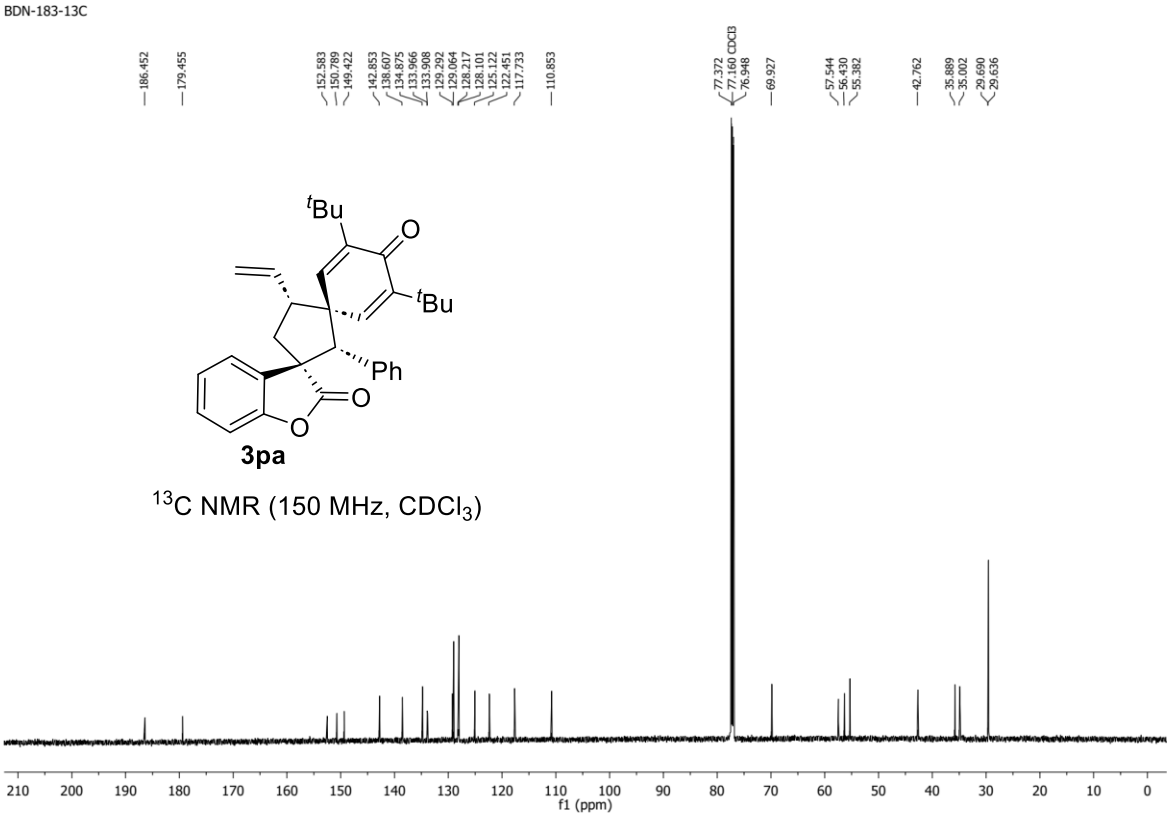

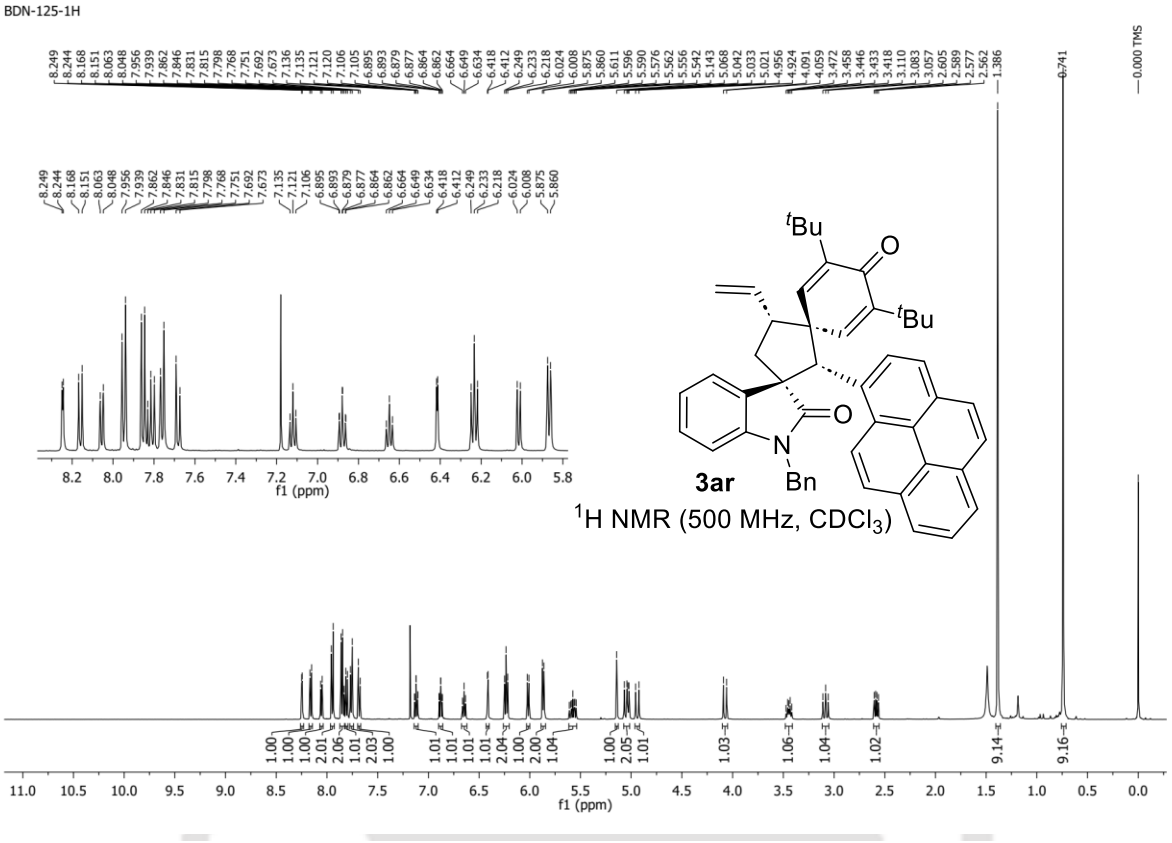

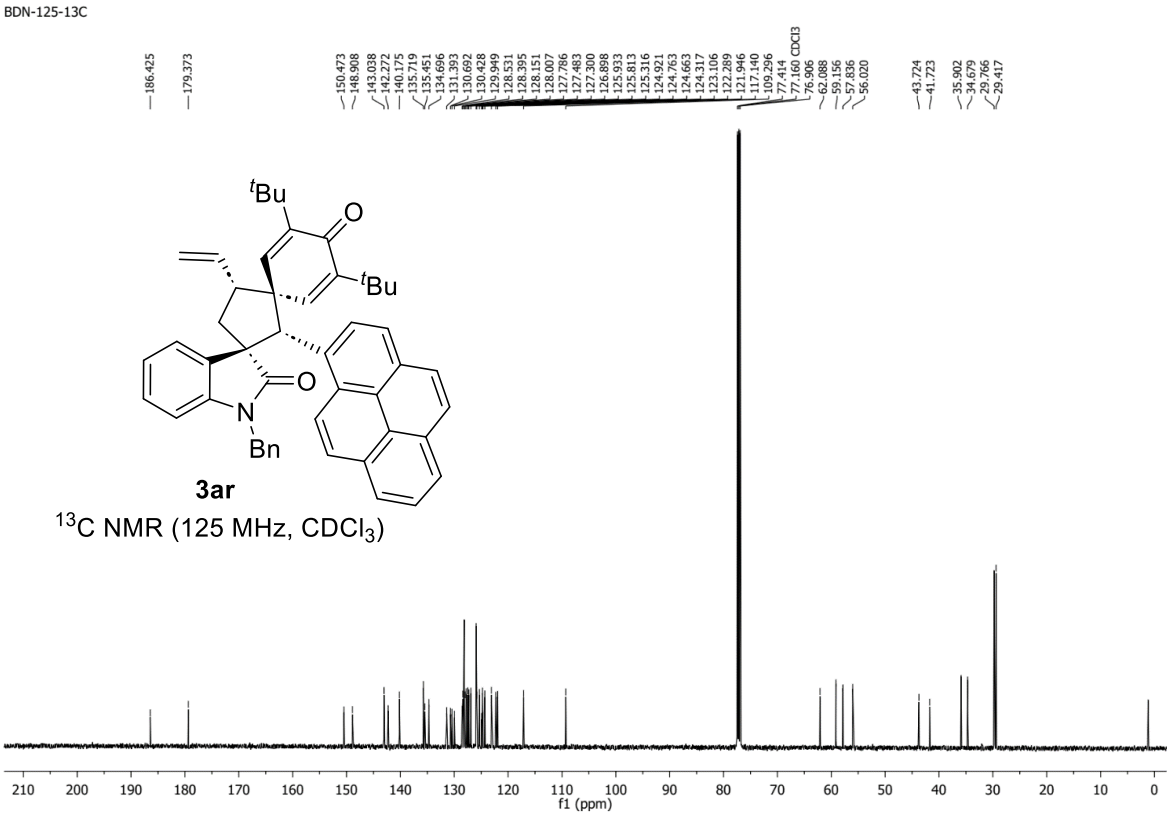

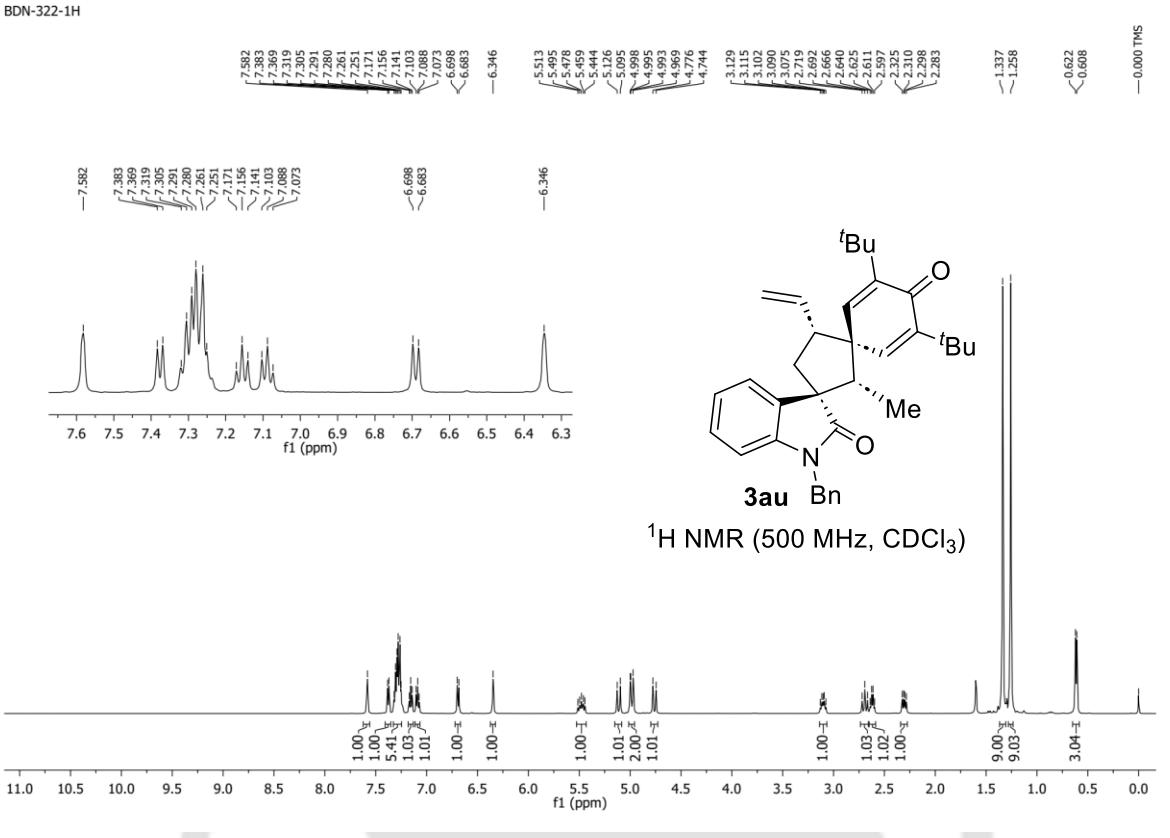

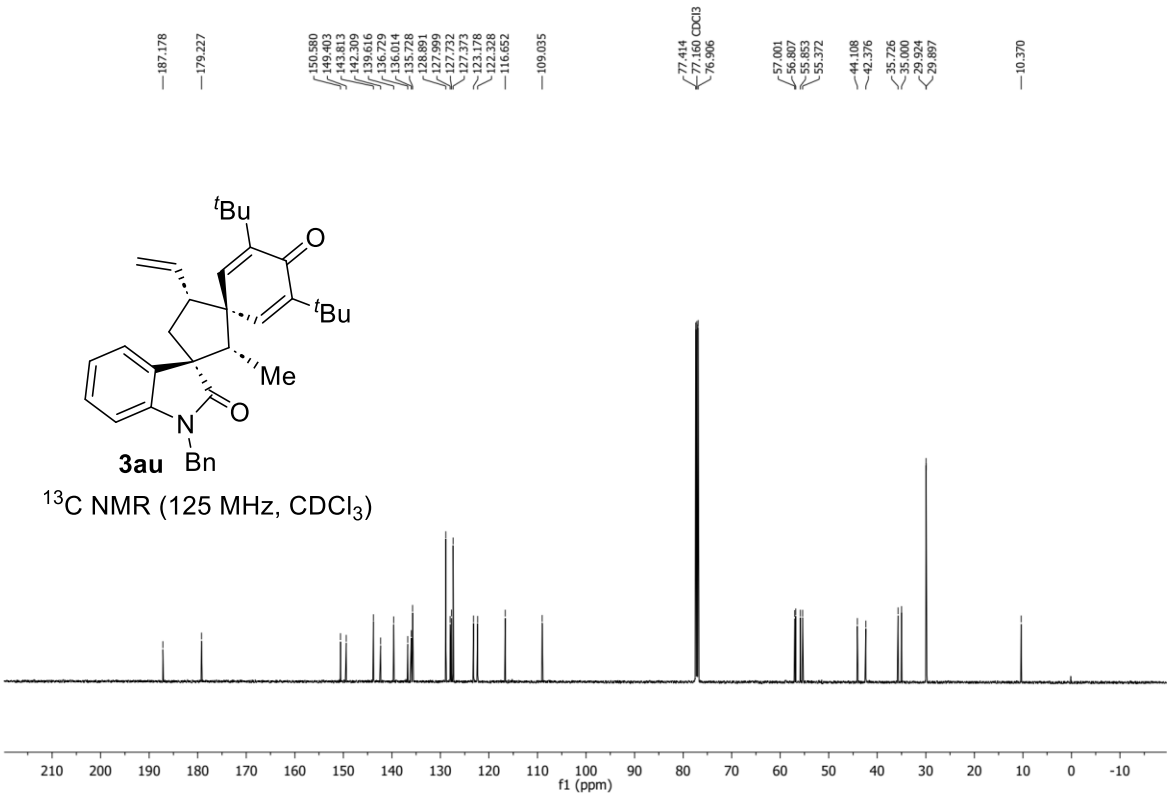

Chapter III

[3+3]-Annulation of 2,4-Dienals with Aziridines: Access to Fused Morpholines

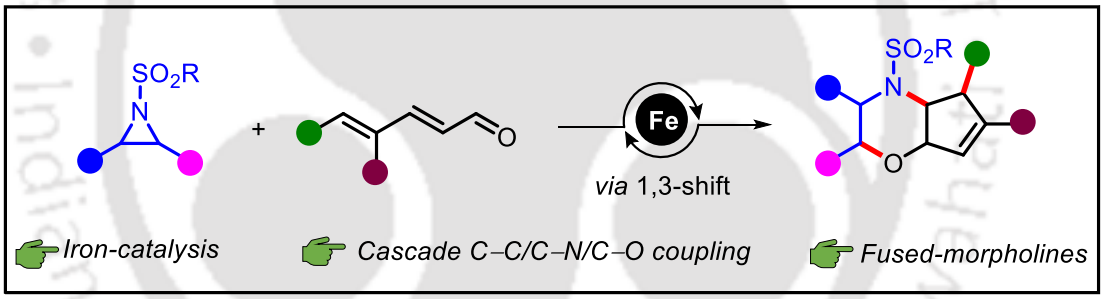

[3+3]-Annulation of 2,4-Dienals with Aziridines: Access to Fused Morpholines

In recent years, the synthesis of fused five- and six-membered ring systems has become key research domain, as these scaffolds are commonly found in natural and medicinal products.[1,2] Their rigid conformations and moderate ring sizes allow them to exhibit a range of desirable physicochemical properties. As a result, the development of synthetic methods to foster such molecular frameworks has become a front-line research area. However, conventional synthetic approaches for such fused systems typically rely on expensive catalysts and are inefficient in terms of atom and step economy. Hence, cost effective methods for synthesis of these structural units using readily accessible catalysts and reactants is a formidable challenge and highly desirable.[3] In this regard, iron-catalyzed reactions have emerged as a promising approach.[4] Due to iron's abundance, sustainability, and minimal-toxicity nature, it is often referred to as a "metal with minimal safety concerns." Additionally, α, β-unsaturated aldehydes have proven to be valuable feedstocks for synthesizing versatile molecular frameworks.[5] Specifically, 2,4-dienals, when exposed to Lewis or Brønsted acid, undergo electro-cyclization leading to the formation of cyclic oxyallyl cation intermediates.[6-8] These intermediates are highly useful for constructing fused organic scaffolds by facilitating the formation of C−C and C−O bonds *via* interrupted *iso*-Nazarov cyclization. However, such reactivity of dienals remains largely unexplored and associated with challenges as 2,4 dienals are also prone to undergo 1,2- as well as 1,4-nucleophilc addition reactions. Thus, regioselective reactivity of such systems are high demand in organic synthesis. Meanwhile, aziridines have garnered significant attention as vital precursor to construct a wide range of ubiquitous fused *N*-heterocyclic scaffolds.[9-11] Due to ease of accessibility and high stability, aziridines continues to be captivating interest in terms of diversity-oriented synthesis of organic scaffolds. Pertinently, coupling of 2,4-dienals with small heterocyclic strained rings remains unexplored and this would be valuable for expanding the reactivity of 2,4-dienals and constructing fused heterocyclic frameworks. Thus, we envisioned merging 2,4-dienal and aziridine under iron catalysis could afford fused morpholine derivatives in a cost effective, atom and step-economic approach. Further, morpholine derivatives emerged as a prominent core structural unit due to their profuse prominence in pharmacophores (Figure 3.1).[12] In addition, U. S. FDA approved morpholine containing drugs ranked 9th position among nitrogen-containing small molecules.[13] This chapter delineates an effective Fe-catalyzed [3+3]-annulation approach by employing aziridines and 2,4-dienals to

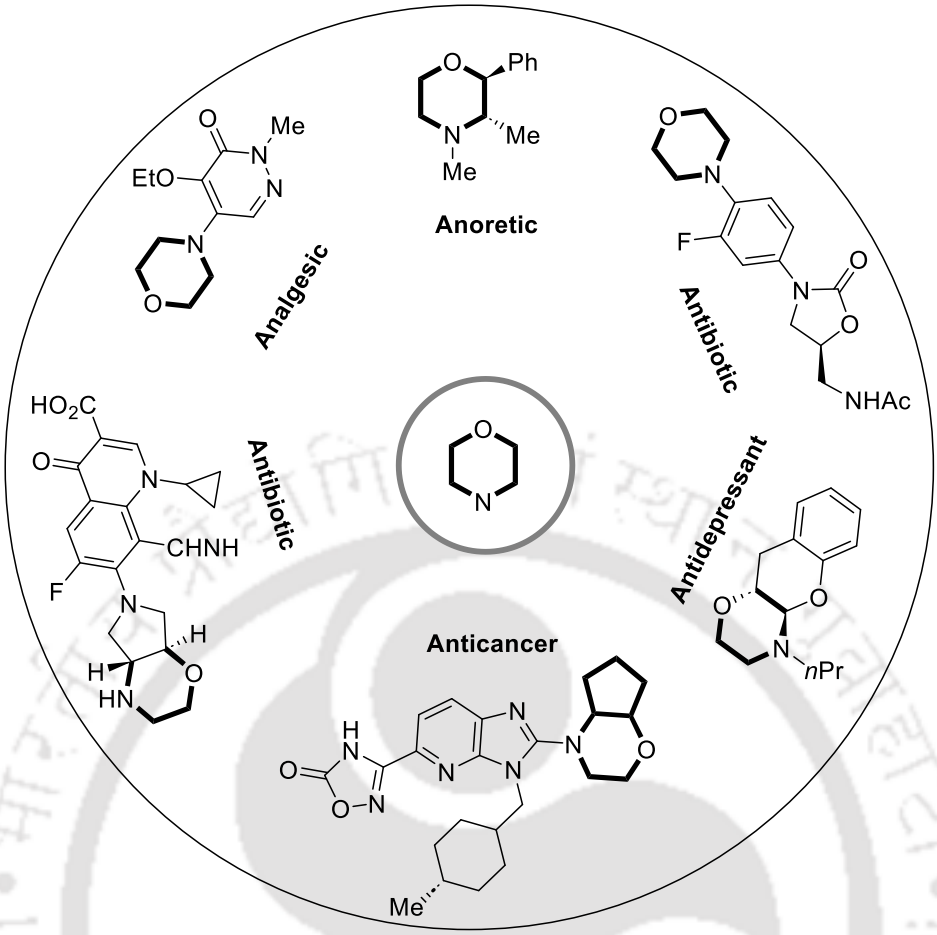

Figure 3.1. Selective Examples of Morpholine Containing Pharmacophores

afford fused-morpholine core. The methodology proceeds *via* an *iso*-Nazarov cyclisation involving 1,3-sigmatropic shift along with ring expansion chemistry.

3.1 Interrupted *Iso*-Nazarov Cyclization Reactions of 2,4-dienals

Moreau and co-workers described Fe-mediated dearomative coupling of 2,4-dienals with indoles (Scheme 3.1).[6] The reaction involves [3+2]-annulation *via* interrupted *iso*-Nazarov path. Further, the umpolung reactivity of *N*-acetylindoles indoles provides a lucrative technique to convey fused indoline derivatives.

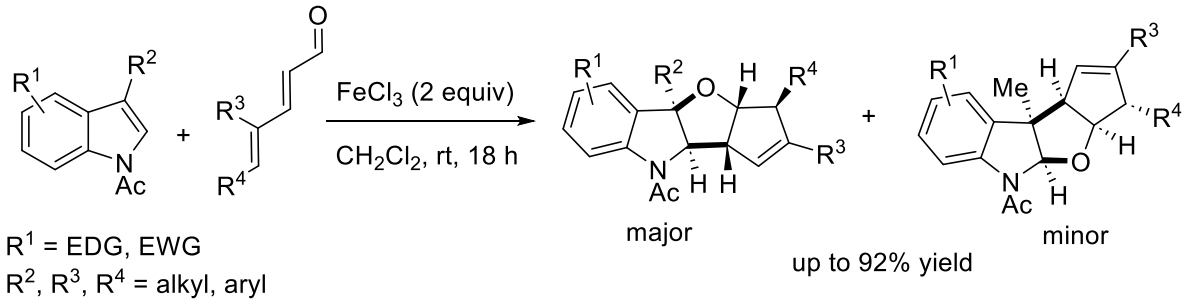

Scheme 3.1. Fe-Mediated [3+2]-Annulation of Dienals with Indoles

Riveira and co-workers showed a multicomponent synthetic strategy for the synthesis of bio-relevant cyclopenta[b]furan-2-one scaffolds by reacting 2,4-dienals with Meldrum's acid in presence of alcohol (Scheme 3.2).[7] The protocol uses inexpensive reagents to furnish cyclopentane fused 2-furanones involving stereoselective trapping of cyclic oxa-allyl cationic intermediate.

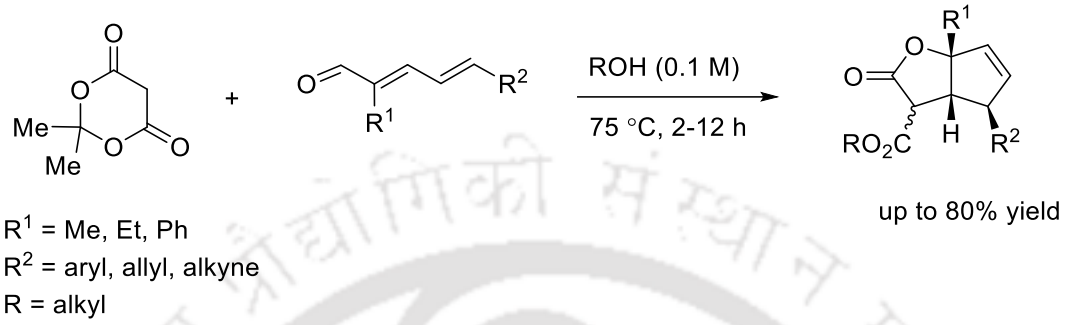

Scheme 3.2. Multicomponent Domino Cyclization of 2,4-Dienals and Meldrum's Acid

A Brønsted acid-mediated interrupted *iso*-Nazarov reactivity using 2,4-dienals was depicted by Moreau group (Scheme 3.3).[8] The strategy leads to synthesis of polycyclic scaffolds by employing 2,4-dienals with azadienes in presence of hydrochloric acid at room temperature. The reaction is believed to procced *via* domino cyclization of cyclopentadienol intermediate with azadiene to furnish the polycyclic product with high yields and stereoselectivity.

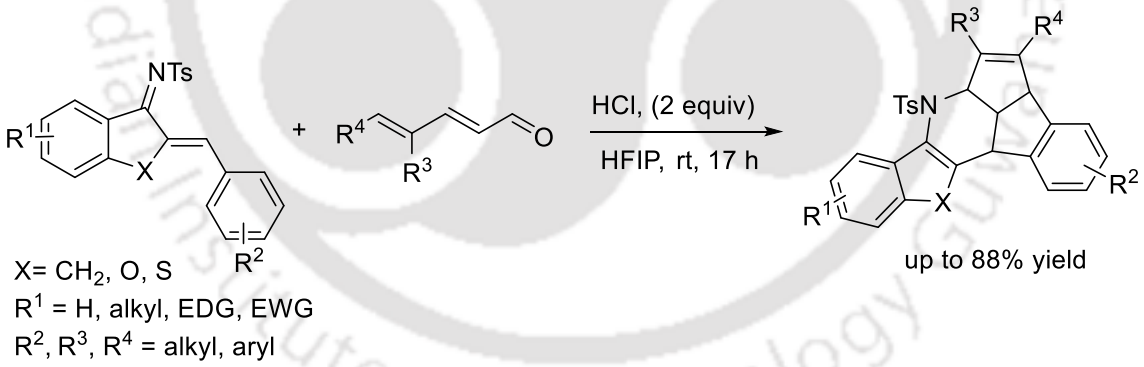

Scheme 3.3. Brønsted Acid-Mediated Polycylization of 2,4-Dienals with Azadienes

3.2 Synthesis of Fused Heterocycles Using Aziridines

Wang group demonstrated a [3+3]-annulation of aziridines with 2-indolylmethanols under Sc(III)-catalysis to synthesize tetrahydro-β-carbolines or fused piperidines (scheme 3.4).[9] In addition, the protocol was extended for synthesis of tetrahydroisoquinolines by coupling of aziridines and benzylic alcohols under similar reaction conditions.

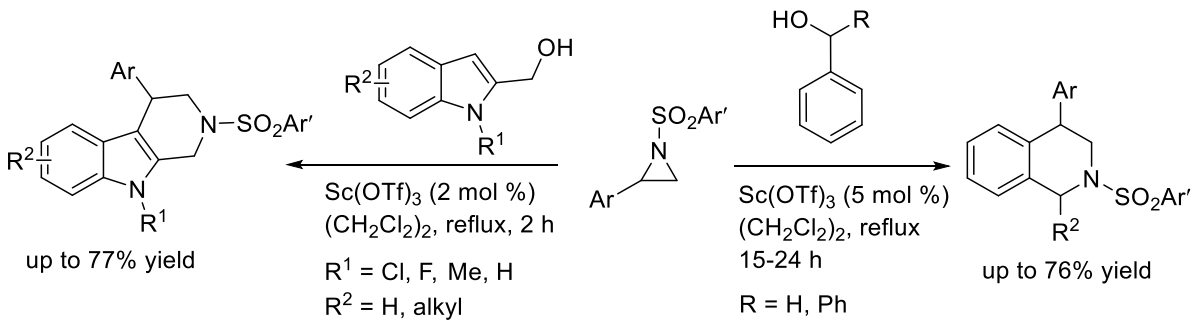

Scheme 3.4. Sc-Catalyzed Synthesis of Fused Piperidines

A unique methodology for synthesis of indolines using aziridine and alcohol under copper catalysis was developed (Scheme 3.5).[10] The synthetic route involves a stereospecific ring-opening of aziridine followed by a Cu(II)-mediated C−H amination to yield indolines in high yields.

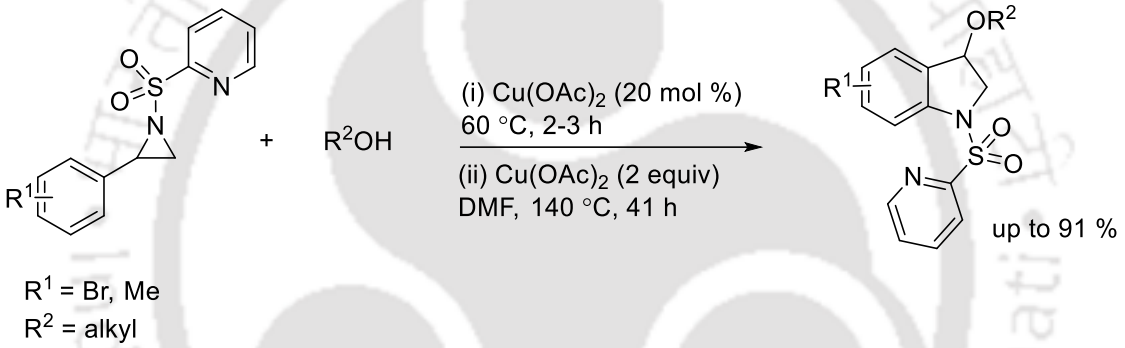

Scheme 3.5. Cu-Catalyzed Synthesis of Indolines

Our group reported photoredox catalysis for the synthesis of fused imidazolidines via annulation of aziridines with cyclic secondary amines (Scheme 3.6).[11] The reaction path proceeds *via* a S_N2 ring-opening of aziridine and C−H amination. The protocol showed well potential and tolerance to a wide range of functional group to afford fused imidazolidines in high yields.

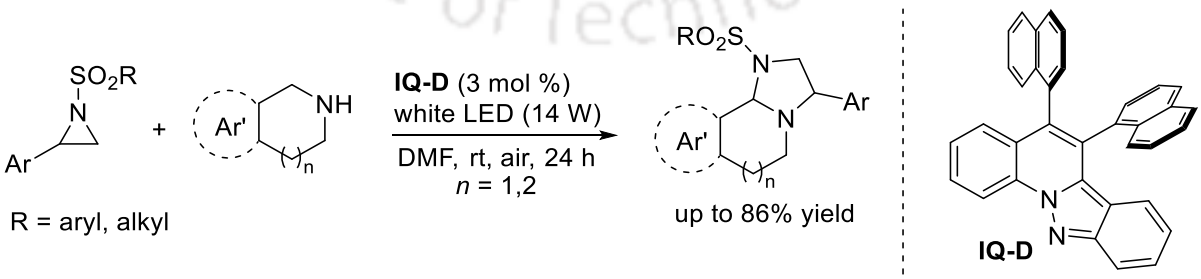

Scheme 3.6. Photoredox Catalyzed Synthesis of Fused Imidazolidines

3.3 Present Study

We report here Fe-catalyzed [3+3]-annulation of diversely substituted aziridines and 2,4-dienals. This synthetic methodology offers construction bio-relevant fused morpholine derivatives. At the outset, we began our optimization studies by reacting **1a** with **2a** as model substrates in the presence of Lewis acids and solvents (Table 3.1-3.2). Among the iron-based Lewis acids *viz*., anhydrous $FeCl_3$., $FeCl_3$•$6H_2O$, $Fe(NO_3)_3$•$9H_2O$, $Fe(acac)_3$ tested, the former in $(CH_2Cl)_2$ at 80 °C resulted **3aa** in 82% yield in 6 h. Screening of other Lewis acids *viz*., $AlCl_3$, $CuCl_2$, $CoCl_2$, $Cu(OTf)_2$, $Sc(OTf)_3$, and BF_3•OEt_2 resulted in inferior results (Table 3.1). Further, $(CH_2Cl)_2$ emerged as the solvent of choice, outperforming CH_2Cl_2, THF, toluene, acetonitrile, methanol and DMF (Table 3.2). Additionally, varying the temperature did not improve the yield of **3aa** (Table 3.2, entry 7-8). In the absence of the catalyst (Table 3.2, entry 9), the reaction did not furnish the annulated product, indicating the essential role of the Lewis acid in driving the reaction.

Optimization of the Reaction Conditions

Table 3.1. Screening of Lewis acid[a]

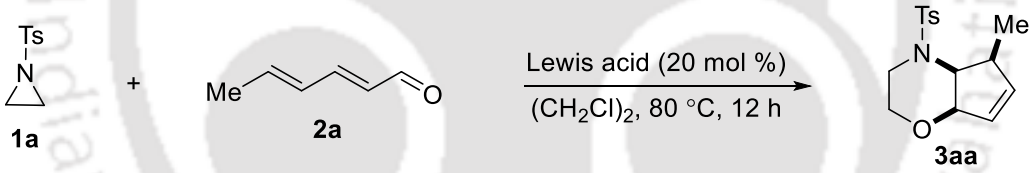

Entry	Lewis acid	Yield (%)[b]
1	**$FeCl_3$**	**82**
2	$FeCl_3$•$6H_2O$	66
3	$Fe(NO_3)_3$•$9H_2O$	63
4	$Fe(acac)_3$	nr
5	$AlCl_3$	56
6	$FeCl_2$	32
7	$CoCl_2$	nr
8	$CuCl_2$	nr

9	$Cu(OTf)_2$	59
10	BF_3•OEt_2	68
11	–	nr

[a]Reaction conditions: **1a** (0.2 mmol), **2a** (0.24 mmol), Lewis acid (20 mol %), $(CH_2Cl)_2$ (1 mL), 80 °C. [b]Isolated yield.

Table 3.2. Screening of Solvent[a]

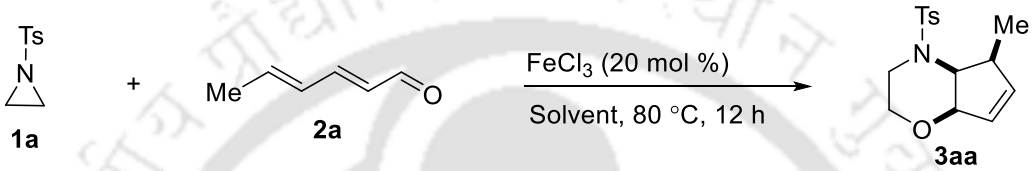

Entry	Solvent	Yield (%)[b]
1	CH_2Cl_2	73
2	THF	61
3	toluene	54
4	CH_3CN	48
5	MeOH	22
6	DMF	26
7[c]	$(CH_2Cl)_2$	49
8[d]	$(CH_2Cl)_2$	70

[a]Reaction conditions: **1a** (0.2 mmol), **2a** (0.24 mmol), Lewis acid (20 mol %), $(CH_2Cl)_2$ (1 mL), 80 °C. [b]Isolated yield. [c]At room temperature. [d]At 50 °C.

Having the optimized conditions, we examined the scope of the method by reacting different substituted aziridines **1b-x** with **2a** as standard substrate (Table 3.3). *N*-substituted aziridines with trifluoromethyl **1b**, bromine **1c** and methoxy **1d** at the sulfonyl aryl ring produced **3ba-ca** in 64-76% yields. Similarly, 2-naphthyl sulfonyl group **1e** gave **3ea** in 76% yield. In contrast,

Table 3.3. Substrate Scope of with Respect to Aziridines[a,b]

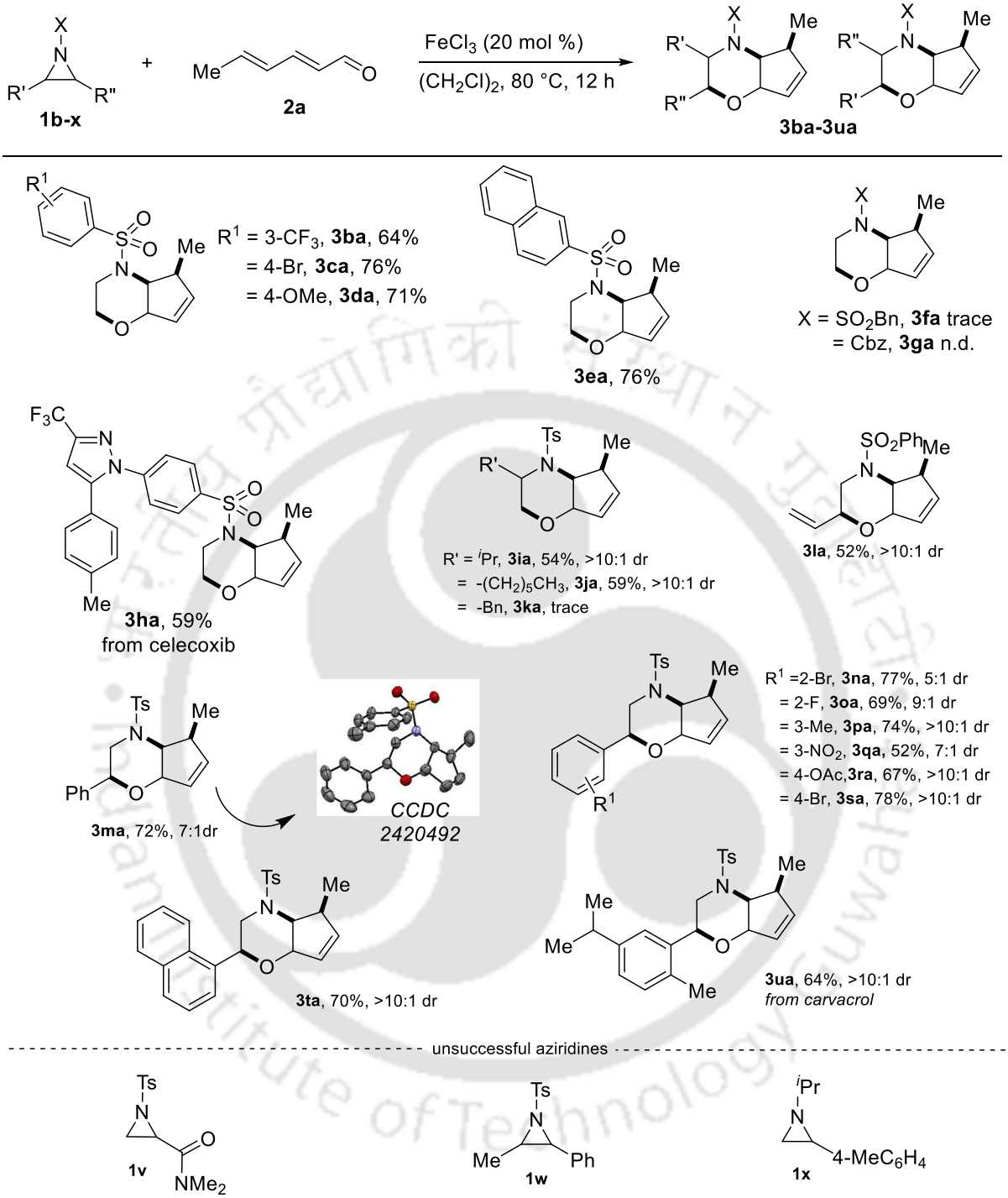

[a]Reaction conditions: **1b-x** (0.2 mmol), **2a** (0.2 mmol), $FeCl_3$ (20 mol %), $(CH_2Cl)_2$ (1 mL), 80 °C, 12 h. [b]Isolated yield.

aziridines having *N*-substitution with benzyl **1f** resulted in **a** trace amount of **3fa**, while, benzyl chloroformate (Cbz) **1g** group did not yield the target product. Pleasingly, aziridine bearing celecoxib unit **1h** furnished **3fa** in 59% yield. Moreover, aziridines having iso-propyl **1i** and

hexyl **1j** substitutions resulted the morpholines **3ia** and **3ja** in 54% and 59% yields, respectively with >10:1 dr. However, benzyl substitution **1k** produced **3ka** with a trace amount. In addition, vinyl aziridine **1l** successfully led to **3la** in 52% yield with >10:1 dr. Moreover, phenyl substituted aziridine **1m** afforded **3ma** in 72% in yield with 7:1 dr. The structure of **3ma** wasconfirmed by *X*-ray analysis (CCDC 2420492), which suggests that there might be 1,3-methyl shift during the reaction. Aziridines bearing more substituted aryl rings with different electron- withdrawing and donating groups, 2-bromo **1n**, 2-fluoro **1o**, 3-methyl**1p**, 3-nitro **1q**, 4-brormo **1r** and 4-acetoxy **1s** furnished **3na-sa** in 52-78% yields with ≥5:1 dr. Further, naphthylsubstituted aziridine **1t** yielded **3ta** in 70% yield and >10:1 dr, whereas, aziridine derived from carvacrol **1u** furnished in **3ua** 64% yield and >10:1 dr. In contrast, aziridine containing amide group **1v** failed to deliver the target product which may due to co-ordination of Fe-catalyst with amide group. Similarly, disubstituted aziridine **1w** and unactivated aziridine **1x** were unsuccessful substrates.

Table 3.4. Substrate Scope of with Respect to Dienals[a,b]

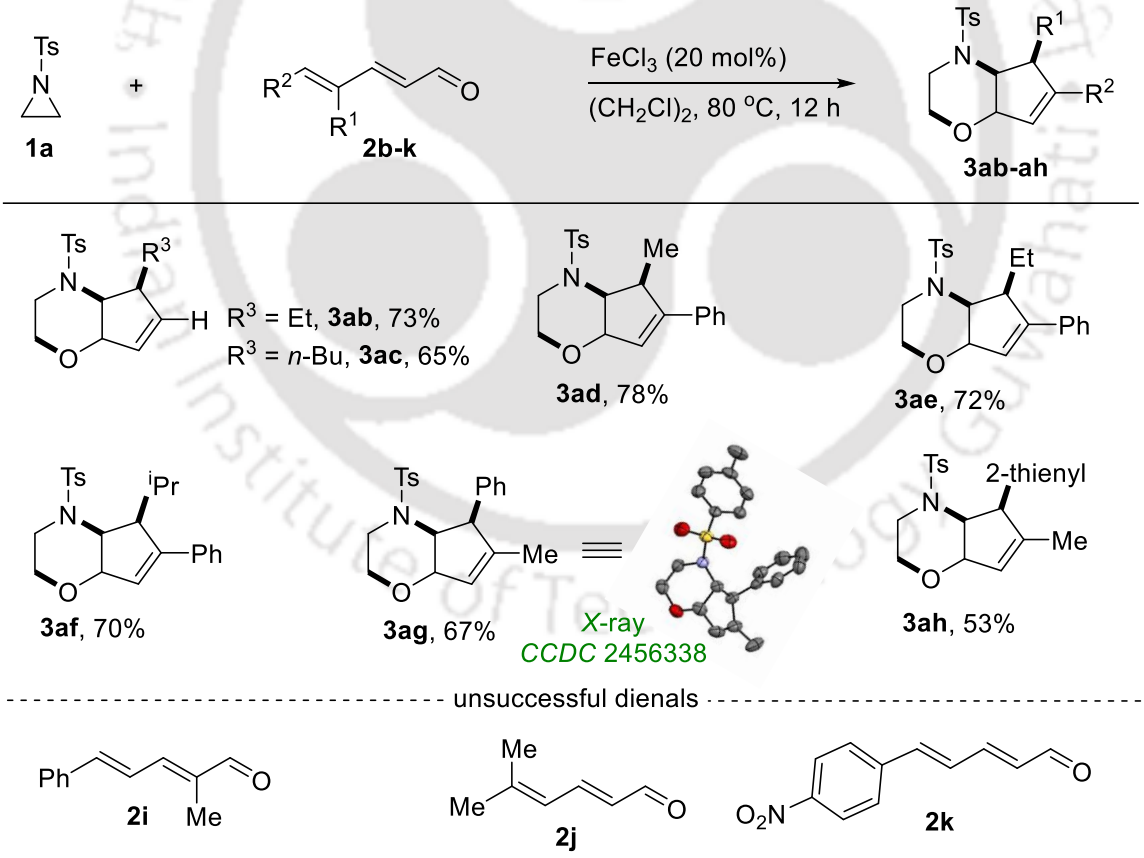

[a]Reaction conditions: **1a** (0.2 mmol), **2b-k** (0.2 mmol), $FeCl_3$ (20 mol %), $(CH_2Cl)_2$ (1 mL), 80 °C, 12 h. [b]Isolated yield.

We further extended the substrate scope by reacting substituted dienals **2b-k** with aziridine **1a** as standard substrate (Table 3.4). 2,4-heptadienal **2d** and 2,4-nonadienal **2c** furnished **3ab** and **3ad** in 79% and 65% in yields, respectively. Dienals bearing phenyl substitution at C-4 position **2d-f** produced the cycloadducts **3ad-af** in 70-78% yields. In addition, dienal having aliphatic substitution at C-4 position and aromatic substitution at C-5 position **2g** yielded **3ag** in 67% yield. The structure of **3ag** was confirmed by X-ray analysis (CCDC 2456338). Delightfully, thienyl substituted dienal **2h** successfully delivered **3ah** 53% in yield. However, dienals **2i**, **2j** and **2k** were failed to furnish the target annulated products, which may be due to more steric encumbrance at C2-center and electron deficiency of dienals to form the Fe-coordinated electrocyclic intermediate.

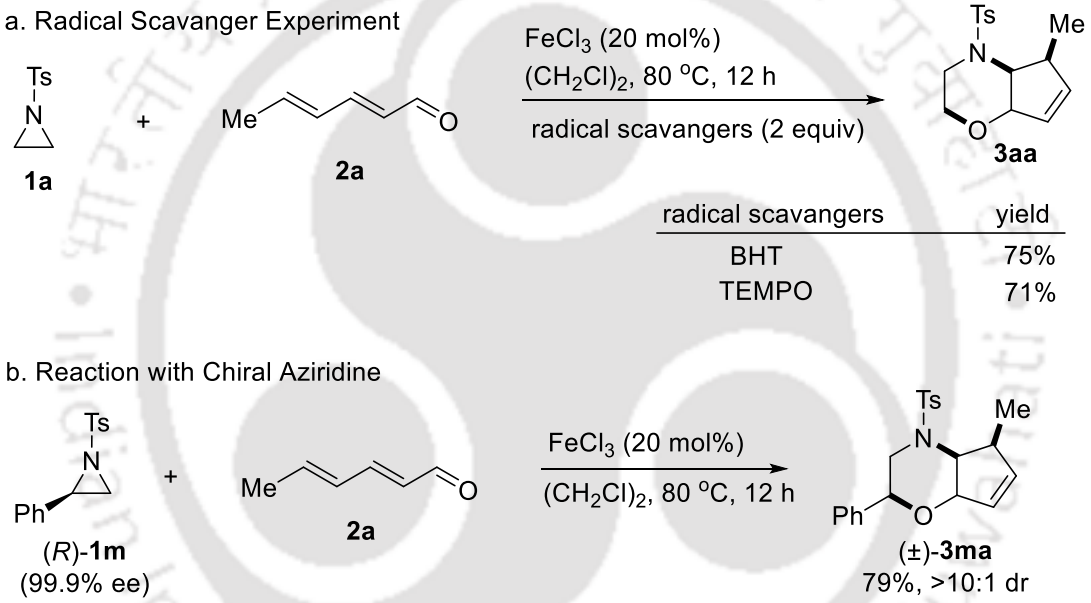

Scheme 3.7. Control Experiments

To gain insight into the reaction pathway, control experiments were performed. The reaction of **1a** and **2a** in presence of TEMPO and BHT under the standard conditions resulted in formation of **3aa** which suggests that the reaction does not involve any radical pathway (Scheme 3.7a). Further, reaction of enantiopure aziridine (R)-**1m** with **2a** with lead to racemic mixture of **3ma** in 79% yield with >10:1 dr (Scheme 3.7b). Based on the experimental results and literature precedents,[14,15] coordination of Fe(III) with dienal **2** may form the ionic species **A**, which then undergoes conrotatory 4π electrocyclization to form the cyclic oxyallyl cation **B** (Scheme 3.8). Heterolytic ring opening of aziridine **1** followed by [3+3]-annulation with **B** may

lead to formation of transition state **D** *via* **C**. Further, a sigmatropic 1,3-methyl shift might furnish the desired cycloadduct **3**.

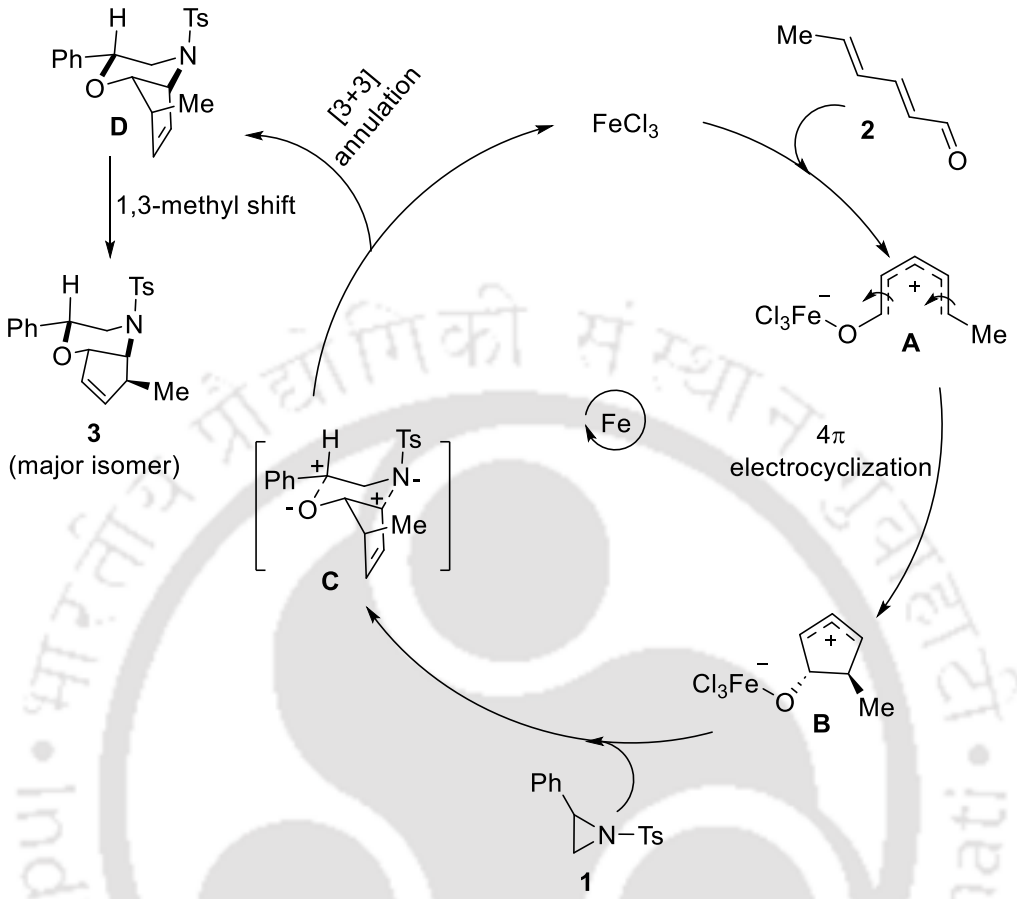

Scheme 3.8. Plausible Reaction Mechanism

To elaborate the synthetic utility, scale-up synthesis was conducted using **1a** and **2a**. The reaction occurred to give **3aa** in 69% yield (Scheme 3.9). This suggests the scalability approach of the designed protocol. To further showcase the versatility of the fused morpholine framework, diverse post-synthetic modification of **3** was performed (Scheme 3.10). Epoxidation of **3aa** with *m*-CPBA resulted in formation **4**, indicating the tolerance of the scaffold to oxidative functionalization. Further, hydrogenation of **3ma** using palladium-charcoal yielded morpholine derivative **5**, demonstrating reductive adaptability. In addition, Suzuki coupling of **3sa** with 3,4-(methylenedioxy)phenylboronic acid furnished **6**, showcasing the amenability of morpholine core to late-stage diversification. These transformations underscore the synthetic flexibility and derivatization potential of the morpholine core. These findings describe the potentiality of the synthesized morpholine to under go further transformation.

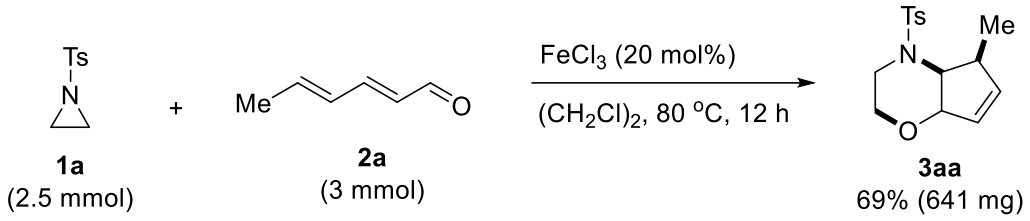

Scheme 3.9. Scale-up Synthesis

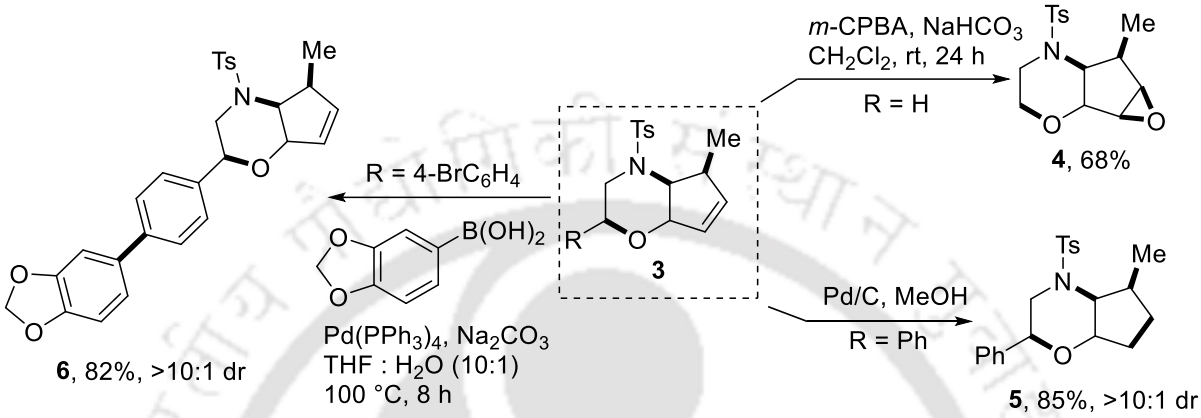

Scheme 3.10. Post-synthetic Transformations

In summary, we have presented an Fe-catalyzed [3+3]-annulation of 2,4-dienals with aziridines. This reaction features an interrupted *iso*-Nazarov 4π-electrocyclization and 1,3-sigmatropic shift, resulting in the formation of bio-relevant fused morpholine frameworks. Key advantages of this method include the use of iron catalyst, substrate scope, diastereoselectivity and synthetic utility.

3.4 Experimental Section

General information. $FeCl_3$ (98%), $FeCl_3$•$6H_2O$ (>98%), $Fe(NO_3)_3$•$9H_2O$ (98%), $FeCl_2$ (98%), $Fe(acac)_3$ (97%), $CuCl_2$ (97%), $CoCl_2$ (97%), $Cu(OTf)_2$ (98%) and BF_3•OEt_2 purchased from Aldrich, TCI and SRL Chemicals, used as received. Aziridines[16,17] and 2,4-dienals[18] were prepared according to literature. SRL silica gel G/GF 254 plates were used for analytical TLC and SRL silica gel (100-200 mesh) was used for column chromatography. Compound spots were visualized using UV lamp (254 nm) and iodine. NMR (^1H, ^{13}C, ^{19}F and NOESY) spectra were recorded with Bruker Ascend 400, 500 and 600 MHz spectrometers using $CDCl_3$ as solvent and TMS as an internal standard. Chemical shifts (δ) and spin-spin coupling constant (*J*) are reported in ppm and in Hz, respectively, and other data are reported as mentioned: s = singlet, d = doublet, t = triplet, m = multiplet. HRMS was recorded with Q-Tof ESI-MS

instrument. Perkin Elmer FT-IR spectrometer was used to record IR spectra. Melting points were determined using a Büchi B-540 apparatus and are uncorrected. HPLC analysis was carried out using a Waters-2489 with YMC Chiral ART Cellulose-SC column utilizing isopropanol and hexane as eluent. Single crystal X-ray data of **3ka** was collected on a Bruker SMART APEX equipped with a CCD area detector using Mo/Kα radiation and the structure was solved by direct method using SHELXL-19 (Göttingen, Germany).

General Procedure for Preparation of Aziridines.[17]

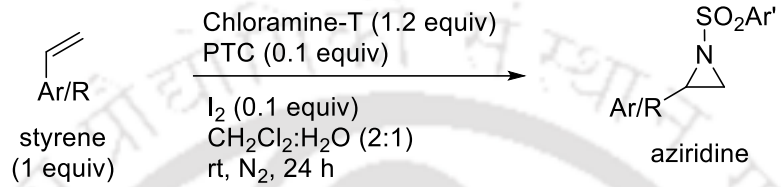

To a stirred solution of the alkene (1 mmol, 1 equiv) and benzyltriethylammonium chloride (PTC) (0.1 mmol, 23 mg) in CH_2Cl_2/H_2O (2:1, 15 mL) were added chloramine-T (1.2 mmol, 251 mg) and iodine (0.1 mmol, 26 mg) at room temperature under N_2 atmosphere. The stirring was allowed to continue for additional 24 h. Then the reaction mixture was treated with saturated aqueous $Na_2S_2O_3$ solution (10 mL) and extracted with CH_2Cl_2 (3 x 10 mL). Drying (Na_2SO_4) and evaporation of the solvent gave a residue that was purified on silica gel column chromatography using hexane and ethyl acetate as eluent to yield aziridine.

General Procedure for Preparation of Chiral Aziridine.[17]

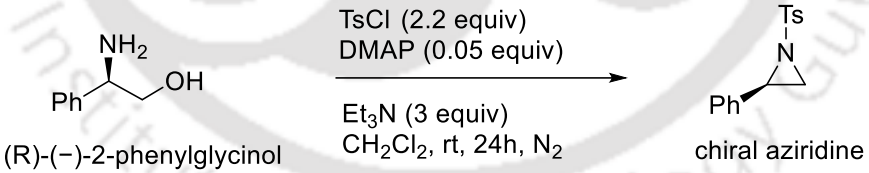

To a stirred solution of (R)-(−)-2-phenylglycinol (1 mmol, 137 mg), TsCl (2.2 mmol, 420 mg) and DMAP (0.05 mmol, 6mg) in dry CH_2Cl_2 (20 mL) at 0 °C, a solution of triethylamine (3 mmol, 420 µL) in dry CH_2Cl_2 (5 mL) was added and the stirring was allowed to continue for additional 24 h. Then the mixture was treated with a saturated aqueous NH_4Cl solution (20 mL) and extracted with CH_2Cl_2 (3 x10 mL). Drying (Na_2SO_4) and evaporation of the solvent gave a residue that was purified on silica gel column chromatography using hexane and ethyl acetate as eluent to yield chiral aziridines.

General Procedure for Preparation of 2,4-Dienal.[18]

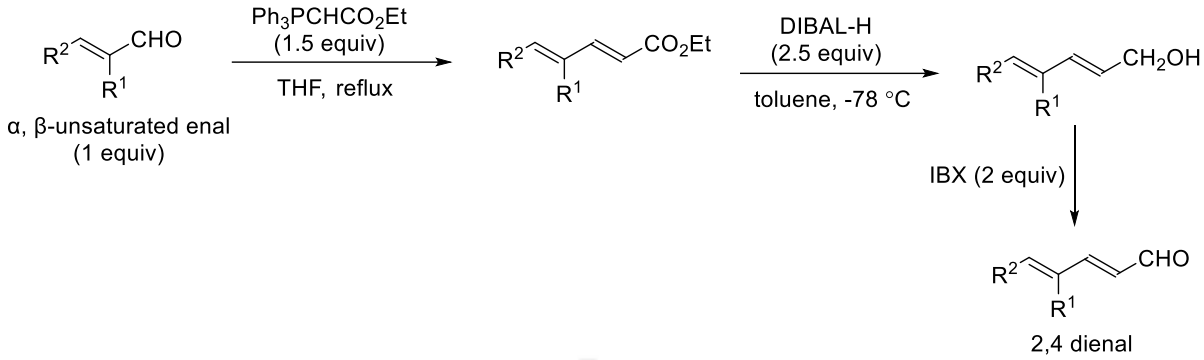

A solution of Ph_3PCHCO_2Et (3 mmol, 1 g) and *α*, *β*-unsaturated enal (2.5 mmol) in THF (20 mL) was allowed to reflux till completion (monitored by TLC). The reaction mixture was cooled to room temperature and evaporation of the solvent resulted in crude mixture which was purified on silica gel column chromatography using hexane and ethyl acetate as eluent to yield the unsaturated ester.

The unsaturated ester was dissolved in dry toluene (20 mL) and allowed to stir at -78 °C under an argon atmosphere for 10 minutes. DIBAL-H (5.0 mL) was added dropwise and the stirring was continued for additional 12 h. Then the reaction mixture was quenched with saturated aqueous NH_4Cl solution (10 mL) and the resultant mixture was filtered. Evaporation of the filtrate gave a residue that was purified on silica gel column chromatography using hexane and ethyl acetate as eluent to yield the unsaturated alcohol.

To a solution of the obtained alcohol in DMSO (5 mL), IBX (4.5 mol, 1.2 g) was added and the stirring was continued at room temperature. Upon completion (monitored by TLC), the reaction mixture was treated with cooled H_2O (5 mL). The organic part was extracted with ethyl acetate. Drying (Na_2SO_4) and evaporation of the solvent gave a residue that was purified on silica gel column chromatography using hexane and ethyl acetate as eluent to yield 2,4-dienals.

General Procedure for the Annulation of Dienals with Aziridines. To a stirred solution of **1** (0.2 mmol) and **2** (0.24 mmol) in $(CH_2Cl)_2$ (1 mL), $FeCl_3$ (20 mol %, 7 mg) was added and the mixture was allowed to stir at 80 °C for 12 h. The reaction mixture was cooled to room temperature, diluted with CH_2Cl_2 (10 mL) and passed through a short pad of celite. Evaporation of the solvent gave a residue, that was purified by silica gel column chromatography using hexane/ethyl acetate as eluent to yield **3**. The dr was determined using ^1H NMR analysis.

Scale-up Synthesis of 3aa. To a stirred solution of **1a** (2.5 mmol, 493.5 mg) and **2a** (3 mmol, 288 mg) in $(CH_2Cl)_2$ (5 mL), $FeCl_3$ (20 mol %), 81 mg) was added and the mixture was allowed to stir at 80 °C for 12 h. The reaction mixture was cooled to room temperature, diluted with CH_2Cl_2 (20 mL), washed with brine (5 mL) and water (5 mL). Drying (Na_2SO_4) and evaporation of solvent gave a residue that was purified on silica gel column chromatography using ethyl acetate/hexane as eluent to yield **3aa** in 69% (641 mg).

Synthesis of 4. To an ice-cold solution of **3aa** (0.2 mmol, 59 mg) and $NaHCO_3$ (0.5 mmol, 42 mg) in CH_2Cl_2 (3 mL), *m*CPBA (0.5 mmol, 86 mg) was added portion wise. The reaction mixture was allowed to stir for 24 h at room temperature and quenched with saturated $Na_2S_2O_3$. The organic layer was extracted using CH_2Cl_2 (3 x 5 mL). Drying (Na_2SO_4) and evaporation of the solvent gave a residue that was purified on silica gel column chromatography using ethyl acetate/hexane as eluent to yield **4** in 68% (42 mg).

Synthesis of 5. To a stirred solution of **3ka** (0.2 mmol, 74 mg) in MeOH (2 mL), Pd/C (10 mol %, 2 mg) added and the reaction was allowed to stir under hydrogen balloon for 12 h at room temperature. The reaction mixture was passed through a short celite pad using EtOAc (10 mL). Evaporation of the solvent gave a residue that was purified on silica gel column chromatography using ethyl acetate/hexane as eluent to yield **5** in 85% (63 mg).

Synthesis of 6. In a pressure tube, **3qa** (0.2 mmol, 90 mg), 3,4-(methylenedioxy)phenylboronic acid (0.4 mmol, 66 mg), Na_2CO_3 (0.4 mmol, 42 mg), toluene (1 mL), ethanol (1 mL) and water (100 µL) were added and purged with argon for 10 minutes. $Pd(PPh_3)_4$ (2 mol % , 5 mg) was added and the mixture was allowed to stir at 100 °C for 8 h. After completion (monitored by TLC), the mixture was diluted with ethyl acetate (20 mL) and washed with water (5 mL). Drying (Na_2SO_4) and evaporation of the solvent gave a residue which was purified on silica gel column chromatography using hexane/ethyl acetate as eluent to afford **6** in 82% (80 mg).

Control Experiments

Radical Scavengers Experiment (Scheme 7a). To a stirred solution of **1a** (0.2 mmol, 39.5 mg) and **2a** (0.24 mmol, 23 mg) in $(CH_2Cl)_2$ (1 mL), $FeCl_3$ (20 mol %, 7 mg) followed by TEMPO or BHT (0.4 mmol) were added and the mixture was allowed to stir at 80 °C for 12 h.

The reaction mixture was purified as according to general procedure to isolate **3aa**. Using BHT the isolated yield of **3aa** was 75% (44 mg) while using BHT the yield was 71% (42 mg).

Experiment with Chiral Aziridine (R)-1m (Scheme 7b). To a stirred solution of (R)-**1m** (0.2 mmol, 54.6 mg) and **2a** (0.24 mmol, 23 mg) in $(CH_2Cl)_2$ (1 mL), $FeCl_3$ (20 mol %, 7 mg) was added and the mixture was allowed to stir at 80 °C for 12 h. The reaction mixture was purified as according to general procedure to isolate **3ma** in 79% (58.3 mg) yield. The HPLC analysis of **3ma** using YMC Chiral ART Cellulose-SC column, (hexane/^{i}PrOH = 95: 05, flow rate: 1 mL/min, λ= 254 nm) suggested the product as racemic.

3.5 Characterization Data

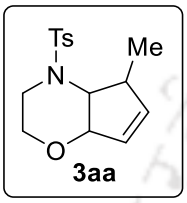

5-Methyl-4-tosyl-2,3,4,4a,5,7a-hexahydrocyclopenta[b][1,4]oxazine 3aa. Analytical TLC on silica gel; 9:1 hexane/ethyl acetate R_f = 0.22; thick colorless liquid; yield 82% (49 mg); ^{1}H NMR (500 MHz, $CDCl_3$) δ 7.74-7.73 (m, 2H), 7.33 (d, *J* = 8.0 Hz, 2H), 6.04-6.03 (m, 1H), 5.83-5.81 (m, 1H), 3.91-3.90 (m, 1H), 3.70 (d, *J* = 15.0 Hz, 1H), 3.64-3.62 (m, 1H), 3.52 (d, *J* = 15.0 Hz, 1H), 3.32- 3.26 (m, 1H), 3.01-2.92 (m, 2H), 2.44 (s, 3H), 1.17-1.15 (m, 3H); ^{13}C NMR (125 MHz, $CDCl_3$) δ 143.8, 143.6, 138.1, 130.0, 128.5, 127.1, 76.0, 62.3, 61.6, 41.7, 39.1, 21.6, 16.4; FT-IR (neat) 2959, 2870, 1597, 1349, 1340, 1158, 1093, 933, 767, 659, 591 cm^{-1}; HRMS (ESI) m/z $[M+H]^+$ calcd for $C_{15}H_{20}NO_3S$: 294.1158, found: 294.1168.

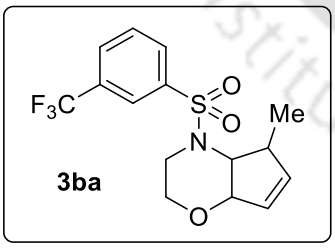

5-Methyl-4-((3-(trifluoromethyl)phenyl)sulfonyl)-2,3,4,4a,5,7a-hexahydrocyclopenta[b][1,4]oxazine 3ba. Analytical TLC on silica gel; 9:1 hexane/ethyl acetate, R_f = 0.20; thick colorless liquid; yield 64% (44 mg); ^{1}H NMR (500 MHz, $CDCl_3$) δ 8.10 (s, 1H), 8.04 (d, *J* = 8.0 Hz, 2H), 7.88 (d, *J* = 7.5 Hz, 2H), 7.72 (t, *J* = 8.0 Hz, 1H), 5.91-5.90 (m, 1H), 5.18 (d, *J* = 5.5 Hz, 1H), 4.82 (s, 1H), 3.76-3.74 (m, 3H), 3.60 (d, *J* = 12.5 Hz, 1H), 3.48-3.44 (m, 1H), 3.10-3.05 (m, 1H), 3.66-3.31 (m, 1H), 1.00 (d, *J* = 7.5Hz, 3H); ^{13}C NMR (125 MHz, $CDCl_3$) δ 141.3, 139.7, 132.4 (J_{C-F} = 33.3 Hz), 130.3 130.1, 129.4 (J_{C-F} = 3.5

Hz), 126.4 (J_{C-F} = 269.8 Hz), 125.2, 124.2 (J_{C-F} = 3.5 Hz), 80.9, 64.2, 59.4, 45.3, 41.7, 15.2; ^{19}F NMR (470 MHz, $CDCl_3$) δ -62.84; FT-IR (neat) 2963, 2927, 2870, 1326, 1164, 1133, 1071, 957, 696, 598 cm^{-1}; HRMS (ESI) m/z $[M+H]^+$ calcd for $C_{15}H_{17}F_3NO_3S$: 348.0876, found: 348.0870.

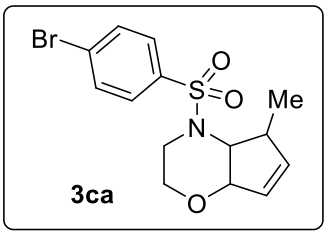

4-((4-Bromophenyl)sulfonyl)-5-methyl-2,3,4,4a,5,7a hexahydrocyclopenta[b][1,4]oxazine 3ca. Analytical TLC on silica gel; 9:1 hexane/ethyl acetate R_f = 0.22; thick colorless liquid; yield 76% (54 mg); ^{1}H NMR (500 MHz, $CDCl_3$) δ 7.73-7.66 (m, 4H), 6.04 (d, *J* = 6.0 Hz, 1H), 5.84-5.82 (m, 1H), 3.94-3.93 (m, 1H), 3.69 (d, *J* = 15.0 Hz, 1H), 3.63-3.60 (m, 1H), 3.57 (d, *J* = 11.5 Hz, 1H), 3.33-3.27 (m, 1H), 3.06-3.00 (m, 1H), 2.95-2.92 (m, 1H), 1.15 (d, *J* = 7.0 Hz, 3H); ^{13}C NMR (125 MHz, $CDCl_3$) δ 143.8, 140.2, 132.7, 128.6, 128.5, 127.7, 76.2, 62.4, 61.7, 41.8, 39.1, 16.5. FT-IR (neat) cm^{-1} 2959, 2870, 1574, 1388, 1352, 1163, 1095, 987, 933, 735, 612, 577; HRMS (ESI) m/z $[M+H]^+$ calcd for $C_{14}H_{17}BrNO_3S$: 358.0107, found: 358.0103.

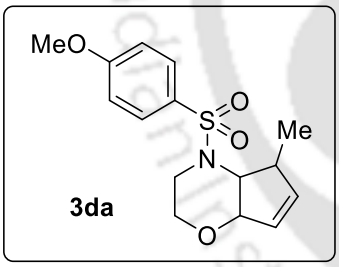

4-((4-Methoxyphenyl)sulfonyl)-5-methyl-2,3,4,4a,5,7a-hexahydrocyclopenta[b][1,4]oxazine 3da. Analytical TLC on silica gel; 9:1 hexane/ethyl acetate, R_f = 0.18; thick colorless liquid; yield 71% (43 mg); ^{1}H NMR (500 MHz, $CDCl_3$) δ 7.79 (d, *J* = 9.0 Hz, 2H), 7.00 (d, *J* = 9.0 Hz, 2H), 6.037 (d, *J* = 6.0 Hz, 1H), 5.83-5.81 (m, 1H), 3.93-3.91 (m, 1H), 3.88 (s, 3H), 3.68 (d, *J* = 14.5 Hz, 1H), 3.6-3.60 (m, 1H), 3.53 (d, *J* = 11.5 Hz, 1H), 3.31-3.25 (m, 1H), 3.05-3.00 (m, 1H), 2.96-2.90 (m, *J* = 6.8 Hz, 1H), 1.16 (d, *J* = 7.0 Hz, 3H); ^{13}C NMR (125 MHz, $CDCl_3$) δ 163.0, 143.9, 132.7, 129.3, 128.6, 114.5, 76.1, 62.4, 61.6, 55.7, 41.7, 39.1, 16.5. FT-IR (neat) 2959, 2925, 2870, 1454, 1384, 1159, 1073, 987, 657 cm^{-1}; HRMS (ESI) m/z $[M+H]^+$ calcd for $C_{15}H_{20}NO_4S$: 310.1108, found: 310.1109.

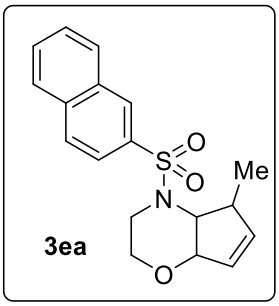

5-Methyl-4-(naphthalen-2-ylsulfonyl)-2,3,4,4a,5,7a-hexahydrocyclopenta[b][1,4]oxazine 3ea. Analytical TLC on silica gel; 9:1 hexane/ethyl acetate, R_f = 0.23; thick colorless liquid; yield 76% (49 mg); ^{1}H NMR (500 MHz, $CDCl_3$) δ 8.43 (s, 1H), 8.00 (t, *J* = 9.0 Hz, 2H), 7.93 (d, *J* = 8.0 Hz, 1H), 7.82-7.80 (m, 1H), 7.67-7.61 (m, 2H), 6.05 (d, *J* = 6.0 Hz, 1H), 5.82-5.81 (m, 1H), 3.93-3.92 (m, 1H), 3.78-3.72 (m, 2H), 3.52 (d, *J* = 11.0 Hz, 1H), 3.36-3.30 (m, 1H), 3.01-2.95 (m, 2H), 1.19 (d, *J* = 7.0 Hz, 3H); ^{13}C NMR (125 MHz, $CDCl_3$) δ 143.9, 137.9, 134.9, 132.3, 129.8, 129.3, 129.0, 128.6, 128.5, 128.0, 127.8, 122.3, 76.2, 62.6, 61.8, 41.8, 39.1, 16.5; FT-IR (neat) 2959, 2925, 2870, 1454, 1348, 1159, 1073, 987, 657 cm^{-1}; HRMS (ESI) m/z $[M+H]^+$ calcd for $C_{18}H_{20}NO_3S$: 330.1158, found: 330.1167.

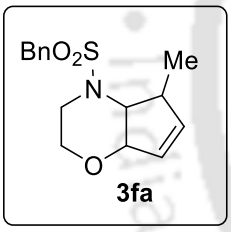

4-(Benzylsulfonyl)-5-methyl-2,3,4,4a,5,7a hexahydrocyclopenta[b]-[1,4]oxazine 3fa. HRMS (ESI) *m/z* $[M+H]^+$ calcd for $C_{15}H_{20}NO_3S$: 294.1158, found: 294.1152.

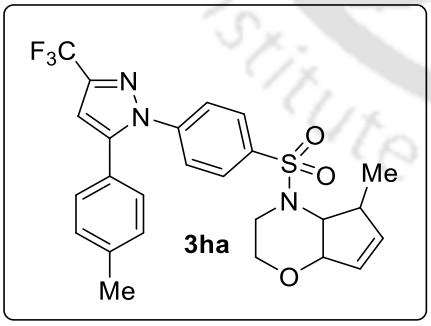

5-Methyl-4-((4-(5-(p-tolyl)-3-(trifluoromethyl)-1H-pyrazol-1-yl)phenyl)sulfonyl)-2,3,4,4a,5,7a-hexahydrocyclopenta[b][1,4]oxazine 3ha. Analytical TLC on silica gel; 9:1 hexane/ethyl acetate, R_f = 0.20; thick colorless liquid; yield 59% (59.5 mg); ^{1}H NMR (500 MHz, $CDCl_3$) δ 7.85 (d, *J* = 8.5 Hz, 2H), 7.50 (d, *J* = 9.0 Hz, 2H), 7.17 (d, *J* = 5.0Hz, 2H), 7.09 (d, *J* = 8.0 Hz, 2H), 6.75 (s, 1H), 6.04 (d, *J* = 6.0 Hz, 1H), 5.83-5.81 (m, 1H), 3.89-3.88 (m, 1H), 3.70 (d, *J* = 14.5 Hz, 1H), 3.61-3.58 (m, 1H), 3.55 (d, *J*

= 11.5 Hz, 1H), 3.33-3.28 (m, 1H), 3.01-2.90 (m, 2H), 2.38 (s, 3H), 1.15 (d, J = 7.0 Hz, 3H); ^{13}C NMR (125 MHz, $CDCl_3$) δ 145.4, 144.7 (J_{C-F} = 38.5 Hz), 144.4, 144.1, 143.9, 143.8, 142.6, 140.6, 139.9, 129.8, 128.8, 128.5, 128.0, 125.9 (J_{C-F} = 267.5 Hz), 125.8, 124.3, 122.2, 120.1, 117.9, 106.4, 76.1, 62.4, 61.8, 41.8, 39.1, 21.4, 16.5; ^{19}F NMR (470 MHz, $CDCl_3$) δ -62.44; FT-IR (neat) 2926, 2872, 1471, 1354 , 1237, 1162,1096, 975, 749, 629 cm^{-1}; HRMS (ESI) m/z $[M+H]^+$ calcd for $C_{25}H_{25}F_3N_3O_3S$: 504.1563, found: 504.1561.

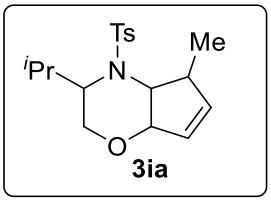

3ia

3-Isopropyl-5-methyl-4-tosyl-2,3,4,4a,5,7a-hexahydrocyclopenta[b]-[1,4]oxazine 3ia. Analytical TLC on silica gel; 11:1 hexane/ethyl acetate, R_f = 0.28; thick colorless liquid; yield 54% (36 mg); major diastereomer (>10:1 dr); ^{1}H NMR (500 MHz, $CDCl_3$) δ 7.74 (d, J = 8.0 Hz, 2H), 7.30 (d, J = 8.0 Hz, 2H), 5.95 (d, J = 6.0 Hz, 1H), 5.59-5.57 (m, 1H), 4.59 (d, J = 7.5 Hz, 1H), 3.80 (t, J = 7.5 Hz, 1H), 3.38-3.35 (m, 1H), 3.32-3.28 (m, 1H), 3.20-3.16 (m, 1H), 2.91-2.88 (m, 1H), 2.44-2.39 (m, 4H), 1.16 (d, J = 7.0 Hz, 3H), 0.85 (d, J = 6.5 Hz, 3H), 0.768 (d, J = 6.5 Hz, 3H); ^{13}C NMR (125 MHz, $CDCl_3$) δ 143.2, 141.7, 136.6, 129.6, 127.6, 127.2, 77.6, 70.7, 58.7, 44.8, 43.7, 30.4, 21.5, 18.3, 18.2, 18.0; FT-IR (neat) 2960, 2928, 2873, 1340, 1165, 1090, 666 547 cm^{-1}; HRMS (ESI) m/z $[M+H]^+$ calcd for $C_{18}H_{26}NO_3S$: 336.1628, found: 336.1626.

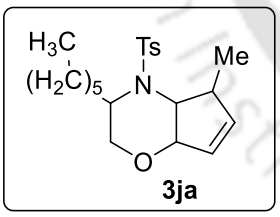

3ja

3-Hexyl-5-methyl-4-tosyl-2,3,4,4a,5,7a-hexahydrocyclopenta[b][1,4]oxazine 3ja. Analytical TLC on silica gel; 11:1 hexane/ethyl acetate, R_f = 0.30; colorless liquid; yield 59% (44 mg); major diastereomer (>10:1 dr); ^{1}H NMR (400 MHz, $CDCl_3$) δ 7.74 (d, J = 8.4 Hz, 2H), 7.31 (d, J = 8.0 Hz, 2H), 5.96-5.94 (m, 1H), 5.64-5.61 (m, 1H), 4.55-4.52 (m, 1H), 3.78 (t, J = 6.8 Hz, 1H), 3.56-3.50 (m, 1H), 3.40-3.35 (m, 1H), 3.21-3.16 (m, 1H), 2.94-2.90 (m, 1H), 2.42 (s, 3H), 1.40-1.34 (m, 1H), 1.27-1.14 (m, 12H), 0.88 (t, J = 6.8 Hz, 3H); ^{13}C NMR (125 MHz, $CDCl_3$) δ 143.4, 142.0, 136.9, 129.7, 128.0, 127.3, 76.6, 66.7, 59.3, 46.5, 43.4, 32.4, 31.812, 29.2, 25.3, 22.6, 21.6, 18.1, 14.1; FT-IR (neat) 2955, 2927, 2858, 1340, 1163, 1090, 1003, 813, 664, 546 cm^{-1}; HRMS (ESI) m/z $[M+H]^+$ calcd for $C_{21}H_{32}NO_3S$: 378.2097, found: 378.2094.

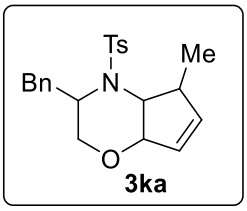

3-Benzyl-5-methyl-4-tosyl-2,3,4,4a,5,7a-hexahydrocyclopenta[b][1,4]oxazine 3ka. Yield: trace. HRMS (ESI) m/z $[M+H]^+$ calcd for $C_{22}H_{26}NO_3S$: 384.1628, found: 384.1625.

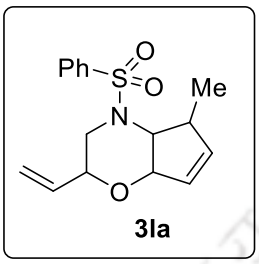

5-Methyl-4-tosyl-2-vinyl-2,3,4,4a,5,7a-hexahydrocyclopenta[b][1,4]oxazine 3la. Analytical TLC on silica gel; 11:1 hexane/ethyl acetate, R_f = 0.26; thick colorless liquid; yield 52% (31 mg); major diastereomer (>10:1 dr); ^{1}H NMR (500 MHz, $CDCl_3$) δ 7.86 (d, *J* = 7.0 Hz, 2H), 7.60-7.57 (m, 1H), 7.53-7.50 (m, 2H), 5.98 (d, *J* = 6.5 Hz, 1H), 5.68-5.61 (m, 2H), 5.22 (d, *J* = 17.5 Hz, 1H), 5.14 (d, *J* = 10.5 Hz, 1H), 4.63 (d, *J* = 7.0 Hz, 1H), 4.11-4.08 (m, 1H), 3.79 (t, *J* = 6.5 Hz, 1H), 3.48-3.44 (m, 1H), 3.37-3.33 (m, 1H), 2.99-2.96 (m, 1H), 1.15 (d, *J* = 7.0 Hz, 3H); ^{13}C NMR (125 MHz, $CDCl_3$) δ 142.4, 139.7, 135.0, 132.8, 129.2, 128.0, 127.4, 118.1, , 76.6, 67.949, 46.0, 43.1, 18.1; FT-IR (neat) 3003, 2989, 2964, 1448, 1346, 1275, 1258, 1166, 764, 750 cm^{-1}; HRMS (ESI) m/z $[M+H]^+$ calcd for $C_{16}H_{20}NO_3S$: 306.1158, found: 306.1159.

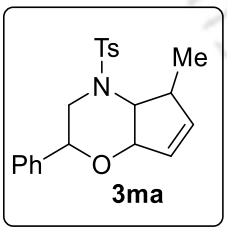

5-Methyl-2-phenyl-4-tosyl-2,3,4,4a,5,7a-hexahydrocyclopenta[b][1,4]oxazine 3ma. Analytical TLC on silica gel; 11:1 hexane/ethyl acetate, R_f= 0.28; colorless solid; mp 118-119 °C; yield 72% (52 mg); major diastereomer (7:1 dr); ^{1}H NMR (400 MHz, $CDCl_3$) δ 7.81 (d, *J* = 8.4 Hz, 2H), 7.38 (d, *J* = 8.0 Hz, 2H), 7.31-7.28 (m, 4H), 7.19-7.17 (m, 2H), 6.07-6.05 (m, 1H), 5.90-5.87 (m, 1H), 4.14-4.12 (m, 1H), 3.88-3.84 (m, 2H), 3.73-3.70 (m, 1H), 3.16-3.10 (m, 1H), 3.04-2.96 (m, 1H), 2.46 (s, 3H), 1.20 (d, *J* = 7.2 Hz, 3H); ^{13}C NMR (100 MHz, $CDCl_3$) δ 143.8, 143.7, 138.6, 138.2, 130.1, 128.7, 128.6, 128.3, 127.2, 126.1, 61.2,

47.6, 39.1, 21.7, 16.4; FT-IR (neat) 2960, 2926, 2873, 1453, 1162, 1090, 1005, 699, 662, 595, 548 cm^{-1}; HRMS (ESI) m/z $[M+H]^+$ calcd for $C_{21}H_{24}NO_3S$: 370.1471, found: 370.1479.

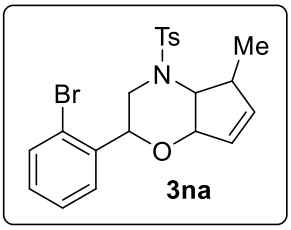

2-(2-Bromophenyl)-5-methyl-4-tosyl-2,3,4,4a,5,7a-hexahydrocyclopenta[b][1,4]oxazine 3na. Analytical TLC on silica gel; 11:1 hexane/ethyl acetate, R_f= 0.26; colorless solid; mp 124-125 °C; yield 77% (69 mg) major diastereomer (5:1 dr); ^{1}H NMR (400 MHz, $CDCl_3$) δ 7.87 (d, *J* = 8.4 Hz, 2H), 7.48-7.46 (m, 1H), 7.71-7.39 (m, 1H), 7.34 (d, *J* = 8.0 Hz, 2H), 7.30-7.27 (m, 1H), 7.1-7.10 (m, 1H), 6.10-6.08 (m, 1H), 5.91-5.88 (m, 1H), 4.37-4.33 (m, 1H), 4.15-4.13 (m, 1H), 4.02-4.01 (m, 1H), 3.72-3.69 (m, 1H), 3.04-3.00 (m, 1H), 2.97-2.91 (m, 1H), 2.44 (s, 3H), 1.25 (d, *J* = 6.8 Hz, 3H); ^{13}C NMR (100 MHz, $CDCl_3$) δ 144.0, 143.7, 138.1, 132.6, 130.0, 129.6, 128.6, 128.0, 127.9, 127.6, 121.8, 72.9, 61.1, 46.0, 38.9, 21.7, 16.4; FT-IR (neat) 2958, 2927, 2873, 1343, 1163, 1089, 756, 665, 552 cm^{-1}; HRMS (ESI) m/z $[M+H]^+$ calcd for $C_{21}H_{23}BrNO_3S$: 448.0577, found: 448.0576.

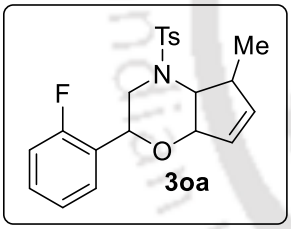

2-(2-Fluorophenyl)-5-methyl-4-tosyl-2,3,4,4a,5,7a-hexahydrocyclopenta[b][1,4]oxazine 3oa. Analytical TLC on silica gel; 11:1 hexane/ethyl acetate, R_f= 0.27; thick colorless liquid; yield 69% (53 mg) major diastereomer (9:1 dr); ^{1}H NMR (400 MHz, $CDCl_3$) δ 7.83 (d, *J* = 8.1 Hz, 2H), 7.37(d, *J* = 8.0 Hz, 2H), 7.34-7.31 (m, 1H), 7.27-7.21 (m, 1H), 7.11-7.07 (m, 1H), 7.02-6.99 (m, 1H), 6.09-6.07 (m, 1H), 5.88-5.85 (m, 1H), 4.14-4.11 (m, 1H), 4.03-3.97 (m, 2H), 3.69-3.66 (m, 1H), 3.11-3.05 (m, 1H), 3.02-2.98 (m, 1H), 2.45 (s, 3H), 1.25 (d, *J* = 7.2 Hz, 3H); ^{13}C NMR (100 MHz, $CDCl_3$) δ 160.7 (J_{C-F} = 244.8 Hz), 143.8, 143.7, 138.1, 130.2, 129.6 (J_{C-F} = 8.1 Hz), 128.5, 127.4 (J_{C-F} = 3.9 Hz), 127.2, 125.9 (J_{C-F} = 13.8 Hz), 124.5 (J_{C-F} = 3.4 Hz), 115.2 (J_{C-F} = 21.1 Hz), 76.6, 67.4 (J_{C-F} = 2.4 Hz), 61.3, 46.8, 39.1, 21.6, 16.3; ^{19}F NMR (470 MHz, $CDCl_3$) δ -123.52; FT-IR (neat) 2958, 2928, 2875, 1492, 1455, 1344, 1162, 1108, 1088, 760, 665, 546 cm^{-1}; HRMS (ESI) m/z $[M+H]^+$ calcd for $C_{21}H_{23}FNO_3S$: 388.1377, found: 388.1381.

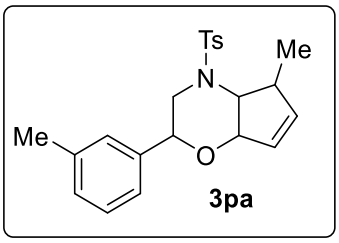

5-Methyl-2-(m-tolyl)-4-tosyl-2,3,4,4a,5,7a-hexahydrocyclopenta[b][1,4]oxazine 3pa. Analytical TLC on silica gel; 11:1 hexane/ethyl acetate, R_f= 0.30; thick colorless liquid; yield 74% (57 mg); major diastereomer (>10:1 dr); ^{1}H NMR (400 MHz, CDCl3 δ 7.73 (d, *J* = 8.4 Hz, 2H), 7.30(d, *J* = 8.4 Hz, 2H), 7.13 (m, *J* = 7.6 Hz, 1H), 7.01 (d, *J* = 7.2 Hz, 1H), 6.93 (s, 1H), 6.89 (d, *J* = 7.6 Hz, 1H), 6.00-5.98 (m, 1H), 5.83-5.80 (m, 1H), 4.05-4.04 (m, 1H), 3..80-3.79 (m, 1H), 3.77 (s, 1H), 3.65-3.62 (m, 1H), 3.09-3.03 (m, 1H), 2.96-2.89 (m, 1H), 2.38 (s, 3H), 2.24 (s, 3H), 1.12 (d, *J* = 6.80 Hz, 3H); ^{13}C NMR (125 MHz, $CDCl_3$) δ 143.8, 143.6, 138.5, 138.3, 138.2, 130.1, 129.1, 128.7, 128.5, 127.2, 126.6, 123.2, 76.9, 73.6, 61.2, 47.6, 39.0, 21.7, 21.5, 16.4; FT-IR (neat) 3056, 2926, 2872, 1332, 1161, 1089, 815, 664, 546 cm^{-1}; HRMS (ESI) m/z $[M+H]^+$ calcd for $C_{22}H_{26}NO_3S$: 384.1628, found: 384.1644.

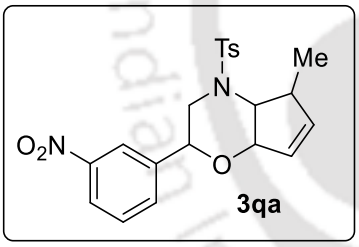

5-Methyl-3-(3-nitrophenyl)-4-tosyl-2,3,4,4a,5,7a-hexahydrocyclopenta[b][1,4]oxazine 3qa. Analytical TLC on silica gel; 9:1 hexane/ethyl acetate, R_f= 0.24; thick yellow liquid; yield 52% (43 mg); major diastereomer (7:1 dr) ; ^{1}H NMR (400 MHz, $CDCl_3$) δ 8.15-8.13 (m, 1H), 8.08-8.07 (s, 1H), 7.82 (d, *J* = 8.4 Hz, 2H), 7.55-7.48 (m, 2H), 7.40 (d, *J* = 8.0 Hz, 2H), 6.10-6.08 (m, 1H), 5.91-5.88 (m, 1H), 4.20-4.18 (m, 1H), 4.04-4.03 (m, 1H), 4.02-4.01 (m, 1H), 3.76-3.72 (m, 1H), 3.12-3.06 (m, 1H), 3.02-2.95 (m, 1H), 2.47 (s, 3H), 1.17 (d, *J* = 7.2 Hz, 3H); ^{13}C NMR (100 MHz, $CDCl_3$) δ 148.5, 144.1, 144.0, 140.8, 137.9, 132.1, 130.2, 129.6, 128.3, 127.2, 123.2, 121.2, 72.6, 61.1, 47.4, 39.0, 21.7, 16.4; FT-IR (neat) 2961, 2927, 2871, 1530, 1347, 1161, 1090, 808, 749, 665, 546 cm^{-1}; HRMS (ESI) m/z $[M+H]^+$ calcd for $C_{21}H_{23}N_2O_5S$: 415.1322, found: 415.1326.

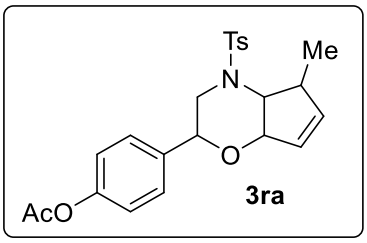

4-(5-Methyl-4-tosyl-2,3,4,4a,5,7a-hexahydrocyclopenta[b][1,4]oxazin-3-yl)phenyl acetate 3ra. Analytical TLC on silica gel; 11:1 hexane/ethyl acetate, R_f = 0.25; thick colorless liquid; yield 67% (57 mg); major diastereomer (>10:1 dr); ^{1}H NMR (600 MHz, $CDCl_3$) δ 7.79 (d, *J* = 7.8 Hz, 2H), 7.37 (d, *J* = 7.8 Hz, 2H), 7.21 (d, *J* = 7.8 Hz, 2H), 7.04 (d, *J* = 7.8 Hz, 2H), 6.06 (d, *J* = 6.0 Hz, 1H), 5.88-5.87 (m, 1H), 4.14 (s, 1H), 3.89-3.84 (m, 2H), 3.73-3.71 (m, 1H), 3.12 (dd, *J* = 10.8, 14.5 Hz, 1H), 3.00-2.95 (m, 1H), 2.45 (s, 3H), 2.27 (s, 3H), 1.18 (d, *J* = 7.2 Hz, 3H); ^{13}C NMR (150 MHz, $CDCl_3$) δ 169.4, 150.5, 143.9, 143.7, 138.1, 136.2, 130.2, 128.6, 127.3, 127.2, 121.8, 73.0, 61.1, 47.5, 39.0, 21.7, 21.2, 16.4; FT-IR (neat) 2956, 2928, 2873, 1759, 1507, 1341, 1194, 1161, 1089, 665, 546 cm^{-1}; HRMS (ESI) m/z $[M+H]^+$ calcd for $C_{23}H_{26}NO_5S$: 428.1526, found: 428.1537.

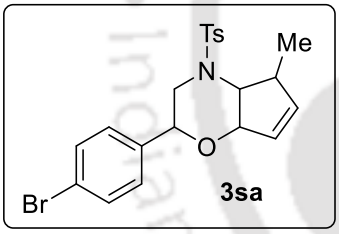

2-(4-Bromophenyl)-5-methyl-4-tosyl-2,3,4,4a,5,7a-hexahydrocyclopenta[b][1,4]oxazine 3sa. Analytical TLC on silica gel; 11:1 hexane/ethyl acetate, R_f = 0.28; thick colorless liquid; yield 78% (67 mg); major diastereomer (>10:1 dr); ^{1}H NMR (400 MHz, $CDCl_3$) δ 7.79 (d, *J* = 8.0 Hz, 2H), 7.44 (d, *J* = 8.4 Hz, 2H), 7.37 (d, *J* = 8.0 Hz, 2H), 7.07 (d, *J* = 8.4 Hz, 2H), 6.07-6.05 (m, 1H), 5.89-5.86 (m, 1H), 4.14-4.12 (m, 1H), 3.87-3.81 (m, 1H), 3.72-3.69 (m, 1H), 3.09-3.02 (m, 1H), 3.00-2.93 (m, 1H), 3.10 (M, 1H), 2.45 (s, 3H), 1.17 (d, *J* = 7.2 Hz, 3H); ^{13}C NMR (100 MHz, $CDCl_3$) δ 143.9, 143.7, 138.1, 137.6, 131.7, 130.2, 128.5, 127.7, 127.2, 122.2, 76.9, 72.9, 61.1, 47.5, 39.0, 21.7, 16.4; FT-IR (neat) 2927, 2873, 1596, 1489, 1335, 1161, 1089, 1009, 816, 667, 551cm^{-1}; HRMS (ESI) m/z $[M+H]^+$ calcd for $C_{21}H_{23}BrNO_3S$: 448.0577, found: 448.0583.

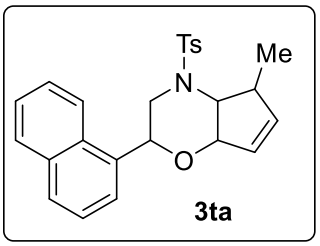

5-Methyl-2-(naphthalen-1-yl)-4-tosyl-2,3,4,4a,5,7a-hexahydrocyclopenta[b][1,4]oxazine 3ta. Analytical TLC on silica gel; 11:1 hexane/ethyl acetate, R_f= 0.30; thick colorless liquid; yield 70% (58 mg); major diastereomer (>10:1 dr); ^{1}H NMR (400 MHz, $CDCl_3$) δ 7.77-7.70 (m, 5H), 7.59 (s, 1H), 7.39-7.37 (m, 2H), 7.32 (d, *J* = 8.0 Hz, 2H), 7.21-7.18 (m, 1H), 6.03-6.01 (m, 1H), 5.87-5.84 (m, 1H), 4.13-4.11 (m, 1H), 4.01-3.98 (m, 1H), 3.91-3.87 (m, 1H), 3.69-3.66 (m, 1H), 3.16-3.09 (m, 1H), 3.00-2.94 (m, 1H), 2.39 (s, 3H), 1.38 (d, *J* = 7.2 Hz, 3H); ^{13}C NMR (125 MHz, $CDCl_3$) δ 143.8, 143.7, 138.2, 136.0, 133.3, 133.2, 130.2, 128.7, 128.4, 128.1, 127.8, 127.2, 126.3, 126.2, 125.0, 123.9, 77.0, 73.7, 61.2, 47.7, 39.1, 21.7, 16.4; FT-IR (neat) 2960, 2927, 2871, 1598, 1333, 1162, 1089, 815, 665, 546 cm^{-1}; HRMS (ESI) m/z $[M+H]^+$ calcd for $C_{25}H_{26}NO_3S$: 420.1628, found: 384.1651.

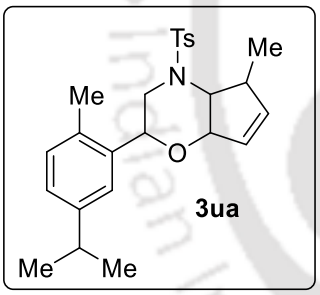

2-(5-Isopropyl-2-methylphenyl)-5-methyl-4-tosyl-2,3,4,4a,5,7a-hexahydrocyclopenta[b][1,4]oxazine 3ua. Analytical TLC on silica gel; 11:1 hexane/ethyl acetate, R_f= 0.32; thick colorless liquid; yield 64% (55 mg); major diastereomer (>10:1 dr); ^{1}H NMR (400 MHz, $CDCl_3$) δ 7.79 (d, *J* = 8.0 Hz, 2H), 7.34 (d, *J* = 8.4 Hz, 2H), 7.10 (s, 1H), 7.03-7.02 (m, 2H), 6.08 (dd, *J* =1.2, 6.4 Hz 1H), 5.92-5.89 (m, 1H), 4.21-4.19 (m, 1H), 4.15 (dd, *J* = 2.0, 10.4 Hz, 1H), 3.78-3.75 (s, 2H), 3.16 (dd, *J* = 10.8, 14.8 Hz, 1H), 3.06-3.01 (m, 1H), 2.86-2.79 (m, 1H), 2.44 (s, 3H), 2.09 (s, 3H), 1.21-1.17 (m, 9H); ^{13}C NMR (125 MHz, $CDCl_3$) δ 147.0, 143.7, 143.6, 138.2, 136.4, 132.2, 130.5, 130.0, 128.8, 127.3, 125.8, 124.0, 77.2, 71.0, 61.1, 46.3, 39.0, 33.9, 24.2, 24.0, 21.6, 18.7, 16.5; FT-IR (neat) 2959, 2926, 2871, 1455, 1345, 1162, 1090, 985, 748, 662, 594, 550 cm^{-1}; HRMS (ESI) m/z $[M+H]^+$ calcd for $C_{25}H_{32}NO_3S$: 426.2097, found: 426.2105.

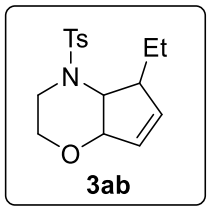

5-Ethyl-4-tosyl-2,3,4,4a,5,7a-hexahydrocyclopenta[b][1,4]oxazine 3ab. Analytical TLC on silica gel; 9:1 hexane/ethyl acetate, R_f = 0.20; thick colorless liquid; yield 73% (44 mg); ^{1}H NMR (400 MHz, $CDCl_3$) δ 7.74 (d, *J* = 8.0 Hz, 2H), 7.33 (d, *J* = 8.0 Hz, 2H), 6.17-6.15 (m, 1H), 5.86-5.83 (m, 1H), 3.90-3.88 (m, 1H), 3.76-3.67 (m, 2H), 3.49 (d, *J* = 11.2 Hz, 1H), 3.35-3.27 (m, 1H), 2.98-2.92 (m, 1H), 2.84-2.8 (m, 1H), 2.44 (s, 3H), 1.91-1.81 (m, 1H), 1.38-1.30 (m, 1H), 0.99 (t, *J* = 7.2 Hz, 3H); ^{13}C NMR (125 MHz, $CDCl_3$) δ 143.5, 141.5, 138.1, 129.9, 129.0, 127.0, 75.6, 62.0, 58.9, 45.5, 41.6, 23.1, 21.5, 11.2; FT-IR (neat) 3283, 29251598, 1431, 1326, 1157, 1092, 841, 750, 661, 550 cm^{-1}; HRMS (ESI) m/z $[M+H]^+$ calcd for $C_{16}H_{22}NO_3S$: 308.1315, found: 308.1321.

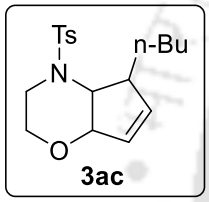

5-Butyl-4-tosyl-2,3,4,4a,5,7a-hexahydrocyclopenta[b][1,4]oxazine 3ac. Analytical TLC on silica gel; 9:1 hexane/ethyl acetate, R_f = 0.24; thick colorless liquid; yield 65% (43 mg); ^{1}H NMR (400 MHz, $CDCl_3$) δ 7.74 (d, *J* = 8.4 Hz, 2H), 7.33 (d, *J* = 8.0 Hz, 2H), 6.16-6.14 (m, 1H), 5.85-5.82 (m, 1H), 3.90-3.89 (m, 1H), 3.73-3.70 (m, 2H), 3.50- 3.47 (m, 1H), 3.34-3.26 (m, 1H), 3.01-2.94 (m, 1H), 2.84-2.83 (m, 1H), 2.43 (s, 3H), 1.78-1.72 (m, 1H), 1.44-1.25 (m, 5H), 0.91 (t, *J* = 6.8 Hz, 3H); ^{13}C NMR (125 MHz, $CDCl_3$) δ 143.6, 141.9, 138.3, 130.0, 129.0, 127.2, 75.7, 62.2, 59.7, 44.3, 41.7, 30.2, 29.6, 23.0, 21.6, 14.1; FT-IR (neat) 2925, 2859, 1598, 1452, 1350, 1160, 1080, 953, 815, 660, 592 cm^{-1}; HRMS (ESI) m/z $[M+H]^+$ calcd for $C_{18}H_{26}NO_3S$: 336.1628, found: 336.1625.

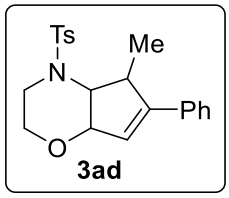

5-Methyl-6-phenyl-4-tosyl-2,3,4,4a,5,7a-hexahydrocyclopenta[b][1,4]oxazine 3ad. Analytical TLC on silica gel; 11:1 hexane/ethyl acetate, R_f = 0.22; thick colorless liquid; yield 78% (58 mg); major diastereomer (>10:1 dr); ^{1}H NMR (500 MHz, $CDCl_3$) δ 7.77 (d, *J* = 8.5 Hz, 2H), 7.34-7.32 (m, 4H), 7.30-7.29 (m, 3H), 5.91 (t, *J* = 2.5 Hz, 1H), 4.02-4.00 (m, 1H), 3.87-3.84 (m, 1H), 3.75 (d, *J* = 14.5 Hz, 1H), 3.53-

3.51 (m, 1H), 3.41-3.36 (m, 2H), 3.06-3.01 (m, 1H), 2.44 (s, 3H), 1.19 (d, J = 7.0 Hz, 3H); ^{13}C NMR (125 MHz, $CDCl_3$) δ 154.5, 143.7, 138.1, 135.8, 130.1, 128.4, 128.2, 127.2, 127.0, 124.2, 74.8, 62.1, 61.9, 41.9, 39.8, 21.6, 16.0; FT-IR (neat) 3054, 2927, 1598, 1447, 1349, 1159, 1085, 1022, 761, 670, 593 cm^{-1}; HRMS (ESI) m/z $[M+H]^+$ calcd for $C_{21}H_{24}NO_3S$: 370.1471, found: 370.1468.

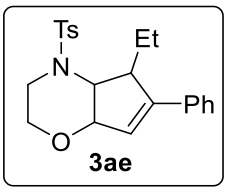

5-Ethyl-6-phenyl-4-tosyl-2,3,4,4a,5,7a-hexahydrocyclopenta[b][1,4]oxazine 3ae. Analytical TLC on silica gel; 11:1 hexane/ethyl acetate, R_f = 0.22; thick colorless liquid; yield 72% (55 mg); major diastereomer (>10:1 dr); ^{1}H NMR (500 MHz, $CDCl_3$) δ 7.78 (d, J = 8.0 Hz, 2H), 7.34-7.29 (m, 7H), 5.92 (s, 1H), 4.12-4.09 (m, 1H), 4.06-4.05 (m, 1H), 3.74 (d, J = 14.5 Hz, 1H), 3.52-3.46 (m, 2H), 3.42-3.36 (m, 1H), 3.06-3.01 (m, 1H), 2.44 (s, 3H), 1.80-1.75 (m, 2H), 0.66 (t, J = 7.0 Hz, 3H); ^{13}C NMR (125 MHz, $CDCl_3$) δ 153.0, 143.7, 138.1, 136.2, 130.1, 128.4, 128.1, 127.2, 126.6, 125.7, 75.0, 61.7, 56.6, 44.9, 41.8, 21.6, 19.6, 8.2; FT-IR (neat) 2965, 2982, 1598, 1350, 1336, 1162, 1089, 970, 757, 670, 549 cm^{-1}; HRMS (ESI) m/z $[M+H]^+$ calcd for $C_{22}H_{26}NO_3S$: 384.1628, found: 384.1629.

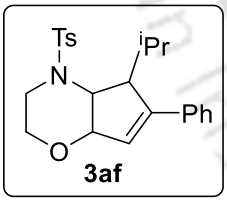

5-Isopropyl-6-phenyl-4-tosyl-2,3,4,4a,5,7a-hexahydrocyclopenta[b][1,4]oxazine 3af. Analytical TLC on silica gel; 11:1 hexane/ethyl acetate, R_f = 0.24; thick colorless liquid; yield 70% (55.5 mg); major diastereomer (>10:1 dr); ^{1}H NMR (500 MHz, $CDCl_3$) δ 7.80 (d, J = 8.5 Hz, 2H), 7.35-7.31 (m, 4H), 7.29-7.27 (m, 3H), 5.82-5,81 (m, 1H), 4.36 (t, J = 6.0 Hz, 1H), 4.13-4.12 (m, 1H), 3.74-3.70 (m, 1H), 3.46-3.43 (m, 3H), 3.04-3.01 (m, 1H), 2.44 (s, 3H), 2.23-2.17 (m, 1H), 1.14 (d, J = 7.5 Hz, 3H), 0.75 (d, J = 7.0 Hz, 3H); ^{13}C NMR (125 MHz, $CDCl_3$) δ 153.4, 143.7, 138.0, 136.5, 130.0, 128.3, 128.0, 127.4, 127.0, 126.2, 75.2, 59.8, 55.4, 51.2, 41.3, 27.2, 21.6, 20.1, 17.1; FT-IR (neat) 2957, 2927, 2872, 1493, 1347, 1335, 1159, 1085, 939, 761, 666, 544 cm^{-1}; HRMS (ESI) m/z $[M+H]^+$ calcd for $C_{23}H_{28}NO_3S$: 398.1784, found: 398.1785.

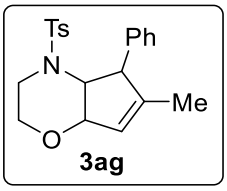

6-Methyl-5-phenyl-4-tosyl-2,3,4,4a,5,7a-hexahydrocyclopenta[b][1,4]oxazine 3ag. Analytical TLC on silica gel; 11:1 hexane/ethyl acetate, R_f = 0.26; thick colorless liquid; yield 67% (48.5 mg); major diastereomer (>10:1 dr); ^{1}H NMR (500 MHz, $CDCl_3$) δ 7.24-7.20 (m, 5H), 7.02-6.97 (m, 4H), 5.76-5,75 (m, 1H), 4.30-4.27 (m, 1H), 4.25-4.23 (m, 1H), 3.82-3.75 (m, 2H), 3.71 (d, *J* = 11.5 Hz, 1H), 3.43-3.38 (m, 1H), 3.33-3.27 (m, 1H), 2.34 (s, 3H), 1.51 (s, 3H); ^{13}C NMR (125 MHz, $CDCl_3$) δ 151.2, 142.9, 139.2, 137.4, 129.5, 128.8, 128.6, 127.0, 126.9, 125.2, 76.3, 63.4, 62.7, 53.1, 41.3, 21.5, 16.2; FT-IR (neat) 2961, 2917, 2869, 1644, 1599, 1332, 1157, 1081, 951, 761, 669, 577 cm^{-1}; HRMS (ESI) m/z $[M+H]^+$ calcd for $C_{21}H_{24}NO_3S$: 370.1471, found: 308. 370.1474.

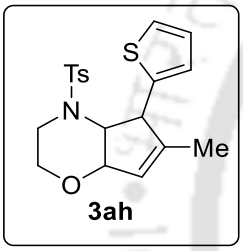

6-Methyl-5-(thiophen-2-yl)-4-tosyl-2,3,4,4a,5,7a-hexahydrocyclopenta [b][1,4]oxazine 3ah. Analytical TLC on silica gel; 11:1 hexane/ethyl acetate, R_f = 0.24; thick colorless liquid; yield 53% (40 mg); major diastereomer (>10:1 dr); ^{1}H NMR (500 MHz, $CDCl_3$) δ 7.72 (d, *J* = 8.0 Hz, 2H), 7.33 (d, *J* = 8.0 Hz, 2H), 7.19 (d, *J* = 5.0 Hz, 1H), 6.95-6.93 (m, 1H), 6.78 (d, *J* = 3.5 Hz, 1H), 5.15 (s, 1H), 4.93 (s, 1H), 3.96 (d, *J* = 4.0 Hz, 1H), 3.76-3.72 (m, 2H), 3.55 (d, *J* = 12.5 Hz, 1H), 3.45-3.40 (m, 1H), 3.13-3.08 (m, 1H), 2.44 (s, 3H), 1.70 (s, 3H); ^{13}C NMR (125 MHz, $CDCl_3$) δ 145.5, 143.7, 140.9, 137.1, 130.0, 127.3, 127.1, 125.0, 124.5, 122.8, 82.3, 64.5, 59.1, 55.4, 41.4, 21.7, 15.9; FT-IR (neat) 2918, 2853, 1439, 1351, 1275, 1262, 1163, 1090, 953, 762, 750, 666 cm^{-1}; HRMS (ESI) m/z $[M+H]^+$ calcd for $C_{19}H_{22}NO_3S_2$: 376.1036, found: 376.1041.

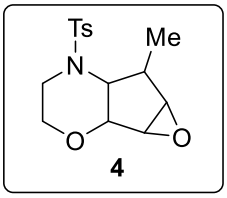

6-methyl-5-tosyloctahydrooxireno[2',3':4,5]cyclopenta[1,2-b][1,4]oxazine 4. Analytical TLC on silica gel; 9:1 hexane/ethyl acetate, R_f = 0.18; thick colorless liquid; yield 68% (42 mg); ^{1}H NMR (500 MHz, $CDCl_3$) δ 7.71 (d, *J* = 8.0 Hz, 2H),

7.32 (d, J = 8.0 Hz, 2H), 3.70-3.66 (m, 1H), 3.61 (d, J = 4.5 Hz, 1H), 3.57-3.54 (m, 1H), 3.47-3.44 (m, 1H), 3.38-3.35 (m, 2H), 3.28-3.18 (m, 1H), 3.00-2.94 (m, 1H), 2.43 (s, 3H), 2.34-2.28 (m, 1H), 1.21 (d, J = 7.0 Hz, 3H); ^{13}C NMR (125 MHz, $CDCl_3$) δ 143.8, 138.0, 130.1, 127.2, 72.4, 64.1, 59.1, 57.2, 54., 41.4, 33.7, 21.6, 12.7; FT-IR (neat) 2966, 2874, 1597, 1454, 1351, 1161, 1106, 985, 773, 666, 554 cm^{-1}; HRMS (ESI) m/z $[M+H]^+$ calcd for $C_{15}H_{20}NO_4S$: 310.1108, found: 310.1094.

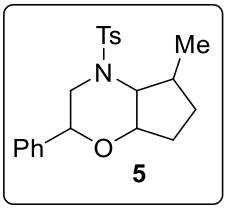

5-Methyl-2-phenyl-4-tosyloctahydrocyclopenta[b][1,4]oxazine 5. Analytical TLC on silica gel; 9:1 hexane/ethyl acetate, R_f = 0.22; thick colorless liquid; yield 85% (63 mg); major diastereomer (10:1 dr); ^{1}H NMR (400 MHz, $CDCl_3$) δ 7.79 (d, J = 8.0 Hz, 2H), 7.35-7.28 (m, 5H), 7.233-7.21 (m, 2H), 3.00-3.96 (m, 1H), 3.76-3.72 (m, 2H), 3.59-3.56 (m, 1H), 3.13-3.07 (m, 1H), 2.44 (s, 3H), 2.40-2.34 (m, 1H), 2.1-2.02 (m, 1H), 1.98-1.89 (m, 1H), 1.75-1.68 (m, 1H), 1.27-1.17 (m, 2H), 1.06 (d, J = 6.8 Hz, 3H); ^{13}C NMR (100 MHz, $CDCl_3$) δ 143.6, 138.9, 138.4, 130.0, 128.6, 128.3, 127.2, 126.0, 76.5, 75.3, 63.0, 46.6, 31.7, 29.2, 29.0, 21.6, 17.7; FT-IR (neat) 2950, 2927, 2872, 1452, 1341, 1156, 1093, 1068, 985, 939, 657 cm^{-1}; HRMS (ESI) m/z $[M+H]^+$ calcd for $C_{21}H_{26}NO_3S$: 372.1628, found: 372.1626.

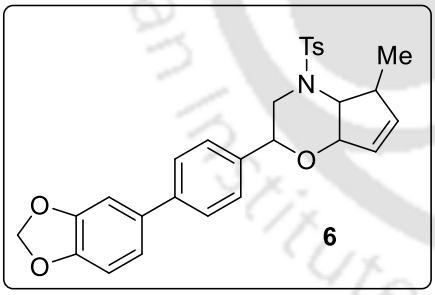

2-(4-(Benzo[d][1,3]dioxol-5-yl)phenyl)-5-methyl-4-tosyl-2,3,4,4a,5,7a-hexahydrocyclopenta[b][1,4]oxazine 6 Analytical TLC on silica gel; 9:1 hexane/ethyl acetate, R_f = 0.23; colorless solid; mp139-140 °C; yield 82% (80 mg); major diastereomer (>10:1 dr); ^{1}H NMR (400 MHz, $CDCl_3$) δ 7.82 (d, J = 8.4 Hz, 2H), 7.46 (d, J = 8.0 Hz, 2H), 7.39 (d, J = 8.0 Hz, 2H), 7.23 (d, J = 8.4 Hz, 2H), 7.01-6.99 (m, 2H), 6.87 (d, J = 8.8 Hz, 1H), 6.08-6.06 (m, 1H), 5.99 (s, 2H), 5.90-5.88 (m, 1H), 4.15-4.14 (m, 1H), 3.91-3.87 (m, 2H), 3.74-3.71(m, 1H), 3.20-3.13 (m, 1H), 3.05-2.98 (m, 1H), 2.46 (s, 3H), 1.20 (d, J = 7.0 Hz, 3H); ^{13}C NMR (100 MHz, $CDCl_3$) δ 148.2, 147.3, 143.8, 143.7, 141.0, 138.1, 137.2, 135.1, 130.1, 128.6, 127.2, 127.1, 126.5, 120.7, 108.7, 107.7, 101.3, 76.9, 73.3, 61.1, 47.5, 39.1, 21.7,

16.4; FT-IR (neat) 2959, 2927, 2875, 1501, 1481, 1335, 1225, 1161, 1088, 808, 665, 544 cm^{-1}; HRMS (ESI) m/z $[M+H]^+$ calcd for $C_{28}H_{28}NO_5S$: 490.1683, found: 490.1677.

Crystal Structure and Data of 3am (major isomer)

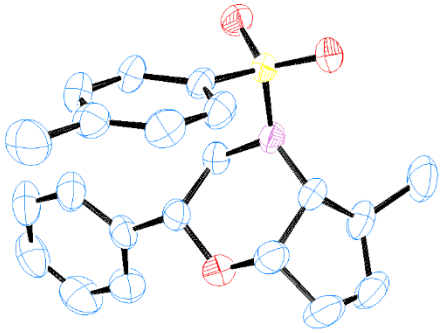

Figure 2. ORTEP diagram of **3ma** (major isomer) with 50% probability (CCDC 2420492). H-Atoms omitted for clarity.

Sample Preparation for Crystal Growth. Compound **3ma** was dissolved in a minimum volume of acetonitrile and kept at room temperature for slow evaporation (3 days). The needle shape crystals were then subjected to X-ray diffraction.

Identification code	**3ma**
Empirical formula	C21 H23 N O3 S
Formula weight	396.46
Crystal habit, colour	Needle/Colorless
Temperature, *T*/K	296 K
Wavelength, λ/Å	0.71073
Crystal system	'monoclinic'
Space group	'P 21/n'
Unit cell dimensions	a= 9.5601(7) Å
	b= 19.4270(11) Å
	c= 11.3119(6) Å

	α = 90
	β = 113.535(7)
	γ = 90
Volume, V/Å^3	1926.1(2)
Z	4
Calculated density, Mg·m^{-3}	1.274
Absorption coefficient, μ/mm^{-1}	0.188
F(000)	784.0
θ range for data collection	2.87 to 28.54°
Limiting indices	-11 ≤ h ≤ 11, –23 ≤ k ≤ 13, –10≤ l ≤ 13
Reflection collected / unique	2955/2736
Completeness to θ	99.9%
Absorption correction	Multi-scan
Max. and min. transmission	0.959 and 0.945
Refinement method	'SHELXL-2019/1 (Sheldrick, 2019)'
Data / restraints / parameters	3399/0/237
Goodness–of–fit on F^2	1.032
Final R indices [I>2sigma(I)]	R1 = 0.0432, wR2 = 0.1083
R indices (all data)	R1 = 0.0564, wR2 = 0.1173

3.6 References

1. Lovering, F.; Bikker, J.; Humblet, C. *J. Med. Chem*. **2009**, *52*, 6752. (b) Bauer, M. R.; Fruscia, P. D.; Lucas, S. C. C.; Michaelides, I. N.; Nelson, J. E; Storera, R. Ian; Whitehurst, B. C. *RSC Med. Chem*. **2021**, *12*, 448.
2. (a) Ma, J.; Chen, S.; Bellotti, P.; Wagener, T.; Daniliuc, C.; Houk, K. N.; Glorius, F. *Nat. Catal*. **2022**, *5*, 405. (b) Xue, Y.; Dong, G. *Acc. Chem. Res*. **2022**, *55*, 2341. (c) Ye, D.; Lu, H.; He, Y.; Zheng, Z.; Wu, J.; Wei, H. *Nat Commun*. **2022**, *13*, 3337. (d) Han, N. Lv, J.-C.; Zhang, P.; Huang, Y.-R.; Xu, Z.-X.; Xu, K.; Wang, X.-F.; Li, X.; Chung, L. W.; Li, C.-C. *Chem* **2024** *10*, 190. (e) Zhu, M.; Gao, Y.-J.; Huang, X.-L.; Li, M.; Zheng, C.; You, S.-L.; *Nat. Commun*. **2024**, *15*, 2462.
3. (a) Trost, B. M.; *Angew. Chem., Int. Ed.* **1995**, *34*, 259. (b) Hayashi, Y. *Chem. Sci.* **2016**, *7*, 866.
4. (a) Bolm, C.; Legros, J.; Paih, J. Le; Zani, L. *Chem. Rev*. **2004**, *104*, 6217. (b) Sherry, B. D.; Fürstner, A. *Acc. Chem. Res*. **2008**, *41*, 150. (c) Bauer, I.; Knölker, H.-J. *Chem. Rev*. **2015**, *115*, 3170. (d) Fürstner, A. *ACS Cent. Sci*. **2016**, *2*, 778.
5. (a) Jensen, K. L.; Dickmeiss, G.; Jiang, H.; Albrecht, Ł.; Jørgensen, K. A. *Acc. Chem. Res*. **2012**, *45*, 248. (c) Curti, C.; Battistini, L.; Sartori, A.; Zanardi, F. *Chem. Rev*. **2020**, *120*, 2448.
6. (a) Marques, A.-S.; Coeffard, V.; Chataigner, I.; Vincent, G.; Moreau, X. *Org. Lett*. **2016**, *18*, 5296.
7. Riveira, M. J.; Marcarino, M. O.; La-Venia, A. *Org. Lett*. **2018**, *20*, 4000.
8. Marques, A.-S.; Duhail, T.; Marrot, J.; Chataigner, I.; Coeffard, V.; Vincent, G.; Moreau, X. *Angew. Chem., Int. Ed*. **2019**, *58*, 9969.
9. Wang, S.; Chai, Z.; Zhou, S.; Wang, S.; Zhu, X.; Wei, Y. *Org. Lett*. **2013**, *15*, 2628.
10. Mal, A.; Goswami, G.; Wani, I. A.; Ghorai, M. K. *Chem. Commun*. **2017**, *53*, 10263.
11. Vijay, M.; Kumar, S. V.; Satheesh, V.; Ananthappan, P.; Srivastava, H. K.; Ellairaja, S.; Vasantha, V. S.; Punniyamurthy, T. *Org. Lett*. **2019**, *21*, 7649.
12. (a) Vliet, L. A. van; Rodenhuis, N.; Dijkstra, D.; Wikström, H. *J. Med. Chem*. **2000**, *43*, 2871. (b) Delost, M. D.; Smith, D. T.; Anderson, B. J.; Njardarson, J. T. *J. Med. Chem.* **2018**, *61*, 10996. (c) Lenci, E.; Calugi, L.; Trabocchi, A. *ACS Chem. Neurosci*. **2021**, *12*, 378. (d) Kourounakis, A. P.; Xanthopoulos, D.; Tzara, A. *Med. Res. Rev*. **2020**, *40*, 709.

13. Marshall, C. M.; Federice, J. G.; Bell, C. N.; Cox, P. B.; Njardarson, J. T. *J. Med. Chem*. **2024**, *67*, 11622.
14. Liu, H.; Jia, H.; Shi, W.; Wang, C.; Zhang, C.; Guo, H. *Org. Lett*. **2018**, *20*, 3570.
15. (a) Carpenter, B. K. *J. Am. Chem. Soc*. **1995**, *117*, 6337. (b) Deslongchampsa, G; Deslongchamps, P. *Org. Biomol. Chem*. **2016,** *14*, 7754. (c) Obeida, A.-H.; Hannedouche, J. *Adv. Synth. Catal*. **2023**, *365*, 1100.
16. Higuchi, D.; Matsubara, S.; Kadowaki, H.; Tanaka, D.; Murakami, K. *Chem. -Eur. J.* **2023**, *29*, e202301071.
17. Karjee, P.; Sarkar, T.; Kar, S.; Punniyamurthy, T. *J. Org. Chem*. **2020**, *85*, 8261.
18. Jia, Z.-J.; Zhou, Q.; Zhou, Q.-Q.; Chen, P.-Q.; Chen, Y.-C. *Angew. Chem., Int. Ed*. **2011**, *50*, 8638.

3.7 HPLC Chromatogram

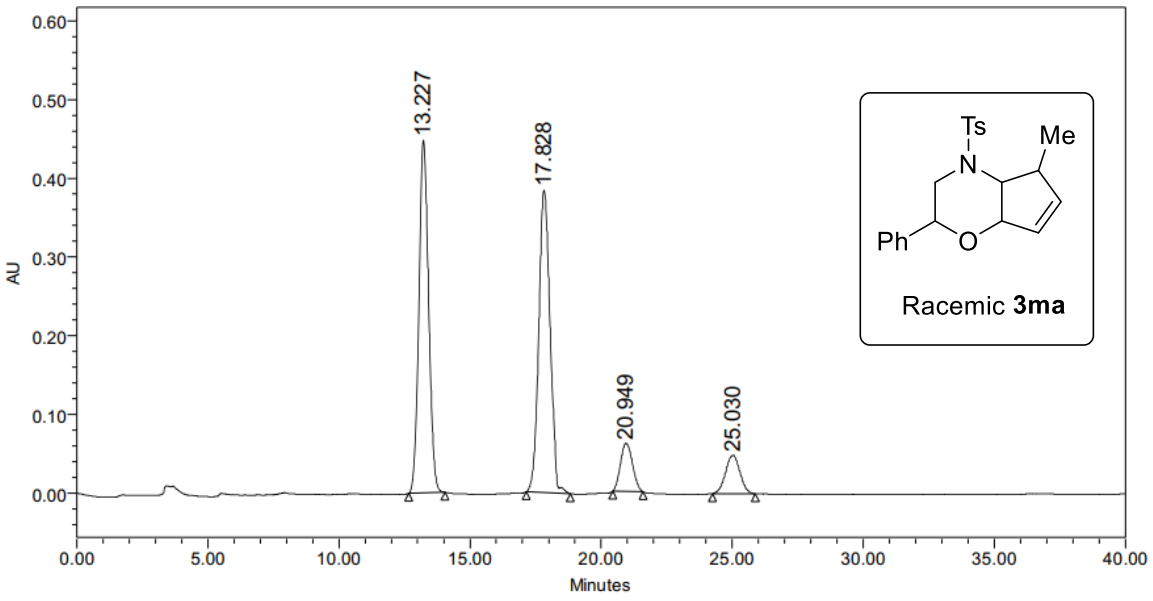

	RT	Area	% Area	Height
1	13.227	11430547	42.83	448468
2	17.828	11455660	42.92	384234
3	20.949	1943403	7.28	60837
4	25.030	1859016	6.97	48829

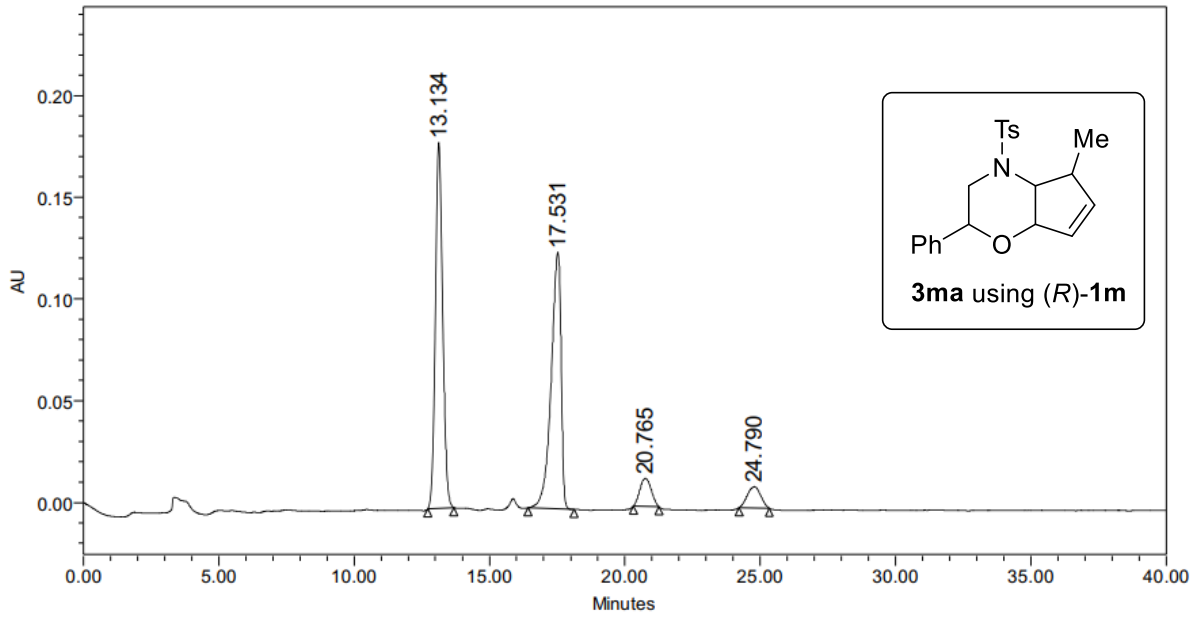

	RT	Area	% Area	Height
1	13.134	3349920	45.77	179703
2	17.531	3204012	43.78	126117
3	20.765	406171	5.55	13722
4	24.790	358155	4.89	10396

3.8 Selected NMR Spectra

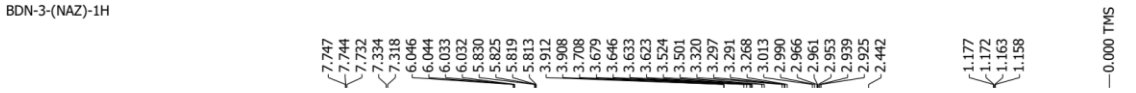

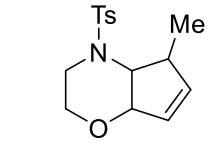

3aa

^{1}H (500 MHz NMR, $CDCl_3$)

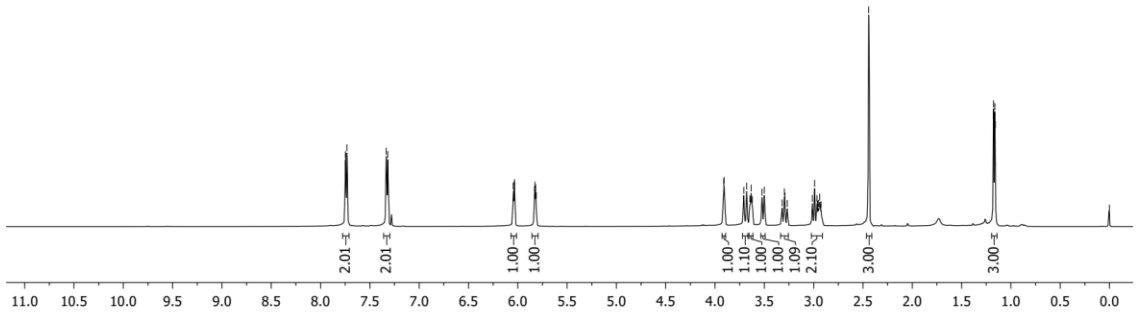

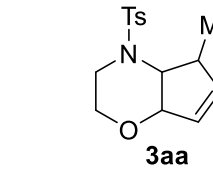

3aa

^{13}C NMR (125 MHz, $CDCl_3$)

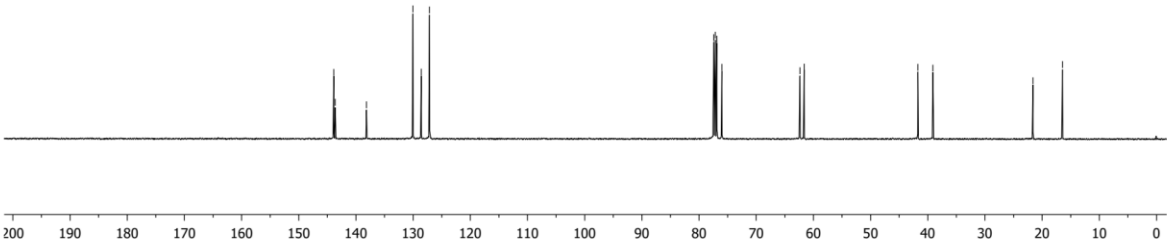

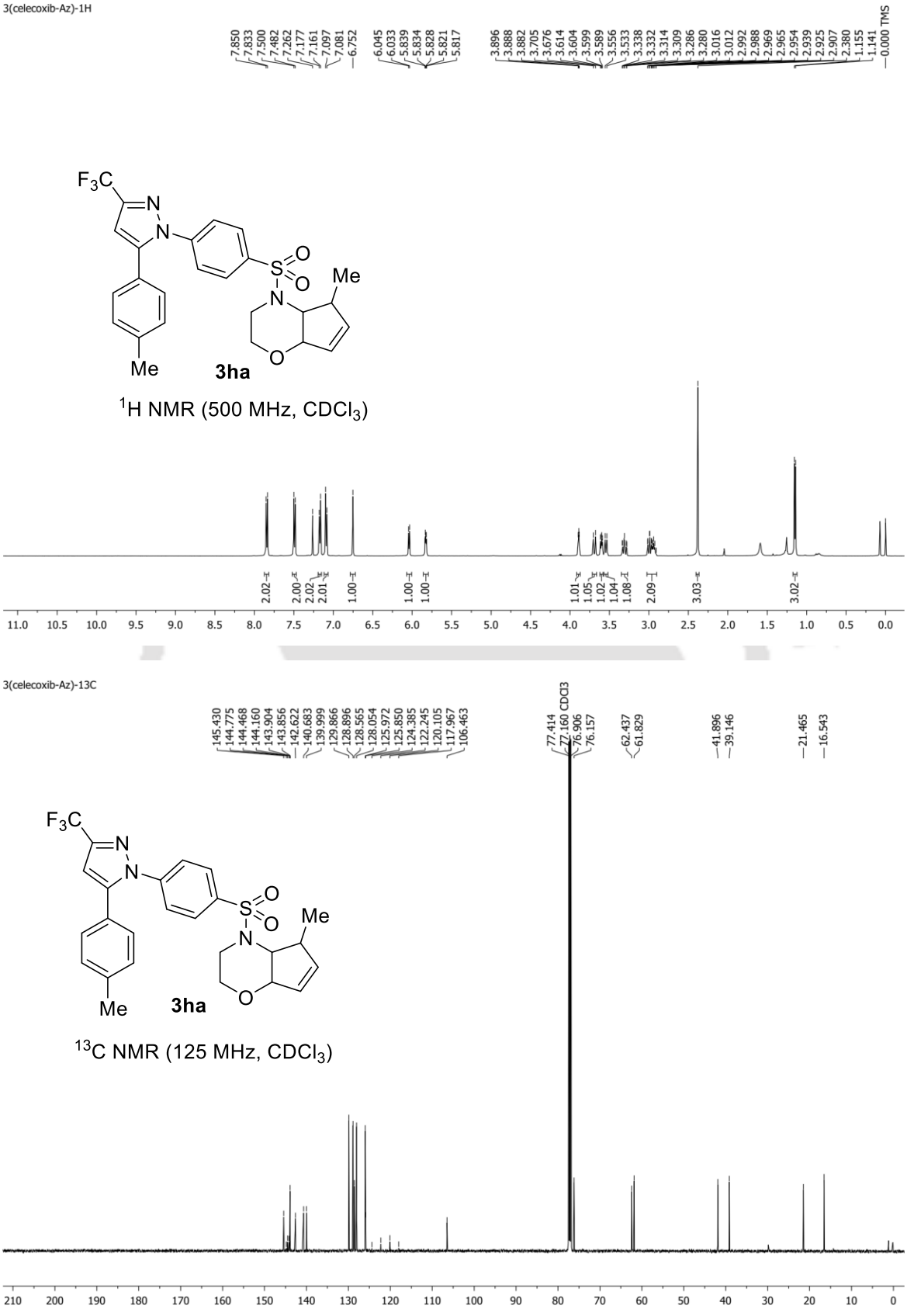

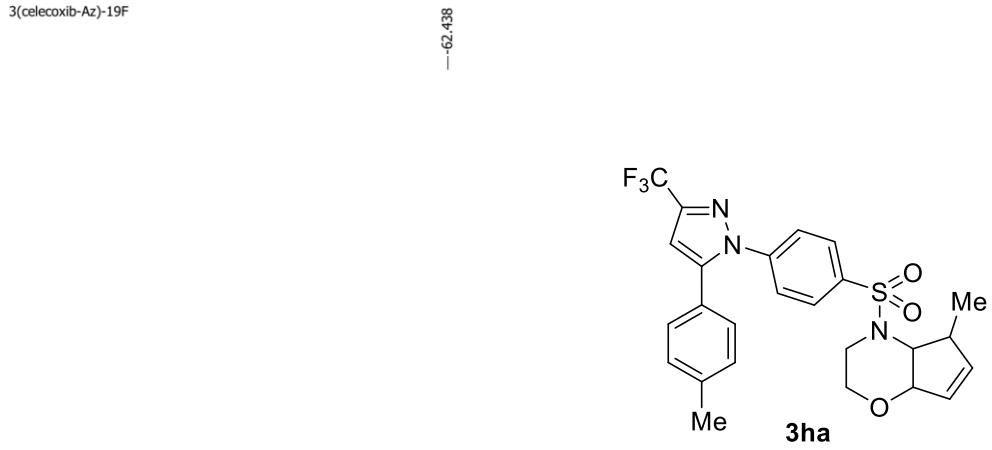

^{19}F NMR (470 MHz, $CDCl_3$)

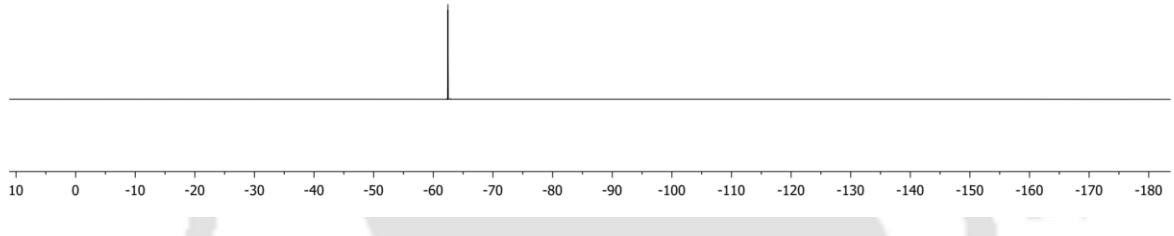

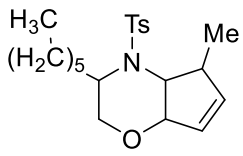

^{1}H NMR (400 MHz, $CDCl_3$)

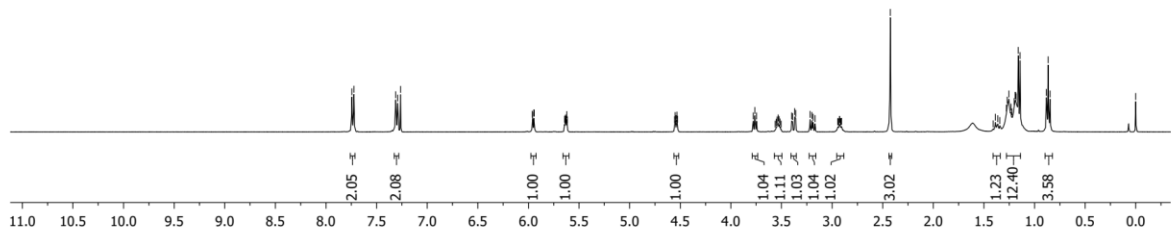

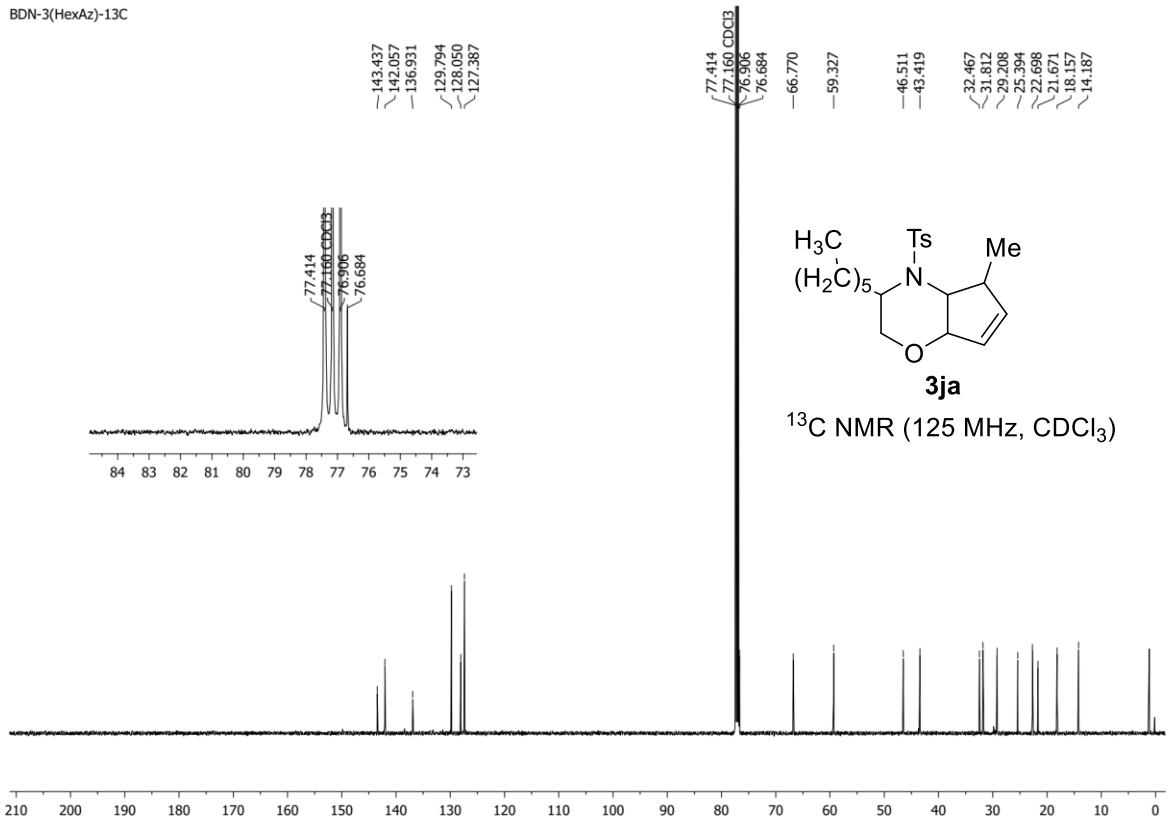

3ja

^{13}C NMR (125 MHz, $CDCl_3$)

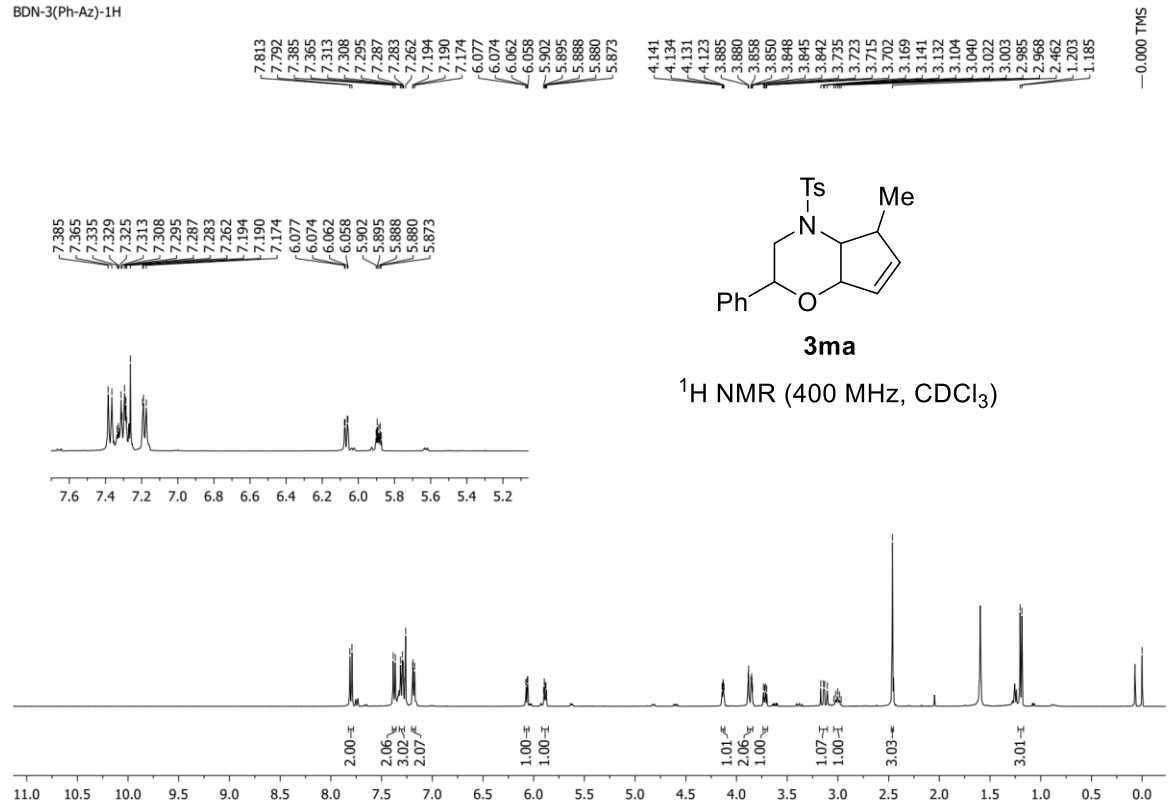

3ma

^{1}H NMR (400 MHz, $CDCl_3$)

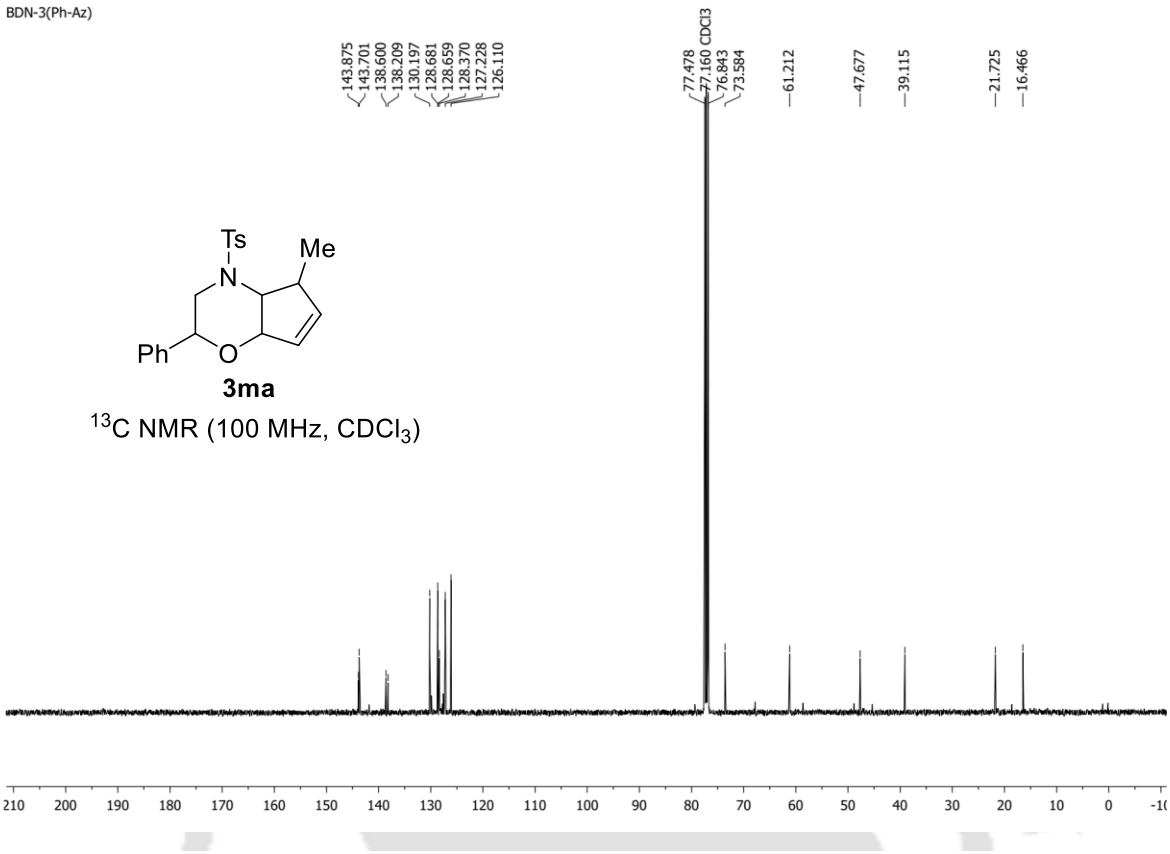

3ma

^{13}C NMR (100 MHz, $CDCl_3$)

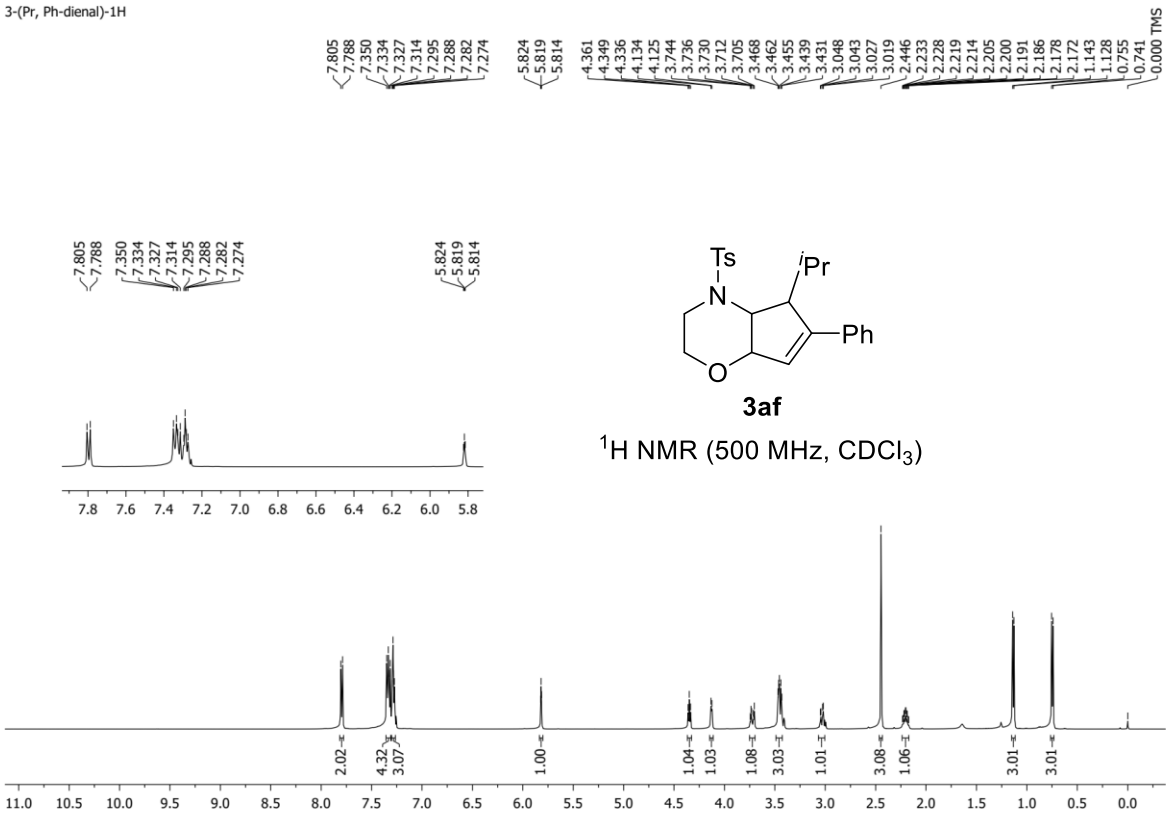

3af

^{1}H NMR (500 MHz, $CDCl_3$)

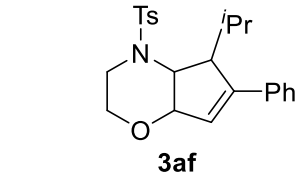

3af

^{13}C NMR (125 MHz, $CDCl_3$)

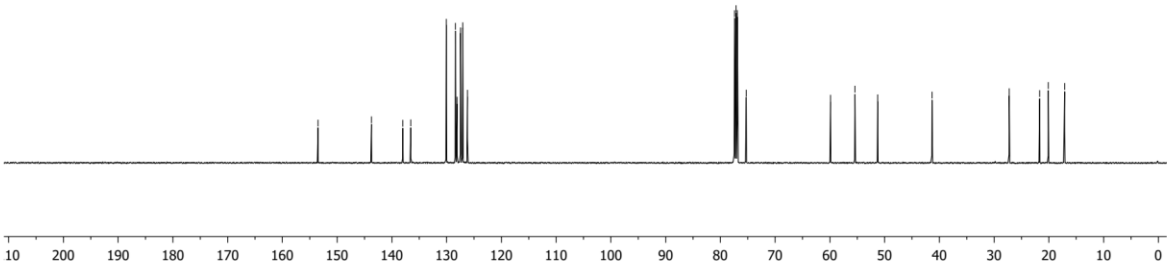

Chapter IV

Cascade C−H/C−C-Activation/Annulation of Quinoline *N*-oxides and Cyclopropenones

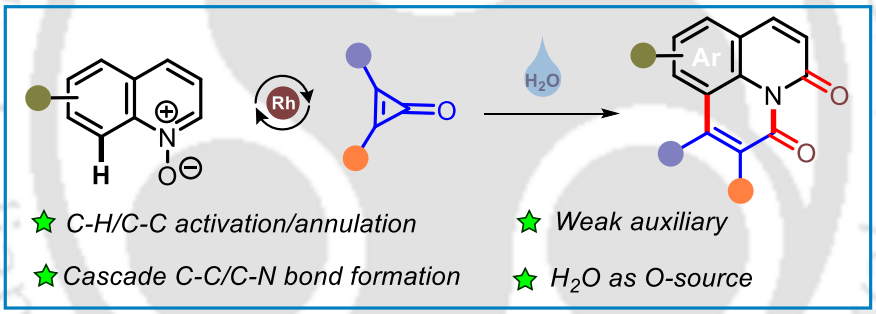

Chem. Commun. **2025**, *61*, 7875

Cascade C−H/C−C Activation/Annulation of Quinoline *N*-oxides and Cyclopropenones

Tandem C−C and C−heteroatom bond formation has become a prominent tool for designing cyclic scaffolds, as such strategies affords effective route for multistep functionalization of the reactants.[1] In this realm, cascade annulation reactions involving C−H/C−C activation strategy has gained substantial attention in current timeline.[2] These strategies have simplified the lengthy multistep synthesis process in a sustainable way. Further, the facile activation of unactivated or inert molecules for further functionalization *via* C−H/C−C activation surged as a robust strategy in modern organic chemistry. In this vein, directing group assisted synthesis or modification of indispensable molecular frameworks has become an engrossing technique.[3] Along this line, site-selective C−H functionalization of quinoline core using auxiliary installed quinoline, specially, quinoline *N*-oxide has gained profuse interest.[4,5] Under transition metal-catalysis quinoline *N*-oxide assists C2/C8−H functionalization. However, there has been significant progress in the functionalization of the more reactive C2–H bond.[4] Thus, C8–H functionalization gained considerable attention.[5] Further, strategies involving C−H activation and annulation with a quinoline core remain largely unexplored due to challenges such as selecting appropriate coupling partners, finding easily accessible reactants, and optimizing reaction conditions. These strategies have potential to explore new domains of chemical space, offering a more sustainable approach to produce diversely substituted cyclic scaffolds. In this context, three-membered aromatic ring, cyclopropenone surge as an appealing coupling partner.[6] The inherent ring strain in these compounds assist easy ring opening, which can result in the formation of 1,3-dipolar species that typically act as acyl-surrogates. In addition, their fascinating reactivity in C−H/C−C activation/annulation incentivized to utilize cyclopropenone as the preferred coupling partner. Hence, integrating quinoline *N*-oxide and cyclopropenone may unfold new arena for C−H/C−C activation/annulation strategies. In this chapter, we report coupling of quinoline *N*-oxide with cyclopropenone in a unique pathway to form tricyclic 2-quinolone derivatives. Further, 2-quinolones are the core structural units of a library ubiquitous molecules having various medicinal importance (Figure 1).[7] The reaction proceeds *via* Rh-catalyzed C8−H activation of quinolone N-oxide and C−C bond activation of cyclopropenone that convey the route for construction of 2-quinolones involving a sequential C−C and C−N bond formation.

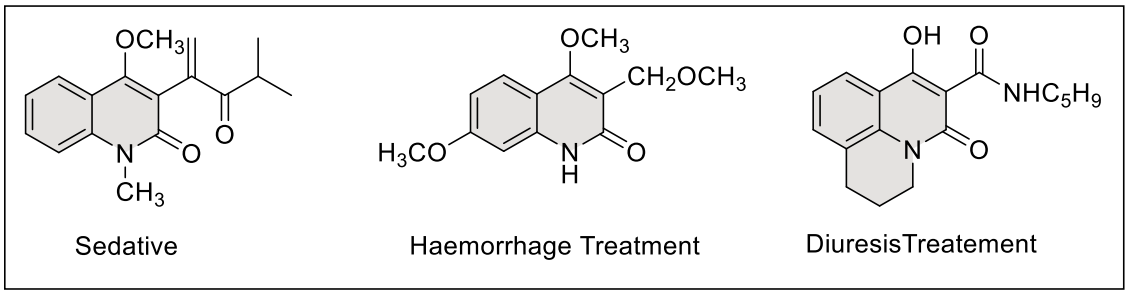

Figure 4.1. Selective Examples of Bio-relevant 2-Quinolones

4.1 C−H Functionalization using Quinoline *N*-oxides

Fagnou and co-workers reported C2-arylation of quinoline *N*-oxides using aryl bromide under Pd-catalysis (Scheme 4.1).[8] The in situ generated Pd/phosphine complex plays the crucial role to stabilize the C2-activated complex of quinoline oxide that ultimately led to C2-funtionalized product with aryl bromide.

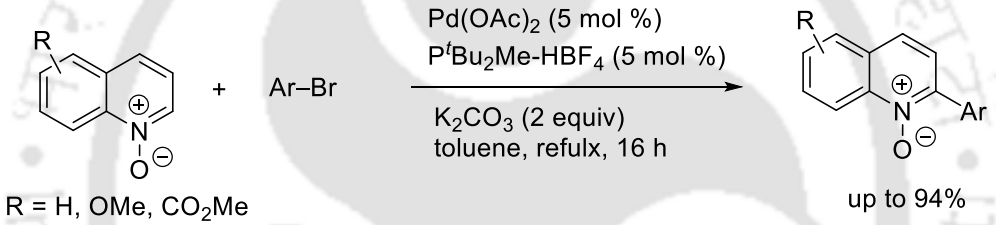

Scheme 4.1. Pd-catalyzed C2-arylation of quinoline *N*-oxides using aryl bromide

An efficient method for C8−H functionalization of quinoline N-oxide was described by Chang group (Scheme 4.2).[9] In this approach, reaction of qninoline *N*-oxide with tosyl azide under Ir-catalysis resulted in C8−amidation of quinoline *N*-oxide. Ir-catalyst favoured C8-activation over C2-position predominantly to yield the functionalized product in high yield.

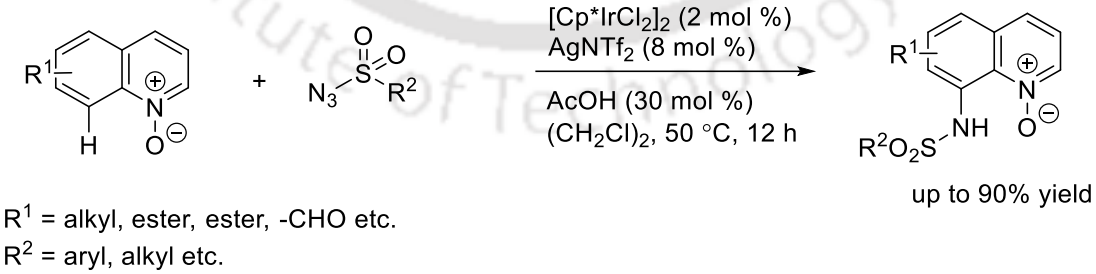

Scheme 4.2. Ir-catalyzed C8-amidation of quinoline *N*-oxides using azides

An effective approach of C8−H alkylation has been achieved to deliver alkylated quinolines using quinoline *N*-oxides with oxa/azabenzonorbornadienes under Rh-catalysis (Scheme 4.3).[10] The reaction showed well compatibility to execute the functionalized product by

retention of the heterobicyclic core. Transformation of the functionalized product to synthetically important scaffolds highlight its practical features.

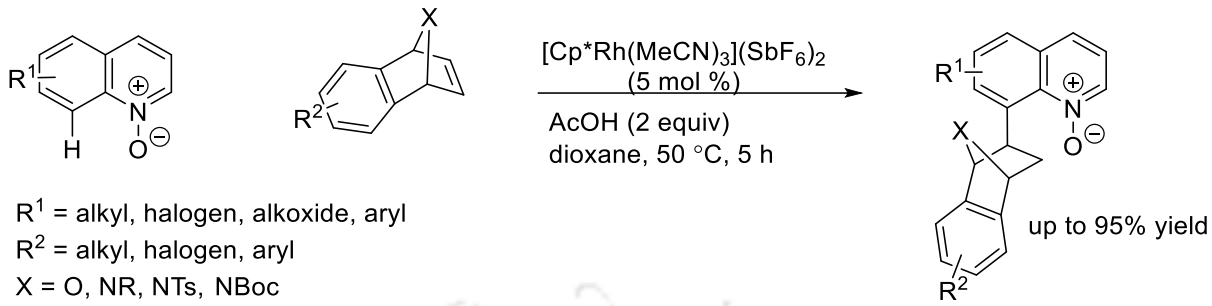

Scheme 4.3. Rh-catalyzed C8-alkylation of quinoline *N*-oxide with oxa/azabenzonorbornadienes

Our group reported Co-catalyzed C8−H alkylation strategy reacting quinoline *N*-oxide with cyclopropanol (Scheme 4.4).[11] The strategy provides a robust technique of alkylation by merging C-H activation and ring-opening reaction in a step-and atom economic fashion.

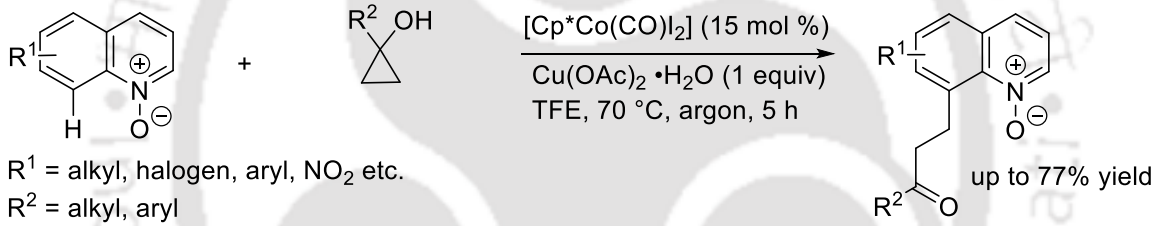

Scheme 4.4. Co-catalyzed C8−H alkylation using quinoline *N*-oxide with cyclopropanol

4.2 Coupling of Cyclopropenones using C−H/C−C Bond Activation

Li and co-workers developed coupling of cyclopropenones with a range of arenes using Rh-catalyzed C−H/C−C activation (Scheme 5).[12] A wide variety of arenes and cyclopropenones were coupled efficiently to form chalcone derivatives under mild reaction conditions. Further, isolation of reaction intermediates provided detailed investigation of the reaction pathways.

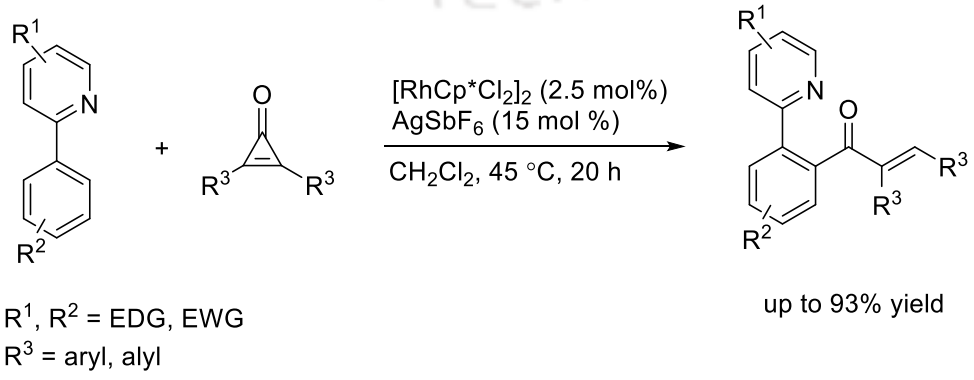

Scheme 4.5. Rh-catalyzed coupling of arenes and cyclopropenones

Wu- and co-workers reported an unprecedented [5+1]-annulation was achieved using aryl substituted anilines with cyclopropenones under Ru-catalyst (Scheme 6).[13] This protocol offers a streamline approach for bio-relevant phenanthridine skeletons. The role of H_3BO_3 was crucial to exhibit the annulated product in good yields.

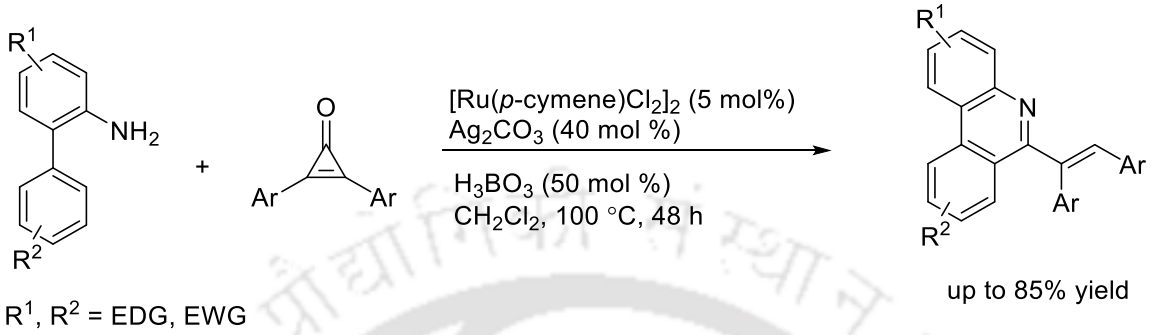

Scheme 4.6. Ru-catalyzed [5+1]-annulation of anilines with cyclopropenones

A straight forward Rh-catalyzed dual C−H functionalization of indoles was realized with the pyridyl auxiliary employing $K_2S_2O_8$ as oxidant (Scheme 7).[14] This approach offered coupling of indoles with cyclopropenone *via* a sequential C−H/C−C/C−H bonds activation. Diversely substituted indoles and cyclopropenones with electron withdrawing and donating groups were well behaved to furnish the indole fused cyclopentenone derivatives.

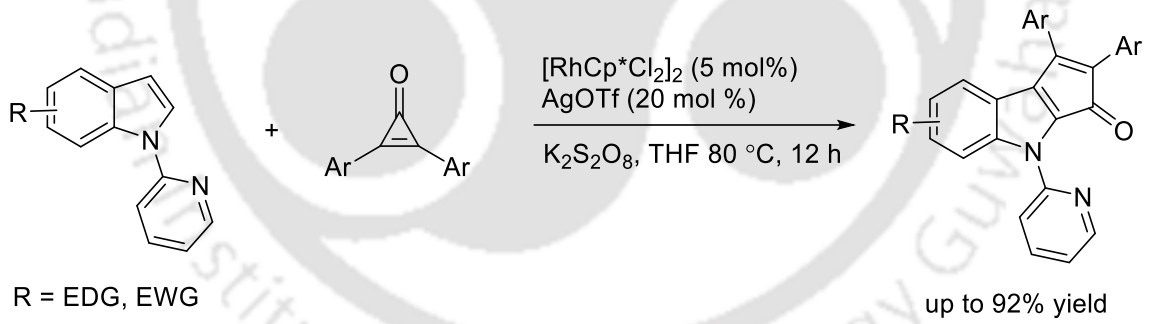

Scheme 4.7. Rh-catalyzed dual C−H functionalization of indoles with cyclopropenones

4.3 Present Study

Here we present an efficient Rh-catalyzed annulative coupling of quinoline N-oxides with cyclopropenones *via* C−H/C−C bond activation/annulation approach. The methodology provides a facile approach for merging C−H activation and ring expansion strategy involving a sequential C−C and C−N bonds formation, leading to generation of functionalized 2-quinolone derivatives. Our optimization studies initiated by employing quinoline *N*-oxide **1a** and diphenylcyclopropenone **2a** as the test substrates under various catalysts, additives,

oxidants and solvents (Table 4.1-4.3). To our delight, the reaction delivered coupled product**3aa** in 73% yield when the substrates were stirred utilizing $[RhCp^*Cl_2]_2$ (5 mol %), $AgBF_4$ (20 mol %) and Ag_2O (1 equiv) in mixture of $(CH_2Cl)_2/H_2O$ (20:1) at 90 °C under argon atmosphere for 2 h (Table 4.1, entry 1). Screening of other additives, $AgSbF_6$ and $AgNTf_2$, proved less effective than $AgBF_4$ (Table 4.1). Of the oxidants tested, Ag_2O outperformed AgOAc, Ag_2CO_3, $Cu(OAc)_2$, Cu_2O, and O_2 (Table 4.2). Among the solvents screened, $(CH_2Cl)_2$ served as the preferred, while TFE, MeOH, toluene, CH_3CN, THF, and DMF yielded less favourable results (Table 4.3, entry 1-5). Further, control experiments revealed that a combination of the Rh-catalyst, additive, oxidant, with a trace amount of water were essential furnish **3aa** (Table 4.3, entry 6-9). The structure of **3aa** was confirmed by single crystal X-ray analysis (CCDC 2382651).

Optimization of Reaction Conditions

Table 4.1. Screening of Additive[a]

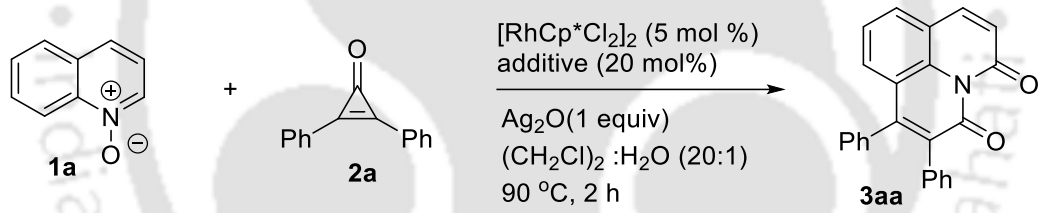

Entry	Additive	Yield (%)[b]
1	**$AgBF_4$**	**73**
2	$AgSbF_6$	62
3	$AgNTf_2$	57

[a]Reaction conditions: **1a** (0.2 mmol), **2a** (0.24 mmol), $[RhCp^*Cl_2]_2$ (5 mol %), additive (20 mol %), Ag_2O (0.2 mmol), $(CH_2Cl)_2$ (1 mL), H_2O (50 µL), 90 °C, argon atmosphere, 2 h. [b]Isolated yield.

Table 4.2. Screening of Oxidant[a]

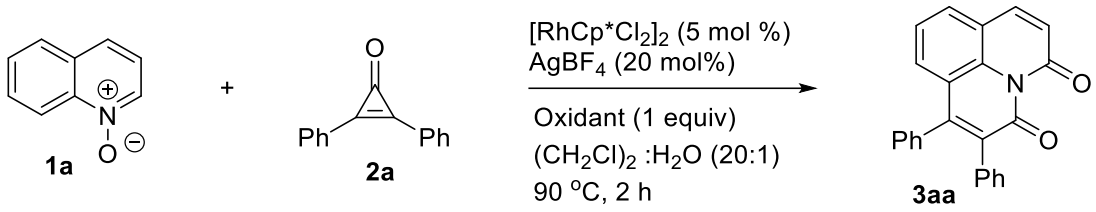

Entry	Oxidant	Yield (%)[b]
1	AgOAc	54
2	Ag_2CO_3	63
3	$Cu(OAc)_2$	28
4	Cu_2O	18
5[c]	O_2	20
6[d]	–	23
7[e]	Ag_2O	44
8[f]	Ag_2O	66

[a]Reaction conditions: **1a** (0.2 mmol), **2a** (0.24 mmol), $[RhCp^*Cl_2]_2$ (5 mol %), $AgBF_4$ (20 mol %), oxidant (0.2 mmol), $(CH_2Cl)_2$ (1 mL), H_2O (50 µL), 90 °C, argon atmosphere, 2 h. [b]Isolated yield. [c]O_2 balloon used. [d]Without oxidant. [e]Ag_2O (0.1 mmol). [f]Ag_2O (0.4 mmol).

Table 4.3. Screening of Solvent[a]

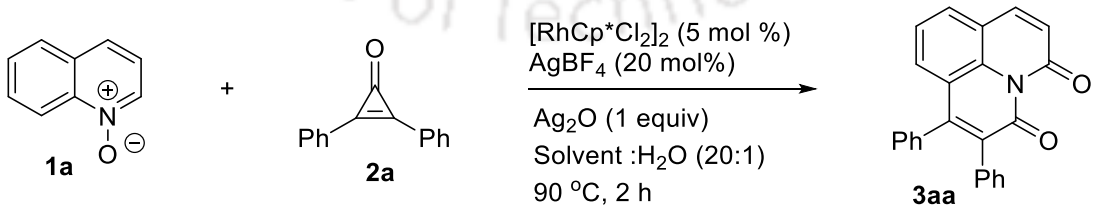

Entry	Oxidant	Yield (%)[b]
1	MeOH	trace

2	toluene	55
3	CH_3CN	42
4	THF	48
5	DMF	38
6[c]	H_2O	nd
7[e]	$(CH_2Cl)_2$	trace
8[f]	$(CH_2Cl)_2$	65
9[g]	$(CH_2Cl)_2$	nd

[a]Reaction conditions: **1a** (0.2 mmol), **2a** (0.24 mmol), $[RhCp^*Cl_2]_2$ (5 mol %), additive (20 mol %), Ag_2O (0.2 mmol), $(CH_2Cl)_2$ (1 mL), H_2O (50 μL), 90 °C, argon atmosphere, 2 h. [b]Isolated yield. [c] only H_2O (1 mL). [e]At 50 °C. [f]At 120 °C. [g]Without $[RhCp^*Cl_2]_2$.

To evaluate the practicality of the method, the scope of the protocol was examined by coupling differently substituted quinoline *N*-oxides **1b-t** with **2a** as the model substrate (Table 4.4). Quinoline *N*-oxides with substituents at the 3-position with bromo **1c**, methyl **1d** and phenyl **1e** produced the annulated products **3ca-ea** in 69-74% yields. Further, substrates bearing trifluoromethyl **1f** group delivered **3fa** in 62% yield. Heterocyclic substitution with thienyl group **1g** yielded **3ga** in 64% yield. Similarly, 4-methyl substituted quinoline *N*-oxides **1h** produced **3ha** in 74% yield. Moreover, quinoline *N*-oxides bearing substituents at the 5-position with phenyl **1i** and 2-napththyl **1j** furnished **3ia** and **3ja** in 67% and 65% yields, respectively. Functional groups, bromo **1k**, methoxy **1l**, nitro **1m** and ester **1n** at the 6-position afforded **3ka-na** in 48-77% yields. To our delight, reaction of quinoline *N*-oxides tethered with gemfibrozil **1q**, ibuprofen **1r**, probenecid **1s** and adamantane **1t** efficiently resulted in the target products **3qa-ta** with 58-65% yields. However, reaction 2-methyl **1b** was unsuccessful due to unavailability reactive site, while 7-methyl **1o** and 7,8-benzo-quinoline **1p** *N*-oxides also exhibited no annulation, might be due to steric hindrance during metal-complex formation.

Inspired by the results, we further extended the scope of the reaction for a series of substituted cyclopropenones **2b-n** with **1a** as the standard substrate (Table 4.5). Reaction of cyclopropenones 3-methylphenyl **2b** furnished **3ab** in 68% yield and 3-trifluoromethylphenyl

2c produced **3ac** in 69% yield. Similarly, cyclopropenones bearing bromo **2d**, fluoro **2e** and methyl **2f** groups at the 4-position of the aryl rings delivered **3ad-af** in 71-76% yields, while

Table 4.4. Substrate Scope of Quinoline *N*-oxides[a]

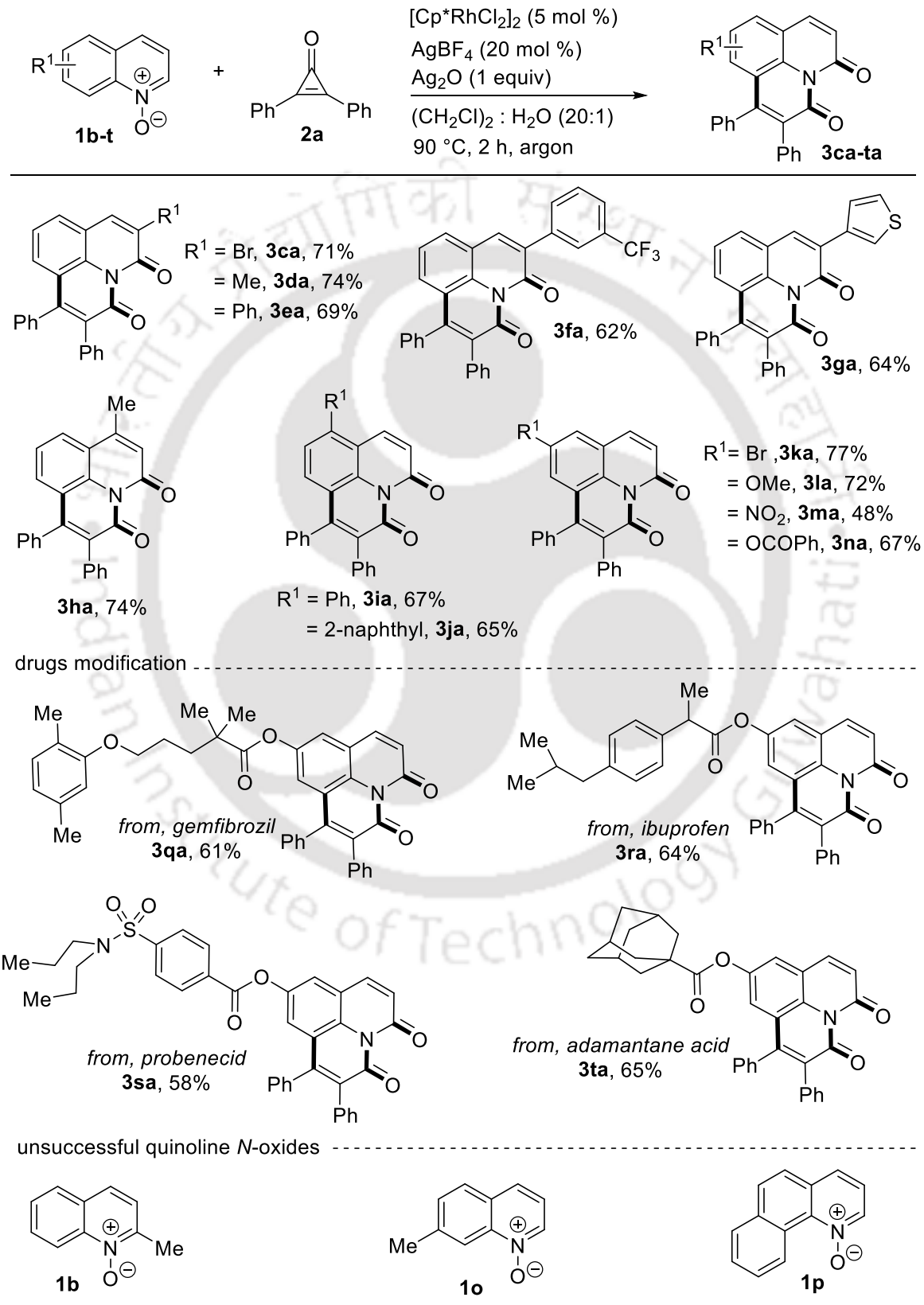

[a]Reaction conditions: **1b-t** (0.2 mmol), **2a** (0.24 mmol), $[RhCp^*Cl_2]_2$ (5 mol %), $AgBF_4$ (20 mol %), Ag_2O (0.2 mmol), $(CH_2Cl)_2$ (1 mL), H_2O (50 µL), 90 °C, argon, 2 h. [b]Isolated yield.

Table 4.5. Substrate Scope of Cyclopropenones[a]

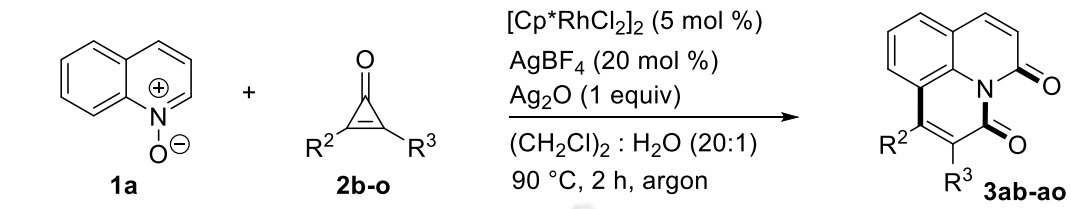

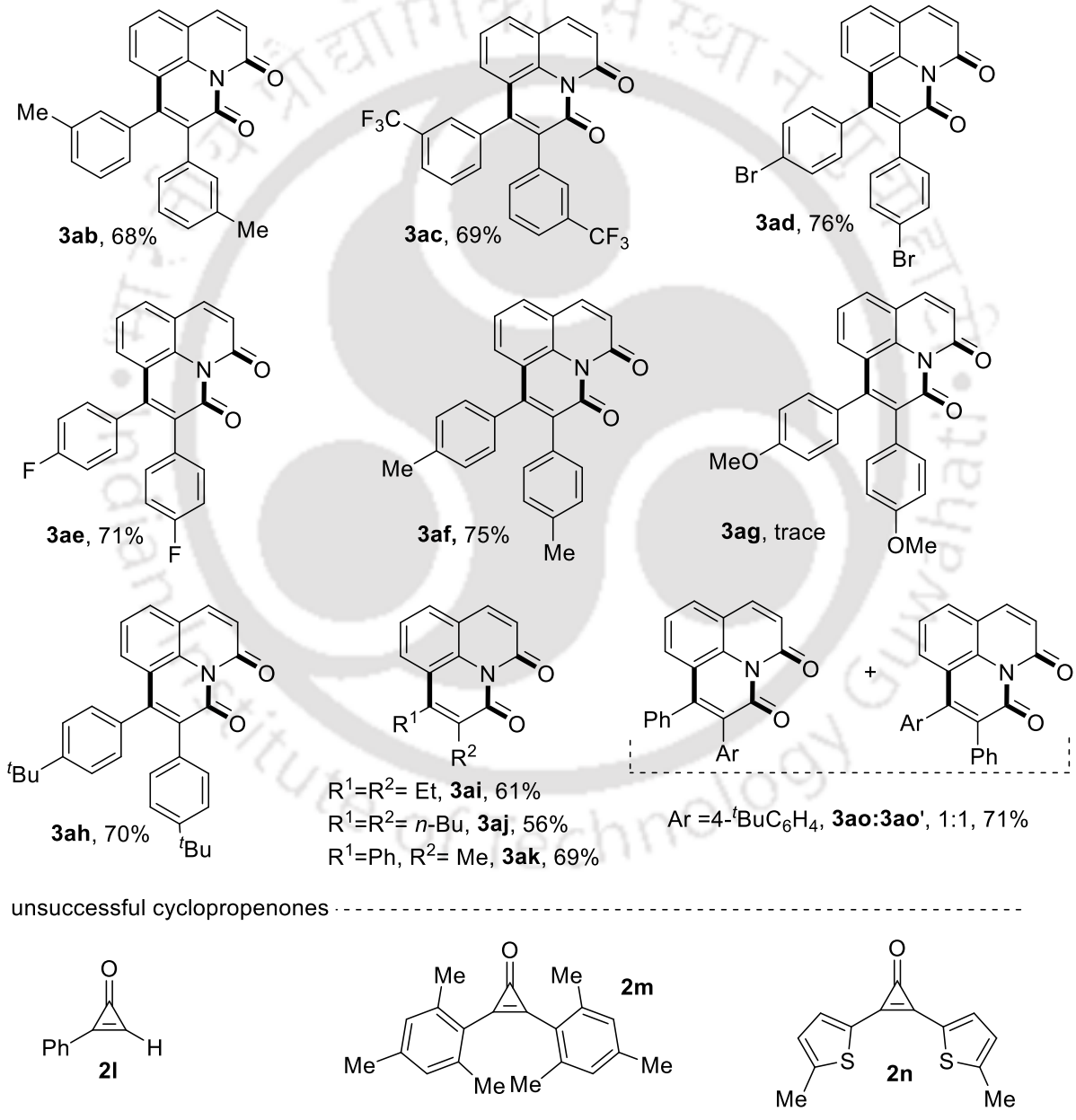

[a]Reaction conditions: **1a** (0.2 mmol), **2b-n** (0.24 mmol), $[RhCp^*Cl_2]_2$ (5 mol %), $AgBF_4$ (20 mol %), Ag_2O (0.2 mmol), $(CH_2Cl)_2$ (1 mL), H_2O (50 µL), 90 °C, argon, 2 h. [b]Isolated yield.

the aryl ring containing 4-methoxy group **2g** led to **3ag** in a trace amount, may be attributed to complex formation with metal catalyst. However, substitution with bulky 4-*tert*-butyl **2h** afforded **3ah** in 70% yield. Further, alkyl substituted cyclopropenones **2i** and **2j** gave **3ai** and **3aj** in 61% and 56% yields, respectively, whereas the reaction of unsymmetrical **2k** delivered **3ak** in in 69% yield while **2o** produced mixture diastereomer **3ao**:**3ao'** with 1:1 dr. However, **2l** decomposed to give phenylacetylene under the reaction conditions, and CPs with mesitylene **2m** and thienyl **2n** groups remain unsuccessful substrates to yield the target products which might be due to the steric hindrance and the formation of a sulphur complex with the catalyst, respectively.

To get insight into the reaction, preliminary mechanistic experiments were performed (Scheme 4.8). Reactions of **1a** with **2a** in the presence of radical scavengers, TEMPO and BHT were performed independently (Scheme 4.8a). The reactions led to the formation of **3aa**, indicating that radical pathway is not involved. Further, H/D exchange study in the absence of **2a** using D_2O as a co-solvent led to 48% deuterium incorporation at the C8-position of **1a**. This reveals that the C−H activation step may be reversible (Scheme 4.8b). Moreover, the kinetic isotope experiments employing **1a** and [D1]-**1a** with **2a** as the model substrates exhibited k_H/k_D value of 1.58 (for competitive) and 1.23 (for parallel), attributing that the C−H activation step might be involved in the rate-determining step (Scheme 4.8c). In addition, the reaction of **1a** with **2a** in the presence of $H_2{}^{18}O$ produced **3aa-^{18}O**, suggesting that water could be the source of the carbonyl oxygen (Scheme 4.8d(i)). Further, the product was observed when the reaction of **2a** with 2-quinolone **4** was performed under standard conditions (Scheme 4.8d(ii)). This result disclose that 2-quinolone formation may not occur during initial stage. The reaction of **2a** with $H_2{}^{18}O$ yielded the labelled **2a-^{18}O**, indicating that an oxygen atom exchange with water may have taken place (Scheme 4.8d(iii)). Additionally, the HRMS analysis of the reaction mixture detected the formation of Rh-species **D** (Scheme 4.8e).

A plausible mechanism is depicted in scheme 4.9 based on experimental results and literature.[15] Firstly, Rh-dimer with Ag(I)-salt can produce the active Rh-species **A**, which may undergo the reversible C8−H activation to form the five-membered rhodacycle **B**. Then intermolecular oxidative addition with **2a** may furnish **C**, which subsequently lead to formation of **D** *via* migratory insertion. Nucleophilic addition of water to **D** may afford **E** which on water elimination convert to **F**. Then a deprotonation path can generate intermediate **G**, which might

undergo a reductive elimination to afford **3aa** and **H**. Further oxidation of **H** using Ag(I) can lead to the active catalyst **A** to complete the catalytic cycle.

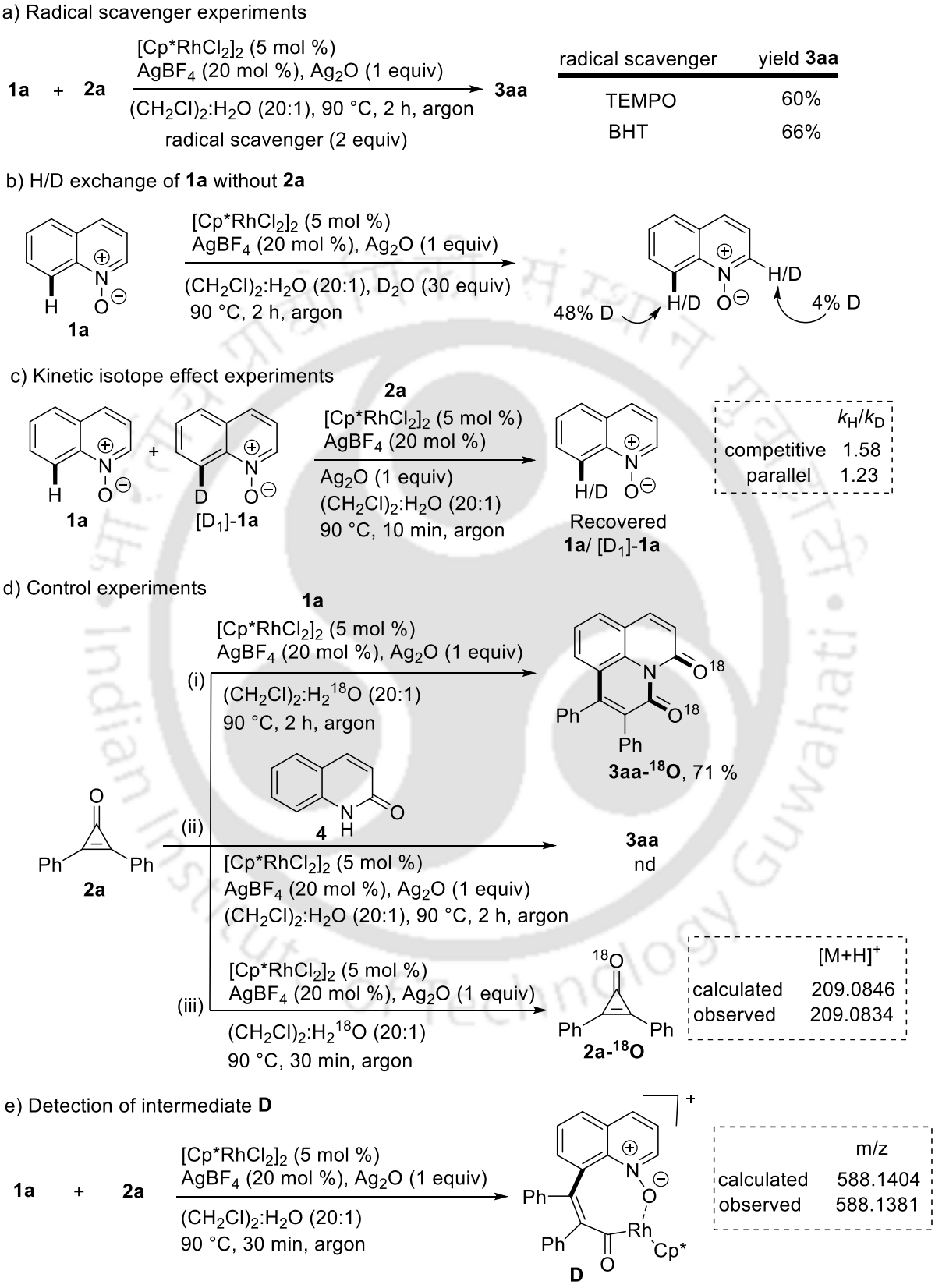

Scheme 4.8. Preliminary Mechanistic Experiments

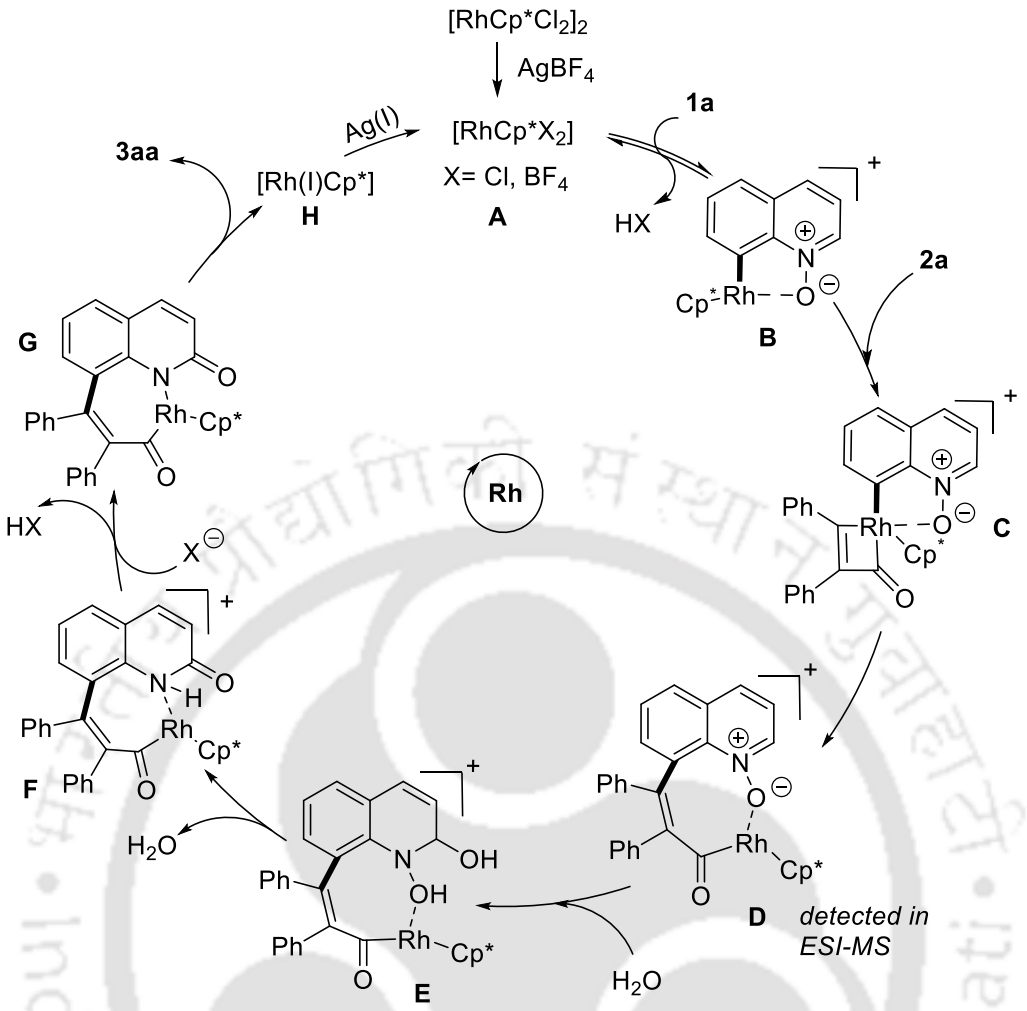

Scheme 4.9. Plausible Reaction Mechanism

To showcase the synthetic utility, scale-up synthesis using **1a** and **2a** as the model substrates afforded **3aa** in 61% yield (Scheme 4.10a). Further, post-synthetic transformations of **3aa** in presence of BH_3•SMe_2 produced 1,2-dihydroquinoline derivative **6** selectively in 68% yield (Scheme 4.10b). The structure of **6** was confirmed using single crystal X-ray analysis (CCDC 2382652). Moreover, Suzuki coupling of **3ka** using phenylboronic acid delivered **7** in 74% yield (Scheme 4.10c). These outcomes collectively underscore not only the scalability of the protocol but also the broad derivatization potential of the fused 2-oxindole framework.

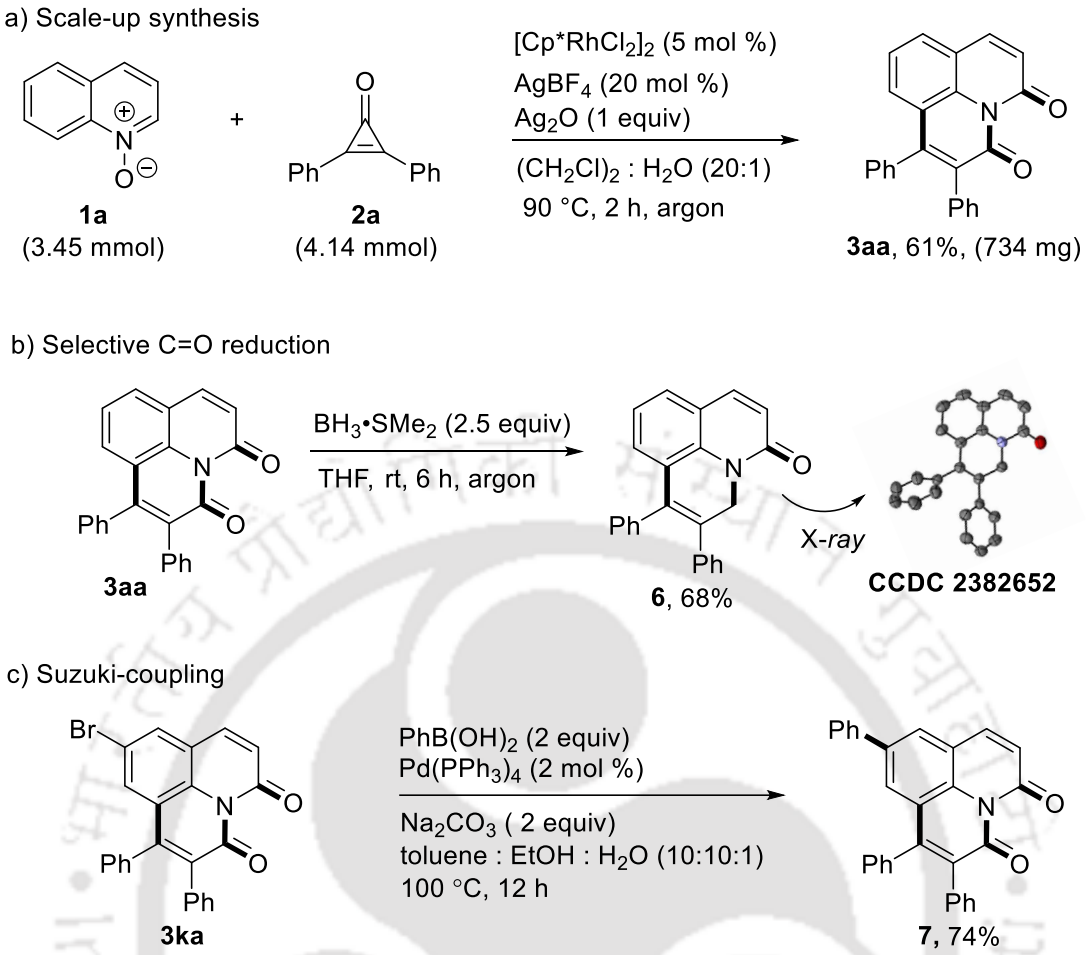

Scheme 4.10. Synthetic Utility

In summary, we have described a Rh-catalyzed annulation of quinoline *N*-oxides with cyclopropenones *via* cascade C−H/C−C bond activation approach that furnish functionalized 2-quinolone derivatives. Sequential C−C/C−N bond formation, merging strained ring reactivity with C−H/C−C activation strategy, water as O-source, drugs modification and post synthetic utility are the important practical features.

4.4 Experimental Section

General Information. Quinolines, $[RhCp^*Cl_2]_2$ (97%), $AgSbF_6$ (99%), $AgNTf_2$ (97%), Ag_2O (99%), AgOAc (≥99.9%), $AgBF_4$ (98%), Ag_2CO_3 (99%), Cu_2O ((≥99.9%), $Cu(OAc)_2$ (98%) and *m*-CPBA (≥77%) of Aldrich used as received. Quinoline N-oxides[15a] and cyclopropenones[2] were prepared according to the reported procedure. SRL silica gel G/GF 254 plates were used for analytical TLC and SRL silica gel (100-200 mesh) was used for column chromatography while compound spots were visualized using UV lamp (254 nm) and iodine. NMR (^1H, ^{13}C, ^{19}F and NOESY) spectra were recorded with Bruker Ascend 400, 500 and 600 MHz

spectrometers using $CDCl_3$ as solvent and TMS as an internal standard. Chemical shifts (δ) and spin-spin coupling constant (*J*) are reported in ppm and in Hz, respectively, and other data are reported as mentioned: s = singlet, d = doublet, t = triplet, m = multiplet. HRMS was recorded with a quadrupole time-of-flight electrospray ionization (ESI) mass spectrometer (Agilent6546). Perkin Elmer FT-IR spectrometer was used to record IR spectra. Melting points were determined using a Büchi B-540 apparatus and are uncorrected. Single crystal X-ray data was collected on a Bruker SMART APEX equipped with a CCD area detector using Mo/Kα radiation and the structure was solved by direct method using SHELXL-19 (Göttingen, Germany).

General Procedure for the Synthesis of Quinoline *N*-Oxides.[11,16]

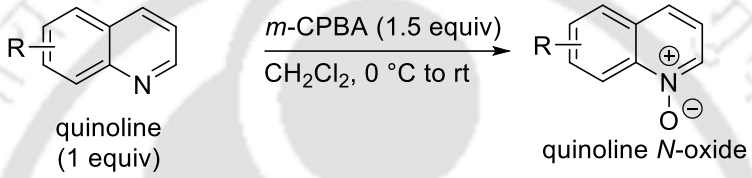

To a stirred solution of quinoline (1 mmol) in CH_2Cl_2 (3 mL), *m*-CPBA (1.5 mmol, 259 mg) was added portion-wise at 0 °C and the reaction mixture was allowed to stir 12 h at room temperature under air. The reaction mixture was quenched with a saturated aqueous solution of $NaHCO_3$ (10 mL) and extracted with CH_2Cl_2 (3 x 15 mL). Drying (Na_2SO_4) and evaporation of the solvent gave a residue that was purified on silica gel column chromatography to afford desired *N*-oxides **1**.

General Procedure for Synthesis of Cyclopropenones.[14,17]

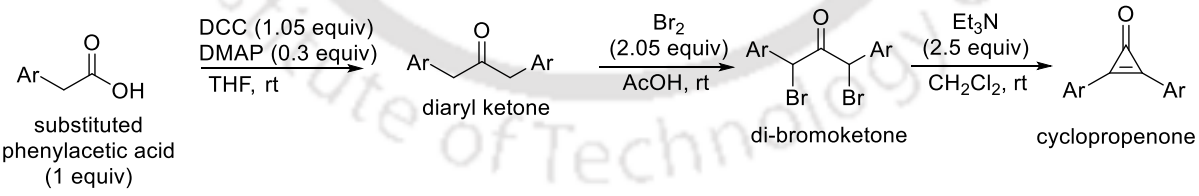

To a stirred solution of DCC (5.3 mmol, 1.1 g) and DMAP (1.5 mmol, 183 mg) in THF (10 mL), substituted phenylacetic acid (5 mmol) was added and the reaction was allowed to stir for 90 minutes at room temperature. Upon completion, the reaction mixture was passed through a short pad of celite. Evaporation of the solvent gave a residue that was purified by column chromatography to afford diaryl ketone.

The above diaryl ketone (1 mmol) was dissolved in acetic acid (2 mL) and bromine (2.05 mmol, 106 µL) in acetic acid (1 mL) was added drop wise over 10 minutes and the resultant mixture was stirred for 3 h at room temperature. Then, the reaction mixture was poured into an ice-cold water, and filtered to get a solid of dibromoketone. To a stirred solution of dibromoketone in CH_2Cl_2 (5 mL), triethylamine (2.5 mmol, 360 µL) was added and the stirring was continued for an additional 1 h. The reaction mixture was then diluted with CH_2Cl_2 (5 mL), washed with 1 N HCl (2 X 5 mL), brine (5 mL) and dried over Na_2SO_4. Evaporation of the solvent gave a residue which was purified on silica gel column chromatography using hexane/ethyl acetate as eluent to yield cyclopropenones **2**.

Procedure for Rh-Catalyzed C−H/C−C Activation and Annulation of Quinolines with Cyclopropenones. In a pressure tube, quinoline *N*-oxide **1** (0.2 mmol), cyclopropenone **2** (0.24 mmol), $[RhCp^*Cl_2]_2$ (0.01 mmol, 6 mg), $AgBF_4$ (0.04 mmol, 8 mg), Ag_2O (0.2 mmol, 46 mg), H_2O (50 µL) and $(CH_2Cl)_2$ (1 mL) were stirred for 2 h at 90 °C under argon atmosphere. Then, the reaction mixture was diluted using CH_2Cl_2 (20 mL) and passed through a short pad of celite. Evaporation of the solvent gave a residue that was purified on silica gel column chromatography using hexane/ethyl acetate as eluent to furnish the annulated product **3**.

Scale-up Synthesis of 3aa. In a pressure tube, quinoline *N*-oxide **1a** (3.44 mmol, 500 mg), cyclopropenone **2a** (4.1 mmol, 850 mg), $[RhCp^*Cl_2]_2$ (0.17 mmol, 106 mg), $AgBF_4$ (1.7 mmol, 134.5 mg), Ag_2O (3.4 mmol, 797 mg), H_2O (0.25 mL) and $(CH_2Cl)_2$ (5 mL) were stirred for 2 h at 90 °C under argon atmosphere. Purifications using above general method furnished **3aa** in 61% yield (734 mg).

Post-synthetic Transformations

Synthesis of 6. To an ice-cold solution of **3aa** (0.1 mmol, 35 mg) in THF (1 mL), BH_3•SMe_2 (0.25 mmol, 25 µL) was added and the reaction mixture was stirred for 6 h at room temperature under nitrogen atmosphere. Evaporation of solvent produced a residue which was purified on silica gel column chromatography using hexane/ethyl acetate to yield **6** in 68% (23 mg) yield.

Synthesis of 7. In a pressure tube, **3ka** (0.1 mmol, 43 mg), phenylboronic acid (0.2 mmol, 25 mg), Na_2CO_3 (0.2 mmol, 21 mg), toluene (1 mL), ethanol (1 mL) and water (100 µL) were added and the resultant mixture was degassed using argon. Then, $Pd(PPh_3)_4$ (2 mol %, 2.5 mg) was added and the mixture was stirred at 100 °C for 8 h. Upon completion, the mixture was diluted with ethyl acetate (20 mL), washed with water (5 mL) and dried (Na_2SO_4). Evaporation

of the solvent lead to a residue that was purified on silica gel column chromatography using hexane and ethyl acetate to get **7** in 74% (31.5 mg) yield.

Preliminary Mechanistic Experiments

Radical Scavenger Experiment (Scheme 4.8a). In a pressure tube charged with quinoline *N*-oxide **1a** (0.2 mmol, 29 mg), diphenylcyclopropenone **2a** (0.24 mmol, 49.5 mg), $[RhCp^*Cl_2]_2$ (0.01 mmol, 6 mg), $AgBF_4$ (0.04 mmol, 8 mg), Ag_2O (0.2 mmol, 46 mg), TEMPO or BHT (0.4 mmol), H_2O (50 µL) and $(CH_2Cl)_2$ (1 mL) was stirred for 2 h at 90 °C under argon atmosphere. The reaction mixture was then cooled to room temperature, diluted with CH_2Cl_2 (20 mL) and passed through celite pad. Evaporation of the solvent gave a residue which was purified using general procedure to yield **3aa**. Using TEMPO the recovered yield of **3aa** was 60% (42 mg), while with BHT the yield was 66% (46 mg).

H/D Exchange Experiment of 1a with D_2O in Absence of 2a (Scheme 4.8b). A pressure tube charged with quinoline *N*-oxide **1a** (0.2 mmol, 29 mg), $[RhCp^*Cl_2]_2$ (0.01 mmol, 6 mg), $AgBF_4$ (0.04 mmol, 8 mg), Ag_2O (0.2 mmol, 46 mg), H_2O (50 µL), $(CH_2Cl)_2$ (1 mL) and D_2O (6 mmol, 110 µL) was allowed to stir for 2 h at 90 °C under argon atmosphere. The reaction mixture was cooled to room temperature, diluted with CH_2Cl_2 (20 mL) and passed through short celite pad. After evaporation of the solvent, resultant residue was purified using general procedure to recover the starting material (86%, 25 mg). ^1H NMR analysis of the recovered starting material confirmed the deuterium incorporation was 48% at C8 position while 4% at C2 position.

Preparation of Quinoline *N*-oxide-8-d_1 [D_1]-1a. A pressure tube charged with quinoline *N*-oxide **1a** (1 mmol, 145 mg), $[RhCp^*Cl_2]_2$ (0.02 mmol, 12 mg), $AgSbF_6$ (0.08 mmol, 28 mg), PivOH (0.1 mmol, 11 mg), CD_3CO_2D (5 mmol, 305 µL), D_2O (0.5 mL) and $(CH_2Cl)_2$ (1 mL) was stirred at 110 °C for 48 h. The reaction mixture was cooled to room temperature, diluted using with CH_2Cl_2 (20 mL) and passed through a short celite pad. The residue produced after evaporation of the solvent was purified according to general procedure to afford [D_1]-**1a** in 84% yield (123 mg). ^1H NMR analysis confirmed the deuterium incorporation at C8 position of the recovered starting material was 93%.

Kinetic Isotope Effect Experiments (Scheme 4.8c)

Competitive Kinetic Isotope Experiment. A pressure tube charged with **1a** (0.2 mmol, 29 mg), [D_1]-**1a** (0.2 mmol, 32 mg), **2a** (0.24 mmol, 49.5 mg), $[RhCp^*Cl_2]_2$ (0.01 mmol, 6 mg), $AgBF_4$ (0.04 mmol, 8 mg), Ag_2O (0.2 mmol, 46 mg), H_2O (50 µL) and $(CH_2Cl)_2$ (1 mL) was

allowed to stir for 10 minutes at 90 °C under argon atmosphere. The quinoline *N*-oxide 1a/[D1]-**1a** was recovered using the general procedure, yielding 73% (22.5 mg). The KIE value for recovered **1a**/[D_1]-**1a** was calculated as k_H/k_D =1.58 from ^{1}H NMR analysis.

Parallel Kinetic Isotope Experiment. Two pressure tubes were separately charged with **1a** (0.2 mmol, 29 mg) or [D_1]-**1a** (0.2 mmol, 32 mg), **2a** (0.24 mmol, 49.5 mg), [RhCp*Cl_2]$_2$ (0.01 mmol, 6 mg), $AgBF_4$ (0.04 mmol, 4 mg), Ag_2O (0.2 mmol, 46 mg), H_2O (50 µL) and $(CH_2Cl)_2$ (1 mL) and allowed to stirred for 10 minutes at 90 °C under argon atmosphere. The two reaction mixtures were combined, and quinoline *N*-oxide **1a**/[D1]-**1a** was recovered using the general procedure in 73% (20 mg) yield. The KIE value was calculated as k_H/k_D = 1.23 from ^{1}H NMR analysis.

Control Experiments (Scheme 4.8d)

i) Reaction of 1a and 2a in presence of $H_2{}^{18}O$. In a pressure tube, **1a** (0.2 mmol, 29 mg), **2a** (0.24 mmol, 49.5 mg), [RhCp*Cl_2]$_2$ (0.01 mmol, 6 mg), $AgBF_4$ (0.04 mmol, 8 mg), Ag_2O (0.2 mmol, 46 mg), $(CH_2Cl)_2$ (1 mL) and $H_2{}^{18}O$ (50 µL) were stirred for 2 h at 90 °C under argon atmosphere. The reaction mixture was cooled to room temperature and purified according to general procedure to get of **3aa-^{18}O** in 71% yield (49.5 mg). (ESI) *m/z* $[M+H]^+$ calcd for $[C_{24}H_{16}N^{18}O_2]^+$ (**3aa-^{18}O**): 354.1272, found 354.1263.

ii) Reaction of 2a with 4. In a pressure tube, 2-quinolone **4** (0.2 mmol, 29 mg), **2a** (0.24 mmol, 49.5 mg), [RhCp*Cl_2]$_2$ (0.01 mmol, 6 mg), $AgBF_4$ (0.04 mmol, 8 mg), Ag_2O (0.2 mmol, 46 mg), H_2O (50 µL) and $(CH_2Cl)_2$ (1 mL) were stirred for 2 h at 90 °C under argon atmosphere. The reaction mixture was cooled to room temperature and HRMS analysis confirmed no **3aa** was formed.

iii) Reaction of 2a with $H_2{}^{18}O$ in Absence of 1a. A pressure tube charged with **2a** (0.1 mmol, 21 mg), [RhCp*Cl_2]$_2$ (0.05 mmol, 3 mg), $AgBF_4$ (0.02 mmol, 4 mg), Ag_2O (0.1 mmol, 23 mg), $(CH_2Cl)_2$ (0.5 mL) and $H_2{}^{18}O$ (25 µL) was stirred for 0.5 h at 90 °C under argon atmosphere. The reaction mixture was cooled to room temperature and HRMS analysis of the crude reaction mixture: (ESI) *m/z* $[M+H]^+$ calcd for $[C_{15}H_{11}{}^{18}O]^+$ (**2a-^{18}O**): 209.0846, found 209.0834.

Detection of Intermediate D (Scheme 4.8e). A pressure tube charged with quinoline *N*-oxide **1a** (0.1 mmol, 14.5 mg), diphenylcyclopropenone **2a** (0.12 mmol, 25 mg), [RhCp*Cl_2]$_2$ (0.005 mmol 3 mg), $AgBF_4$ (0.02 mmol, 4 mg), Ag_2O (0.1 mmol, 23 mg), H_2O (25 µL) and $(CH_2Cl)_2$ (0.5 mL) was allowed to stir for 0.5 h at 90 °C under argon atmosphere. HRMS analysis of the

crude reaction mixture: (ESI) *m/z* $[M]^+$ calcd for $[C_{34}H_{31}NO_2Rh]^+$ (intermediate **D**): 588.1404, found 588.1381.

4.5 Characterization Data

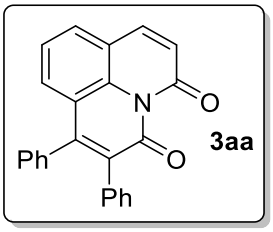

1,2-Diphenyl-3H,5H-pyrido[3,2,1-ij]quinoline-3,5-dione 3aa. Analytical TLC on silica gel; 3:2 hexane/ethyl acetate R_f = 0.3; brown solid; mp 247-248 °C; yield 73% (51 mg); ^{1}H NMR (500 MHz, $CDCl_3$) δ 7.74 (d, *J* = 10.0 Hz, 1H), 7.67 (d, *J* = 7.5 Hz, 1H), 7.44 (d, *J* = 8.0 Hz, 1H), 7.32-7.29 (m, 4H), 7.18-7.12 (m, 7H), 6.79 (d, *J* = 10.0 Hz, 1H); ^{13}C NMR (125 MHz, $CDCl_3$) δ 161.9, 161.8, 148.2, 139.9, 135.3, 134.9, 134.4, 134.3, 131.1, 130.9, 130.6, 129.9, 128.3, 128.2, 127.6, 127.5, 124.4, 123.8, 121.1, 119.5; FT-IR (neat) 2924, 1719, 1627, 1443, 1252, 1148, 947, 700 cm^{-1}; HRMS (ESI) *m/z* $[M+H]^+$ calcd for $C_{24}H_{16}NO_2$: 350.1176, found 350.1171.

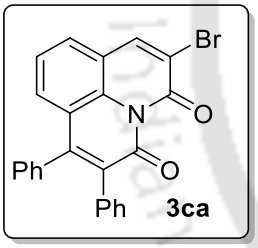

6-Bromo-1,2-diphenyl-3H,5H-pyrido[3,2,1-ij]quinoline-3,5-dione 3ca. Analytical TLC on silica gel; 7:3 hexane/ethyl acetate R_f = 0.4; brown solid; mp 255-256 °C; yield 71% (62 mg); ^{1}H NMR (500 MHz, $CDCl_3$) δ 8.20 (s, 1H), 7.64 (d, *J* = 7.5 Hz, 1H), 7.46 (d, *J* = 8.0 Hz, 1H), 7.34-7.2 (m, 4H), 7.16-7.11 (m, 7H); ^{13}C NMR (125 MHz, $CDCl_3$) δ 161.3, 157.4, 148.3, 141.4, 135.1, 134.3, 134.2, 134.1, 131.3, 130.8, 129.9, 129.8, 128.3, 127.72, 127.70, 124.2, 121.2, 119.4, 119.2; FT-IR (neat) 2923, 1725, 1616, 1448, 1234, 1616, 960, 699 cm^{-1}; HRMS (ESI) *m/z* $[M+H]^+$ calcd for $C_{24}H_{15}NO_2Br$: 428.0281, found 428.0272.

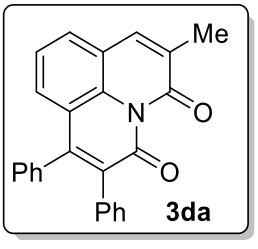

6-Methyl-1,2-diphenyl-3H,5H-pyrido[3,2,1-ij]quinoline-3,5-dione 3da. Analytical TLC on silica gel; 7:3 hexane/ethyl acetate R_f = 0.4; brown solid; mp 230-231

°C; yield 74% (54 mg); ^{1}H NMR (500 MHz, $CDCl_3$) δ 7.60-7.58 (m, 2H), 7.35-7.34 (m, 1H), 7.29-7.26 (m, 4H), 7.11-7.11 (m, 7H), 2.33 (s, 3H); ^{13}C NMR (125 MHz, $CDCl_3$) δ 162.8, 162.0, 148.2, 136.4, 135.5, 134.5, 134.2, 134.1, 132.9, 130.9, 129.9, 129.8, 129.7, 123.7, 120.7, 119.4, 17.698; FT-IR (neat) 2923, 1715, 1459, 1442, 1150, 765 752, 702 cm^{-1}; HRMS (ESI) *m/z* $[M+H]^+$ calcd for $C_{25}H_{18}NO_2$: 364.1332, found 364.1333.

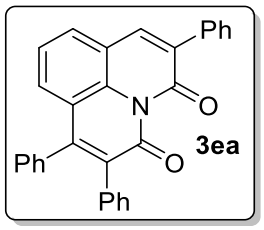

1,2,6-Triphenyl-3H,5H-pyrido[3,2,1-ij]quinoline-3,5-dione 3ea. Analytical TLC on silica gel; 7:3 hexane/ethyl acetate R_f = 0.4; brown solid; mp 258-259 °C; yield 69% (59 mg); ^{1}H NMR (500 MHz, $CDCl_3$) δ 7.85 (s, 1H), 7.78-7.76 (m, 2H), 7.71-7.70 m, 1H), 7.48 (t, *J* = 7.0 Hz, 2H), 7.43-7.40 (m, 2H), 7.32-7.29 (m, 4H), 7.17-7.13 (m, 7H); ^{13}C NMR (125 MHz, $CDCl_3$) δ 161.9, 161.6, 148.1, 137.0, 135.4, 134.9, 134.5, 134.4, 131.0, 130.6, 130.5, 129.9, 129.1, 128.9, 128.5, 128.3, 128.2, 127.6, 127.5, 123.8, 120.7, 119.4; FT-IR (neat) 2922, 1721, 1664, 1444, 1275, 1153, 753, 698 cm^{-1}; HRMS (ESI) *m/z* $[M+H]^+$ calcd for $C_{30}H_{20}NO_2$: 426.1489, found 426.1490.

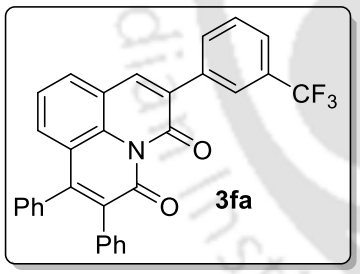

1,2-Diphenyl-6-(3-(trifluoromethyl)phenyl)-3H,5H-pyrido-[3,2,1-ij]quinoline-3,5-dione 3fa. Analytical TLC on silica gel; 7:3 hexane/ethyl acetate R_f = 0.35; brown solid; mp 262-263 °C; yield 62% (61 mg); ^{1}H NMR (500 MHz, $CDCl_3$) δ 8.01 (d, *J* = 10.0 Hz, 2H), 7.91 (s, 1H), 7.75 (d, *J* = 7.0 Hz, 1H), 7.68 (d, *J* = 7.5 Hz, 1H), 7.60 (t, *J* = 8.0 Hz, 1H), 7.46 (d, *J* = 7.5 Hz, 1H), 7.35-7.30 (m, 4H), 7.19-7.14 (m, 7H); ^{13}C NMR (125 MHz, $CDCl_3$) δ 161.8, 161.2, 148.2, 137.9, 136.1, 135.2, 134.5, 134.4, 134.3, 133.4, 132.6, 131.1 (J_{C-F} = 32.0 Hz), 131.0, 130.97, 130.95 129.9, 128.954, 128.3, 128.3, 127.6, 125.9 (J_{C-F} = 3.8 Hz), 125.5 (J_{C-F} = 4.0 Hz), 125.2 (J_{C-F} = 270.7 Hz), 124.0, 120.8, 119.1; ^{19}F NMR (470 MHz, $CDCl_3$) δ -62.50; FT-IR (neat) 3059, 2922, 1720, 1663, 1442, 1332, 1217, 1153, 1124, 1075, 750, 697 cm^{-1}; HRMS (ESI) *m/z* $[M+H]^+$ calcd for $C_{31}H_{19}F_3NO_2$: 494.1362, found 494.1356.

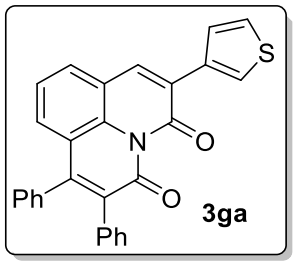

1,2-Diphenyl-6-(thiophen-3-yl)-3H,5H-pyrido[3,2,1-ij]quinoline-3,5-dione 3ga. Analytical TLC on silica gel, 7:3 hexane/ethyl acetate R_f = 0.42; brown solid; mp 244-245 °C; yield 64% (56 mg); ^{1}H NMR (400 MHz, $CDCl_3$) δ 8.32-8.31 (m, 1H), 8.00 (s, 1H), 7.72-7.70 (m, 1H), 7.61-7.59 (m, 1H), 7.41-7.39 (m, 2H), 7.33-7.29 (m, 4H), 7.18-7.13 (m, 7H); ^{13}C NMR (150 MHz, $CDCl_3$) δ 162.0, 161.2, 148.1, 135.4, 134.8, 134.7, 134.5, 134.4, 133.8, 131.0, 130.5, 130.3, 129.9, 129.0, 128.3, 128.2, 127.6, 127.5, 126.8, 126.6, 125.4, 123.8, 120.6, 119.3; FT-IR (neat) 2924, 1719, 1661, 1444, 1149, 699 cm^{-1}; HRMS (ESI) *m/z* $[M+H]^+$ calcd for $C_{28}H_{18}NO_2S$: 432.1053, found 432.1050.

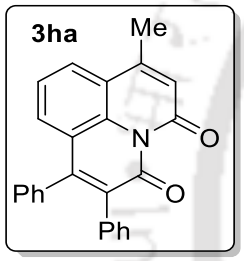

7-Methyl-1,2-diphenyl-3H,5H-pyrido[3,2,1-ij]quinoline-3,5-dione 3ha. Analytical TLC on silica gel; 3:2 hexane/ethyl acetate R_f = 0.32; brown solid; mp 230-231 °C; yield 73% (52.5 mg); ^{1}H NMR (500 MHz, $CDCl_3$) δ 7.83 (d, *J* = 7.5 Hz, 1H), 7.43 (d, *J* = 8.0 Hz, 1H), 7.33-7.29 (m, 4H), 7.16-7.11 (m, 7H), 6.67 (s, 1H), 2.53 (s, 3H); ^{13}C NMR (125 MHz, $CDCl_3$) ^{13}C NMR (125 MHz, $CDCl_3$) δ 161.7, 161.6, 148.2, 147.7, 135.5, 134.8, 134.3, 134.2, 131.0, 130.9, 129.9, 128.3, 128.2, 127.6, 127.5, 127.1, 123.5, 123.4, 121.2, 120.6, 19.417; FT-IR (neat) 3057, 2923, 1720, 1664, 1443, 1256, 1205, 1146, 744, 710 cm^{-1}; HRMS (ESI) *m/z* $[M+H]^+$ calcd for $C_{25}H_{18}NO_2$: 364.1332, found 364.1338.

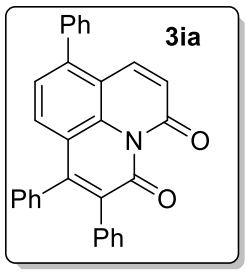

1,2,8-Triphenyl-3H,5H-pyrido[3,2,1-ij]quinoline-3,5-dione 3ia. Analytical TLC on silica gel; 3:2 hexane/ethyl acetate R_f = 0.3; brown solid; mp 210-211 °C; yield 67% (56 mg); ^{1}H NMR (400 MHz, $CDCl_3$) δ 7.81 (d, *J* = 10.0 Hz, 1H), 7.54-7.48 (m,

3H), 7.46 (d, *J* = 8.0 Hz, 1H), 7.40-7.37 (m, 2H), 7.34-7.28 (m, 4H), 7.17-7.14 (m, 7H), 6.714 (d, *J* = 10.0 Hz, 1H); ^{13}C NMR (100 MHz, $CDCl_3$) δ 162.1, 161.7, 148.1, 144.1, 138.4, 138.0, 135.6, 135.4, 134.3, 134.0, 130.9, 130.6, 130.0, 129.9, 128.8, 128.6, 128.3, 128.3, 127.6, 127.5, 125.4, 123.8, 120.2, 117.3; FT-IR (neat) 3057, 1727, 1667, 1442, 1275, 1147, 763, 697 cm^{-1}; HRMS (ESI) *m/z* $[M+H]^+$ calcd for $C_{30}H_{20}NO_2$: 426.1489, found 426.1491.

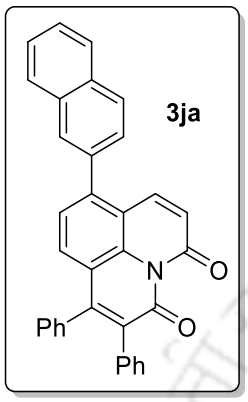

8-(Naphthalen-2-yl)-1,2-diphenyl-3H,5H-pyrido[3,2,1-ij]quinoline-3,5-dione 3ja. Analytical TLC on silica gel; 7:3 hexane/ethyl acetate R_f = 0.33; brown solid; mp 231-232 °C; yield 65% (61.5 mg); ^{1}H NMR (400 MHz, $CDCl_3$) δ 8.00 (d, *J* = 8.4 Hz, 1H), 7.95-7.91 (m, 2H), 7.86-7.83 (m, 2H), 7.61-7.56 (m, 2H), 7.51-7.47 (m, 2H), 7.37-7.31 (m, 4H), 7.19-7.16 (m, 7H), 6.72 (d, *J* = 10.0 Hz, 1H); ^{13}C NMR (125 MHz, $CDCl_3$) δ 162.1, 161.7, 148.2, 144.1, 138.1, 135.8, 135.6, 135.4, 134.3, 134.0, 133.1, 133.0, 130.9, 130.6, 129.9, 129.3, 128.5, 128.3, 128.3, 127.9, 127.6, 127.5, 127.1, 127.0, 125.6, 123.9, 120.3, 117.4.; FT-IR (neat) 5034, 2924, 1724, 16649, 1570, 1441, 1275, 1148, 763, 750, 702 cm^{-1}; HRMS (ESI) *m/z* $[M+H]^+$ calcd for $C_{34}H_{22}NO_2$: 476.1645, found 476.1648.

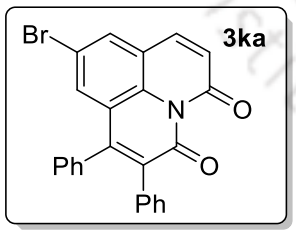

9-Bromo-1,2-diphenyl-3H,5H-pyrido[3,2,1-ij]quinoline-3,5-dione 3ka. Analytical TLC on silica gel; 3:2 hexane/ethyl acetate R_f = 0.30; brown solid; mp 251-252 °C; yield 77% (66 mg); ^{1}H NMR (500 MHz, $CDCl_3$) δ 7.78 (d, *J* = 2.5 Hz, 1H), 7.66 (d, *J* = 10.0 Hz, 1H), 7.49 (d, *J* = 2.5 Hz, 1H), 7.32-7.31 (m, 3H), 7.18-7.15 (m, 3H), 7.12-7.10 (m, 4H), 6.81 (d, *J* = 10.0 Hz, 1H); ^{13}C NMR (125 MHz, $CDCl_3$) δ 161.3, 161.2, 147.1, 138.7, 135.5, 134.6, 133.9, 133.8, 132.9, 132.6, 130.7, 129.7, 128.6, 128.5, 127.7, 127.6, 125.6, 122.9, 121.0, 116.9; FT-IR (neat) 3060, 1723, 1565, 1444, 1252, 1153, 1113, 741, 699 cm^{-1}; HRMS (ESI) *m/z* $[M+H]^+$ calcd for $C_{24}H_{15}NO_2Br$: 428.0281, found 428.0283.

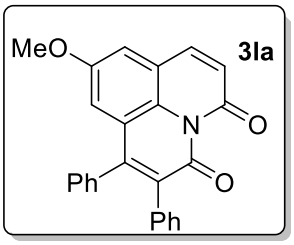

9-Methoxy-1,2-diphenyl-3H,5H-pyrido[3,2,1-ij]quinoline-3,5-dione 3la. Analytical TLC on silica gel; 3:2 hexane/ethyl acetate R_f = 0.28; brown solid; mp 245-246 °C; yield 72% (54 mg); ^{1}H NMR (500 MHz, $CDCl_3$) δ 7.67 (d, *J* = 9.5 Hz, 1H), 7.31-7.28 (m, 3H), 7.17-7.10 (m, 8H), 6.96 (d, *J* = 2.5 Hz, 1H), 6.79 (d, *J* = 9.5 Hz, 1H), 3.7 (s, 3H).; ^{13}C NMR (125 MHz, $CDCl_3$) δ 161.7, 161.7, 155.5, 147.8, 139.5, 135.3, 135.0, 134.4, 130.9, 129.8, 129.4, 128.3, 128.3, 127.5, 127.5, 125.1, 122.5, 120.5, 117.0, 114.7, 55.872; FT-IR (neat) 3060, 2922, 1715, 1590, 1461, 1349, 1291, 1148, 1054, 764, 750, 702 cm^{-1}; HRMS (ESI) *m/z* $[M+H]^+$ calcd for $C_{25}H_{18}NO_3$: 380.1281, found 380.1286.

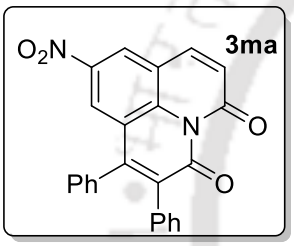

9-Nitro-1,2-diphenyl-3H,5H-pyrido[3,2,1-ij]quinoline-3,5-dione 3ma. Analytical TLC on silica gel; 1:1 hexane/ethyl acetate R_f = 0.27; brown solid; mp 275-276 °C; yield 48% (38 mg); ^{1}H NMR (400 MHz, $CDCl_3$) δ 8.52 (d, *J* = 2.4 Hz, 1H), 8.27 (d, *J* = 2.4 Hz, 1H), 7.83 (d, *J* = 9.6 Hz, 1H), 7.37-7.35 (m, 3H), 7.20-7.19 (m, 3H), 7.15-7.12 (m, 4H), 6.918 (d, *J* = 10.0 Hz, 1H); ^{13}C NMR (100 MHz, $CDCl_3$) δ 160.9, 160.6, 147.3, 143.4, 138.9, 138.3, 136.2, 134.0, 133.4, 130.7, 129.7, 129.1, 128.9, 128.1, 127.8, 126.4, 125.0, 124.6, 122.0, 119.8; FT-IR (neat) 6063, 2929, 1733, 1527, 1447, 1334, 747, 700 cm^{-1}; HRMS (ESI) *m/z* $[M+H]^+$ calcd for $C_{24}H_{15}N_2O_4$: 395.1026, found 395.1032.

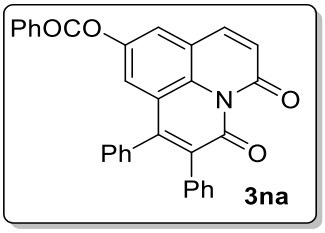

3,5-Dioxo-1,2-diphenyl-3H,5H-pyrido[3,2,1-ij]quinolin-9-yl benzoate 3na. Analytical TLC on silica gel; 3:2 hexane/ethyl acetate R_f = 0.37; brown solid; mp 212-213 °C; yield 67% (64 mg); ^{1}H NMR (500 MHz, $CDCl_3$) δ 8.15 (d, *J* = 8.5 Hz, 2H), 7.72 (d, *J* = 10.0 Hz, 1H), 7.66 (t, *J* = 7.5 Hz, 1H), 7.57 (d, *J* = 2.5 Hz, 1H), 7.51 (t, *J* = 8.0 Hz, 2H), 7.31-7.30 (m, 3H), 7.25-7.4 (m, 1H), 7.17-7.14 (m, 7H), 6.84 (d, *J* = 10.0 Hz, 1H).; ^{13}C

NMR (125 MHz, $CDCl_3$) 165.1, 161.5, 147.5, 146.6, 139.3, 135.3, 134.9, 134.2, 134.1, 132.7, 130.8, 130.4, 129.8, 128.8, 128.5, 128.4, 127.7, 127.6, 125.4, 123.7, 123.5, 122.4, 120.53; FT-IR (neat) 3060, 2925, 1726, 1592, 1449, 1248, 1147, 1061, 750, 702 cm^{-1}; HRMS (ESI) *m/z* $[M+H]^+$ calcd for $C_{31}H_{20}NO_4$: 470.1387, found 470.1389.

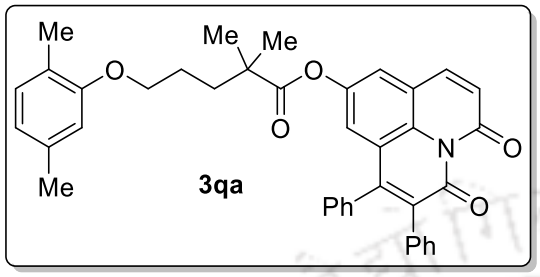

3,5-Dioxo-1,2-diphenyl-3H,5H-pyrido[3,2,1-ij]quinolin-9-yl 5-(2,5-dimethylphenoxy)-2,2-dimethylpentanoate 3qa. Analytical TLC on silica gel; 7:3 hexane/ethyl acetate R_f = 0.35; brown sticky liquid; yield 61% (72 mg); ^{1}H NMR (500 MHz, $CDCl_3$) δ 7.62 (d, *J* = 10.0 Hz, 1H), 7.33 (d, *J* = 2.5 Hz, 1H), 7.25-7.20 (m, 3H), 7.16-7.14 (m, 3H), 7.13-7.10 (m, 4H), 7.07 (d, *J* = 2.5 Hz, 1H), 7.00 (d, *J* = 7.0 Hz, 1H), 6.80 (d, *J* = 9.5 Hz, 1H), 6.68 (d, *J* = 7.5 Hz, 1H), 6.59 (s, 1H), 3.91 (t, *J* = 6.0 Hz, 2H), 2.30 (s, 3H), 2.12 (s, 3H), 1.87-1.83 (m, 2H), 1.80-1.76 (m, 2H), 1.32 (s, 6H); ^{13}C NMR (125 MHz, $CDCl_3$) δ 176.4, 161.5, 156.9, 147.5, 146.7, 139.2, 136.6, 135.1, 134.8, 132.5, 130.8, 130.5, 129.8, 128.44, 128.40, 127.7, 127.6, 125.2, 123.6, 123.4, 123.3, 122.3, 120.9, 120.4, 112.0, 67.6, 42.6, 37.2, 25.3, 25.1, 21.5, 15.9; FT-IR (neat) 3059, 2925, 1727, 1667, 1450, 1251, 1149, 1105, 705 cm^{-1}; HRMS (ESI) *m/z* $[M+H]^+$ calcd for $C_{39}H_{36}NO_5$: 598.2588, found 598.2584.

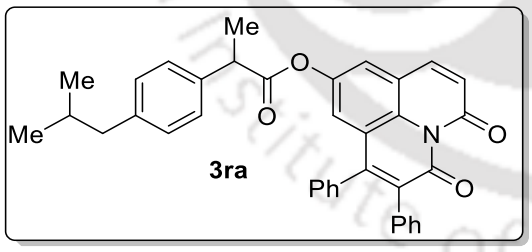

3,5-Dioxo-1,2-diphenyl-3H,5H-pyrido[3,2,1-ij]quinolin-9-yl 2-(4-isobutylphenyl)propanoate 3ra. Analytical TLC on silica gel; 7:3 hexane/ethyl acetate R_f = 0.38; brown sticky liquid; yield 64% (70.5 mg); ^{1}H NMR (400 MHz, $CDCl_3$) δ 7.63 (d, *J* = 9.6 Hz, 1H), 7.31-7.28 (m, 4H), 7.22 (d, *J* = 8.0 Hz, 2H), 7.16-7.14 (m, 3H), 7.12-7.09 (m, 6H), 7.04 (d, *J* = 2.8 Hz, 1H), 6.79 (d, *J* = 9.6 Hz, 1H), 3.91-3.85 (m, 1H), 2.46 (d, *J* = 7.2 Hz, 2H), 1.88-1.81 (m, 1H), 1.56 (d, *J* = 7.2 Hz, 3H), 0.91 (d, *J* = 6.8 Hz, 6H); ^{13}C NMR (125 MHz, $CDCl_3$) δ 173.2, 161.4, 147.4, 146.5, 141.1, 139.2, 136.9, 135.1, 134.9, 134.1, 132.6, 130.8, 129.8, 129.7, 128.4, 127.7, 127.6, 127.2, 125.2, 123.4, 123.1, 122.2, 120.3, 45.2, 45.1, 30.3, 22.5, 18.6; FT-IR (neat) 3056, 2954, 1755, 1727, 1455, 1443, 1286,

1250,1145, 765, 750, 702 cm^{-1}; HRMS (ESI) *m/z* $[M+H]^+$ calcd for $C_{37}H_{32}NO_4$: 554.2326, found 554.2320.

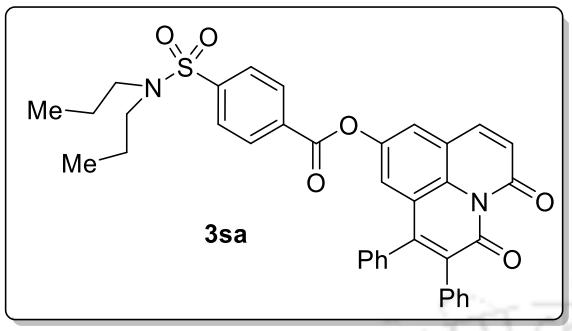

3,5-dioxo-1,2-diphenyl-3H,5H-pyrido[3,2,1-ij]quinolin-9-yl 4-(*N*,*N*-dipropylsulfamoyl)benzoate 3sa. Analytical TLC on silica gel; 7:3 hexane/ethyl acetate R_f = 0.33; brown sticky liquid; yield 58% (74 mg); ^1H NMR (400 MHz, $CDCl_3$) δ 8.27 (d, *J* = 8.4 Hz, 2H), 7.93 (d, *J* = 8.4 Hz, 2H), 7.72 (d, *J* = 9.6 Hz, 1H), 7.58 (d, *J* = 2.8 Hz, 1H), 7.30-7.27 (m, 3H), 7.25 (d, *J* = 2.8 Hz, 1H), 7.18-7.12 (m, 7H), 6.85 (d, *J* = 9.6 Hz, 1H), 3.13-3.09 (m, 4H), 1.58-1.50 (m, 5H), 0.89 (t, *J* = 7.6 Hz, 6H); ^{13}C NMR (100 MHz, $CDCl_3$) δ 163.8, 161.4, 161.4, 147.4, 146.2, 145.6, 139.1, 135.5, 134.9, 134.0, 132.9, 132.0, 131.0, 130.8, 129.8, 128.5, 128.5, 127.7, 127.6, 127.3, 125.5, 123.4, 123.2, 122.5, 120.6, 50.0, 22.0, 11.2. FT-IR (neat) 3057, 9965, 2931, 1725, 1452, 1342, 1251, 1153, 1071, 992, 751, 701 cm^{-1}; HRMS (ESI) *m/z* $[M+H]^+$ calcd for $C_{37}H_{33}N_2O_6S$: 633.2054, found 633.2055.

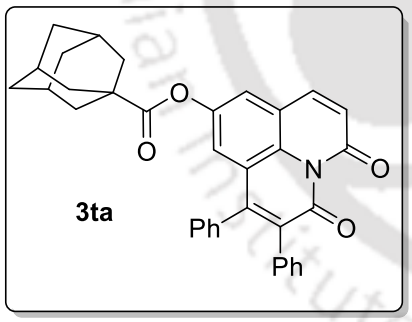

3,5-Dioxo-1,2-diphenyl-3H,5H-pyrido[3,2,1-ij]quinolin-9-yl adamantane-1-carboxylate 3ta. Analytical TLC on silica gel, 7:3 hexane/ethyl acetate R_f = 0.40; brown sticky liquid; yield 65% (66 mg); ^1H NMR (400 MHz, $CDCl_3$) δ 7.67 (d, *J* = 9.6 Hz, 1H), 7.39 (d, *J* = 2.4 Hz, 1H), 7.32-7.28 (m, 3H), 7.17-7.10 (m, 7H), 7.07 (d, *J* = 2.8 Hz, 1H), 6.81 (d, *J* = 9.6 Hz, 1H), 2.06 (s, 3H), 2.00 (d, *J* = 2.4 Hz, 6H), 1.78-1.70 (m, 6H); ^{13}C NMR (150 MHz, $CDCl_3$) δ 176.1, 161.5, 161.5, 147.5, 146.8, 139.2, 135.1, 134.9, 134.2, 132.5, 130.8, 129.9, 128.4, 127.6, 127.6, 125.2, 123.4, 122.2, 120.3, 41.2, 38.7, 36.4, 27.9; FT-IR (neat) 2907, 2853, 1726, 1449, 1207, 1180, 1048, 703 cm^{-1}; HRMS (ESI) *m/z* $[M+H]^+$ calcd for $C_{35}H_{30}NO_4$: 528.2169, found 528.2169.

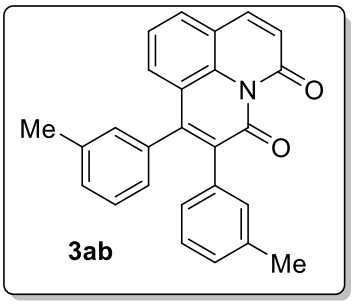

1,2-Di-*m*-tolyl-3H,5H-pyrido[3,2,1-ij]quinoline-3,5-dione 3ab. Analytical TLC on silica gel; 3:2 hexane/ethyl acetate R_f = 0.33; brown solid; mp 223-224 °C; yield 68% (52 mg); ^{1}H NMR (500 MHz, $CDCl_3$) δ 7.73 (d, *J* = 9.5 Hz, 1H), 7.66 (d, *J* = 7.5 Hz, 1H), 7.44-7.43 (m, 1H), 7.31(t, *J* = 7.5 Hz, 1H), 7.19 (t, *J* = 7.5 Hz, 1H), 7.09 (d, *J* = 7.5 Hz, 1H), 7.05 (t, *J* = 7.5 Hz, 1H), 7.00 (s, 1H), 6.96-6.89 (m, 4H), 6.79 (d, *J* = 10.0 Hz, 1H), 2.28 (s, 3H), 2.21 (s, 3H); ^{13}C NMR (125 MHz, $CDCl_3$) δ 161.93, 161.90, 148.2, 139.9, 137.8, 136.9, 135.3, 134.8, 134.4, 134.2, 131.5, 131.1, 130.5, 130.4, 128.9, 128.2, 128.1, 127.9, 127.4, 126.9, 124.4, 123.7, 121.2, 119.4, 21.5, 21.4; FT-IR (neat) 3054, 2922, 1718, 1665, 1258, 1137, 837, 774, 703 cm^{-1}; HRMS (ESI) *m/z* $[M+H]^+$ calcd for $C_{26}H_{20}NO_2$: 378.1489, found 378.1496.

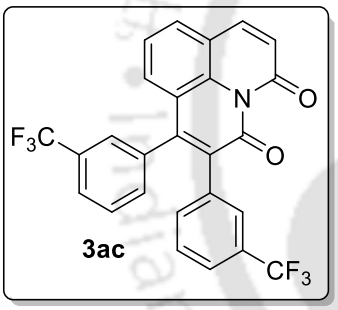

1,2-Bis(3-(trifluoromethyl)phenyl)-3H,5H-pyrido[3,2,1-ij]quinoline-3,5-dione 3ac. Analytical TLC on silica gel; 3:2 hexane/ethyl acetate R_f = 0.3; colourless solid; mp 240-241 °C; yield 67% (68 mg); ^{1}H NMR (500 MHz, $CDCl_3$) δ 7.77-7.73 (m, 2H), 7.59 (d, *J* = 8.0 Hz, 1H), 7.48 (t, *J* = 7.8 Hz, 1H), 7.44 (d, *J* = 7.5 Hz, 1H), 7.40-7.37 (m, 4H), 7.35-7.31 (m, 2H), 7.30 (s, 1H), 6.82 (d, *J* = 9.5 Hz, 1H); ^{13}C NMR (125 MHz, $CDCl_3$) δ 161.5, 161.0, 147.5, 140.0, 135.7, 135.0, 134.6, 134.2, 133.6, 133.0, 131.5, 131.1 (J_{C-F} = 33.0 Hz), 130.7, 130.1 (J_{C-F} = 32.0 Hz), 129.2, 128.3, 127.8 (J_{C-F} = 3.8 Hz), 126.7 (J_{C-F} = 3.6 Hz), 125.4 (J_{C-F} = 3.8 Hz), 124.6 (J_{C-F} = 3.6 Hz), 124.6, 124.3, 122.7 (J_{C-F} = 270.6 Hz), 122.5 (J_{C-F} = 270.5 Hz), 120.1, 119.7; ^{19}F NMR (470 MHz, $CDCl_3$) δ -63.00, -63.05; FT-IR (neat) 3064, 1723, 1666, 1433, 1331, 1123, 1075, 834, 707 cm^{-1}; HRMS (ESI) *m/z* $[M+Na]^+$ calcd for $C_{26}H_{13}F_6NO_2Na$: 508.0743, found 508.0739.

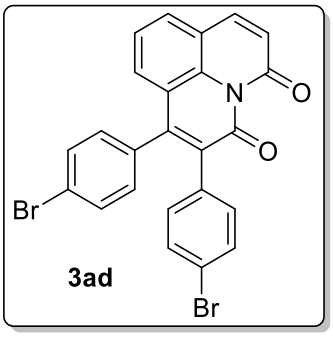

3ad

1,2-Bis(4-bromophenyl)-3H,5H-pyrido[3,2,1-ij]quinoline-3,5-dione 3ad. Analytical TLC on silica gel, 3:2 hexane/ethyl acetate R_f = 0.32; dark brown solid; mp 272-273°C; yield 76% (76.5 mg); ^{1}H NMR (400 MHz, $CDCl_3$) δ 7.74 (d, *J* = 9.6 Hz, 1H), 7.70 (dd, *J* = 1.6, 7.3 Hz, 1H), 7.49-7.47 (m, 2H), 7.39-7.32 (m, 4H), 7.02-6.99 (m, 4H), 6.79 (d, *J* = 9.6 Hz, 1H); ^{13}C NMR (125 MHz, $CDCl_3$) δ 161.6, 161.2, 147.2, 139.9, 134.9, 133.9, 133.4, 132.9, 132.5, 131.9, 131.4, 131.1, 131.1, 130.8, 124.5, 124.0, 122.9, 122.2, 120.5, 119.6; FT-IR (neat) 3062, 2924, 1717, 1567, 1486, 1252, 1148, 1071, 1011, 802, 776 cm^{-1}; HRMS (ESI) *m/z* $[M+H]^+$ calcd for $C_{24}H_{14}Br_2NO_2$: 505.9386, found 505.9394.

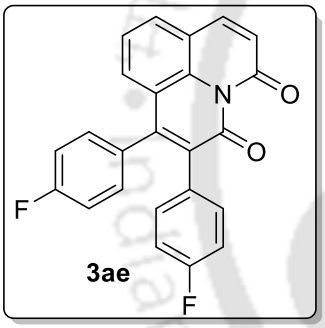

3ae

1,2-Bis(4-fluorophenyl)-3H,5H-pyrido[3,2,1-ij]quinoline-3,5-dione 3ae. Analytical TLC on silica gel; 3:2 hexane/ethyl acetate R_f = 0.29; dark brown solid; mp 255-256 °C; yield 71% (54 mg); ^{1}H NMR (500 MHz, $CDCl_3$) δ 7.74 (d, *J* = 10.0 Hz, 1H), 7.69 (d, *J* = 7.5 Hz, 1H), 7.41 (d, *J* = 7.5 Hz, 1H), 7.34 (t, *J* = 8.0 Hz, 1H), 7.11-7.08 (m, 4H), 7.04 (t, *J* = 8.0 Hz, 2H), 6.90 (t, *J* = 8.5 Hz, 2H), 6.79 (d, J = 9.5 Hz, 1H; ^{13}C NMR (125 MHz, $CDCl_3$) δ 163.5 (d, J_{C-F} = 247.7 Hz), 163.1 (d, J_{C-F} = 246.1 Hz), 161.6, 161.5, 147.5, 139.9, 134.9, 133.8, 132.7 (d, J_{C-F} = 8.1 Hz), 131.7 (d, J_{C-F} = 8.1 Hz), 131.1 (d, J_{C-F} = 3.6 Hz), 130.9, 130.8, 130.1 (J_{C-F} = 3.7 Hz), 124.5, 123.9, 120.9, 119.6, 115.8 (d, J_{C-F} = 21.7 Hz), 114.9, (d, J_{C-F} = 21.3 Hz); ^{19}F NMR (470 MHz, $CDCl_3$) δ -112.31, -113.85; FT-IR (neat) 3069, 1721, 1600, 1507, 1224, 1155, 838, 816 cm^{-1}; HRMS (ESI) *m/z* $[M+H]^+$ calcd for $C_{24}H_{14}FNO_2$: 386.0987, found 386.0974.

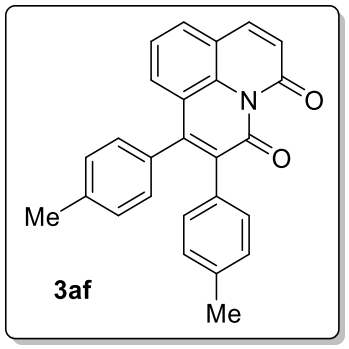

1,2-Di-p-tolyl-3H,5H-pyrido[3,2,1-ij]quinoline-3,5-dione 3af. Analytical TLC on silica gel; 3:2 hexane/ethyl acetate R_f = 0.32; brown solid; mp 268-269 °C; yield 75% (55.5 mg); ^{1}H NMR (400 MHz, $CDCl_3$) δ 7.72 (d, *J* = 9.6 Hz, 1H), 7.64 (dd, *J* = 1.5, 7.5 Hz, 1H), 7.44 (dd, *J* = 1.5, 8.0 Hz, 1H), 7.30 (d, *J* = 7.6 Hz, 1H), 7.12 (d, J = 8.0 Hz, 2H), 7.04-6.97 (m, 7H), 6.78 (d, *J* = 9.6 Hz, 1H), 2.34 (s, 3H), 2.25 (s, 3H); ^{13}C NMR (100 MHz, $CDCl_3$) δ 162.0, 161.9, 147.9, 139.8, 137.9, 137.1, 134.8, 134.3, 132.5, 131.4, 131.1, 130.8, 130.4, 129.8, 129.0, 128.3, 124.4, 123.7, 121.4, 119.4, 21.44, 21.41; FT-IR (neat) 3025, 2920, 1720, 1569, 1252, 1147, 1113, 838, 798, 748 cm^{-1}; HRMS (ESI) *m/z* $[M+H]^+$ calcd for $C_{26}H_{20}NO_2$: 378.1489, found 378.1492

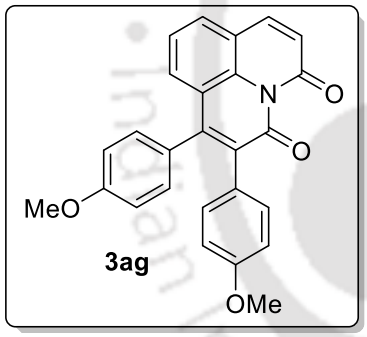

1,2-Bis(4-methoxyphenyl)-3H,5H-pyrido[3,2,1-ij]quinoline-3,5-dione 3ag. Yield: trace; HRMS (ESI) *m/z* $[M+H]^+$ calcd for $C_{26}H_{20}NO_4$: 410.1387, found 410.1396.

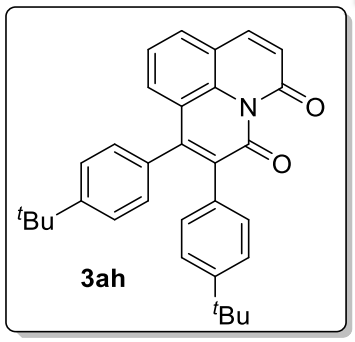

1,2-Bis(4-(*tert*-butyl)phenyl)-3H,5H-pyrido[3,2,1-ij]quinoline-3,5-dione 3ah. Analytical TLC on silica gel; 7:3 hexane/ethyl acetate R_f = 0.35; brown solid; mp 265-266 °C; yield 70% (63 mg); ^{1}H NMR (500 MHz, $CDCl_3$) δ 7.73 (d, *J* = 9.5 Hz, 1H),

7.65 (d, *J* = 7.5 Hz, 1H), 7.55 (d, *J* = 8.0 Hz, 1H), 7.32-7.27 (m, 3H), 7.15 (d, *J* = 8.5 Hz, 2H), 7.04 (t, *J* = 8.0 Hz, 4H), 6.78 (d, *J* = 9.5 Hz, 1H), 1.28 (s, 9H), 1.22 (s, 9H); ^{13}C NMR (125 MHz, $CDCl_3$) δ 161.9, 151.2, 150.1, 148.2, 139.9, 134.9, 134.4, 132.5, 131.4, 131.1, 130.6, 130.4, 129.7, 125.0, 124.4, 124.3, 123.7, 121.3, 119.4, 34.7, 34.5, 31.34, 31.33; FT-IR (neat) 2959, 1722, 1567, 1457, 1254, 1152, 1115, 837, 812, 752 cm^{-1}; HRMS (ESI) *m/z* $[M+H]^+$ calcd for $C_{32}H_{32}NO_2$: 462.2428, found 462.2435.

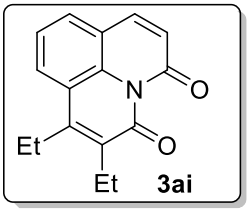

1,2-Diethyl-3H,5H-pyrido[3,2,1-ij]quinoline-3,5-dione 3ai. Analytical TLC on silica gel; 7:3 hexane/ethyl acetate R_f = 0.4; sticky brown liquid; yield 61% (31 mg); ^{1}H NMR (600 MHz, $CDCl_3$) δ 7.89 (d, *J* = 8.4 Hz, 1H), 7.66 (d, *J* = 9.6 Hz, 1H), 7.61 (d, *J* = 7.2 Hz, 1H), 7.44 (t, *J* = 7.8 Hz, 1H), 6.73 (d, *J* = 9.6 Hz, 1H), 2.95-2.91 (m, 2H), 2.81-2.77 (m, 2H), 1.32 (t, *J* = 7.8 Hz, 3H), 1.24 (t, *J* = 7.8 Hz, 3H); ^{13}C NMR (150 MHz, $CDCl_3$) δ 162.1, 147.1, 139.9, 135.2, 134.5, 129.8, 127.3, 124.3, 123.9, 120.0, 119.7, 22.134, 21.1, 14.4, 13.8.; FT-IR (neat) 2970, 1715, 1456, 1234, 1124, 839, 751 cm^{-1}; HRMS (ESI) *m/z* $[M+H]^+$ calcd for $C_{16}H_{16}NO_2$: 254.1176, found 254.1171.

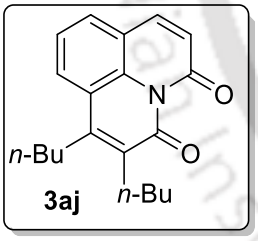

1,2-Dibutyl-3H,5H-pyrido[3,2,1-ij]quinoline-3,5-dione 3aj. Analytical TLC on silica gel; 7:3 hexane/ethyl acetate R_f = 0.4; brown liquid; yield 56% (34 mg); ^{1}H NMR (500 MHz, $CDCl_3$) δ 7.85 (d, *J* = 8.0 Hz, 1H), 7.66 (d, *J* = 10.0 Hz, 1H), 7.60 (d, *J* = 7.5 Hz, 1H), 7.43 (t, *J* = 8.0 Hz, 1H), 6.72 (d, *J* = 9.5 Hz, 1H), 2.88 (t, *J* = 8.0 Hz, 2H), 2.75 (t, *J* = 8.0 Hz, 2H), 1.59-1.45 (m, 8 H), 1.03 (t, *J* = 7.5 Hz, 3H), 0.97 (t, *J* = 7.5 Hz, 3H); ^{13}C NMR (125 MHz, $CDCl_3$) δ 162.2, 162.1, 146.0, 139.8, 134.4, 134.3, 129.7, 127.4, 124.2, 123.8, 120.3, 119.6, 32.1, 31.4, 28.8, 27.7, 23.3, 23.3, 14.1, 14.0; FT-IR (neat) 2957, 2928, 2862, 1717, 1662, 1568, 1251, 1125, 838, 751 cm^{-1}; HRMS (ESI) *m/z* $[M+H]^+$ calcd for $C_{20}H_{24}NO_2$: 310.1802, found 310.1805.

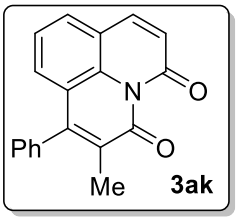

2-Methyl-1-phenyl-3H,5H-pyrido[3,2,1-ij]quinoline-3,5-dione 3ak. Analytical TLC on silica gel; 3:2 hexane/ethyl acetate R_f= 0.35; brown solid; mp 245-246 °C; yield 69% (39.5 mg); ^{1}H NMR (400 MHz, $CDCl_3$) δ 7.72 (d, *J* = 9.6 Hz, 1H), 7.61-7.60 (m, 1H), 7.56-7.49 (m, 3H), 7.26-7.21 (m, 4H), 6.78 (d, *J* = 9.6 Hz, 1H), 2.06 (s, 3H); ^{13}C NMR (125 MHz, $CDCl_3$) δ 162.8, 162.0, 147.2, 140.0, 135.9, 134.1, 130.7, 130.3, 129.9, 129.0, 128.8, 128.6, 124.3, 123.8, 121.3, 119.4, 15.2; DEPT-135 (125 MHz, $CDCl_3$) 140.0 (upward), 130.3 (upward), 129.9 (upward), 129.0 (upward), 128.7 (upward), 128.6 (upward), 124.3 (upward), 123.8 (upward), 15.2 (upward); FT-IR (neat) 3063, 1720, 1632, 1569, 1351, 1253, 1129, 761 cm^{-1}; HRMS (ESI) *m/z* $[M+H]^+$ calcd for $C_{19}H_{14}NO_2$: 288.1019, found 288.1019.\

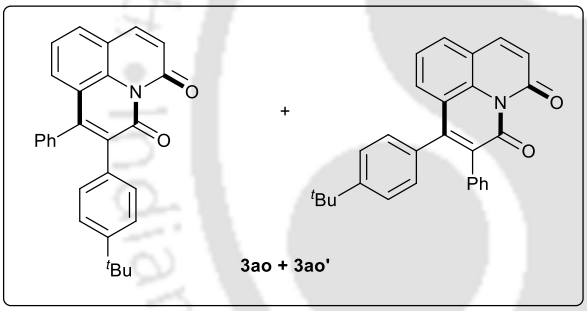

2-(4-(*tert*-Butyl)phenyl)-1-phenyl-3H,5H-pyrido[3,2,1-ij]quinoline-3,5-dioneb (3ao) and 1-(4-(*tert*-Butyl)phenyl)-2-phenyl-3H, 5H-pyrido[3,2,1-ij]quinoline-3,5-dione (3ao'). Analytical TLC on silica gel; 3:2 hexane/ethyl acetate R_f= 0.4; thick brown liquid; yield 69% (58 mg); 1:1 mixture; ^{1}H NMR (500 MHz, $CDCl_3$) δ 7.73 (d, *J* = 9.5 Hz, 2H), 7.66-7.63 (m, 2H), 7.50 (d, *J* = 8.0 Hz, 1H), 7.43 (d, *J* = 7.0 Hz, 1H), 7.32-7.26 (m, 7H), 7.17-7.12 (m, 9H), 7.07-7.02 (m, 4H), 6.78 (d, *J* = 9.5 Hz, 2H), 1.29 (s, 9H), 1.23 (s, 9H); ^{13}C NMR (125 MHz, $CDCl_3$) δ 162.0, 161.9, 161.87, 161.86, 151.3, 150.3, 148.3, 147.7, 140.0, 139.9, 135.5, 135.0, 134.9, 134.5, 134.4, 134.3, 132.2, 131.2, 131.1, 131.0, 130.7, 130.6, 130.5, 130.0, 129.6, 128.2, 128.1, 127.5, 127.4, 125.1, 124.5, 124.45, 124.44, 123.7, 121.3, 121.2, 119.5, 119.4, 34.7, 34.5, 31.4, 31.3; FT-IR (neat) 3063, 2960, 1723, 1454, 1254, 1150, 947, 837, 701 cm^{-1}; HRMS (ESI) *m/z* $[M+H]^+$ calcd for $C_{28}H_{24}NO_2$: 406.1802, found 406.1790.

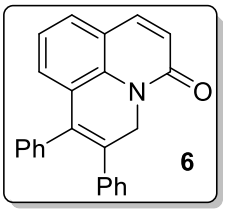

6,7-Diphenyl-3H,5H-pyrido[3,2,1-ij]quinolin-3-one 6. Analytical TLC on silica gel; 9:1 hexane/ethyl acetate R_f = 0.35; colorless solid; mp 203-204 °C; yield 68% (23 mg); ^{1}H NMR (500 MHz, $CDCl_3$) δ 7.75 (d, *J* = 9.5 Hz, 1H), 7.38 (d, *J* = 8.0 Hz, 1H), 7.29-7.26 (m, 2H), 7.25-7.22 (m, 1H), 7.17-7.09 (m, 7H), 7.01 (t, *J* = 7.5 Hz, 1H), 6.94 (d, *J* = 7.5 Hz, 1H), 6.78 (d, *J* = 9.5 Hz, 1H), 5.21 (s, 2H); ^{13}C NMR (125 MHz, $CDCl_3$) δ 161.7, 139.1, 138.4, 136.8, 135.5, 132.2, 132.0, 130.7, 128.5, 128.5, 128.2, 127.6, 127.4, 127.3, 124.8, 122.2, 121.2, 119.7, 49.0; FT-IR (neat) 3056, 2924, 1644, 1582, 1466, 830, 749, 696 cm^{-1}; HRMS (ESI) *m/z* $[M+H]^+$ calcd for $C_{24}H_{18}NO$: 336.1383, found 336.1384.

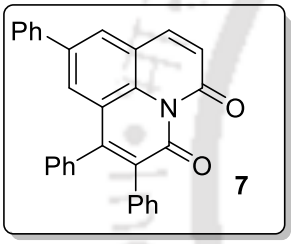

1,2,9-Triphenyl-3H,5H-pyrido[3,2,1-ij]quinoline-3,5-dione 7. Analytical TLC on silica gel; 7:3 hexane/ethyl acetate R_f = 0.35; brown solid; mp 245-246 °C; yield 74% (31.5 mg); ^{1}H NMR (500 MHz, $CDCl_3$) δ 7.86 (d, *J* = 2.0 Hz, 1H), 7.80 (d, *J* = 10.0 Hz, 1H), 7.64 (d, *J* = 2.0 Hz, 1H), 7.437 (dt, *J* = 7.5, 15.0 Hz, 4H), 7.46-7.40 (m, 1H), 7.37-7.34 (m, 3H), 7.32-7.29 (m, 7H), 6.83 (d, *J* = 10.0 Hz, 1H); ^{13}C NMR (100 MHz, $CDCl_3$) δ 161.7, 161.7, 148.2, 139.9, 139.0, 137.0, 135.2, 134.8, 134.3, 134.1, 130.9, 129.9, 129.4, 129.2, 129.0, 128.4, 128.4, 128.1, 127.63, 127.60, 127.1, 124.8, 121.6, 119.9; FT-IR (neat) 3055, 2923, 2853, 1723, 1454, 1259, 1154, 757, 699 cm^{-1}; HRMS (ESI) *m/z* $[M+H]^+$ calcd for $C_{30}H_{20}NO_2$: 426.1489, found 426.1472.

Crystal Data and Structure Refinement for 3aa

Sample Preparation for Crystal Growth. The compounds **3aa** was dissolved in a minimum volume of acetonitrile and kept at room temperature for slow evaporation for 2 days. The crystals were then subjected to *X*-ray diffraction.

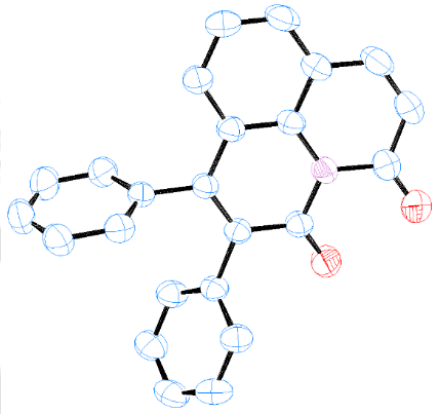

Figure 2. ORTEP diagram of 1,2-diphenyl-3H,5H-pyrido[3,2,1-ij]quinoline-3,5-dione **3aa** with 50% ellipsoid (CCDC 2382651). H-Atoms are omitted for clarity.

Identification code	**3aa**
Empirical formula	'C24 H15 N O2'
Formula weight	349.37
Crystal habit, color	Needle, colorless
Crystal size, mm^3	0.25 x 0.21 x 0.19
Temperature, *T*/K	297 K
Wavelength, λ/Å	0.71073
Crystal system	'Monoclinic'
Space group	' P 21/n'
Unit cell dimensions	a = 9.3265 (7) Å
	b = 16.1716 (11) Å
	c = 11.8420 (8) Å
	α = 90
	β = 92.342 (2)
	γ = 90
Volume, *V*/$Å^3$	1784.6 (2)

Z	4
Calculated density, g cm^{-3}	1.300
Absorption coefficient, μ/mm^{-1}	0.083
F(000)	728.0
θ range for data collection	2.52 to 25.08°
Limiting indices	$-11 \leq h \leq 11$, $-19 \leq k \leq 19$, $-14 \leq l \leq 14$
Reflection collected / unique	3162/2251
Completeness to θ	99.7%
Absorption correction	None
Max. and min. transmission	0.984 and 0.979
Refinement method	SHELXL-2019/1 (Sheldrick, 2019)
Data / restraints / parameters	3162/0/245
Goodness–of–fit on F^2	1.089
Final R indices [I>2sigma(I)]	R1 = 0.0589, wR2 = 0.1293
R indices (all data)	R1 = 0.0913, wR2 = 0.1553

Crystal Data and Structure Refinement for 6

Sample Preparation for Crystal Growth. The compounds **6** was dissolved in a minimum volume of acetonitrile and kept at room temperature for slow evaporation for 2 days. The crystals were then subjected to *X*-ray diffraction.

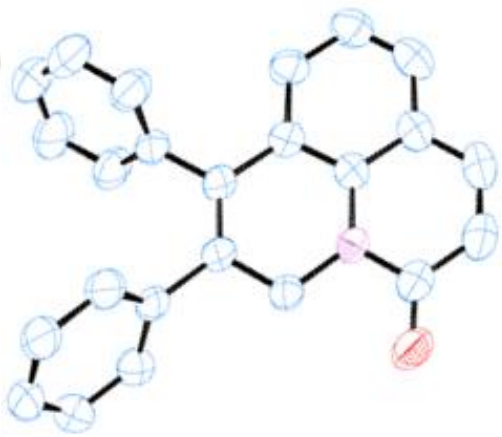

Figure 3. ORTEP diagram of **6** with 50% ellipsoid (CCDC 2382652). H-Atoms are omitted for clarity.

Identification code	**6**
Empirical formula	'C24 H17 N O'
Formula weight	335.38
Crystal habit, color	Block, Colorless
Crystal size, mm^3	0.27 x 0.24 x 0.20
Temperature, *T*/K	295 K
Wavelength, λ/Å	0.71073
Crystal system	'Orthorhombic'
Space group	'P b c a'
Unit cell dimensions	a = 6.9180 (7) Å
	b = 16.8553 (17) Å
	c = 29.099 (3) Å
	α = 90
	β = 90
	γ = 90
Volume, *V*/$Å^3$	3393.1 (6)
Z	8
Calculated density, g cm^{-3}	1.313
Absorption coefficient, μ/mm^{-1}	0.080
F(000)	1408.0
θ range for data collection	2.52 to 26.39°
Limiting indices	$-8 \leq h \leq 8$, $-21 \leq k \leq 21$, $-36 \leq l \leq 36$
Reflection collected / unique	3429/2109
Completeness to θ	98.3%
Absorption correction	None
Max. and min. transmission	0.984 and 0.979
Refinement method	SHELXL-2019/1 (Sheldrick, 2019)
Data / restraints / parameters	3429/0/244
Goodness–of–fit on F^2	1.110
Final *R* indices [*I*>2sigma(*I*)]	R1 = 0.0591, wR2 = 0.0999
R indices (all data)	R1 = 0.1169, wR2 = 0.1247

4.6 References

1. (a) Song, G.; Wang, F.; Li, X. *Chem. Soc. Rev*. **2012**, *41*, 3651. (b) Rogge, T.; Kaplaneris, N.; Chatani, N.; Kim, J.; Chang, S.; Punji, B.; Schafer, L. L.; Musaev, D. G.; Wencel-Delord, J.; Roberts, C. A.; Sarpong, R.; Wilson, Z. E.; Brimble, M. A.; Johansson, M. J.; Ackermann, L. *Nat. Rev. Methods Primers* **2021**, *1*, 43. (c) Dalton, T.; Faber, T.; Glorius, F. *ACS Cent. Sci*. **2021**, *7*, 245. (d) Docherty, J. H.; Lister, T. M.; McArthur, G.; Findlay, M. T.; Domingo-Legarda, P.; Kenyon, J.; Choudhary, S.; Larrosa, I. *Chem. Rev*. **2023**, *123*, 7692.
2. (a) Umeda, N.; Tsurugi, H.; Satoh, T.; Miura, M. *Angew. Chem., Int. Ed*. **2008**, *47*, 4019. (b) Shiota, H.; Ano, Y.; Aihara, Y.; Fukumoto, Y.; Chatani, N. *J. Am. Chem. Soc*. **2011**, *133*, 14952. (c) Ackermann, L. *Acc. Chem. Res*. **2014**, *47*, 281. (d) Misal Castro, L. C.; Obata, A.; Aihara, Y.; Chatani, N. *Chem.-Eur. J.* **2016**, *22*, 1362. (f) Saha, S.; Debnath, B.; Talukdar, K.; Karjee, P.; Mandal, S.; Punni-yamurthy, T. *Org. Lett*. **2023**, *25*, 3352.
3. (a) Engle, K. M.; Mei, T. S.; Wasa, M.; Yu, J. Q. *Acc. Chem. Res*. **2012,** *45*, 788. (b) Corbet, M.; De Campo, F. *Angew. Chem., Int. Ed*. **2013**, *52*, 9896. (c) Zhang, F.; Spring, D. R. *Chem. Soc. Rev*. **2014**, *43*, 6906. (d) De Sarkar, S.; Liu, W.; Kozhushkov, S. I.; Ackermann, L. *Adv. Synth. Catal*. **2014**, *356*, 1461. (e) Gensch, T.; Hopkinson, M. N.; Glorius, F.; Wencel-Delord, J. *Chem. Soc. Rev*. **2016**, *45*, 2900. (f) Zhang, Q.; Shi, B.-F. *Acc. Chem. Res*. **2021**, *54*, 2750.
4. Wang, D.; Désaubry, L.; Li, G.; Huang, M.; Zheng, S. *Adv. Synth. Catal*. **2021**, *363*, 2.
5. Basak, S.; Paul, T.; Mandal, S.; Karjee, P.; Nanjegowda, M. V.; Punniyamurthy, T. *Synthesis* **2023**, *55*, 3454.
6. Shah, T. A.; De, P. B.; Pradhan, S.; Banerjee, S.; Punniyamurthy, T. *Chem.-Asian J.* **2019**, *14*, 4520.
7. (a) Joseph, B.; Darro, F.; Béhard, A.; Lesur, B.; Collignon, F.; Decaestecker, C.; Frydman, A.; Guillaumet, G.; Kiss, R. *J. Med. Chem*. **2002**, 45, 2543. (b) Michael, J. P. *Nat. Prod. Rep*. **2003**, *20*, 476. (c) Lebreux, F.; Quiclet-Sire, B.; Zard, S. Z. *Org. Lett*. **2009**, *11*, 2844. (d) Ukrainets, I. V.; Sidorenko, L. V.; Golik, M. Y.; Chernenok, I. M.; Grinevich, L. A.; Davidenko, A. A. *Sci. Pharm*. **2018**, *86*, 12.
8. Campeau, L.-C.; Stuart, D. R.; Leclerc, J.-P.; Bertrand-Laperle, M.; Villemure, E.; Sun, H.-Y.; Lasserre, S.; Guimond, N.; Lecavallier, M.; Fagnou, K. *J. Am. Chem. Soc*. **2009**, *131*, 3291.

9. Hwang, H.; Kim, J.; Jeong, J.; Chang, S. J. Am. Chem. Soc. **2014**, 136, 10770.
10. Li, D. Y.; Huang, Z. L.; Liu, P. N. *Org. Lett.* **2018**, *20*, 2028.
11. Mandal, S.; Paul, T.; Karjee, P.; Barman, M.; Punniyamurthy, T. Org. Lett. **2023**, *25*, 7805.
12. Yu, S.; Li, X. *Org. Lett*. **2014**, *16*, 1220.
13. Chen, J.; Tang, B. L.; Liu, X. X.; Lv, G. H.; Shi, Y. S.; Huang, T. L.; Xing, H. N.; Guo, X. Y.; Hai, L.; Wu, Y. *Org. Chem. Front*. **2020**, *7*, 2944.
14. Zhang, Y.-B.; Li, B.-S.; Xu, G.-J.; Sun, W.; Sun, M. *Org. Lett*. **2023**, *25*, 3922.
15. (a) Chen, X.; Cui, X.; Wu, Y. *Org. Lett*. **2016**, *18*, 2411. (b) Zhao, W. T.; Gao, F.; Zhao, D. B. *Angew. Chem., Int. Ed*. **2018**, *57*, 6329. (c) Haito, A.; Chatani, N. *Chem. Commun*. **2019**, *55*, 5740. (d) Haito, A.; Chatani, N. *Chem. Commun*. **2019**, *55*, 5740. (e) Shi, Y.; Xing, H.; Huang, T.; Liu, X.; Chen, J.; Guo, X.; Li, G.-B.; Wu, Y. *Chem. Commun*. **2020**, *56*, 1585. (f) Mandal, S.; Karjee, P.; Saha, S.; Punniyamurthy, T. *Chem. Commun*. **2023**, *59*, 2823.
16. Dhiman, A. K.; Gupta, S. S.; Sharma, R.; Kumar, R.; Sharma, U. *J. Org. Chem*. **2019**, *84*, 12871.
17. (a) Poloukhtine, A.; Popik, V. V. *J. Org. Chem*. **2003**, *68*, 7833. (b) Kuzmanich, G.; Gard, M. N.; Garcia-Garibay, M. A. *J. Am. Chem. Soc*. **2009**, *131,* 11606. (c) Vanos, C. M.; Lambert, T. H. *Angew. Chem., Int. Ed*. **2011**, *50*, 12222.

4.7 Selected NMR Spectra

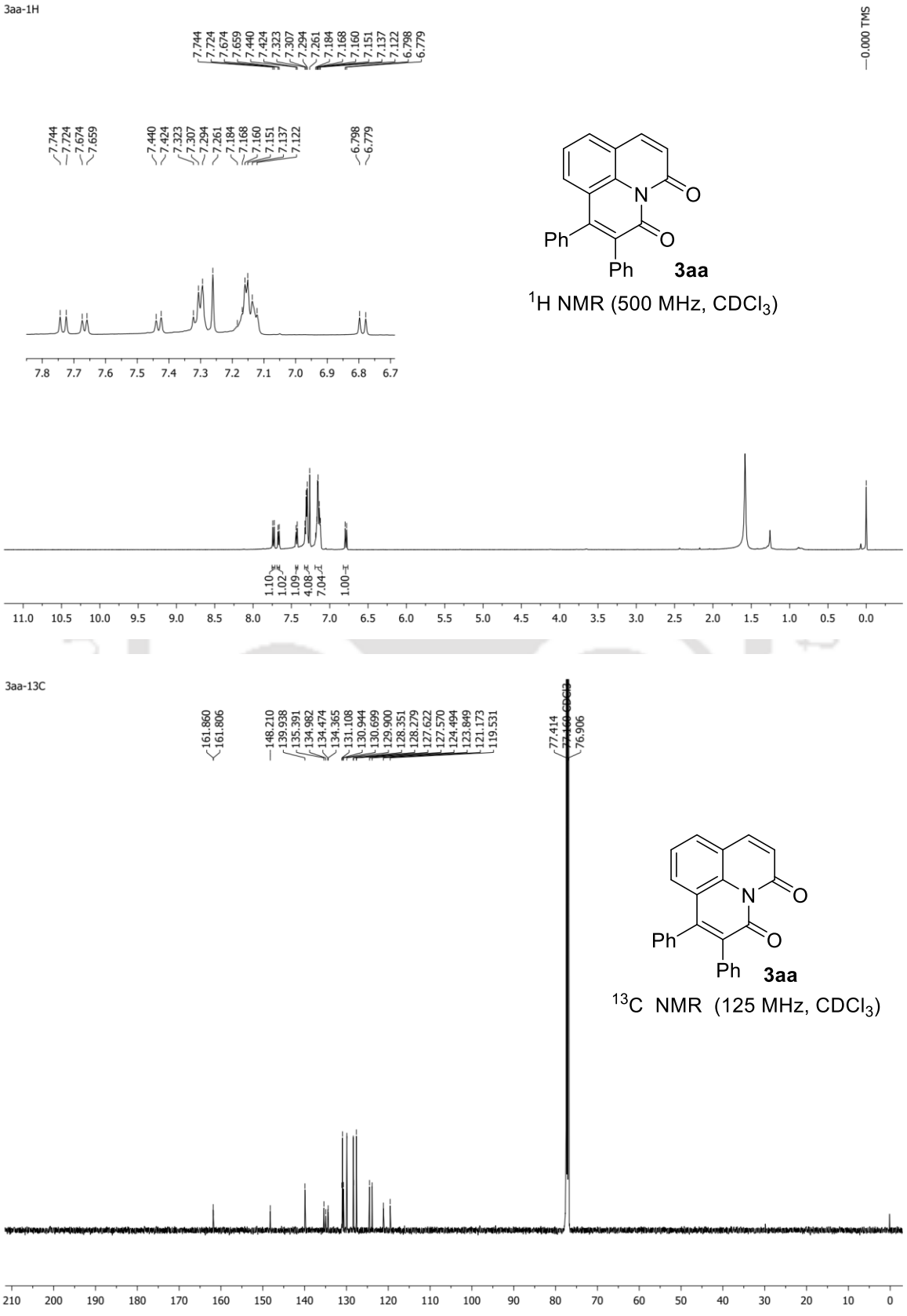

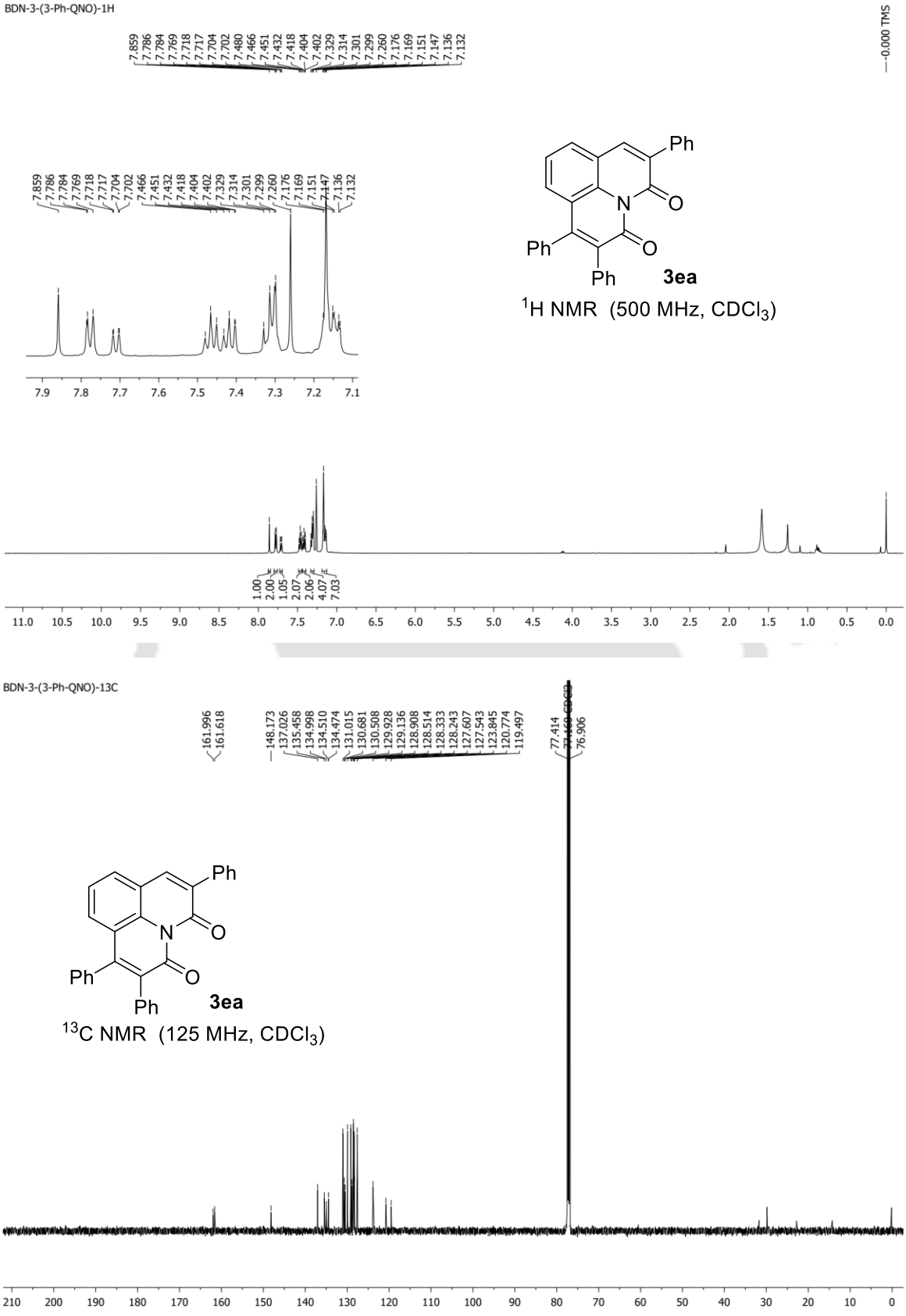

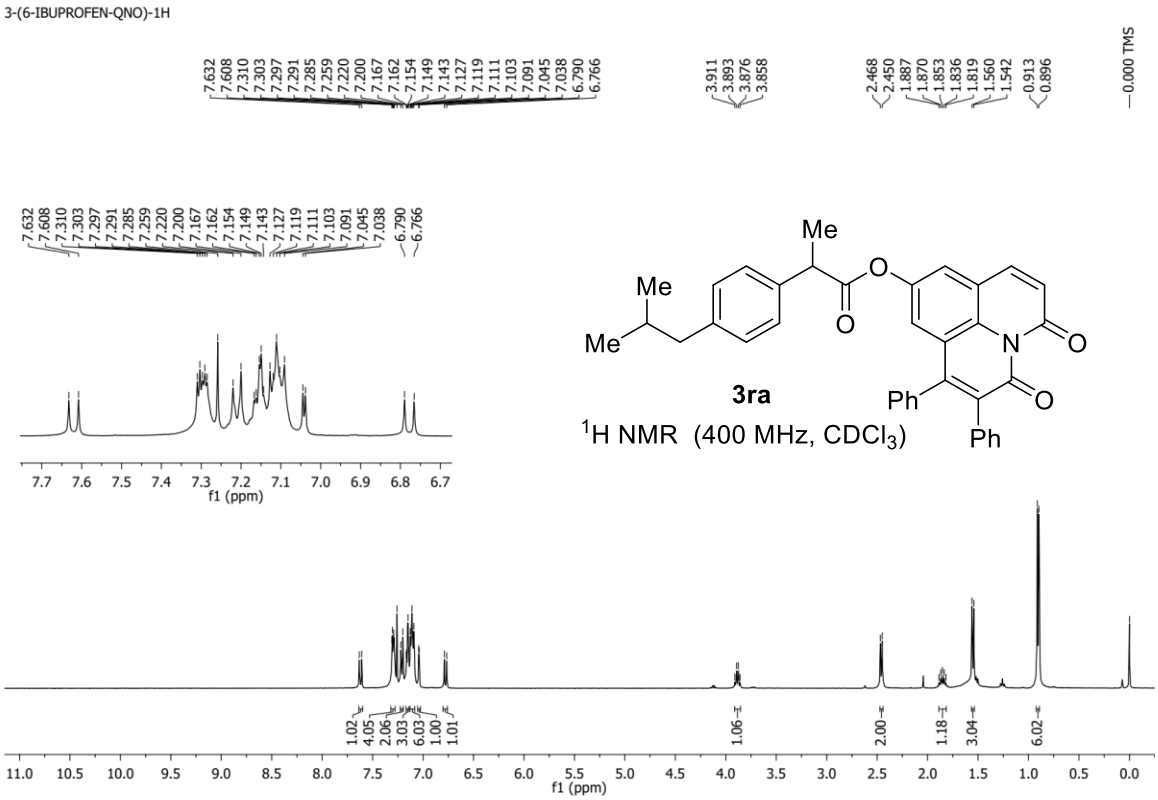

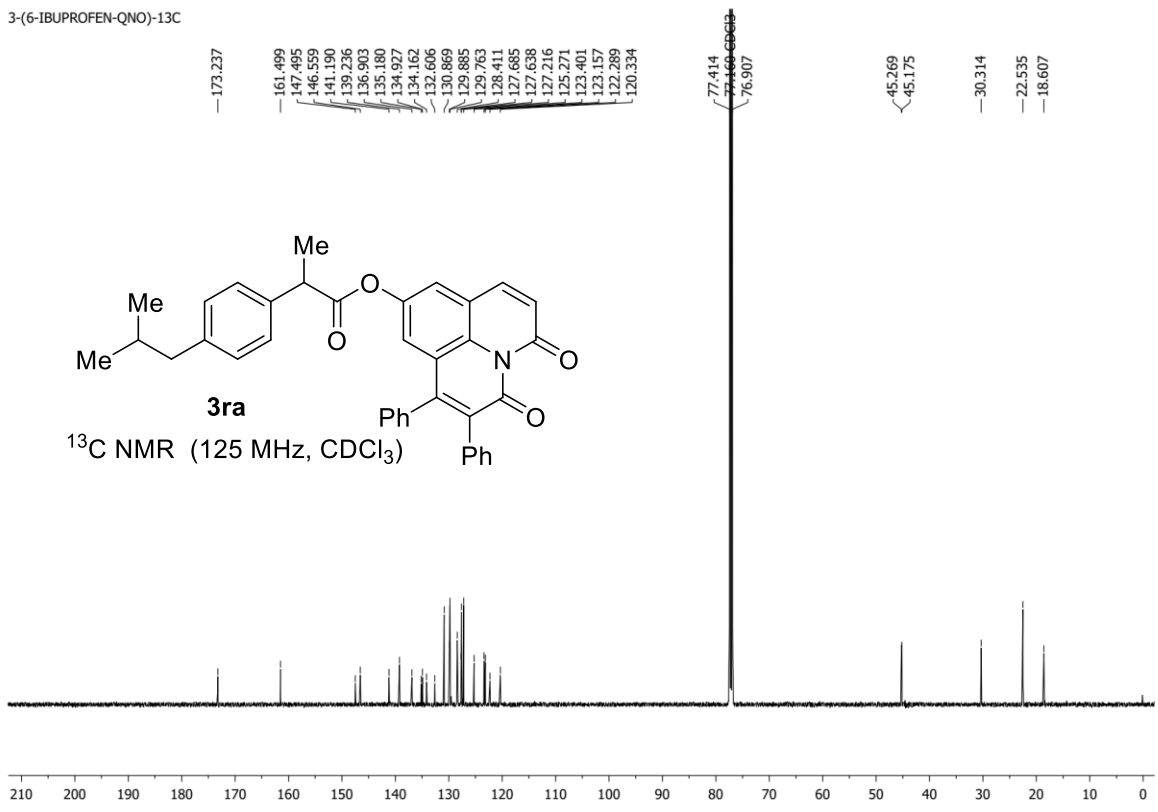

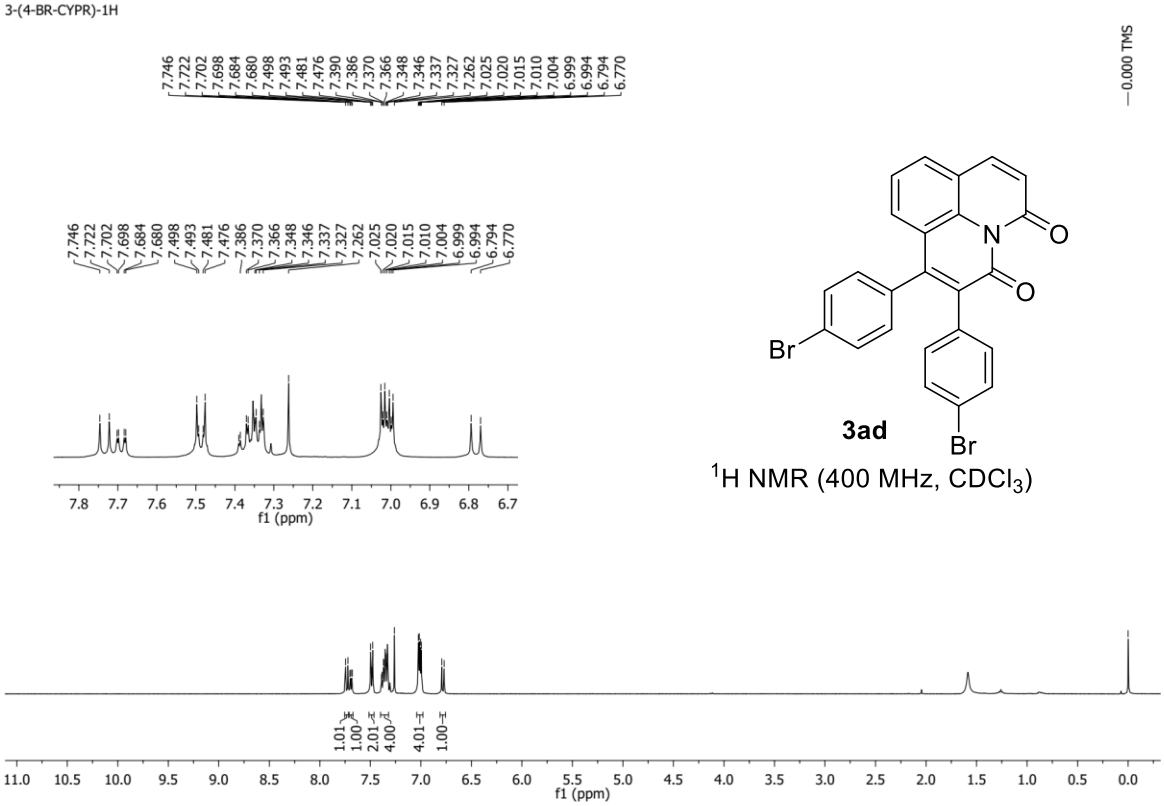

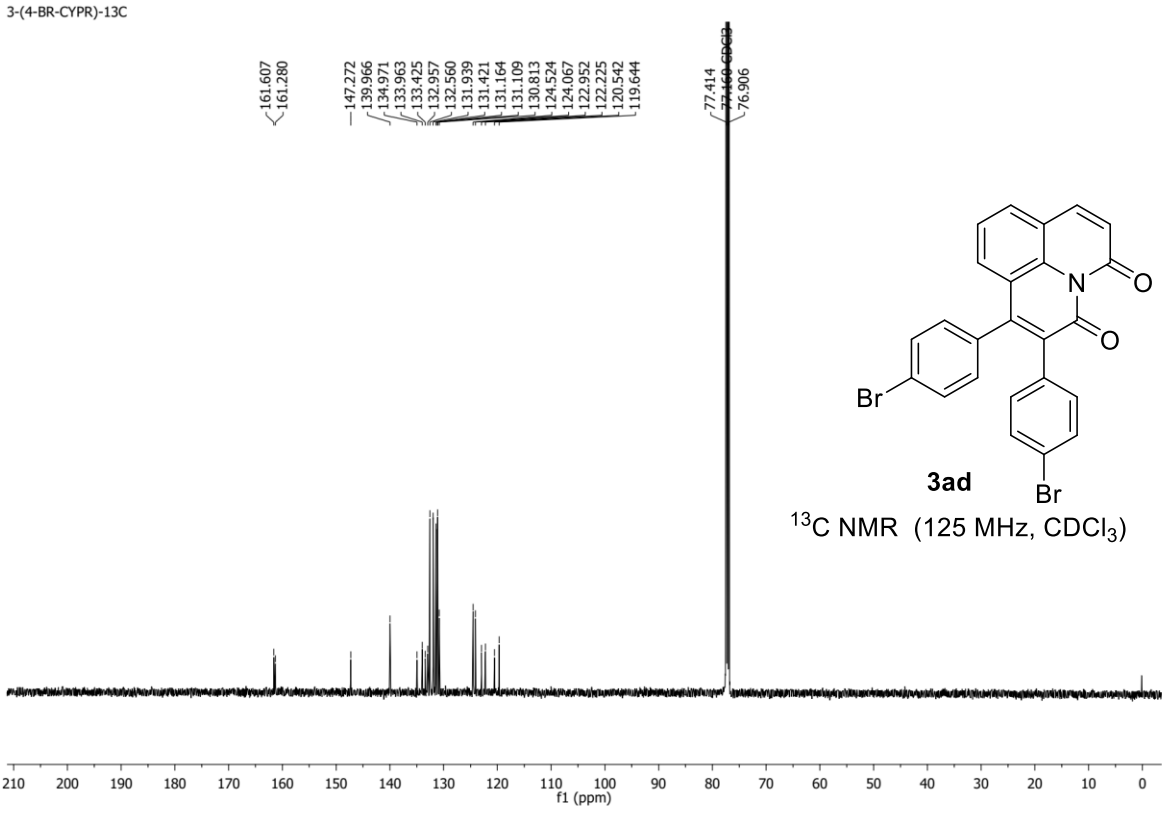

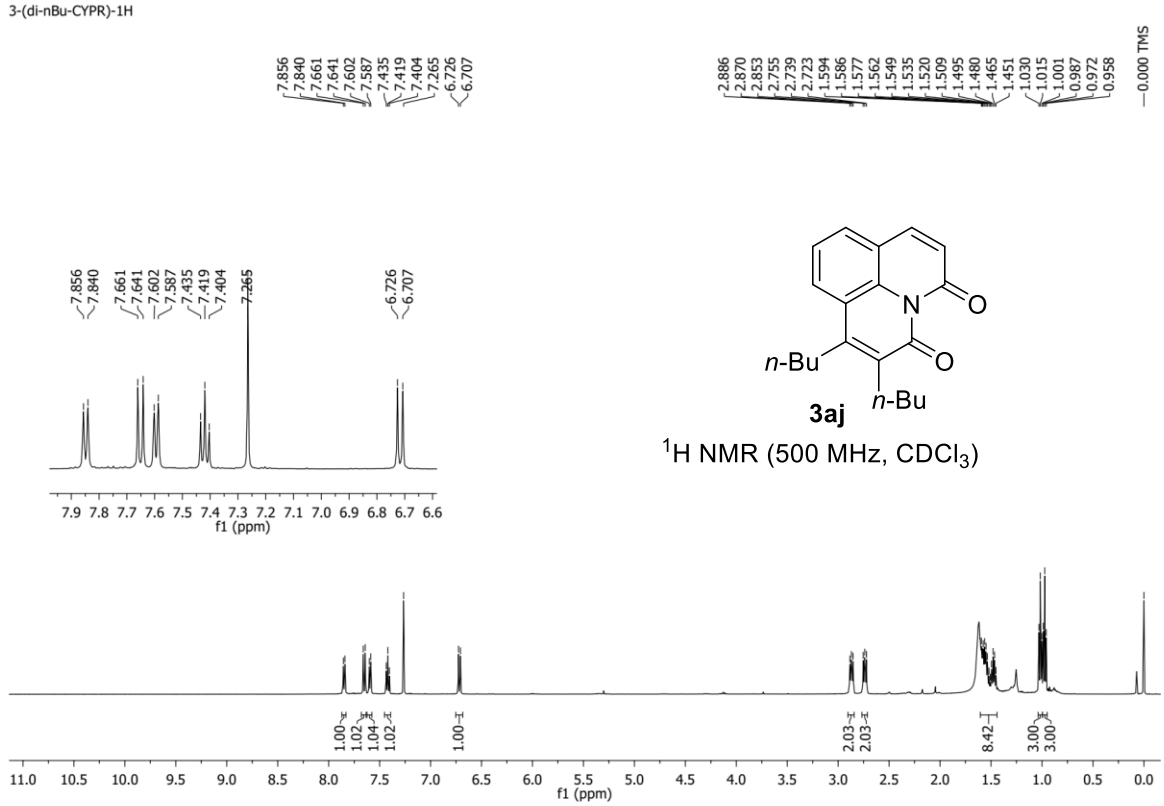

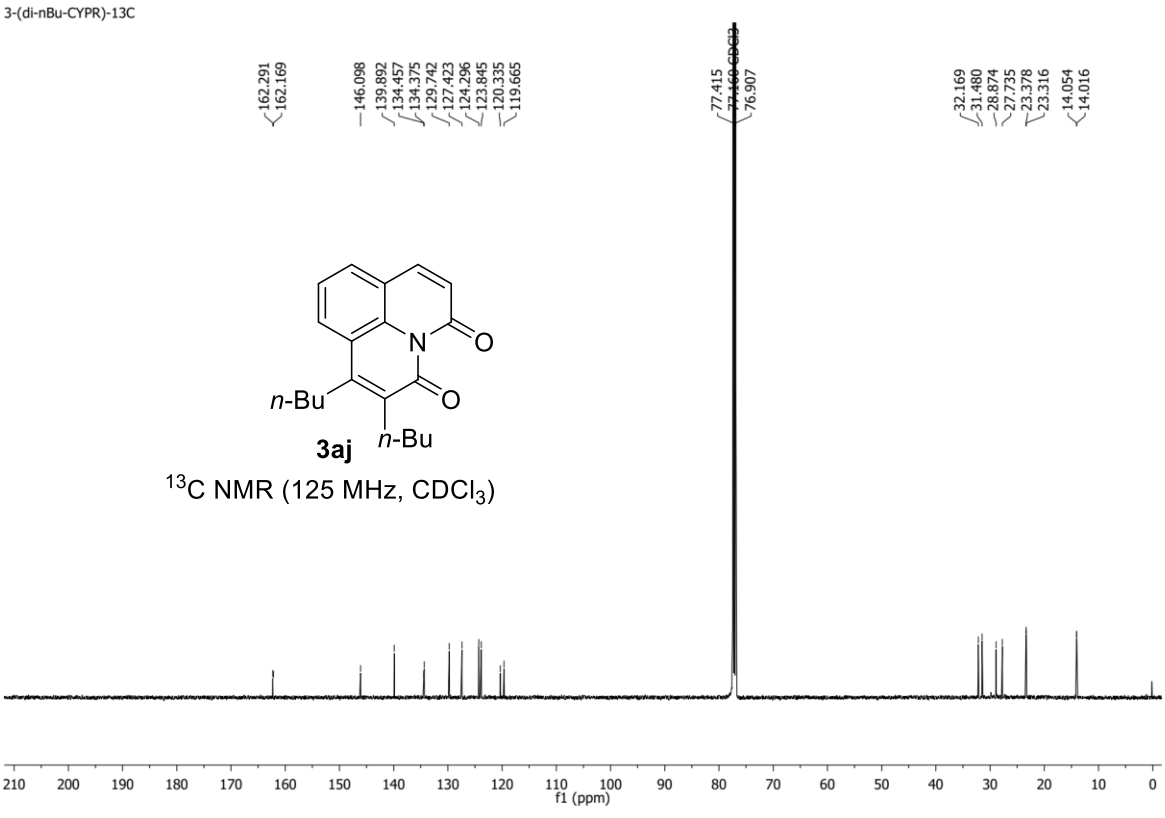

Thesis Overview

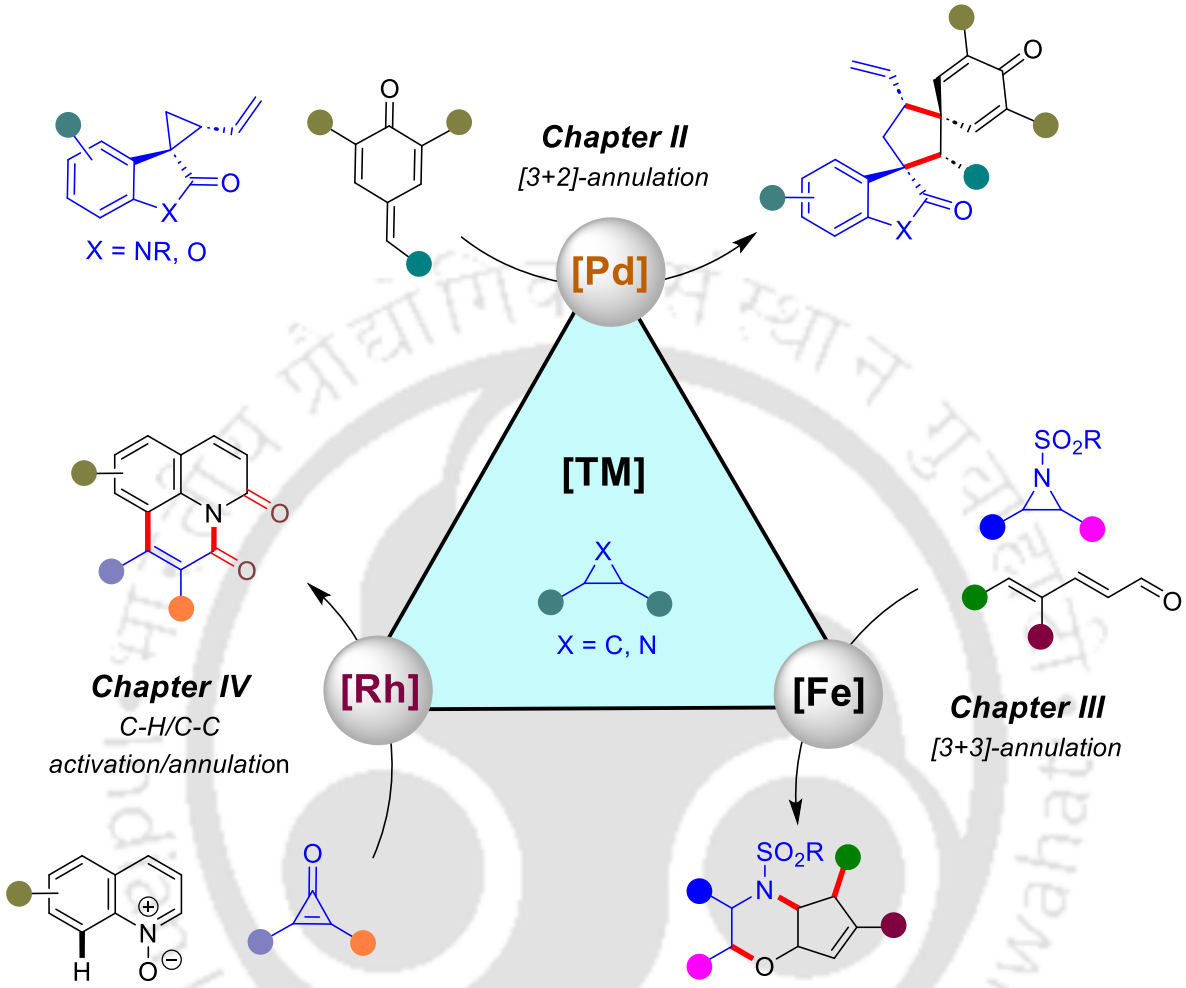

Summary

This thesis presents research on the distinct reactivities of three-membered rings, such as vinylcyclopropane, aziridines and cyclopropenones, exploring their potential for constructing spiro and heterocyclic scaffolds. The key findings from comprehensive experimental and DFT studies are discussed.

In chapter I, we highlighted the significance of spiro- and heterocyclic scaffolds and their recent advancements in synthesis of such relevant structural frameworks using strained ring systems. The ease of accessibility and facile reactivity under transition-metal-catalysis of these strained rings with diversified reagents, have marked a significant milestone in broadening the synthetic chemical landscape to achieve new objectives.

Chapter II illustrates a palladium-catalyzed [3+2]-annulation of spirovinylcyclopropyl oxindoles with *p*-quinone methides. The protocol afforded a prospective route to the functionalized bis-spirocyclopentane oxindoles *via* C−C bond formation at room temperature. Substate scope with wide range of functional group tolerance, DFT-mechanistic study and the cytotoxicity of the synthesized spiro-derivative against cancer cells demonstrates its potential for synthetic applications.

Chapter III describes a [3+3]-annulation of aziridines with dienals under iron-catalysis. The strategy showed an effective method for C−O and C−N bond formation leading to bio-relevant morpholine derivative. The reaction occurs through an iron-catalyzed ring-opening/cyclization of aziridine with a cyclic oxalyl-cation, generated *via* the iso-Nazarov pathway. Use of easily accessible reagents, inexpensive iron catalyst and post-synthetic transformations to synthesize fused morpholines are the major findings of the protocol.

Chapter IV showcased an auxiliary-assisted rhodium-catalyzed annulation of quinoline *N*-oxide with cyclopropenone that follows a C−H/C−C activation and annulation. The synthetic route involves C8−H functionalization followed by a sequential C−C and C−N bond formation to furnish functionalized 2-quinolone derivatives. The notable aspects of the findings include broad substrate scope, functional group diversity, drug modifications, post-synthetic transformations, and mechanism insights.

Strained small-ring systems enable efficient access to diverse spiro- and heterocycles. Our methodologies provide versatile strategies for constructing structurally varied spiro and heterocyclic compounds.

List of Publications

1. **Debnath**, **B**.; Sarkar, T.; Karjee, P.; Purkayastha, S. K.; Guha, A. K.; Punniyamurthy, T. Palladium-Catalyzed Annulative Coupling of Spirovinylcyclopropyl Oxindoles with *p*-Quinone Methides. *J. Org. Chem*. **2023**, *88*, 9704.
2. **Debnath, B**.; Mandal, S.; Saha, S.; Karjee, P.; Punniyamurthy, T. Rh-Catalyzed [3+3]-Annulation of Quinolines with Cyclopropenones: Access to Functionalized 2-Quinolones. *Chem. Commun.* **2025**, *61*, 7875.
3. Sarkar, T.; Talukdar, K.; Das, B. K.; Shah, T. A.; **Debnath**, **B.**; T. Punniyamurthy, T. The Transition-Metal-Catalyzed Stereoselective Ring-Expansion of Vinyl-aziridines and Vinyloxiranes. *Org. Biomol. Chem*. **2021**,*19*, 3776.
4. Sarkar, T.; Shah, T. A.; Maharana, P. K.; **Debnath**, **B.**; Punniyamurthy, T. Dual Metallaphotoredox Catalyzed Directed C(sp2)−H Functionalization: Access to C−C/Heteroatom Bonds. *Eur. J. Org. Chem*. **2022**, e202200541.
5. Karjee, P.; Mishra, M.; **Debnath**, **B.**; Punniyamurthy, T. Expedient $Ni(OTf)_2$/Visible Light Photoredox-Catalyzed Annulation of Donor-Acceptor Cyclopropanes with Cyclic Secondary Amines. *Chem. Commun*. **2022**, *58*, 8670.
6. Basak, S.; Paul, T.; Maharana, P. K.; **Debnath**, **B.**; Punniyamurthy, T. Transition-Metal-Catalyzed Directing Group Assisted C4−H Carbon−Carbon Bond Formation of Indole. *Synlett*. **2023**, *34*, 759.
7. Saha, S.; **Debnath**, **B.**; Talukdar, K.; Karjee, P.; Mandal, S.; Punniyamurthy, T. Cascade C–H Activation/Annulation of Sulfoxonium Ylides with Vinyl Cyclopropanes: Access to Cyclopropane-Fused α-Tetralones. *Org. Lett*. **2023**, *25*, 3352.
8. Karjee, P.; Mandal, S.; **Debnath**, **B.**; Namdev, N.; Punniyamurthy, T. Expedient (3+3)-Annulation of in situ Generated Azaoxyallyl Cations with Diaziridines. *Chem. Commun*. **2023**, *59*, 8270.
9. Saha, S.; Bhattacharyya, H.; Karjee, P.; **Debnath**, **B**.; Verma, K.; Punniyamurthy, T. Expedient C−H Allylation of Sulfoxonium Ylides: Merging C−H and C−C/C−Het Bond Activation. *Chem. Commun*. **2023**, *59*, 14173.
10. Karjee, P.; **Debnath**, **B**.; Mandal, S.; Saha, S.; Punniyamurthy, T. One-Pot C−N/C−C Bond Formation and Oxidation of Donor-Acceptor Cyclopropanes with Tetrahydroisoquinolines: Access to Benzo-Fused Indolizines. *Chem. Commun*. **2024**, *60*, 4068.

11. Mandal, S.; Barman, M.; **Debnath**, **B**.; Punniyamurthy, T. Dual C(sp3)–H and C(sp2)–H Activation of 8-Methylquinoline N-Oxides: A Route to Access C7–H Bond. *Org. Lett*. **2024**, *26*, 7560.
12. Karjee, P.; Shah, T. A.; Mandal, S.; **Debnath, B**.; Punniyamurthy, T. Recent Advancement on Ring Expansion of Bicyclic Diaziridines to Access *N*-Heterocyclic Compounds. *Eur. J. Org. Chem*. **2024**, e202401057.

Conference Attended

1. **B. Debnath**, T. Sarkar, P. Karjee and T. Punniyamurthy, "Palladuim-Catalyzed [3+2]-Cycloaddition of Spirovinylcyclopropyl Oxindoles with *p*-Quinone Methides" CRSI NSC-28, IIT Guwahati, February 4-6, 2022.
2. **B. Debnath**, T. Sarkar, P. Karjee, S. K. Purkayastha, A. K. Guha and T. Punniyamurthy, "Palladium-Catalyzed Annulative Coupling of Spirovinylcyclopropyl Oxindoles with *p*-Quinone Methides" RIC, IIT Guwahati, May 14-16, 2023.
3. **B. Debnath**, T. Sarkar, P. Karjee, S. K. Purkayastha, A. K. Guha and T. Punniyamurthy, "Palladium-Catalyzed Annulative Coupling of Spirovinylcyclopropyl Oxindoles with *p*-Quinone Methides" CRSI NSC-32, BITS Pilani, February 2-4, 2024.
4. **B. Debnath**, T. Sarkar, P. Karjee, S. K. Purkayastha, A. K. Guha and T. Punniyamurthy, "Palladium-Catalyzed Annulative Coupling of Spirovinylcyclopropyl Oxindoles with *p*-Quinone Methides" FICS-2024, IIT Guwahati, December 2-4, 2024.